PHD

PROGRAM OF BIOMEDICINE AND BIOTECHNOLOGY

TRANSCRIPTOMIC ANALYSIS OF HOST-PATHOGEN RELATIONSHIP IN *Vibrio vulnificus*

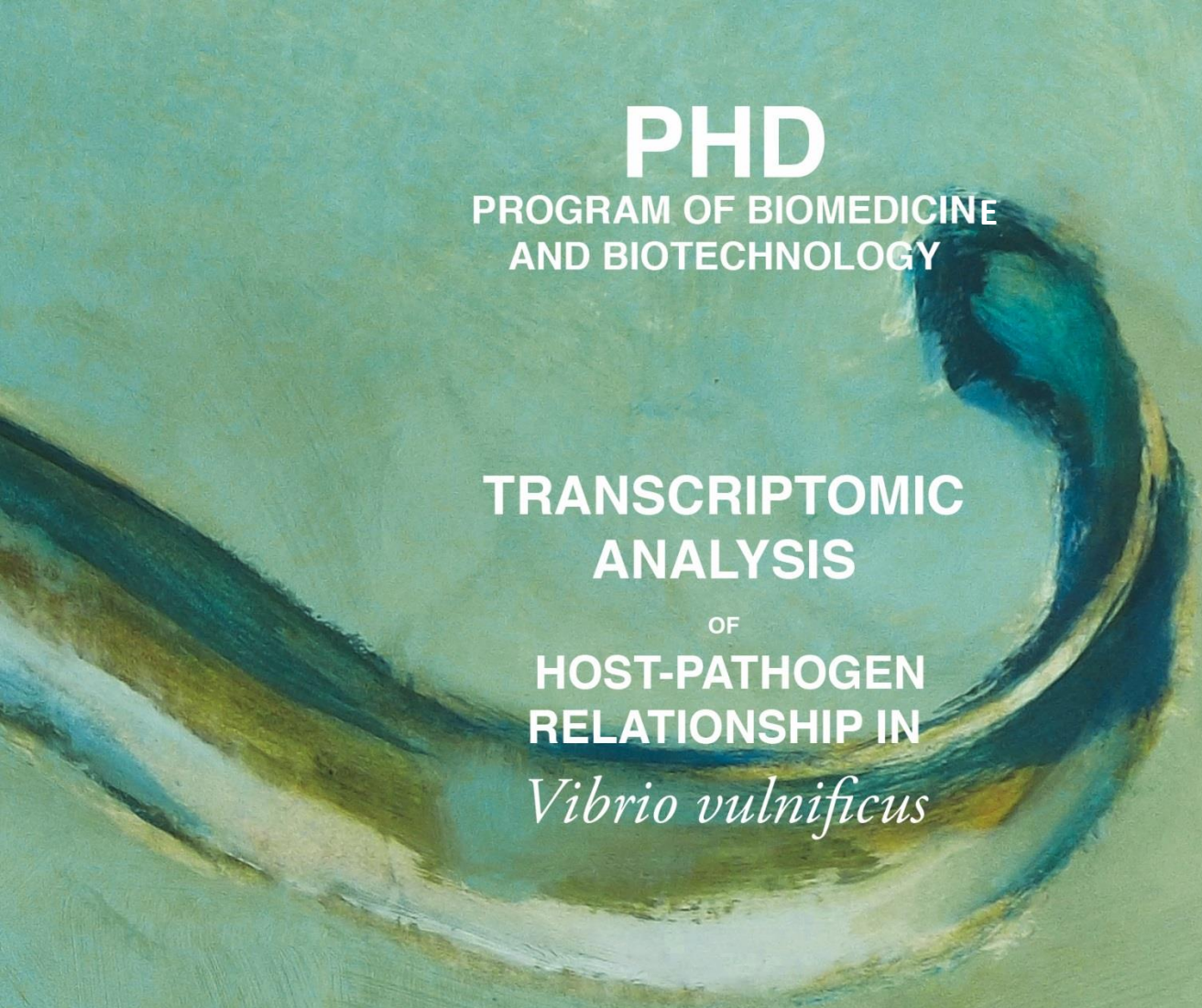

CARLA HERNÁNDEZ CABAÑERO

SUPERVISOR

CARMEN AMARO GONZÁLEZ

Dep. Microbiologia i Ecologia

VNIVERSITAT DE VALÈNCIA

VNIVERSITAT DE VALÈNCIA | BIOTECMED
Estructura de Recerca Interdisciplinar en Biotecnologia i Biomedicina

PROGRAMA DE POSTGRADO EN BIOMEDICINA Y BIOTECNOLOGÍA

TRANSCRIPTOMIC ANALYSIS OF HOST-PATHOGEN RELATIONSHIP IN *Vibrio vulnificus*

Memoria presentada por
Carla Hernández Cabañero
para optar al grado de Doctor con mención internacional
por la Universidad de Valencia

Dirigida por
Dra. **Carmen Amaro González**

Valencia, 2019

La Dra. Carmen Amaro González, catedrática del departamento de Microbiología y Ecología y directora del grupo de Patógenos Acuáticos del Estructura de Recerca Interdisciplinar en Biotecnologia i Biomedicina (ERI BIOTECMED), ambos de la Universidad de Valencia, certifica que Dña. Carla Hernández Cabañero ha realizado bajo su dirección el trabajo titulado "**Transcriptomic analysis of host-pathogen relathionship in *Vibrio vulnificus***" y autoriza la lectura y defensa de la misma para optar al grado de Doctor en Ciencias Biológicas por la Universidad de Valencia.

Y para que así conste a los efectos oportunos, firma la presente en Valencia en Octubre de 2019.

Fdo. Carmen Amaro González

La Dra. Belén Fouz Rodríguez, profesora contratada del departamento de Microbiología y Ecología y miembro del grupo de Patógenos Acuáticos del Estructura de Recerca Interdisciplinar en Biotecnologia i Biomedicina (ERI BIOTECMED), ambos de la Universidad de Valencia, certifica que Dña. Carla Hernández Cabañero ha realizado bajo su tutela el trabajo titulado "**Transcriptomic analysis of host-pathogen relathionship in *Vibrio vulnificus***" y autoriza la lectura y defensa de la misma para optar al grado de Doctor en Ciencias Biológicas por la Universidad de Valencia.

Y para que así conste a los efectos oportunos, firma la presente en Valencia en Octubre de 2019.

Fdo. Belén Fouz Rodríguez

“La imaginación es, por excelencia, la habilidad de descubrir, es aquello que penetra en los mundos invisibles que nos rodean, los mundos de la ciencia.” **Ada Lovelace**

“Como investigadora, los momentos inolvidables de mi vida son excepcionales… Cuando el velo que esconde los secretos de la naturaleza de repente se levanta.”
Gerty Cory

“Por encima de todo, no temas los momentos difíciles. De ellos sale lo mejor.”
Rita Levi-Montalcini

AGRADECIMIENTOS/ ACKNOWLEDGEMENTS

Me gustaría aprovechar este espacio para dedicar unas líneas a todas las personas que en mayor o menor medida han contribuido a esta tesis, porque si algo tengo claro es que de no haber sido por todos vosotros la finalización de este proyecto no habría sido posible. Por ello, espero consideréis este trabajo tan vuestro como mío.

Mi más sincero agradecimiento a mi directora, Carmen Amaro, no solo por haberme dado la oportunidad de formarme en el laboratorio durante el máster y posteriormente haber confiado en mí para la realización de este tesis, sino también por la confianza y el buen trato personal que me has dado durante todos estos años.

A Belén Fouz. Supongo que de no haber realizado el TFG contigo no habría terminado trabajando en este laboratorio, así que en primer lugar gracias por eso. Gracias también por ser la tutora de esta tesis, y por los consejos que me has dado durante estos años, tanto en lo referente al trabajo con peces como en las tareas docentes. Tengo que admitir que las prácticas del máster de acuicultura han sido mis favoritas.

A todos los compañeros del laboratorio. A los que estaban en un principio, por acogerme como a una más desde el primer momento: a David por ser mi guía en los inicios (sin duda alguna tú me enseñaste a trabajar en el laboratorio); a Miguel por las tardes de temazos y los refranes en Valencià; a Celia, por enseñarme a contar células, calcular mois y hacer qPCRs, y por seguir interesándote por mis avances cuando ya habías dejado el lab; a Amparo, por estar siempre ahí para escuchar, charrar y echar una mano, gracias también por enseñarme a trabajar con animales, desde sangrar conejos hasta muestrear anguilas; y a Eva, por tener siempre respuesta a todas, todas mis dudas. También a los compañeros que han ido llegando después, en especial a Paco, desde el máster sufriendo (y ahogando las penas en cerveza) juntos; y a Vero, mi primera estudiante y una gran ayuda durante dos años (todavía te echo de menos). También a Duarte (por el mes de agosto que pasamos juntos trabajando con Chung-Te), Eli, Amparo Jr., Ana, Omar, Carla Jr., Adrián, Sara, Héctor… En definitiva, a todos los que habéis pasado por el lab, porque todos habéis dejado vuestra huella y me habéis ayudado en algún momento. También a Alba, aunque no de lab sí compañera de despacho.

A los compañeros de departamento que me han ayudado, especialmente a Eduardo (por el hielo seco y las medidas de oxígeno) y a Chelo, por ayudarme en los primeros años de docencia.

A Rodolfo, por proporcionarme las anguilas y a Lucas y Silvia por su colaboración en las infecciones realizadas en planta de acuarios. También al servicio de secuenciación, en especial a Amparo, por resolver las dudas que me han surgido a lo largo de los años y por prestarme reactivos cuando ha sido necesario.

Gracias al grupo de fisiología de peces de la UAB, especialmente a Lluis Tort por permitirme pasar tres meses en su grupo y por supuesto a Felipe y Eva, que no solo me enseñasteis a trabajar con las muestras y datos de microarray sino que me hicisteis sentir como una más cada día que pasé en el laboratorio/despacho. Gracias a los dos también por haber estado siempre dispuestos a un Skype cuando he necesitado reanalizar algunos datos. De la estancia en Barcelona gracias también a mi prima Julia, por tan generosamente acogerme en tu casa y regalarme tantas risas y buenos recuerdos que me llevo conmigo.

My second stage was in Blokesch's Lab in EPFL (Switzerland), so thank you very much Melanie for letting me stay with you and your wonderful group for three months and learn so many things. I really appreciate that you treated me as a member of your group inviting me to both lab and personal meetings. I would also like to thank all the lab mates I met there for the kindly personal trait they gave me not only in the lab, but also in the coffee breaks, lunch time, beer time, dinner time, cinema time… Thank you all for made me feel like anyone else in the group. I'm especially grateful to Audrey and Natàlia for finding me some space in the P2.2 and teaching me everything I know about amoeba and confocal microscopy; and Leonardo for practicing your Spanish with me and giving me a break of English speaking. Thank you also to the FSLE building mates, especially to Olivier, for sharing the earliest and darkest breakfasts I have had in my live, and to Giovanni for being the light in that depressing building and make my days during the last month in Lausanne (you are soooo Italian!). Probably we will NEVER EVER meet again but I wish you all the best guys.

A mis amigas, Lucía, Bea, Miriam, Rocío y Ana. Porque aunque cada vez nos juntemos menos (por la tesis y otras circunstancias) seguimos estando ahí las unas para las otras.

A mi grupo paranormaaaaal (¿de verdad vamos a dejar esto como nombre de grupo para la eternidad?). Cris, Vicent, Víctor (estoy absolutamente convencida de que nadie me ha preguntado tanto "¿CÓMO VA LA TESIS?" como tú) y Álvaro, porque aunque penséis que soy una asesina de anguilas, con vosotros siempre he podido desconectar de la tesis. A Víctor también le agradezco las clases de Python (quizá no te lo creas, pero me han ayudado a entender muchas cosas).

A los compañeros de carrera que acabaron siendo amigos, Cris (otra vez), Edgar, David y Elena (aunque nos veamos poquísimo). También a Juan y los compañeros de excursiones, que con el tiempo se han cambiado por horchatas y chocolates.

A TODA mi familia (¡y somos muchos!), al Gen Hernández, a los Cabañero y a los postizos (los García-Navarro y Martínez-Cantos). Gracias a todos por formar parte de mi vida durante tantos años. Mención especial a mi tía Ana (una mezcla entre segunda madre y hermana mayor), gracias por fundar la casa del Joe y la beca Hernández, que me dieron cobijo en Valencia durante 6 años, por los viajes, las clases de estadística, de flamenco… gracias por todo. Y a Marta, por los años (y locuras) compartidos en la casa del Joe, y especialmente por ocuparse del diseño de la portada de esta tesis. También a los peludos de 4 patas de la familia que dan tanto sin pedir nada, los que están y los que ya no están, pero que nos han alegrado la vida compartiendo paseos y siestas con nosotros.

A mis padres, por haber echo de mí la persona que soy, por enseñarme que la constancia y el esfuerzo son las mejores armas para luchar y conseguir mis objetivos, por animarme y apoyarme (sentimental y económicamente) en todas mis decisiones, y en los últimos años, por preocuparos de si se morían o no las anguilas y/o "los bichos". Sin vosotros no habría llegado hasta aquí. Gracias también por haberme dado la mejor amiga que podría tener, mi hermana, porque pese a ser tan distintas (o no) no se me ocurre nadie mejor con quien compartir momentos (buenos y malos) en la vida, ya sea juntas en casa o en la distancia.

A Álvaro, por cargar conmigo la peor parte de esta tesis, por aguantar mi interminable verborrea sobre microarrays, qPCRs, genes y mutantes (sobre todo los días en que llegaba a casa cabreada), aceptando también las estancias que nos han separado a temporadas, los domingos de laboratorio, los fines de semana de escritura de tesis… En definitiva, gracias por cruzarte en mi vida y quedarte en ella. Gracias por convertirte en mi mejor amigo y mi compañero en la vida. Te quiero.

RESUMEN

Vibrio vulnificus es un patógeno bacteriano que habita en ecosistemas costeros de salinidades intermedias localizados en zonas del planeta templadas y cálidas. Esta especie es una de las más sensibles al calentamiento global habiendo experimentado una expansión en su distribución geográfica hacia zonas costeras de aguas frías como las que rodean países tan próximos al círculo polar como como Noruega y Groenlandia, de las que se aísla en las épocas cálidas del año. En su medio natural la bacteria puede encontrarse en un estado metabólico inactivo, conocido como estado VBNC (*viable but not culturable*) que es inducido en circunstancias ambientales adversas (temperaturas por debajo de 10ºC, salinidad menor al 0,5%, carencia de nutrientes…), o metabólicamente activo bien como forma libre natatoria (células planctónicas) o como forma sésil, normalmente asociada a superficies mucosales (especialmente las mucosas externas e internas de los peces) formando biofilms.

Se trata de un patógeno multi-hospedador y zoonótico, capaz de causar una gran variedad de infecciones conocidas como vibriosis animal y humana. La vibriosis animal se manifiesta en forma de brotes o epizootias de elevada mortalidad en piscifactorías de anguila, su hospedador más susceptible. La bacteria infecta a través del agua y se asocia sobre todo a las mucosas del epitelio de las branquias desde donde accede a sangre, prolifera, se distribuye a los órganos internos y causa muerte por septicemia hemorrágica en menos de 24 h, siempre y cuando la temperatura ambiental esté por encima de 25ºC. La vibriosis humana cursa de dos formas principales relacionadas con la ruta de infección que puede ser oral o por contacto. En el primer caso el patógeno se ingiere con marisco o pescado crudo, coloniza el intestino y causa gastroenteritis que puede desde resolverse sin medicación a requerir hospitalización. En el segundo caso, la bacteria suele infectar heridas preexistentes por contacto con agua de mar o peces portadores o enfermos y causar graves infecciones manifestadas como fascitis necrotizante y celulitis que requieren hospitalización, desbridamiento e, incluso, la amputación del miembro infectado. En todos los casos, si el paciente es un paciente de riesgo, la vibriosis humana puede derivar en septicemia y muerte del paciente también en menos de 24 h. De hecho, la OMS y la FAO consideran que es el patógeno ligado a alimentos que causa la mayor mortandad en humanos a escala global. Estudios epidemiológicos demuestran que el principal factor de riesgo en humanos es una elevada concentración de hierro en sangre causada por distintas patologías subyacentes como hepatitis, cirrosis, cáncer de hígado, hemocromatosis

etc. Resulta interesante que, en el caso de las anguilas, la bacteria pueda causar muerte por septicemia incluso en anguilas sanas.

La especie incluye cepas avirulentas y virulentas para múltiples hospedadores por lo que es genéticamente muy variable. Además, es el único *Vibrio* relacionado con casos de zoonosis, en particular, con la transmisión de vibriosis animal a humanos por contacto de piscicultores con anguilas enfermas de piscifactoría. Clásicamente la especie se dividió en biotipos pero, este sistema de clasificación se está abandonando por resultar incompleto y se está sustituyendo por un sistema de clasificación filogenético. Recientemente, se ha propuesto que la especie se divida en 5 linajes filogenéticos y una patovariedad definida por la posesión de un plásmido de virulencia que confiere capacidad para infectar peces y que puede transmitirse por conjugación asociado a un plásmido conjugativo. Para esta patovariedad se propuso el nombre de *piscis*. De acuerdo con este sistema, las cepas zoonóticas constituyen un complejo clonal distribuido por todo el mundo que pertenece al linaje 2 y a la patovariedad *piscis*. También se ha demostrado que el plásmido de virulencia o una parte del mismo, se ha transmitido recientemente a otros linajes, distintos del linaje 2, y a otras especies de patógenos acuáticos como *Aeromonas salmonicida, V. harveyi* y *Photobacterium damselae.*

De todos los factores de virulencia que produce *V. vulnificus* el único que está claramente relacionado con septicemia y muerte es una toxina denominada RtxA1. Esta toxina presenta un módulo externo conservado con secuencias repetidas ricas en glicina que flanquean un módulo interno variable divido en dominios funcionales distintos. Por el dominio externo la toxina se une a la membrana eucariótica y forma un poro permitiendo la translocación del módulo interno, uno de cuyos dominios tiene actividad endoproteolítica, se activa en presencia de inositol 6 fosfato celular y procesa el módulo interno separando los distintos dominios que son los responsables de la actividad citotóxica de la toxina. De momento se han descrito 8 tipos diferentes de toxinas RtxA1. La toxina que producen las cepas del complejo clonal está involucrada en septicemia como así lo han demostrado experimentos realizados con mutantes en anguilas y ratones. Además, se ha demostrado la relación de la toxina con una tormenta de citoquinas temprana en ratones, tormenta que podría explicar la rápida muerte de estos animales y de los humanos por sepsis.

Por tanto, *V. vulnificus* es un patógeno septicémico multi-hospedador que se encuentra en expansión debido a que el calentamiento global favorece las condiciones ambientales óptimas para su proliferación en el ambiente. El estudio de este patógeno es de elevado interés en salud pública, ya que no sólo es responsable de la mayoría de muertes causadas por

infecciones alimentarias a nivel mundial, sino que también es el causante de brotes de elevada mortalidad en piscifactorías que suponen importantes pérdidas económicas para el sector. Precisamente, las piscifactorías constituyen uno de los principales reservorios de este patógeno, favoreciendo su proliferación y eventos de transferencia genética horizontales esenciales en la evolución de la especie y la emergencia de nuevas variantes virulentas.

El primer objetivo general de la presente tesis fue dilucidar los mecanismos de virulencia de este patógeno que le permiten causar septicemia en hospedadores tan distintos como humanos y peces. Puesto que la temperatura ambiental y la concentración de hierro son determinantes a la hora de producirse la septicemia en animales, en el primer caso, y en el hombre, en el segundo, nos hemos planteado como **segundo objetivo general** averiguar el papel que el hierro y la temperatura ambiental tienen como señales que activan la supervivencia de la bacteria dentro y fuera de su hospedador animal. Finalmente, el desenlace de una infección no depende solo de los mecanismos de virulencia específicos del patógeno sino también de la capacidad del hospedador de modular una respuesta inmunitaria adecuada y eliminarlo. Por tanto, para comprender de forma global la relación hospedador-patógeno se deben determinar no solo los mecanismos de virulencia utilizados por el patógeno sino también la estrategia de defensa desplegada por el hospedador durante la infección. En consecuencia, **el tercer objetivo general** fue determinar la respuesta inmunitaria del principal hospedador animal de *V. vulnificus*, la anguila, durante la infección usando distintos tipos de aproximaciones *ex vivo* e *in vivo*. Para conseguir estos objetivos generales, hemos utilizado una cepa representativa del complejo clonal zoonótico (cepa CECT4999 o R99) de genoma secuenciado y anotado y hemos usado modelos de septicemia *in vitro*, *ex vivo* e *in vivo*. Hemos analizado la transcriptómica global de patógeno y hospedador aplicando tecnologías de hibridación con microarrays específicamente diseñados para la cepa problema y para la anguila, en particular, para la detección de los genes de su sistema inmunitario, así como RNAseq y dual-RNAseq, modalidad que permite analizar a partir de la misma muestra, los genes de patógeno y hospedador que son transcritos. Los resultados transcriptómicos pusieron de manifiesto procesos y genes relevantes en la infección que fueron validados aplicando técnicas de mutagénesis dirigida hacia genes concretos del patógeno y usando la cepa parental y sus mutantes en ensayos fenotípicos específicamente diseñados para cada uno de los procesos detectados.

En función de los distintos objetivos, hemos realizado los siguientes experimentos:

1) Para conocer la influencia de la concentración de hierro (ambiental o presente en la sangre del hospedador) en el ciclo de vida de esta bacteria, hemos crecido la cepa parental y un mutante deficiente en el regulador Fur en un medio mínimo en presencia y ausencia de hierro y analizado y comparado los transcriptomas.

2) Para conocer el papel de la temperatura ambiental (del agua o del hospedador) en las estrategias de supervivencia y virulencia de esta bacteria, hemos crecido la cepa parental a temperaturas a las cuales no es virulenta y temperaturas a las cuales es virulenta presentando distintos grados de virulencia y analizado y comparado los transcriptomas.

3) Para comprender los mecanismos que esta especie utiliza para causar septicemia en hospedadores evolutivamente tan distantes como el hombre y la anguila, hemos infectado suero y sangre artificial de anguila y humano, sano y con sobrecarga de hierro y analizado y comparado los transcriptomas.

4) Para conocer cómo responde el hospedador a la infección con *V. vulnificus* hemos realizado experimentos *ex vivo* (sangre artificial; dual RNAseq) e *in vivo* (anguilas infectadas por baño; hibridación con microarrays) y determinado el transcriptoma del hospedador en ambos casos.

5) Para averiguar si la toxina RtxA1 está involucrada en muerte por sepsis al desencadenar una tormenta de citoquinas temprana hemos realizado experimentos *in vivo* infectando células con la cepa parental y una mutante deficiente en la toxina y analizado y comparado el transcriptoma de los animales en distintos compartimentos celulares y a lo largo del tiempo.

La unificación del conjunto de resultados obtenidos en este trabajo nos ha permitido construir una serie de modelos que intentar explicar el ciclo de vida de *V. vulnificus* dentro y fuera de sus principales hospedadores, así como dar respuesta a una serie de incógnitas respecto a la vibriosis en anguila y humanos. Los resultados más relevantes se encuentran resumidos a continuación.

La concentración de hierro y la temperatura ambientales controlan la supervivencia de *V. vulnificus* dentro y fuera de sus hospedadores. Hemos determinado el regulon Fur (Ferric uptake regulator), el estimulón hierro y el estimulón temperatura, definidos como el conjunto de genes del patógeno cuya expresión cambia en función de la presencia o ausencia del regulador Fur, la concentración de hierro en el medio, y la temperatura ambiental, respectivamente. Nuestros resultados demuestran que el hierro es una de las principales señales a las que responde esta bacteria, principalmente a través del regulador global Fur,

capaz de desencadenar una estrategia de supervivencia adaptada al ambiente (medio acuático o sangre del hospedador). Así, cuando el hierro es escaso en el ambiente *V. vulnificus* forma biofilms como estrategia de supervivencia, mientras que cuando el hierro es abundante en el agua (condiciones que se dan en piscifactorías) la bacteria se dispersa de los biofilms y cambia a un modo de vida libre, formando células capsuladas, móviles (gracias a la producción del flagelo) y altamente infectivas. Además, la temperatura también afecta a la supervivencia de *V. vulnificus* en el ambiente y a su virulencia, puesto que es incapaz de infectar a temperaturas inferiores a 20ºC mientras que es altamente infectivo a temperaturas por encima de los 25ºC, siendo 28ºC la temperatura a la que se producen brotes de elevada mortalidad en peces. Nuestros resultados contribuyen a explicar la dependencia entre la temperatura ambiental y la virulencia de este patógeno, ya que muestran que gran parte de las actividades bacterianas que permiten la colonización de los hospedadores (incluidos humanos) como son la movilidad, la quimiotaxis y la secreción de proteasas, así como la producción de una envuelta protectora frente a las defensas del hospedador, aumentan con un aumento en la temperatura y por tanto conllevan un aumento en la probabilidad de infección.

***V. vulnificus* expresa un fenotipo virulento adaptado a hospedador y dependiente de hierro.** Hemos demostrado que *V. vulnificus* no solo responde a los niveles de hierro exógenos sino que, además, los cambia, como consecuencia de su crecimiento en sangre durante la septicemia. Este cambio lo produce probablemente al lisar los glóbulos rojos y liberar hemoglobina. De hecho, 1 de cada 2 genes detectados como diferencialmente expresados en suero/sangre pertenecen al estimulón hierro y/ al regulón Fur). En sangre, el patógeno responde al ataque de señales secretadas por parte del hospedador (por ejemplo, formas reactivas del oxígeno [ROS] y el óxido nítrico por parte de las células del sistema inmunitario) transcribiendo genes para la inactivación de estas señales y para la reparación de la membrana. Además, en la sangre de sus hospedadores la bacteria sobreexpresa una serie de genes destinados a activar un metabolismo anaeróbico que en la anguila depende de la oxidación de compuestos del nitrógeno, mediante respiración de nitratos/nitritos, mientras que en humanos con niveles elevados de hierro en sangre (pacientes de riesgo) depende de la oxidación de compuestos derivados del glicógeno mediante respiración anaeróbica de fumarato. De acuerdo a los resultados transcriptómicos obtenidos en esta tesis y apoyados en estudios previos, proponemos que la señal que desencadena la activación del metabolismo anaeróbico en sangre se transmitiría a través de PspABC (sistema inducido por el estrés generado en la membrana bacteriana) en ambos hospedadores y, en el caso de los humanos, además, parece depender del nivel de catecolaminas detectado a través de QseBC. Fur

también juega un papel central en determinar la fuente de nutrientes preferida por la bacteria bien como apo-Fur, a través de Lrp en anguila, bien como holo-Fur, a través de rutas de señalización desconocidas, en humanos. Una vez en la sangre de sus hospedadores, *V. vulnificus* expresa un fenotipo tóxico adaptado a hospedador, basado en la producción de las toxinas VvhA y RtxA1 y una envoltura protectora que le permiten resistir la acción del complemento del hospedador, multiplicarse de forma eficaz y producir septicemia. Los resultados transcriptómicos sugieren que la concentración de hierro y Fur (a través de otros reguladores transcripcionales globales como SmcR y HlyU) juegan un papel significativo en la activación de VvhA y RtxA1 y, por tanto, en la expresión del fenotipo tóxico. Para confirmar estos resultados transcriptómicos hemos realizado experimentos fenotípicos adicionales cuyos resultados sugieren que en el caso de los pacientes humanos de riesgo, ambas toxinas actúan de forma aditiva desde el principio de la infección, mientras que en anguila actúan de forma secuencial, produciéndose primero la hemolisina VvhA, que genera un cambio en la concentración de hierro en sangre al lisar eritrocitos e induce la activación de $RtxA_3$ que actúa más tardíamente en la infección. La envoltura protectora óptima (en términos de producción de cápsula y antígeno O del lipopolisacárido) frente al sistema inmunitario producida por *V. vulnificus* en la sangre de sus hospedadores susceptibles es un proceso regulado no solo por hierro y Fur, sino también por la temperatura. Así, la bacteria produce una envoltura rica en cápsula sólo en la sangre de humanos con niveles elevados de hierro en sangre que la hace resistente al complemento y la fagocitosis. Este resultado demuestra que la cápsula es absolutamente esencial para resistir y sobrevivir en sangre humana y explica por qué no hay casos de septicemia entre pacientes sanos ya que al no producir cápsula, la bacteria muere en la sangre de estos pacientes. En la sangre de anguila, restrictiva en hierro ya que éste se encuentra unido a transferrina, *V. vulnificus* produce una envoltura rica en antígeno O, pero sólo a temperaturas por encima de 25ºC y de manera óptima a 28ºC (temperatura del agua durante brotes de vibriosis que causan alta mortalidad en piscifactorías). Además, en sangre de anguila la bacteria produce dos proteínas de membrana externa reguladas por hierro y temperatura (una de ellas), una que actúa como receptor específico para la transferrina de peces (Ftbp) y otra que protege a la bacteria del complemento y la fagocitosis (Fpcrp). Ambas proteínas constituyen un "kit de supervivencia en sangre" que está codificado en el plásmido de virulencia y que permite a la bacteria multiplicarse de forma eficaz en la sangre de peces sanos. El kit ha sido transferido entre linajes dentro de la especie y a otros patógenos de peces lo que confirma el papel de la transferencia genética horizontal en la emergencia de nuevos patógenos en el entorno de las piscifactorías.

El T6SS (sistema de secreción de tipo IV), a través de la toxina VgrG, de *V. vulnificus* puede estar implicado en la supervivencia y defensa de la bacteria frente a la fagocitosis y al ataque por las células de la anguila. Nuestros resultados transcriptómicos revelan una sobreexpresión de *vgrG* en presencia de células rojas (CR) de la sangre de anguila, sólo cuando estas son lisadas. Por tanto, la producción de esta toxina podría estar regulada por hierro y estar implicada en la defensa frente al ataque de células eucariotas. Experimentos fenotípicos adicionales sugieren que la toxina VgrG, proteína efectora del T6SS, sí está regulada por hierro y participa en la supervivencia de *V. vulnificus* en su medio natural otorgándole resistencia frente a sus predadores naturales (amebas) y en el interior de sus hospedadores al estar implicado en citotoxicidad a CR de la sangre de anguila. Estos resultados deben considerarse preliminares, y requieren estudios en profundidad para dilucidar el mecanismo molecular que activa la producción y la acción de esta toxina.

En la respuesta inmunitaria de la anguila frente a *V. vulnificus* participan tanto CR como células blancas (CB) sanguíneas. Combinando experimentos *ex vivo* en sangre artificial de anguila, con infecciones de animales *in vivo*, hemos obtenido resultados interesantes sobre la respuesta inmunitaria de la anguila durante la interacción hospedador-patógeno. Así, por primera vez, hemos descrito que las CR nucleadas, como es el caso de las de los peces teleósteos (entre ellos, la anguila) participan en la respuesta inmunitaria frente a patógenos bacterianos septicémicos como *V. vulnificus*. Los resultados obtenidos *ex vivo* aportan múltiples evidencias transcriptómicas de la acción de la toxina RtxA1 sobre las células de la sangre (tanto CR como CB) en forma de genes regulados hacia arriba para reparación del citoesqueleto celular (respuesta a la acción del dominio entrecruzador de actina [ACD] de la toxina), activación del tráfico endosomal (achacable al dominio alfa-beta hidrolasa [ABH] de la toxina) y activación de la muerte celular por apoptosis (por la acción del dominio MCF de la toxina). Además, nuestros resultados muestran que las CR, que son las células más abundantes en la sangre de anguila (10^9 CR/ml, aprox. 1000 CR por cada CB), son transcripcionalmente activas y actúan como células inmunitarias: tras la infección con el patógeno, regularon hacia arriba múltiples genes relacionados con reconocimiento, procesamiento y presentación de antígenos, producción de TNFa y diálogo cruzado con otras células inmunitarias, principalmente linfocitos T y, probablemente, plaquetas y células endoteliales. Nuestros resultados también revelan que las CR pueden actuar como células efectoras, ya que activan la transcripción de genes para galectina3, prostaglandinas, reciclaje de transferrina y coagulación de la sangre (incluida la fibronectina). Entre los diferentes genes relacionados con la conversación cruzada con otras células inmunitarias, destacamos un gen que codifica un tipo

específico de TNFa que responde al LPS (*litnfa*). La concentración de CR en la sangre de la anguila es tan alta que, probablemente, pequeñas cantidades de LITNFa podrían conllevar cambios importantes en la producción de citocinas y quimiocinas. De hecho, entre los transcritos más sobreexpresados hemos observado numerosos genes relacionados con la respuesta a TNFa. Las CB por su parte actúan contra las bacterias activando la transcripción de genes para la producción de ROS y, probablemente, péptidos microcidas, así como de genes que les permiten actuar como células presentadoras de antígeno profesionales (activación de la transcripción de múltiples genes para TLRs, citoquinas y sus receptores, receptores de inmunoglobulinas, etc.), transductores de señal y múltiples retrotransposones. Un resultado especialmente interesante, es la activación de la transcripción del gen que codifica Il17c, una citocina que actúa de manera coordinada con Il6 activando la producción de las mucinas secretadas (Muc5B, la transcripción de cuyo gen también se encuentra activada en CB según nuestros resultados) por las células epiteliales y mucosales. El papel de estas mucinas es atrapar bacterias colaborando en su eliminación de los tejidos de la mucosa, lo que sugiere una conexión entre la inmunidad sistémica con la mucosal. En conjunto, este resultado sugiere que los leucocitos estimulados por el patógeno podrían migrar a los tejidos de la mucosa y secretar directamente mucinas contra el patógeno, hipótesis que quedaría por demostrar. Los resultados obtenidos a partir de experimentos *in vivo* son, si cabe, más interesantes ya que, además de confirmar parte de los resultados obtenido *ex vivo*, sugieren que la anguila responde a la infección por *V. vulnificus* generando una fuerte y rápida respuesta de tipo inflamatoria activada sobre todo por las CR, que parecen ser la principal diana de la toxina RtxA1 *in vivo*. Este hecho constituye un resultado sumamente novedoso y está apoyado por la regulación hacia arriba de miles de genes por parte de las CR en contraposición con cientos de genes por parte de las CB. Además, tanto CR como CB activan una respuesta atípica, en parte debida a la activación de mecanismos de defensa anti-vírica, en respuesta al patógeno que incluyen un RNA de interferencia (RNAi) y que es el gen que se detecta en sangre como el más fuertemente activado a las 12 h de infección. Esta respuesta anti-vírica resulta sorprendente dado que *V. vulnificus* es un patógeno extracelular sin existencia intracelular como la que se requeriría para activar este tipo de respuesta.

La toxina RtxA1 está implicada en la generación de un choque séptico que causa la muerte de las anguilas infectadas por *V. vulnificus*. Comparando los datos transcriptómicos obtenidos en sangre de anguilas infectadas (tanto *ex vivo* como *in vivo*) con la cepa parental del complejo clonal zoónotico de *V. vulnificus* y con los de las infectadas con su mutante deficiente en la toxina RtxA1, hemos podido relacionar la producción de la toxina con una

respuesta temprana de tipo inflamatorio que es sobre todo evidente en los ensayos realizados *in vivo*, lo que relaciona la toxina con muerte por choque tóxico debida a una tormenta temprana de citoquinas, proceso que de manera similar ha sido previamente descrito en ratón. Es más, los resultados obtenidos a partir de los datos de los experimentos *ex vivo* relacionan la toxina RtxA1 además con una tormenta de retrotransposones a nivel celular, fenómeno que se ha descrito muy recientemente asociado a enfermedades humanas no infecciosas y merece un estudio en profundidad. Además, hemos encontrado evidencias de que la respuesta inflamatoria podría relacionarse con un daño masivo seguido de una respuesta transcriptómica muy elevada por parte de las CR, siendo éstas las células de la sangre transcripcionalmente más activas *in vivo*. Finalmente, hemos encontrado evidencias que permiten asociar la toxina con la activación de una respuesta anti-viral *in vivo*, probablemente mediadas por la liberación de RNAi y por el silenciamiento de microRNAs (miRNA-142a) involucrados en la regulación de respuesta inmunitaria protectora, y por tanto en la muerte de la anguila mediada por la toxina.

En resumen, *V. vulnificus* es un patógeno versátil que ha desarrollado múltiples estrategias para sobrevivir en ambientes tan dispares como el agua, las mucosas, la sangre humana, la sangre de anguila, etc. Esta capacidad de adaptación al ambiente, le permite expresar un fenotipo virulento adaptado al hospedador que es dependiente de hierro y que es acentuado por la temperatura, causando muerte por septicemia en hospedadores tan distintos como humanos y peces. El fenotipo virulento está basado en la actividad de las toxinas VvhA y RtxA1 y en la producción de una envoltura protectora generalista pero dependiente de hospedador. En el caso de pacientes humanos de riesgo, esta envoltura está enriquecida en cápsula, mientras que en anguilas está enriquecida en antígeno O y contiene dos proteínas de membrana externa codificadas en el plásmido de virulencia (Fpcrp y Ftbp) que constituyen un "kit de supervivencia en sangre" que confiere capacidad para resistir específicamente la inmunidad innata de los peces, explicando en parte por qué el patógeno es tan virulento en anguilas sanas. Por otro lado, mediante el estudio de la interacción hospedador-patógeno entre esta bacteria y su principal hospedador, la anguila, hemos puesto de manifiesto que tanto las CB como las CR de la sangre de peces teleósteos responden a la infección causada por patógenos bacterianos septicémicos, y que la toxina RtxA1 de *V. vulnificus* está implicada en la generación de una respuesta atípica e intracelular en fases muy tempranas de la infección. Esta respuesta está ligada a una tormenta de citoquinas y/o retrotransposones directamente relacionada con la muerte de los animales.

El conjunto del trabajo realizado en esta tesis aporta gran cantidad de datos transcriptómicos obtenidos del estudio de la relación hospedador-patógeno entre *V. vulnificus* y su hospedador principal, la anguila, abriendo la puerta a nuevas hipótesis para futuras proyectos como el estudio de nuevos factores de virulencia del patógeno (i.e., activación de metabolismo anaeróbico en sangre del hospedador, T6SS) o el desarrollo de nuevas herramientas de inmunoterapia (i.e., miR-142a) para prevenir brotes de *V. vulnificus* en piscifactorías, que constituyen el mayor reservorio para este patógeno y suponen un riesgo para la acuicultura y la salud pública.

ABSTRACT

Vibrio vulnificus is a worldwide distributed pathogen traditionally isolated from temperate aquatic ecosystems, whose geographical distribution is currently spreading due to global warming. The species is genetically variable and only the strains that belong to the zoonotic clonal-complex (serovar E within pathovar *piscis* [formerly biotype 2]) are able to cause disease, with multiple clinical manifestations collectively known as vibriosis, in humans and fishes. The most severe form of vibriosis is hemorrhagic septicemia that, in case of eels it affects healthy animals, while in case of humans mainly affects susceptible patients (those with high levels of free iron in blood [iron-overloaded humans] due to different underlying pathologies). In both cases, septicemia is a very rapid disease that leads to death by sepsis in less than 48 h.

The main **aim** of this thesis is to gain insights into the pathogen's virulence mechanisms that allow it to cause septicemia in hosts as evolutionary distant as human and fish. To this end, we have selected a representative strain of the zoonotic clonal-complex and applied a combination of transcriptomic and single gene approaches using *in vitro* and *ex vivo* models of septicemia to understand how iron and temperature (either outside [water] or inside its host) influence *V. vulnificus* virulence. First, we have analyzed how Fur (Ferric uptake regulator) mediated the global bacterial response to iron (both iron excess and iron starvation conditions). As a result, we have described the **iron stimulon** and **Fur regulon** of *V. vulnificus* and demonstrated that iron, not always throw Fur, controls the entire life cycle of this pathogen, from its survival in the marine environment (including motility and chemotaxis) to its survival in the blood of their hosts (including host-specific mechanisms of resistance to innate immunity). Second, we have described a **host-adapted virulent phenotype** that *V. vulnificus* expresses in the blood of its main susceptible hosts (iron-overloaded humans and healthy eels) by changing metabolism preferences from aerobic to anaerobic (based on amino or glycogen compounds utilization in eels or human blood, respectively) and combining a host-specific protective envelope (capsule enriched for humans and O-antigen enriched for eels) with the common expression of two toxins (VvhA and $RtxA1_3$). Moreover, the zoonotic strains have bypassed the iron requirement of the species for fish infection due to the acquisition of two iron-regulated outer membrane proteins (Ftbp and Fpcrp) involved in resistance to fish innate immunity: Ftbp conferring ability to specifically bind to fish transferrin in order to acquire iron from it; and Fpcrp conferring resistance to fish complement and phagocytosis.

Finally, **temperature** contributes to the host-adapted virulent phenotype, since an increase in temperature (from environmental [around 20ºC] to infective [28ºC for fish and 37ºC for humans] temperatures) entails bacterium fitness which leads to an optimal physiological state that adapts the pathogen for the subsequent host invasion and survival in blood. This, in combination with exogenous iron sources, increases the expression of virulence factors in a host-specific manner.

Given that the outcome of an infection depends not only on the virulent mechanisms expressed by the pathogen but also on the host ability to modulate a **suitable immune response** to eliminate the pathogen, we have also performed *ex vivo* and *in vivo* experiments in order to gain insights into the eel immune response against *V. vulnificus* as well as to understand the host-pathogen relationship. Analyzing the immune transcriptome expressed in eel blood during vibriosis we have proved that eel **RBC (red blood cells)**, as nucleated cells, are transcriptionally active and involved in the immune response against bacterial pathogens not only as antigen recognition, processing and presentation cells but also with ability to produce effectors (i.e., TNF, cytokines, lectins and prostaglandins). Finally, we have also analyzed the immune transcriptome in eel blood during vibriosis caused by a *V. vulnificus* mutant strain lacking $RtxA1_3$ (a strain that cause septicemia but do not kill the animals) and found strong evidence for an early **intracellular** and **atypical immune response** induced by $RtxA1_3$. This atypical response is mainly carried out by RBC and is based on a **rapid cytokine/retrotransposon storm, mediated by a systemic RNAi and an anti-silencing protein,** which by unknown mechanisms could lead to **the inactivation of miRNA-142a** resulting in an exacerbated immune response which eventually causes eel death.

In conclusion, *V. vulnificus* has the ability to express an iron-dependent and host-adapted virulent phenotype based on of a generalist but host-dependent protective envelope plus the common overexpression of $RtxA1_3$ and VvhA. In the case of humans, the envelope is enriched in the capsule, while in eels it contains Fpcrp and Ftbp that together confrom a “survival in fish blood kit” which confers specific ability to resist fish innate immunity. Moreover, host-pathogen interaction studies in *V. vulnificus* and its main host, the eel, have opened the door for new hypothesis and future projects, such as the study of new putative bacterial virulence factors (i.e., T6SS) and the development of new immunotherapeutic tools (i.e., miR-142a) to prevent *V. vulnificus* outbreaks in fish farms, the major reservoir of this pathogen.

ABBREVIATIONS

- $Fe_{(D)}$	supplemented with 100 µM 2,2'-bipyridyl
+Fe	supplemented with 100 µM $FeCl_3$
+Tf	supplemented with 10 µM human apotransferrin
A	Agar
ABH	alpha/beta hydrolase domain
Abs_x	Absorbance at x nm
ACD	Actin cross-linking domain
B	Blood
BALB/c	Bagg Albino
BCA	Bicinchoninic acid assay
Bt	Biotype
CB	chemotaxis buffer
cDNA	complementary DNA
CFU	Colony forming units
CM9	M9 broth supplemented with 0.2% casamino acids
CPD	Cysteine protease domain
Crh	Chromosome
Cy3	cyanide 3
DEGs	Differentially expressed genes
DUF1	Domain with unknown function
ECPs	Extracellular products
EDTA	Ethylenediaminetetraacetic acid
ES	Eel serum
FC	Fold change
Fpcrp	Fish phagocytosis and complement resistance protein
Ftbp	Fish transferrin binding protein
Fur	Ferric uptake regulator
GEO	Gene Expression Omnibus
HMW	high molecular weight
HRP	Horseradish Peroxidase
HS	Human serum
HS+Fe	Iron-overloaded human serum (HS supplemented with 100 µM $FeCl_3$)
i.p.	intra-peritoneal
IFN	Interferon
Ig	Immunoglobulin
Il	Interleukin
InsP6	Inositol hexakisphosphate
IPTG	Isopropyl β-D-1-thiogalactopyranoside
IROMP	iron regulated outer membrane protein

IUCN	International Union for Conservation of Nature
L	Lineage
LB	Luria Bertani broth
LC–MS/MS	liquid chromatography and tandem mass spectrometry
LD_{50}	Lethal dose 50
LPS	Lipopolysaccharide
MA	Motility agar
MARTX	Multifuctional autoprocessing repeat in toxin
Mb	Mega base
MCF	"makes caterpillars floppy"-like domain
MIC	Minimal inhibitory concentration
miRNA	microRNA
MMW	medium molecular weight
moi	multiplicity of infection
mRNA	messenger RNA
MS22	Tricaine methanesulfonate
MSWYE	Marine seawater supplemented with yeast extract
NLR	Nod-like receptor
NO	Nitric oxide
NT	Non tested
nt	nucleotides
OM	Outer membrane
OMP	Outer membrane protein
ORF	Open reading frame
PAMP	Pathogen-associated molecular pattern
PBS	Phosphate buffered saline
PCA	Principal component analysis
pR99	R99 strain pVvBt2
PRR	Patter-recognition receptor
pv.	pathovar
PVDF	Polyvinylidene difluoride
pVvBt2	*V. vulnificus* pv. *piscis* virulence plasmid
R99	*V. vulnificus* pv. *piscis* SerE wild-type representative strain (CECT4999 strain)
RBC	Red blood cells
RID	Rho GTPase inhibitor domain
RIN	RNA integrity number
RNAseq	RNA sequencing
ROS	Reactive oxygen species
rRNA	ribosomal RNA
RRSP	Ras/Rap1 specific emdopeptidase
RT-qPCR	Reverse-transcription quanitative polymerase chain reaction
RTX	repeat in toxin
SCSIE	Servei Central de Suport a la Investigació (Experimental Central Service for Experimental Research)
SDC	sodium deoxicolate

SDS-PAGE	sodium dodecyl sulfate- Polyacrilamide gel electrophoresis
Ser	Serotype
SI	Survival index
T6SS	Type 6 secretion system
TLR	Toll-like receptor
TNF	Tumor necrosis factor
tRNA	transfer RNA
TSA	Tryptone soy agar
VBNC	Viable but nonculturable
vs	versus
WBC	White blood cells

INDEX

INTRODUCTION

1. The pathogen: *Vibrio vulnificus*

The genus *Vibrio* comprises approximately 150 aquatic, gramnegative, oxidase-positive, facultative anaerobic and rod-shaped bacterial species, of which around a dozen have been demonstrated to cause infection in humans and/or fish (http://www.bacterio.net/vibrio.html). Together with *V. cholerae*, *V. vulnificus* is one of the major species within the genus *Vibrio*.

1.1. Taxonomy and phylogeny

V. vulnificus was first defined as a species in 1979 from a series of halophilic, lactose- and indole-positive *Vibrio* isolates, both from clinical and environmental samples, reported in the United States (Farmer, 1979). Almost at the same time, *Vibrio* isolates with similar phenotypic characteristics, but indole-negative, were recovered from diseased eels in Japan (Muroga *et al.*, 1976). Thus, the species was originally subdivided into two different biotypes based on biochemical and host-range differences: Bt1 clustering the indole-positive human and clinical isolates and Bt2 comprising the indole-negative strains isolated from eels (Tison *et al.*, 1982). Later on, in 1999, a third biotype (Bt3) was defined to group isolates from human infection outbreaks among workers of a tilapia fish farm in Israel that differed phenotypically from Bt1 and Bt2 and were avirulent for fish species (Bisharat *et al.*, 1999). In parallel, it was described that some Bt2 strains were potentially virulent for humans (Amaro and Biosca, 1996). The three biotypes are able to infect humans, but only Bt2 can also cause disease in fish. The ability to infect fish relies on a virulence plasmid (pVvBt2) which confers resistance to teleost fish innate immunity and it is present in all Bt2 strains (Amaro *et al.*, 2015). Moreover, Bt2 is further subdivided in three serotype-related groups, one of which, SerE, is considered as truly zoonotic and constitutes a zoonotic clonal-complex within the species (Sanjuán *et al.*, 2011).

The subdivision of the species in biotypes has been historically conserved since the isolates were easily discriminated by phenotypic and genetic tests (Tison *et al.*, 1982; Bisharat *et al.*, 1999; Sanjuán and Amaro, 2004). Nevertheless, as the amount and diversity of *V. vulnificus* isolates has exponentially increased during the last decades, nowadays a completely reliable test (or combination of tests) to discriminate between biotypes does not exist. This issue has been recently solved by the phylogenomic study carried out by Roig *et al.*, (2018). The authors of this study have analyzed the core genomes of 80 *V. vulnificus* strains belonging to the three biotypes and demonstrated that the species is subdivided into five phylogenetic lineages that do not correspond to the current biotypes (**TABLE 1** and **FIGURE 1**). The results of this study also

suggest that the pVvBt2 has been acquired independently by different clones, probably in fish farms. In summary, the authors propose to reconsider the classification of the species to base it on the five phylogenetic lineages plus one pathovar (pv. *piscis*), which groups all the *V. vulnificus* strains with the ability to cause fish disease, meaning those harboring the pVvBt2 (formerly Bt2) (Roig *et al.*, 2018). The pv. *piscis* conserves the subdivision into three serotype-related sublineages, with serE as a zoonotic clonal-complex (Sanjuán *et al.*, 2011; Roig *et al.*, 2018).

TABLE 1 | Brief description of the five *V. vulnificus* phylogenetic lineages (Roig *et al.*, 2018).

Lineage	Description
L1	Bt1 strains involved in human clinical cases related to raw seafood ingestion
L2	Bt1 strains isolated from a variety of sources related to aquaculture context Bt2 (pv. *piscis*) strains isolated from a variety of sources related to aquaculture context
L3	Bt3 strains
L4	Bt1 strains associated to specific geographical area
L5	Bt1 strains associated to specific geographical area

V. vulnificus is a very versatile pathogenic species which includes virulent and avirulent strains that differ in the presence and/or combination of virulence-related genes. Around 90% of the virulence-related genes are present in the core genome of the species, and therefore all *V. vulnificus* strains should be considered potentially virulent for humans, while only the strains carrying the pVvBt2 should be considered as potentially virulent for fish (Roig *et al.*, 2018). Nevertheless, there are some polymorphisms in specific genes that seem plausible to be used to predict the virulent potential of the isolates (i.e., *vcg* and *pilF* (Rosche *et al.*, 2005; Roig *et al.*, 2010)).

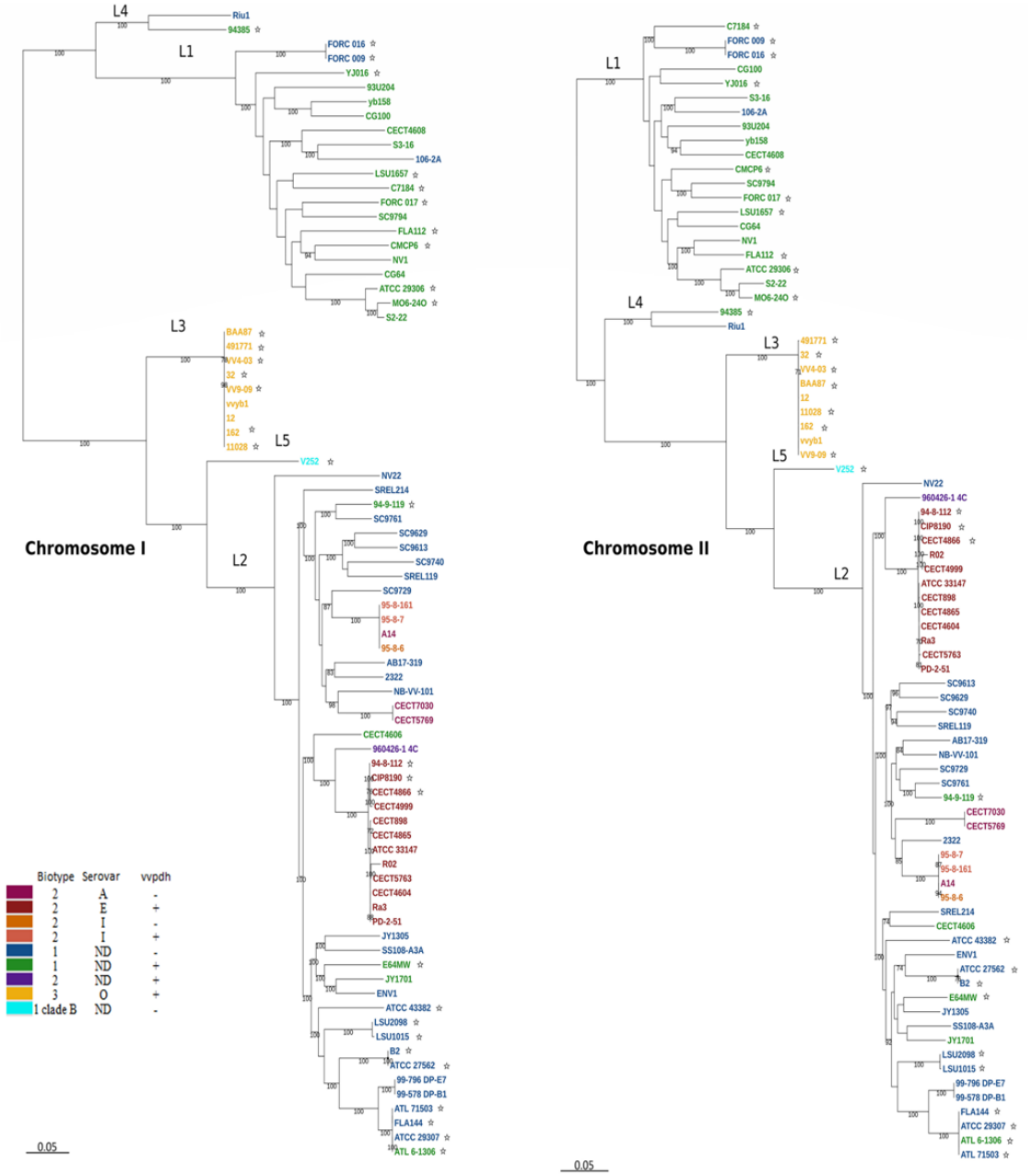

FIGURE 1 | *V. vulnificus* phylogenetic tree reconstructed from chromosome I and chromosome II. Phylogeny is based on single nucleotide polymorphisms on the coding regions in the core genome of the species. Image taken from Roig *et al.*, (2018).

1.2. Zoonotic clonal-complex genome

In 2003 the first genome of *V. vulnificus* was published. It corresponded to a L1 strain (YJ016) isolated from the blood of a septicemic patient in Taiwan (Chen *et al.*, 2003). Since then, multiple genomes of several strains of the species have been sequenced and published (Park *et al.*, 2011; Li *et al.*, 2012; Morrison *et al.*, 2012; Wang *et al.*, 2012; Danin-Poleg *et al.*, 2013), including the R99 (CECT4999, a representative strain of the zoonotic clonal-complex) genome (https://www.ncbi.nlm.nih.gov/nuccore/NZCP014636).

R99 was isolated in 1999 in Spain from the kidney of a diseased European eel (Roig *et al.*, 2018). The main characteristics of its genome are resumed in **TABLE 2** (unpublished results, https://www.ncbi.nlm.nih.gov/genome/189?genomeassemblyid=323426). It is constituted by 4,533 coding DNA sequences distributed in three replicons corresponding to two chromosomes (ChrI and ChrII) and the virulence plasmid (pR99). Putative functions have been assigned to 82% of the coding sequences while the remaining 18% coding sequences with no putative function assigned are considered as predicted hypothetical proteins. The majority of the coding sequences annotated as virulence-related genes are encoded either in ChrII or in the pR99. Concretely, those virulence factors considered as generalist or host-nonspecific are encoded in ChrII while those encoded in pR99 are fish-specific virulence factors, with the exception of RtxA1$_3$ toxin, which is duplicated in both ChrII and pR99.

Overall, the main differences between the main genetic features of R99 and YJ016 strains reveal that: zoonotic clonal-complex genome is larger than L1 genomes (19 kb); and the distribution of proteins in functional categories is slightly different (carbohydrate transport and metabolism related-clusters are more abundant in L1 genomes while replication, recombination and repair related-clusters are predominant in the zoonotic clonal-complex genome). Moreover, out of 469 ORFs (open reading frames) (from which 50% are annotated as hypothetical proteins, 20% as transposases and other mobile elements and the remaining 30% as different cellular process; i.e., carbohydrate transport and metabolism, cell wall biogenesis, transcriptional regulator, etc.) are unique in R99 genome since they are not shared with L1 genomes (unpublished results).

R99 has been used as a model strain throughout the present thesis.

TABLE 2 | Global features of the R99 strain genome (https://www.ncbi.nlm.nih.gov/genome/189?genomeassemblyid=323426).

Location	Size (Mb)	% GC	Predicted proteins	rRNA	tRNA
ChrI	3.39	46.3	3,070	25	103
ChrII	1.7	47.1	1,390	3	13
pR99	0.07	43.8	56	-	-

1.3. Ecology and epidemiology

V. vulnificus is a worldwide distributed pathogen autochthonous from marine and estuarine ecosystems located in temperate, tropical and subtropical areas where water temperature ranges from 10 to 30ºC (Baker-Austin and Oliver, 2018). The preferred habitat of *V. vulnificus* is brackish water (1-2% NaCl) above 18ºC, but it can survive in cold water (below 9ºC) by entering into VBNC (viable but nonculturable) state (Oliver, 2015). Ecological studies suggest that water salinity and temperature, as well as the interaction between both parameters (Takemura *et al.*, 2014), determine the geographical and seasonal distribution of the species. Therefore, the increase in water temperature caused by global warming is leading to the expansion of this bacterial pathogen due to the augment in both the impacted geographical area and the population abundance in currently affected areas (Baker-Austin *et al.*, 2010).

V. vulnificus, as many other aquatic bacteria, shows an extensive range of niches. Thus, it can be encountered in the environment either as a free-living form or associated to biotic (i.e., fish mucosae, algae or chitin exoskeleton of bivalve species) or abiotic (sediments) surfaces by forming biofilms (Oliver, 2015). Moreover, as a free-swimming microorganism it can be concentrated by filter feeders to more than 100 times the concentration in the surrounding aquatic environment (Froelich *et al.*, 2017). Therefore, apart from water, aquatic animals such us fish, oysters, and shrimps, are considered the main environmental reservoirs for this pathogen (Oliver, 2015). However, strains belonging to the pv. *piscis* have never been isolated from oysters, suggesting a fish-niche adaptation for pv. *piscis*. Accordingly, pv. *piscis* has never been related to human foodborne infections (Amaro *et al.*, 2015).

The species is considered a pathogen of public health concern as it is responsible for most of the outbreaks in fish farms as well as for the majority of seafood-associated deaths worldwide, but especially in the United States (Kaspar and Tamplin, 1993; Tao *et al.*, 2012). In

fact, epidemiological data report that among the stated human infections both the hospitalization and mortality rates are high (84 and 25%, respectively) (Oliver, 2015). Epidemiological studies, in accordance with ecological data, also suggest that *V. vulnificus* foodborne infections occur as sporadic cases in warmer months, achieving a maximum in the hottest periods of the year in the geographical areas where the pathogen is an autochthonous species (Baker-Austin *et al.*, 2010; Oliver, 2015). Moreover, the number of reported cases of *V. vulnificus* infections has been increasing dramatically during the last decade due to global warming (Baker-Austin *et al.*, 2010; Baker-Austin and Oliver, 2018), probably together with changes in dietary habits (increase of consumption of raw seafood [sushi]) as well as an increase in population with predisposing risk factors (Horseman and Surani, 2011; Karunasagar, 2014).

2. The main hosts

V. vulnificus constitutes an extremely versatile pathogen that can infect a wide variety of hosts during its life cycle. Humans and fish are considered as the most important ones due to the clinical and economic burden this species pose to both public health and aquaculture industry.

2.1. Humans

V. vulnificus is an opportunistic human pathogen. Independently of the infective strain and the form of the disease (see point 3 “The disease” [p. 42]), the progression of the infection depends on the patient health status, either healthy or susceptible human host. In healthy patients the disease is usually self-limiting and rarely leads to septicemia, while in susceptible patients the disease can lead to death by sepsis depending on a series of predisposing risk factors that result in an increase of free iron level in blood, and from which the most important ones are chronic liver disease, immunodeficiency disorders, gastrointestinal disease, renal disease, and hematological disorders such as hemochromatosis and thalassemia (Horseman and Surani, 2011; Menon *et al.*, 2014). Thus, apart from normal mice, the most used animal model to study human vibriosis is iron-overloaded mice (obtained by injecting iron to the animals previous to the infection) (Amaro *et al.*, 1994).

2.2. Fish

Among fish species, the main hosts of *V. vulnificus* are teleost fish cultured in brackish water at warm temperatures such as Nile tilapia and eel, from which European eel is the most susceptible one (Tison *et al.*, 1982; Fouz and Amaro, 2003; Fouz *et al.*, 2006; Amaro *et al.*, 2015).

Nile tilapia (*Orechromis niloticus*) is a freshwater species that inhabits tropical shallow waters with optimal temperatures between 31-36ºC, although it can live at a range of temperatures between 11-42ºC (Lim and Webster, 2006). The species life expectancy is approximately 10 years and sexual maturity is achieved at 5-6 months age. After fertilization, the female collects the eggs inside its mouth and incubates them for 1-2 weeks until the spawn, which takes place inside nests dug by male specimens. The spawn, and subsequently the life cycle of the species, is controlled by water temperature (Lim and Webster, 2006). Female specimens can spawn continuously as long as the water temperature remains optimum for spawning (over 24ºC) (Lim and Webster, 2006). As the life cycle of the species is well known, Nile tilapia is extensively cultured in many tropical and temperate countries in floating cages or in ponds in large natural lakes (Lim and Webster, 2006).

European eel (*Anguilla anguilla*) is a catadromous fish that presents a complex life cycle with multiple life stages (Tesch, 2003; van Ginneken and Maes, 2005) (**FIGURE 2**). The spawn of the species occurs in the Sargasso Sea from where young larvae (Leptocephali) are transported by ocean currents to continental coasts. Leptocephali larvae metamorphose to glass eels before their arrival to the coast. Once they reach the continent, they enter estuaries and ascend European rivers, metamorphosing to yellow eel and colonizing ponds and lakes where they grow as resident eels until they metamorphose again to silver eels, which means they become sexually mature. At this point, they migrate back to the Sargasso Sea to spawn and die. The eel life cycle takes between 5-20 years and, contrary to many other teleost fish life cycles, it remains poorly understood. In fact, the species reproduction has not been successfully achieved under artificial conditions although big efforts are being done in order to close their production cycle in captivity (developing standardized protocols for production of gametes, embryos, and feeding larvae of European eel) (Palstra *et al.*, 2005; Mes *et al.*, 2016; Jehannet *et al.*, 2017). Thus, to date, eel resources are based on glass eel catches from natural stocks and their subsequent growth in fish farms under intensive conditions until they rise to market size. This situation, exacerbated by the species' commercial importance (the global production of anguilliculture is around 7,000 tons per year), is leading to overexploitation and

overfishing (Nielsen and Prouzet, 2008) which together with several of the species' biological characteristics such as migration-dependent life cycle, single breeding and longevity, and many other anthropogenic factors including climate and oceanic change (factors that are causing the species' habitat destruction) (Friedland *et al.*, 2007; Kirkegaard, 2010) have caused the critical decline of the natural European eel population over the last decades (Dekker, 2003; Henderson *et al.*, 2012). Moreover, the European eel natural stock currently occupies a position in the IUCN (International Union for Conservation of Nature) red list as a critically endangered species and it is considered outside of safe biological limits since 2008 (https://www.iucnredlist.org/species/60344/45833138).

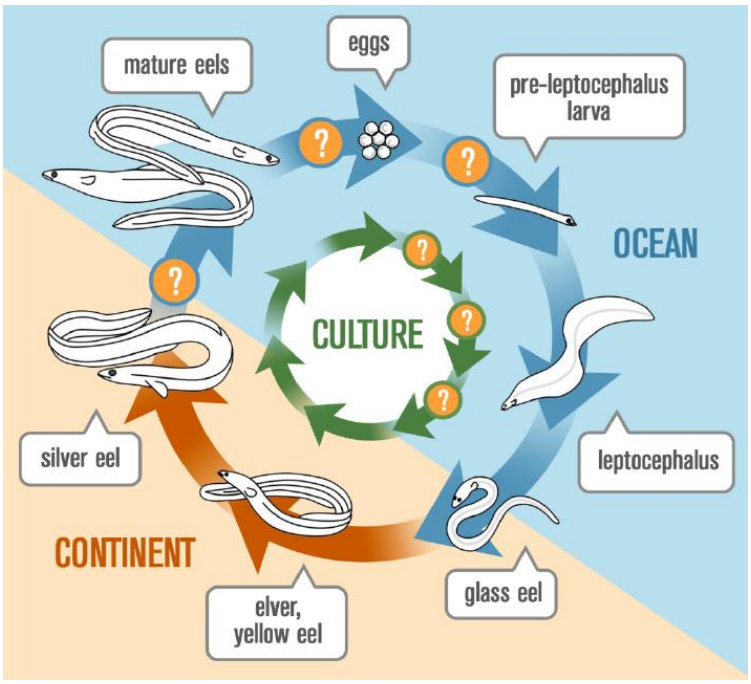

FIGURE 2 | European eel life cycle. Known and unknown stages of eel life cycle both in natural and cultured conditions. Image taken from Callol (2013).

3. The disease: vibriosis

V. vulnificus is a multihost septicemic pathogen that accidentally infects a variety of aquatic animal species (fish, shrimps, oysters, etc.) and humans, causing in all of them diseases (collectively known as vibriosis) with multiple clinical manifestations. The clinical signs associated with vibriosis depend on both the transmission route and the infected host, but in all cases the common result of the disease is an acute septicemia with a high probability of death by sepsis (Oliver, 2015).

In fish, pv. *piscis* causes a disease known as warm-water vibriosis because the most serious outbreaks take place in fish farms where the water temperatures are kept over 25ºC. There are two forms of the disease depending on water salinity, brackish water and freshwater modalities. The brackish water modality is caused by the zoonotic clonal-complex and occurs in form of high mortality outbreaks in eel farms where the water salinity ranges between 0.5-2%; while the freshwater modality is caused by non-zoonotic serotypes and occurs in form of low mortality outbreaks in eel and tilapia farms where water salinity ranges between 0.3-0.9% (Biosca *et al.*, 1991; Amaro and Biosca, 1996; Chen *et al.*, 2006; Fouz *et al.*, 2006). The prime vehicles of transmission are ingestion and contact with contaminated water or even other fishes (diseased fishes or healthy carriers), but the transmission route of the disease is serotype dependent. The zoonotic clonal-complex preferably infects through water while non-zoonotic serotypes infect preferentially by the oral/anal route (mouth or anus) (Fouz *et al.*, 2010; Amaro *et al.*, 2015). Although there are some differences in clinical manifestation between serotypes, the main clinical signs are common and consist of abdominal petechiae, hemorrhages at the base of the dorsal and anal fins and a reddening in the operculum region (**FIGURE 3**) (Amaro *et al.*, 2015). In the case of the zoonotic clonal-complex, the pathogen colonizes the gills and multiplies on the surface forming biofilms. Then, the pathogen crosses the epithelial barrier, invades the bloodstream and spreads to internal organs causing an acute hemorrhagic septicemia, regardless of the immune status of the host, which ends with the death of the animals in less than 48 h. Interestingly, the bacterial population size needed to cause the rapid death of the animals is remarkably lower than that reported to other *Vibrio*-related vibriosis (Valiente and Amaro, 2006; Valiente *et al.*, 2008).

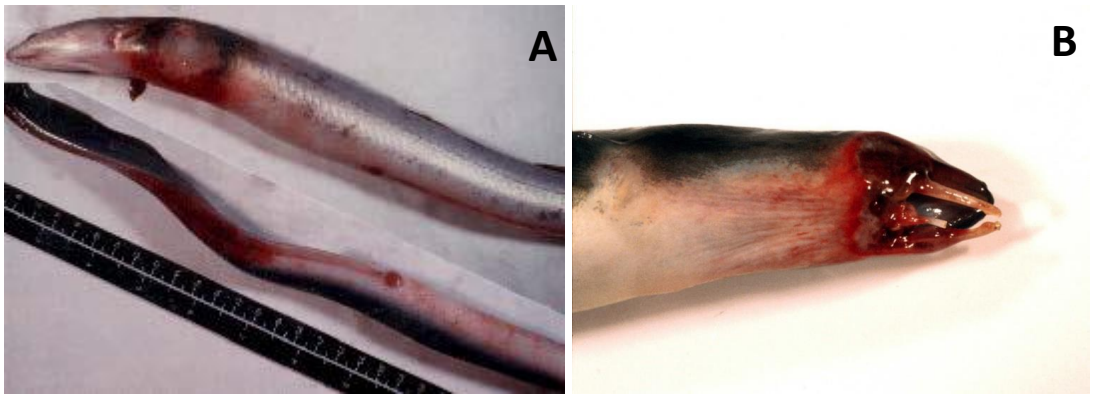

FIGURE 3 | Warm-water vibriosis clinical signs in European eel. A) Eel vibriosis in brackish water caused by the zoonotic clonal-complex. External ulcers are the main differential clinical sign. B) Eel vibriosis in freshwater caused by non-zoonotic serotypes. Jaw degradation is the main differential clinical sign. Images taken from Biosca *et al.*, (1991) and Haenen *et al.,* (2014).

In humans, there are two main forms of the disease according to the transmission route, either contact or ingestion. In both cases, the disease can converge in hemorrhagic septicemia (primary septicemia in case of ingestion of raw contaminated seafood; secondary septicemia in case of wound contact with contaminated water or fish) with similar clinical signs (**FIGURE 4**) that can lead to death depending on the patient's health status (Oliver, 2015). The main predisposing risk factor is a high level of free iron in blood due to different underlying diseases (i.e., chronic liver diseases and hemochromatosis). In fact, the high correlation between sepsis and an underlying disease is well stablished, with less than 5% of the reported cases occurring in healthy patients while patients with at least one of the mentioned predisposing risk factors are 80 times more likely to develop primary septicemia (Horseman and Surani, 2011). In common with fish vibriosis, human disease caused by *V. vulnificus* has a very short incubation time, causing death in 24-72 h (Jones and Oliver, 2009). Finally, *V. vulnificus* is also a zoonotic pathogen (zoonotic clonal-complex strains of pv. *piscis*) as there are reported cases of the pathogen being directly transmitted by contact from diseased fish to humans, mainly in fish farms (Veenstra *et al.*, 1992; Dalsgaard *et al.*, 1996; Amaro *et al.*, 2015).

FIGURE 4 | Common clinical signs of primary (oral transmission) and secondary (contact transmission) septicemia caused by *V. vulnificus* in humans. Cellulitis, erythema and necrotizing fasciitis in the leg of a patient in Taiwan. Image taken from Ceccarelli *et al.*, (2019).

4. Host-pathogen interaction

To better understand the main pathogen and host factors involved in the establishment of vibriosis, the disease can be divided into three main temporal steps: colonization (early steps that occur during the first host-pathogen contact), invasion (blood invasion and spreading to

internal organs), and sepsis (damage phase and death by hemorrhagic septic shock). **The present thesis is focused on the study of host-pathogen relationship using the zoonotic clonal-complex and the eel as a model of infection, but in some approaches human models have been included in order to compare host-adaptation processes in the establishment of vibriosis**. For this reason, the role of each virulence factor is described below taking into account both hosts.

Colonization. In fish, the pathogen is chemo-attracted to gill mucus where it primarily binds to colonize this organ. In this process both the protease Vvp and the capsule are involved, as deficient strains in either the capsule or the protease are significantly unpaired in gill colonization (Amaro *et al.*, 1995; Valiente *et al.*, 2008). In humans, pv. *piscis* only infects wounds by contact with contaminated water or fish while the strains belonging to the rest of lineages can infect either by the oral route or by contact. Wound and intestine colonization seems to be mediated by bacterial adhesins (Paranjpye and Strom, 2005; Jones and Oliver, 2009). In case of oral infection, *V. vulnificus* has to first resist the acid pH of the stomach as well as the bactericidal effect of bile salts by expressing protective LPS (lipopolysaccharide) and several outer membrane proteins related to stress resistance prior to colonizing the intestine (Rhee *et al.*, 2002).

Invasion. Once the pathogen is well-established in the colonized organs, it expresses the RtxA1 toxin, a MARTX (Multifuctional Autoprocessing Repeat in Toxin) family toxin that has been related to invasion in both humans and fish (Satchell, 2007, 2011; Lee *et al.*, 2013). The structure and mechanism of action of *V. vulnificus* RtxA1 are represented in **FIGURE 5**. Briefly, RtxA1 are modular proteins of high molecular weight with conserved external modules that form pores in the membrane of a wide range of eukaryotic cell types. The formed pore is used to translocate the central module of the toxin, which harbors the effector domains that are responsible of the cytotoxicity. These domains are released into the cytosol of the eukaryotic cell by CPD (cysteine protease domain) after its activation by binding the InsP6 (inositol hexakisphosphate) (Gavin and Satchell, 2015). The internal domains known until now are: DUF1 (domain with unknown function) which probably binds prohibitin-1 promoting the translocation of the toxin into the cell; RID (Rho GTPase inhibitor domain) that activates actin depolymerization, altering the cell cytoskeleton; ACD (actin cross-linking domain) that activates actin cross-linking; ABH (alpha/beta hydrolase domain) which binds inositol-3-phosphate inhibiting autophagy and endosomal trafficking; MCF ("makes caterpillars floppy"-like domain) that induces depolarization of the mitochondrial membrane potential causing activation of cell death signaling pathways; and RRSP (Ras/Rap1 specific endopeptidase

domain) which suppresses the ERK-mitogen-activated protein kinase pathway by proteolytically processing Ras and Rap1 GTPases, thus preventing Ras from activating ERK, and inhibiting cell proliferation (Satchell, 2011, 2015; Agarwal *et al.*, 2015; Murciano et al., 2017). *V. vulnificus* can produce several types of RtxA1 that differ in the number and types of effector domains (Satchell, 2011). The zoonotic clonal-complex carries two copies of $RtxA1_3$ in its genome (one in ChrII and the other in pVvBt2) (Roig *et al.*, 2011; Lee *et al.*, 2013) and its structure and mechanism of attack to eukaryotic cells are represented in **FIGURE 6**. This toxin is expressed early during the fish infection and is secreted when the bacterium co-localizes with eukaryotic cells (Lee *et al.*, 2013). In fish, $RtxA1_3$ is involved in phagocytes destruction and tissue damage in gills. Moreover, the toxin causes local inflammation favoring the pathogen entrance into the bloodstream (Callol *et al.*, 2015). Similarly, in humans, $RtxA1_3$ together with the major hemolysin of the species (VvhA), whose role in fish disease remains unknown, causes tissue damage and local inflammation contributing to the pathogen dissemination to blood and internal organs (Jeong and Satchell, 2012).

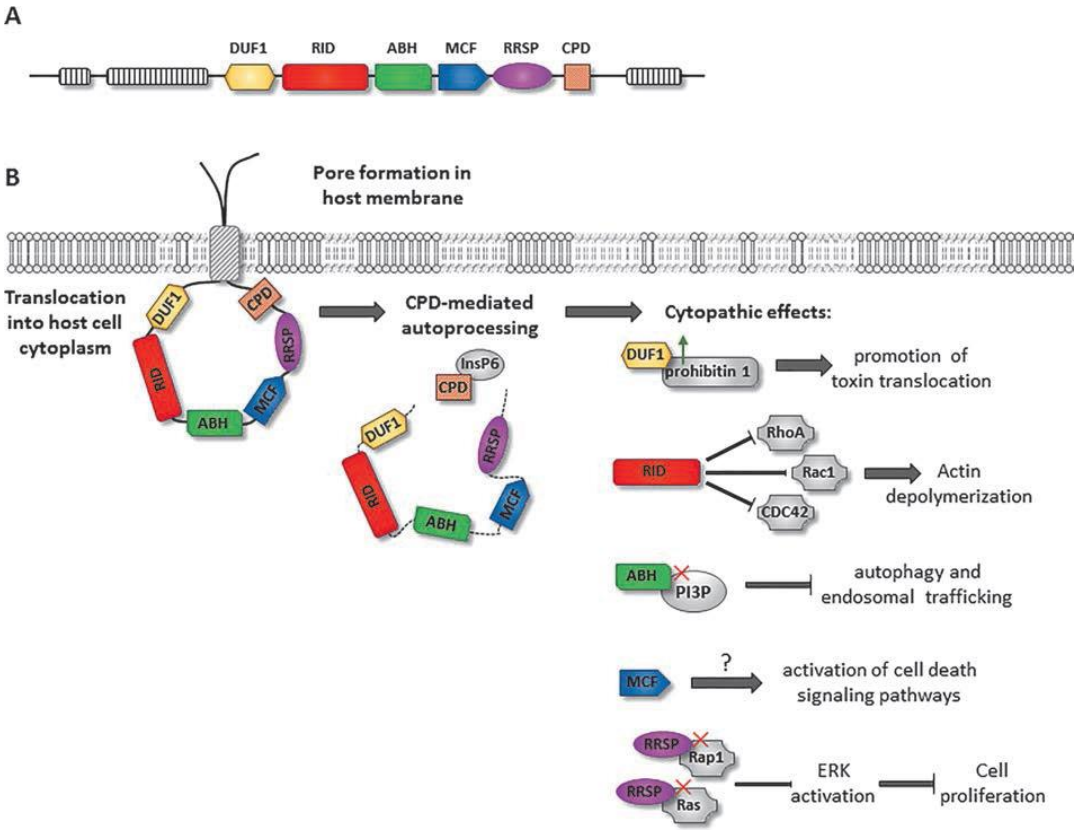

FIGURE 5 | *V. vulnificus* RtxA1 toxins structure (A) and mechanism of action (B). The scheme shows the conserved external modules and the internal module, containing the effector domains represented with different colors. When the toxin is secreted, the external module is associated with the target cell membrane by forming a pore that allows the central module to be exposed to the cytosol. CPD is activated after binding InsP6 and catalyzes the release of the rest of internal domains: DUF1, RID, ACD, ABH; MCF and RRSP. Image taken from Ceccarelli *et al.*, (2019).

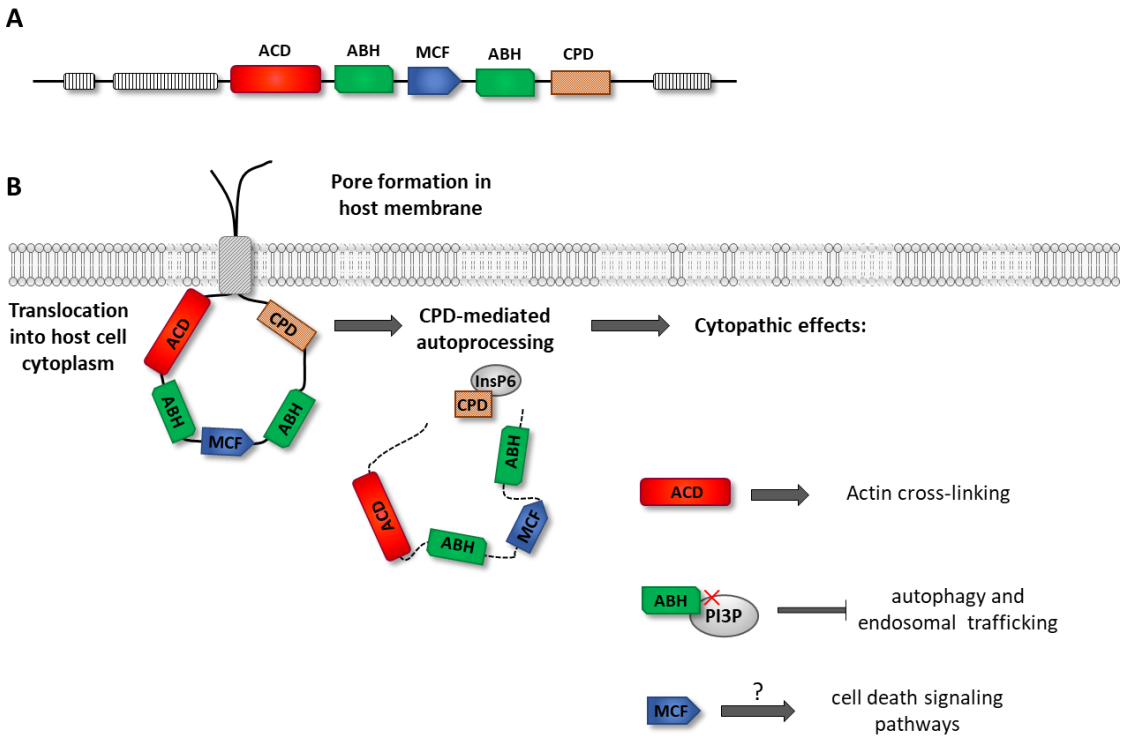

FIGURE 6 | Zoonotic clonal-complex RtxA1$_3$ toxins structure (A) and mechanism of action (B). The scheme shows the conserved external modules and the internal module, containing the effector domains represented with different colors. When the toxin is secreted the external module is associated with the target cell membrane by forming a pore that allows the central module to be exposed to the cytosol. CPD is activated after binding InsP6 and catalyzes the release of the rest of internal domains. Contrary to other RtxA1, RtxA1$_3$ only carry ACD, ABH (duplicated) and MCF. Image taken from Amaro *et al.,* (2019).

Sepsis. Once into the bloodstream *V. vulnificus* is able to survive and multiply in blood, inducing septicemia and host death due to severe injury to tissues and organs. However, to successfully establish sepsis, the pathogen must overcome the main defense mechanisms of the infected host, such as nutritional immunity and innate immunity.

Innate immunity is a primary line of defense against pathogens that basically acts on two levels, humoral immunity and cellular immunity. The humoral immunity is based on the presence of bactericidal and bacteriostatic proteins in blood and mucosal tissues. Serum transferrin and mucosal lactoferrin are among the most effective bacteriostatic proteins. Both proteins bind to iron and reduce their levels in blood and in mucosal tissues below the limits for bacterial growth. Transferrin and lactoferrin are part of nutritional immunity, an ancient mechanism of innate immunity highly conserved among vertebrates (Weinberg, 2009). To overcome these iron restricted conditions in humans, *V. vulnificus* either sequesters iron from

transferrin by using the siderophore vulnibactin or binds directly to the heme group that is present in hemoglobin and derivative proteins (Pajuelo *et al.*, 2014). In fish, pv. *piscis* uses the plasmid protein Ftbp (Fish transferrin binding protein) that binds specifically to teleost fish transferrin (Pajuelo *et al.*, 2015).

Serum complement comprises a series of proteins that take part of the bactericidal proteins of innate immunity. They are produced by the liver as inactive proteins and secreted to the blood and tissues where they will be activated by the pathogens. Once activated, they act in chain (the first activates the second, the second activates the third, and so on). The result of this cascade of complement activation is that the pathogen is marked either for its destruction by lysis or for its further destruction by a phagocyte (opsonophagocytosis) (Williams *et al.*, 2014). LPS and capsule of *V. vulnificus* are involved in resistance to serum complement (Amaro *et al.*, 1994, 1997).

Phagocytes are part of the cellular innate immunity. They directly recognize several markers on the pathogen surface (PAMPs [pathogen associated molecular patterns]) or opsonins (complement proteins or antibodies fixed on the bacterial surface). Then, they phagocyte the pathogen and destroy it. The capsule of *V. vulnificus* confers resistance to both fish and human phagocytes (Amaro *et al.*, 1995; Williams *et al.*, 2014).

In teleost fish, including European eel, erythrocytes or RBC (red blood cells) are nucleated cells present in blood circulation and thus, they could be more than hemoglobin and oxygen transporters (as they are in mammals), meaning that they are able to modify their transcriptome and therefore they could have a potential role in non-respiratory processes, such as cellular innate immunity. In fact, some studies have already suggested an immune function for nucleated teleost fish RBC, mainly based on their ability to detect PAMPs (Morera and MacKenzie, 2011; Morera *et al.*, 2011). Recently, an active antiviral role mediated by autophagy has been attributed to teleost RBC (Pereiro *et al.*, 2017).

If the pathogen successfully evades the innate immune response, a sustained immune response with secretion of several inflammatory cytokines produces a systemic inflammatory syndrome which eventually causes host death (Shin *et al.*, 2002; Chen *et al.*, 2017). In fact, $RtxA1_3$ has been recently related to an early, unbalanced and detrimental systemic inflammatory response in mice (Murciano *et al.*, 2017). In fish, it remains unknown if the innate immune system has a role in the generation of septic shock.

5. Treatment and preventive measures

Patients who show clinical signs of infection caused by *V. vulnificus*, especially those who show signs of septicemia, should be immediately treated. It is important to keep in mind that the disease is very fast (24-72 h) and thus, the mortality rate due to *V. vulnificus* infection is strongly dependent on the time taken after infection to initiate the treatment (Horseman and Surani, 2011; Heng *et al.*, 2017). Recommended treatment usually consists of antibiotic administration since the majority of *V. vulnificus* strains are susceptible to most of the antibiotics approved for clinical use (Heng *et al.*, 2017). However, the extensive use of antibiotics during the past years is leading to an increase in resistant isolates for the most frequent prescribed drugs (Elmahdi *et al.*, 2016; Igbinosa, 2016). In consequence, not only effective treatment but also preventive measurements must be taken in order to reduce *V. vulnificus* infections. In this sense, the best preventive step against foodborne infections caused by *V. vulnificus* is to trace potentially contaminated seafood (by geographical area and harvesting season) and regulate its consumption (i.e., restricting its sale, requiring the application of post-harvest measurements treatments to reduce bacterial numbers (Vugia *et al.*, 2013)). Educational campaigns could also help to raise awareness for people to avoid the ingestion of raw shellfish, especially in geographical areas where *V. vulnificus* is widely spread. A good example of the importance of these measurements is found in the State of California (United States) were the number of deaths by *V. vulnificus* was successfully driven to zero in 2010 (Vugia *et al.*, 2013).

Moreover, fish farms, especially eel farms, constitute a reservoir for the pv. *piscis* of the pathogen and therefore preventive measures should also be taken in the aquaculture context to avoid *V. vulnificus* expansion. Although the manipulation of water physicochemical parameters, to keep them outside the biological limits for *V. vulnificus* proliferation and transmission (freshwater at temperatures below 25ºC and pH below 6), help control the disease (Amaro *et al.*, 1995; Marco-Noales *et al.*, 1999), the optimal preventive measure to avoid outbreaks of this disease is vaccination (Fouz *et al.*, 2001; Esteve-Gassent *et al.*, 2003, 2004). Only vaccination can guarantee that the health status of the animals is adequate to avoid the proliferation and evolution of the pathogen in fish farms as well as human vibriosis outbreaks related to aquaculture context.

6. References

Agarwal, S., Kim, H., Chan, R.B., Agarwal, S., Williamson, R., Cho, W., et al. (2015) Autophagy and endosomal trafficking inhibition by *Vibrio cholerae* MARTX toxin phosphatidylinositol-3-phosphate-specific phospholipase A1 activity. *Nat Commun* **6**.

Amaro, C. and Biosca, E.G. (1996) *Vibrio vulnificus* biotype 2, pathogenic for eels, is also an opportunistic pathogen for humans. *Appl Environ Microbiol* **62**: 1454–1457.

Amaro, C., Biosca, E.G., Fouz, B., Alcaide, E., and Esteve, C. (1995) Evidence that water transmits *Vibrio vulnificus* biotype-2 Infections to eels. *Appl Environ Microbiol* **61**: 1133–1137.

Amaro, C., Biosca, E.G., Fouz, B., Toranzo, A.E., and Garay, E. (1994) Role of iron, capsule, and toxins in the pathogenicity of *Vibrio vulnificus* biotype-2 for mice. *Infect Immun* **62**: 759–763.

Amaro, C., Fouz, B., Biosca, E.G., Marco-Noales, E., and Collado, R. (1997) The lipopolysaccharide o side chain of *Vibrio vulnificus* serogroup E is a virulence determinant for eels. *Infect Immun* **65**: 2475–2479.

Amaro, C., Fouz, B. Sanjuán, E., and Romalde J.L. (2019). Fish vibriosis. In Climate change and infectious fish diseases. CABI, UK. *In press*

Amaro, C., Sanjuán, E., Fouz, B., Pajuelo, D., Lee, C.T., Hor, L., et al. (2015) The fish pathogen *Vibrio vulnificus* biotype 2: epidemiology , phylogeny , and virulence factors involved in warm-water vibriosis. *Microbiol Spectr* **3**.

Baker-Austin, C. and Oliver, J.D. (2018) *Vibrio vulnificus*: new insights into a deadly opportunistic pathogen. *Environ Microbiol* **20**: 423–430.

Baker-Austin, C., Stockley, L., Rangdale, R., and Martinez-Urtaza, J. (2010) Environmental occurrence and clinical impact of *Vibrio vulnificus* and *Vibrio parahaemolyticus*: a European perspective. *Environ Microbiol Rep* **2**: 7–18.

Biosca, E.G., Amaro, C., Esteve, C., Alcaide, E., and Garay, E. (1991) First record of *Vibrio vulnificus* biotype 2 from diseased European eel, *Anguilla anguilla*. *J Fish Dis* **14**: 103–109.

Bisharat, N., Agmon, V., Finkelstein, R., Raz, R., Ben-Dror, G., Lerner, L., et al. (1999) Clinical, epidemiological, and microbiological features of *Vibrio vulnificus* biogroup 3 causing

outbreaks of wound infection and bacteraemia in Israel. *Lancet* **354**: 1421–1424.

Callol, A. (2013) Eelness. Transcriptomic analysis of *Vibio*-induced immune response in European eel (*Anguilla anguilla*). PhD Thesis. Universitat de València.

Callol, A., Pajuelo, D., Ebbesson, L., Teles, M., MacKenzie, S., and Amaro, C. (2015) Early steps in the European eel (*Anguilla anguilla*)-*Vibrio vulnificus* interaction in the gills: role of the RtxA1$_3$ toxin. *Fish Shellfish Immunol* **43**: 502–509.

Ceccarelli, D., Amaro, C., Romalde, J., Suffredini, E., and Vezzulli, L. (2019) *Vibrio* species. In Food Microbiology: Fundamentals and Frontiers, 5th Edition. Doyle,M., Diez-González,F., and Hill,C. (eds). ASM Press. Washington. DC. pp. 347-388.

Chen, C.L., Chien, S.C., Leu, T.H., Harn, H.I.C., Tang, M.J., and Hor, L.I. (2017) *Vibrio vulnificus* MARTX cytotoxin causes inactivation of phagocytosis-related signaling molecules in macrophages. *J Biomed Sci* **24**: 58.

Chen, C.Y., Wu, K.M., Chang, Y.C., Chang, C.H., Tsai, H.C., Liao, T.L., et al. (2003) Comparative genome analysis of *Vibrio vulnificus*, a marine pathogen. *Genome Res* **13**: 2577–2587.

Chen, C.Y., Chao, C. Ben, and Bowser, P.R. (2006) Infection of tilapia *Oreochromis sp*. by *Vibrio vulnificus* in freshwater and low-salinity environments. *J World Aquac Soc* **37**: 82–88.

Dalsgaard, A., Frimodt-Moller, N., Bruun, B., Hoi, L., and Larsen, J.L. (1996) Clinical manifestations and molecular epidemiology of *Vibrio vulnificus* infections in Denmark. *Eur J Clin Microbiol Infect Dis* **15**: 227–232.

Danin-Poleg, Y., Elgavish, S., Raz, N., Efimov, V., and Kashi, Y. (2013) Genome sequence of the pathogenic bacterium *Vibrio vulnificus* biotype 3. *Genome Announc* **1**: e0013613.

Dekker, W. (2003) Did lack of spawners cause the collapse of the European eel, *Anguilla anguilla*? *Fish Manag Ecol* **10**: 365–376.

Elmahdi, S., DaSilva, L. V, and Parveen, S. (2016) Antibiotic resistance of *Vibrio parahaemolyticus* and *Vibrio vulnificus* in various countries: A review. *Food Microbiol* **57**: 128–134.

Esteve-Gassent, M.D., Fouz, B., and Amaro, C. (2004) Efficacy of a bivalent vaccine against eel diseases caused by *Vibrio vulnificu*s after its administration by four different routes. *Fish Shellfish Immunol*. **16**: 93–105.

Esteve-Gassent, M.D., Nielsen, M.E., and Amaro, C. (2003) The kinetics of antibody production in mucus and serum of European eel (*Anguilla anguilla*) after vaccination against *Vibrio vulnificus*: development of a new method for antibody quantification in skin mucus. *Fish Shellfish Immunol* **15**: 51–61.

Farmer 3rd, J.J. (1979) *Vibrio* ("Beneckea") *vulnificus*, the bacterium associated with sepsis, septicaemia and the sea. *Lancet* **314**: 903.

Fouz, B. and Amaro, C. (2003) Isolation of a new serovar of *Vibrio vulnificus* pathogenic for eels cultured in freshwater farms. *Aquaculture* **217**: 677–682.

Fouz, B., Esteve-Gassent, M.D., Barrera, R., Larsen, J.L., and Nielsen, M.E. (2001) Field testing of a vaccine against eel diseases caused by *Vibrio vulnificus* . *Dis Aquat Organ* **45**: 183–189.

Fouz, B., Larsen, J.L., and Amaro, C. (2006) *Vibrio vulnificus* serovar A: an emerging pathogen in European anguilliculture. *J Fish Dis* **29**: 285–291.

Fouz, B., Llorens, A., Valiente, E., and Amaro, C. (2010) A comparative epizootiologic study of the two fish-pathogenic serovars of *Vibrio vulnificus* biotype 2. *J Fish Dis* **33**: 383–390.

Friedland, K.D., Miller, M.J., and Knights, B. (2007) Oceanic changes in the Sargasso Sea and declines in recruitment of the European eel. *ICES J Mar Sci* **64**: 519–530.

Froelich, B.A., Phippen, B., Fowler, P., Noble, R.T., and Oliver, J.D. (2017) Differences in abundances of total *Vibrio spp*., *V. vulnificus*, and *V. parahaemolyticus* in clams and oysters in North Carolina. *Appl Environ Microbiol* **83**: e02265-16.

Gavin, H.E. and Satchell, K.J.F. (2015) MARTX toxins as effector delivery platforms. *Pathog Dis* **73**: 1–9.

Haenen, O.L.M., Fouz, B., Amaro, C., Isern, M.M., Mikkelsen, H., Zrncic, M., et al. (2014). Vibriosis in aquaculture. 16th EAFP Conference, Tempere, Finland, 4th September 2013. *Bull Eur Ass Fish Pathol* **34**: 138–146.

Henderson, P.A., Plenty, S.J., Newton, L.C., and Bird, D.J. (2012) Evidence for a population collapse of European eel (*Anguilla anguilla*) in the Bristol Channel. *J Mar Biol Assoc United Kingdom* **92**: 843–851.

Heng, S.P., Letchumanan, V., Deng, C.Y., Ab Mutalib, N.S., Khan, T.M., Chuah, L.H., et al. (2017) *Vibrio vulnificus*: an environmental and clinical burden. *Front Microbiol* **8**: 997.

Horseman, M.A. and Surani, S. (2011) A comprehensive review of *Vibrio vulnificus*: an important cause of severe sepsis and skin and soft-tissue infection. *Int J Infect Dis* **15**: e157–e166.

Igbinosa, E.O. (2016) Detection and antimicrobial resistance of *Vibrio* isolates in aquaculture environments: implications for public health. *Microb Drug Resist* **22**: 238–245.

Jehannet, P., Heinsbroek, L.T.N., and Palstra, A.P. (2017) Ultrasonography to assist with timing of spawning in European eel. *Theriogenology* **101**: 73–80.

Jeong, H.G. and Satchell, K.J.F. (2012) Additive function of *Vibrio vulnificus* MARTXVv and VvhA cytolysins promotes rapid growth and epithelial tissue necrosis during intestinal infection. *PLoS Pathog* **8**: e1002581.

Jones, M.K. and Oliver, J.D. (2009) *Vibrio vulnificus*: disease and pathogenesis. *Infect Immun* **77**: 1723–1733.

Karunasagar, I. (2014) *Vibrio vulnificus.* In Encyclopaedia of food safety. Motarjemi Y., and Moy G.,T.E. (eds) Elsevier. pp. 564–569.

Kaspar, C.W. and Tamplin, M.L. (1993) Effects of temperature and salinity on the survival of *Vibrio vulnificus* in seawater and shellfish. *Appl Environ Microbiol* **59**: 2425–2429.

Kirkegaard, E. (2010) European eel and aquaculture. DTU Aqua Report 229, National Institute of Aquatic Resources, Technical University of Denmark. pp.19.

Lee, C.T., Pajuelo, D., Llorens, A., Chen, Y.H., Leiro, J.M., Padrós, F., et al. (2013) MARTX of *Vibrio vulnificus* biotype 2 is a virulence and survival factor. *Environ Microbiol* **15**: 419–432.

Li, Z., Chen, H., Chen, X., Zhou, T., Zhao, L., Zhang, C., et al. (2012) Genome sequence of the human-pathogenic bacterium *Vibrio vulnificus* type strain ATCC 27562. *J Bacteriol* **194**: 6954–6955.

Lim, C.E. and Webster, C.D. (2006) Tilapia: biology, culture and nutrition. The Haworth Press, Inc., Binghamton, New York.

Marco-Noales, E., Biosca, E.G., and Amaro, C. (1999) Effects of salinity and temperature on long-term survival of the eel pathogen *Vibrio vulnificus* biotype 2 (serovar E). **65**: 1117–1126.

Menon, M.P., Yu, P.A., Iwamoto, M., and Painter, J. (2014) Pre-existing medical conditions associated with *Vibrio vulnificus* septicaemia. *Epidemiol Infect* **142**: 878–881.

Mes, D., Dirks, R.P., and Palstra, A.P. (2016) Simulated migration under mimicked photothermal conditions enhances sexual maturation of farmed European eel (*Anguilla anguilla*). *Aquaculture*. **452**: 367–372.

Morera, D. and MacKenzie, S.A. (2011) Is there a direct role for erythrocytes in the immune response? *Vet Res* **42**: 89.

Morera, D., Roher, N., Ribas, L., Balasch, J.C., Doñate, C., Callol, A., et al. (2011) Rna-seq reveals an integrated immune response in nucleated erythrocytes. *PLoS One* **6**: e26998.

Morrison, S.S., Williams, T., Cain, A., Froelich, B., Taylor, C., Baker-Austin, C., et al. (2012) Pyrosequencing-based comparative genome analysis of *Vibrio vulnificus* environmental isolates. *PLoS One* **7**: e37553.

Murciano, C., Lee, C.T., Fernández-Bravo, A., Hsieh, T.H., Fouz, B., Hor, L.I., et al. (2017) MARTX toxin in the zoonotic serovar of *Vibrio vulnificus* triggers an early cytokine storm in mice. *Front Cell Infect Microbiol* **7**: 1–19.

Muroga, K., Jo, Y., and Nishibuchi, M. (1976) Pathogenic *Vibrio* isolated from cultured eels. Characteristics and taxonomic status. *Fish Pathog* **11**: 141–145.

Nielsen, T. and Prouzet, P. (2008) Capture-based aquaculture of the wild European eel (*Anguilla anguilla*). In Capture-based aquaculture: global overview Edition: FAO Fisheries Technical Paper 508. Lovatelli, A. and Holthus, P.F. (eds). FAO.

Oliver, J.D. (2015) The biology of *Vibrio vulnificus*. *Microbiol Spectr* **3**: 1–10.

Pajuelo, D., Lee, C.T., Roig, F.J., Hor, L.I., and Amaro, C. (2015) Novel host-specific iron acquisition system in the zoonotic pathogen *Vibrio vulnificus*. *Environ Microbiol* **17**: 2076–2089.

Pajuelo, D., Lee, C.T., Roig, F.J., Lemos, M.L., Hor, L.I., and Amaro, C. (2014) Host-nonspecific iron acquisition systems and virulence in the zoonotic serovar of *Vibrio vulnificus*. *Infect Immun* **82**: 731–744.

Palstra, A.P., Cohen, E.G.H., Niemantsverdriet, P.R.W., Van Ginneken, V.J.T., and Van Den Thillart, G.E.E.J.M. (2005) Artificial maturation and reproduction of European silver eel:

development of oocytes during final maturation. *Aquaculture*. **249**: 533–547.

Paranjpye, R.N. and Strom, M.S. (2005) A *Vibrio vulnificus* type IV pilin contributes to biofilm formation, adherence to epithelial cells, and virulence. *Infect Immun* **73**: 1411–1422.

Park, J.H., Cho, Y.J., Chun, J., Seok, Y.J., Lee, J.K., Kim, K.S., et al. (2011) Complete genome sequence of *Vibrio vulnificus* MO6-24/O. *J Bacteriol* **193**: 2062–2063.

Pereiro, P., Romero, A., Díaz-Rosales, P., Estepa, A., Figueras, A., and Novoa, B. (2017) Nucleated teleost erythrocytes play an Nk-lysin and autophagy-dependent role in antiviral immunity. *Front Immunol* **8**: 1–15.

Rhee, J.E., Rhee, J.H., Ryu, P.Y., and Choi, S.H. (2002) Identification of the *cadBA* operon from *Vibrio vulnificus* and its influence on survival to acid stress. *FEMS Microbiol Lett* **208**: 245–251.

Roig, F.J., Gonzalez-Candelas, F., and Amaro, C. (2011) Domain organization and evolution of multifunctional autoprocessing repeats-in-toxin (MARTX) toxin in *Vibrio vulnificus*. *Appl Environ Microbiol* **77**: 657–668.

Roig, F.J., González-Candelas, F., Sanjuán, E., Fouz, B., Feil, E.J., Llorens, C., et al. (2018) Phylogeny of *Vibrio vulnificus* from the analysis of the core-genome: implications for intra-species taxonomy. *Front Microbiol* **8**: 1–13.

Roig, F.J., Sanjuan, E., Llorens, A., and Amaro, C. (2010) *pilF* polymorphism-based PCR to distinguish *Vibrio vulnificus* strains potentially dangerous to public health. *Appl Environ Microbiol* **76**: 1328–1333.

Rosche, T.M., Yano, Y., and Oliver, J.D. (2005) A rapid and simple PCR analysis indicates there are two subgroups of *Vibrio vulnificus* which correlate with clinical or environmental isolation. *Microbiol Immunol* **49**: 381–389.

Sanjuán, E. and Amaro, C. (2004) Protocol for specific isolation of virulent strains of *Vibrio vulnificus* serovar E (Biotype 2) from environmental samples. *Appl Environ Microbiol* **70**: 7024–7032.

Sanjuán, E., González-Candelas, F., and Amaro, C. (2011) Polyphyletic origin of *Vibrio vulnificus* biotype 2 as revealed by sequence-based analysis. *Appl Environ Microbiol* **77**: 688–695.

Satchell, K.J.F. (2007) MARTX, multifunctional autoprocessing repeats-in-toxin toxins. *Infect*

Immun **75**: 5079–5084.

Satchell, K.J.F. (2015) Multifunctional-autoprocessing repeats-in-toxin (MARTX) Toxins of *Vibrios*. *Microbiol Spectr* **3**.

Satchell, K.J.F. (2011) Structure and function of MARTX toxins and other large repetitive RTX proteins. *Annu Rev Microbiol* **65**: 71–90.

Shin, S.H., Shin, D.H., Ryu, P.Y., Chung, S.S., and Rhee, J.H. (2002) Proinflammatory cytokine profile in *Vibrio vulnificus* septicemic patients' sera. *FEMS Immunol Med Microbiol* **33**: 133–138.

Takemura, A.F., Chien, D.M., and Polz, M.F. (2014) Associations and dynamics of Vibrionaceae in the environment, from the genus to the population level. *Front Microbiol* **5**: 38.

Tao, Z., Larsen, A.M., Bullard, S.A., Wright, A.C., and Arias, C.R. (2012) Prevalence and population structure of *Vibrio vulnificus* on fishes from the northern Gulf of Mexico. *Appl Environ Microbiol* **78**: 7611–7618.

Tesch, F. (2003) The Eel. 3rd Edition. Blackwell Science, Oxford.

Tison, D.L., Nishibuchi, M., Greenwood, J.D., and Seidler, R.J. (1982) *Vibrio vulnificus* biogroup 2: new biogroup pathogenic for eels. *Appl Environ Microbiol* **44**: 640–646.

Valiente, E. and Amaro, C. (2006) A method to diagnose the carrier state of *Vibrio vulnificus* serovar E in eels: development and field studies. *Aquaculture* **258**: 173–179.

Valiente, E., Lee, C.T., Lamas, J., Hor, L., and Amaro, C. (2008) Role of the virulence plasmid pR99 and the metalloprotease Vvp in resistance of *Vibrio vulnificus* serovar E to eel innate immunity. *Fish Shellfish Immunol* **24**: 134–141.

van Ginneken, V.J.T. and Maes, G.E. (2005) The European eel (*Anguilla anguilla*), its life cycle, evolution and reproduction: a Literature Review. *Rev Fish Biol Fish* **15**: 367–398.

Veenstra, J., Rietra, P.J., Stoutenbeek, C.P., Coster, J.M., de Gier, H.H., and Dirks-Go, S. (1992) Infection by an indole-negative variant of *Vibrio vulnificus* transmitted by eels. *J Infect Dis* **166**: 209–210.

Vugia, D.J., Tabnak, F., Newton, A.E., Hernandez, M., and Griffin, P.M. (2013) Impact of 2003 state regulation on raw oyster-associated *Vibrio vulnificus* illnesses and deaths, California, USA. *Emerg Infect Dis* **19**: 1276–1280.

Wang, Z.G., Wu, Z., Xu, S.L., and Zha, J. (2012) Genome sequence of the human-pathogenetic bacterium *Vibrio vulnificus* B2. *J Bacteriol* **194**: 7019.

Weinberg, E.D. (2009) Iron availability and infection. *Biochim Biophys Acta Gen Subj* **1790**: 600–605.

Williams, T.C., Ayrapetyan, M., Ryan, H., and Oliver, J.D. (2014) Serum survival of *Vibrio vulnificus*: role of genotype, capsule, complement, clinical origin, and in Situ incubation. *Pathogens* **3**: 822–832.

HYPOTHESIS AND OBJECTIVES

The **global aim** of this thesis was to gain insights into the understanding of how *V. vulnificus* causes septicemia in hosts as evolutionary distant as human and fish. To this end, we have selected a representative strain of the zoonotic clonal-complex and two *ex vivo* and *in vitro* models of septicemia and we have applied a combination of transcriptomic and single gene approaches.

Our hypotheses were:

1. Iron and temperature (water or host) are two external signals that control virulence in *V. vulnificus*.

2. The interplay between fish erythrocytes and $RtxA1_3$ plays an essential role in fish septicemia.

The outcome of an infection depends on several factors, being the most relevant the virulent mechanisms expressed by the pathogen and the host ability to modulate a suitable immune response to eliminate the pathogen. Thus, a comprehensive understanding of host-pathogen relationship requires knowing the gene expression changes occurring in both the pathogen and the host during the infection (**FIGURE 1**). For this reason, the **specific objectives** to achieve in this work were:

1. To determine *V. vulnificus* relevant virulence factors to trigger infection, specially focusing on:

    a. How does iron influence *V. vulnificus* virulence? **CHAPTER 1**
        i. To study the global bacterial transcriptome *in vitro* at iron restricted and iron rich culture media, using a microarray platform.

    b. How does host innate immunity influence *V. vulnificus* virulence?
        i. To study the global bacterial transcriptome *ex vivo* (serum) using a microarray platform. **CHAPTER 2**
        ii. To study the global bacterial transcriptome *ex vivo* (artificial blood) by using an RNAseq approach. **CHAPTER 4**

    c. How does temperature influence *V. vulnificus* virulence? **CHAPTER 3**
        i. To study the global bacterial transcriptome *in vitro* at different temperatures, using a microarray platform.

2. To determine European eel relevant immune response signals against vibriosis:

    a. How does eel innate immunity respond to infection? Is RtxA1$_3$ toxin involved in triggering a detrimental immune response which favors animal death and bacterial dispersion?

        i. To study the global eel transcriptome *ex vivo* in eel artificial blood infected with *V. vulnificus*, using an RNAseq approach. **CHAPTER 4**

        ii. To study the global transcriptome of eel blood cells *in vivo* during the establishment of the vibriosis, using a microarray platform. **CHAPTER 5**

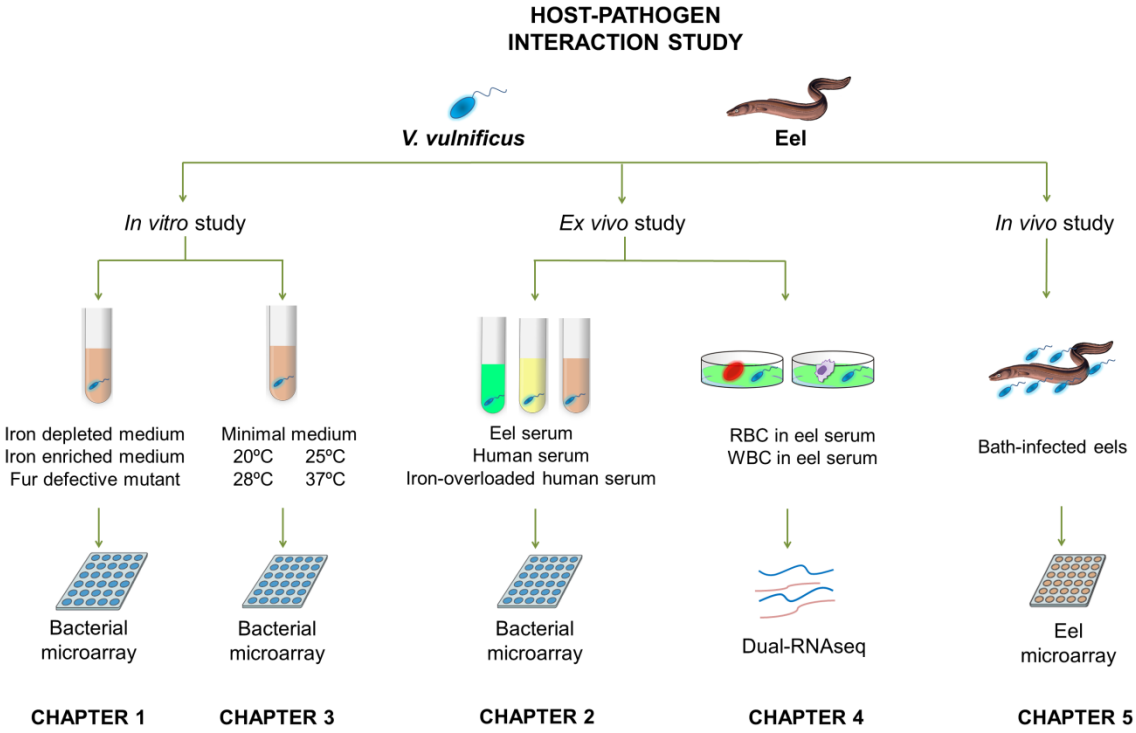

FIGURE 1 | General experimental design followed through this thesis to achieve the proposed objectives.

GENERAL METHODOLOGY

Molecular tools have evolved very fast during the last decades and nowadays there are multiple genomic and transcriptomic tools available that allow researchers to understand the complex biology of species. Of special interests are those functional genomic tools that have evolved to analyze the differential expression of thousands of transcripts at a time (sometimes even studying whole genome transcriptomes [i.e., bacterial genomes]). Microarray technology was one of the first molecular tools adapted to be used in transcriptomic studies, although the introduction of high-throughput technologies for cDNA massive sequencing (RNAseq) has partially replaced it during the last years (Bellin *et al.*, 2009; Wang *et al.*, 2009; Metzker, 2010). However, as molecular tools that can be successfully applied in differential expression analysis, both microarray and RNAseq have advantages and disadvantages and in many cases they might be used as complementary approaches for the same study (Malone and Oliver, 2011; Sîrbu *et al.*, 2012). For example, although RNAseq is more sensitive, it is more expansive, more laborious and only gives results about gene quantification in absolute terms. Microarray tools are cheaper, easier to use and the time taken in the whole process is shorter (Sîrbu *et al.*, 2012). Thus, microarray seems more useful for specific purposes or custom approaches while RNAseq could be better applied in exploratory experiments.

In any case, for gene expression analysis in host-pathogen interaction studies, the major advantage of RNAseq over microarray is that it does not require the pathogen and host cells to be physically separated before sequencing (dual-RNAseq), as it is a probe-independent tool. On the contrary, microarrays are probe-dependent approaches and require immobilized gene-specific DNA probes, in custom and separate platforms for host and pathogen, which hybridize to their corresponding labeled cDNA. Thus, dual-RNAseq allows sequencing and analyzing transcriptomes of two species together without previous treatment to separate samples from each organism and therefore, it is possible to monitor host and pathogen gene expression in parallel (Westermann *et al.*, 2012). **FIGURE 1** shows the fundamental differences between microarray and dual-RNAseq approaches in gene expression analysis. However, dual-RNAseq still has potential limiting factors that must be considered when planning experiments. For instance, eukaryotic cells contain around 150 times more RNA than prokaryotic cells, which must be taken into account when estimating the required sequencing depth, with more reads required for the pathogen than for the host (Westermann *et al.*, 2012). Moreover, this limitation could even make dual-RNAseq impossible to use in gene expression analysis during *in vivo* infections when very few bacteria cause animal death.

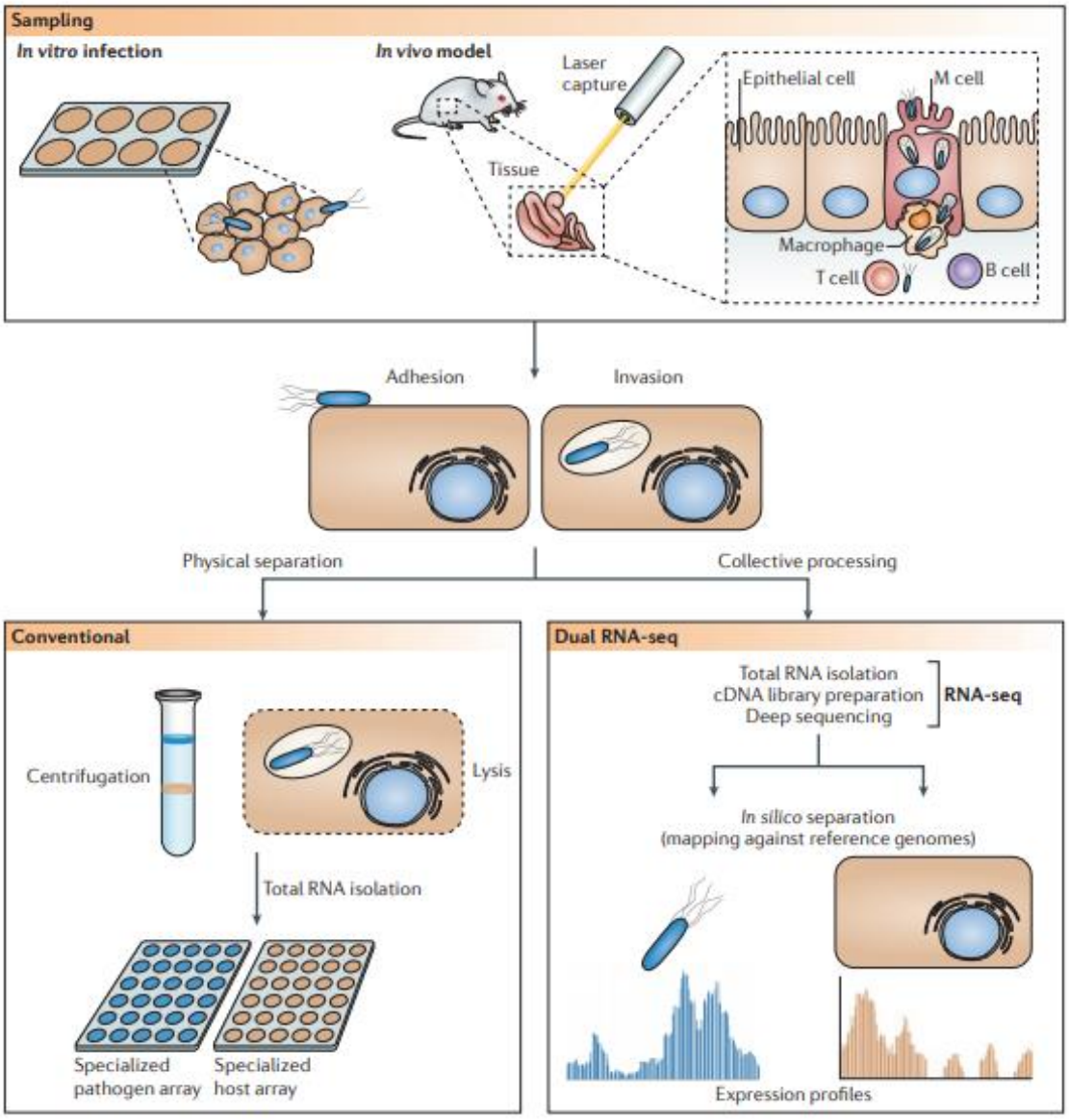

FIGURE 1 | Fundamental differences between microarray and dual-RNAseq approaches in gene expression analysis. Probe-dependent approaches such us microarray require that the host and pathogen cells be physically separated before the hybridization with a set of specific and customized probes. By contrast, probe-independent approaches such us RNAseq enable that two organisms are analyzed collectively (dual-RNAseq) and discrimination of host and pathogen transcripts is done at the bioinformatics step. Image taken from Westermann *et al.*, (2012).

The common approach used throughout this thesis was to combine transcriptomic studies (either using microarray platforms or dual-RNAseq) to identify new hypothetic relevant virulence/immune genes with single gene studies (using mutant bacterial strains) to confirm the transcriptomic results. For this reason, the general procedures followed to obtain microarray and dual-RNAseq data are explained below, while specific methodology used to achieve each objective is detailed in the corresponding chapter.

1. Microarray

Bacteria (*V. vulnificus* R99 strain) and host (European eel) custom designed microarray platforms were used (Agilent ID 041079 and 042990, respectively). Specific platforms, 8x15K for bacteria and 4x44K for eel, were designed with eArray software (Agilent technologies) using 60 nt probes for predicted ORF's (4,553 targets in R99 genome (Pajuelo, 2013) and 44,715 targets in European eel immunotranscriptome (Callol *et al.*, 2015)). The complete design of each platform is available at GEO (Gene Expression Omnibus) database with the accession numbers GPL19040 and GPL16775 for *V. vulnificus* and eel devices, respectively.

In both cases, total RNA was extracted using NucleoZOL (Macherey-Nagel), subjected to DNasa treatment using TURBO^{TM} DNase (Ambion) and cleaned with the RNA Cleanup and Concentration Micro Kit (Thermo Scientific). RNA concentration and integrity were measured using a 2100 Bioanalyzer (Agilent) and only samples with RIN (RNA Integrity Number) ≥ 7.5 were selected to obtain labelled cDNA. The specific labelling steps were slightly modified depending on the origin of each sample (either bacterial or eukaryotic). In case of bacterial samples, cDNA was obtained by mixing 200 µg of the total RNA with 200 ng of T7N9 and was subjected to a transcription reaction to finally obtain cDNA labeled with Cy3 (cyanine 3) dye; while in case of eel samples, 200 µg of the total RNA were directly used for indirect labelling with Cy3 dye. In both cases, 1.65 µg of the obtained cDNA labeled samples were dispensed onto the gasket well on the respective custom slides and were placed in a hybridization oven with rotation at 10 rpm at 65ºC for 17 h. All procedures were performed following manufacturer's instructions for one-color microarray-based gene expression analysis along with Agilent's one-color RNA spikeIn kit. After washing the slides, scanning was performed with an Axon Scanner 4000B.

The data were extracted using Feature extraction software (Agilent technologies) and the quality reports were generated and checked for each microarray. Then, the extracted data of the appropriate quality were analyzed with Genespring 14.5 GX software (Agilent technologies) using the 75% percentile normalization for appropriate comparisons, where values were compared using the most accurate statistical analysis available in the Genespring software to reveal transcriptomic profile differences between tested conditions.

2. Dual-RNAseq

For dual-RNAseq experiments, we obtained samples containing both bacteria and eel blood cells and extracted total RNA using RNeasy MinElute Cleanup kit (Qiagen). Then, total RNA was subjected to DNasa treatment using TURBO™ DNase (Ambion) and cleaned with the RNeasy MinElute Cleanup kit (Qiagen). Once checked RNA concentration and integrity using Qubit, rRNA was depleted from samples using Ribo-Zero™ Gold Removal Kit (Illumina). Finally, libraries construction and NextSeq500 sequencing (between 1 and 30 million reads depending on the sample: 1 million reads for samples that only contained bacterial RNA; 5 million reads for samples that only contained eel RNA; 30 million reads for samples that contained mixed RNA from bacterial and eel) was performed at Servei de Genòmica of SCSIE (Servei Central de Suport a la Investigació Experimental [Central Service for Experimental Research]) of Universitat de València.

Illumina reads were filtered with fastq-mcf software (Aronesty, 2011), aligned with reference genomes using Bowtie2 software (Langmead and Salzberg, 2012) and treated with SAMTools (Li *et al.*, 2009). Finally, differential expression analysis was performed using FeatureCounts (Liao *et al.*, 2014) and EdgeR packages (Robinson *et al.*, 2010).

3. References

Aronesty, E. (2011) Command-line tools for processing biological sequencing data. ea-utils https://expressionanalysis.github.io/ea-utils/: Expression Analysis, Durham, NC.

Bellin, D., Ferrarini, A., Chimento, A., Kaiser, O., Levenkova, N., Bouffard, P., et al. (2009) Combining next-generation pyrosequencing with microarray for large scale expression analysis in non-model species. *BMC Genomics* **10**: 555.

Callol, A., Reyes-Lopez, F.E., Roig, F.J., Goetz, G., Goetz, F.W., Amaro, C., et al. (2015) An enriched European eel transcriptome sheds light upon host-pathogen interactions with *Vibrio vulnificus*. *PLoS One* **10**: e0133328.

Langmead, B. and Salzberg, S.L. (2012) Fast gapped-read alignment with Bowtie 2. *Nat. Methods* **9**: 357–359.

Li, H., Handsaker, B., Wysoker, A., Fennell, T., Ruan, J., Homer, N., et al. (2009) The Sequence Alignment/Map format and SAMtools. *Bioinformatics* **25**: 2078–2079.

Liao, Y., Smyth, G.K., and Shi, W. (2014) featureCounts: an efficient general purpose program for assigning sequence reads to genomic features. *Bioinformatics* **30**: 923–930.

Malone, J.H. and Oliver, B. (2011) Microarrays, deep sequencing and the true measure of the transcriptome. *BMC Biol.* **9**: 34.

Metzker, M.L. (2010) Sequencing technologies - the next generation. *Nat. Rev. Genet.* **11**: 31–46.

Pajuelo, D. (2013) Iron and virulence in the zoonotic pathogen *Vibrio vulnificus*. PhD Thesis. Universitat de València.

Robinson, M.D., McCarthy, D.J., and Smyth, G.K. (2010) edgeR: a Bioconductor package for differential expression analysis of digital gene expression data. *Bioinformatics* **26**: 139–140.

Sîrbu, A., Kerr, G., Crane, M., and Ruskin, H.J. (2012) RNA-Seq vs dual- and single-channel microarray data: sensitivity analysis for differential expression and clustering. *PLoS One* **7**: e50986.

Wang, Z., Gerstein, M., and Snyder, M. (2009) RNA-Seq: a revolutionary tool for transcriptomics. *Nat. Rev. Genet.* **10**: 57–63.

Westermann, A.J., Gorski, S.A., and Vogel, J. (2012) Dual RNA-seq of pathogen and host. *Nat. Rev. Microbiol.* **10**: 618–630.

CHAPTER 1

Role of iron and fur in the life cycle of *Vibrio vulnificus*

Pajuelo, D., **Hernández-Cabanyero, C.**, Sanjuán, E., Lee, C.T., Silva-Hernández, F.X., Hor, L.I., MacKenzie, S., and Amaro, C. (2016) Iron and Fur in the life cycle of the zoonotic pathogen *Vibrio vulnificus*. Environmental Microbiology 18: 4005–4022.

1. Introduction

V. vulnificus is a siderophilic pathogen that requires high levels of free iron in human blood to cause the most severe vibriosis. This statement is based on epidemiological studies on clinical cases of human vibriosis that show a high correlation between death rate by sepsis and high levels of free iron in blood caused by different underlying pathologies (Horseman and Surani, 2011).

Free iron is presumably available to *V. vulnificus* in the nutrient enriched environment characteristic of intensive fish farming industry but it is unavailable inside the hosts due to nutritional immunity, an ancestral mechanism of defense common to fish and mammals (Weinberg, 2009). Thus, iron is present in host tissues either complexed to heme groups, forming part of the hemic proteins such as hemoglobin, or sequestered by transferrin in blood or lactoferrin in secretions, with all of these proteins binding Fe^{3+} with an exceptionally high affinity (Hood and Skaar, 2012). It has been demonstrated that *V. vulnificus* produces two iron uptake systems under starvation *in vitro* and that both of them are required for full virulence in mice and eels, the animal models for human and fish vibriosis, respectively (Pajuelo *et al.*, 2014). The two systems are the siderophore vulnibactin (an exogenous chelating agent that sequesters iron from transferrin) together with its receptor VuuA as well as a receptor for hemin (HupA). However, the expression of both iron uptake systems *in vivo* seems not to be enough for the bacterium to multiply in blood and cause septicemia in healthy humans. Interestingly, strains belonging to the zoonotic clonal-complex can also produce a third iron uptake system encoded in the fish virulence plasmid pVvbt2 (Pajuelo *et al.*, 2015). This system relies on an outer membrane receptor for fish transferrin (Ftbp), which allows the growth of the pathogen in blood and makes it highly virulent for healthy fish, especially eels (LD_{50} [lethal dose 50] for eels around 10-200 CFU/fish) (Amaro *et al.*, 1995; Pajuelo *et al.*, 2015). The deletion of the gene encoding this protein makes the bacterium avirulent for eels, which demonstrate the importance of iron for the bacterium to produce death by sepsis.

The main iron responsive transcriptional factor is Fur (Ferric Uptake Regulator) protein. Initially, Fur was described as a negative regulator that uses iron as a cofactor (holo-repression) to control the transcription of genes related to iron acquisition (Hantke, 2001). However, later studies suggest that Fur could also control other bacterial processes such as acid shock response, chemotaxis, metabolic pathways, bioluminescence and production of toxins and other virulence factors, in some cases through a positive regulation (Troxell and Hassan, 2013). Finally, Fur controls its own transcription as well as that of a few virulence

genes (including those for iron uptake) and two master regulator genes, *smcR* and *rpoS*, in *V. vulnificus* (Lee *et al.*, 2003; Alice *et al.*, 2008; Kim *et al.*, 2013).

In this study, we aimed to unravel the role of iron not only in virulence for humans and fish but also in the life cycle of *V. vulnificus* out of its hosts. Our hypothesis was that exogenous iron acts as a general signal that the bacterium senses and to which it responds by changing the transcription of important genes involved not only in iron uptake but also in its survival both inside and outside its hosts. To this end, we selected a strain belonging to the zoonotic clonal-complex (R99 strain), the only one able to infect both humans and fish, whose genome (sequenced and annotated) was used to design a specific microarray platform (Pajuelo, 2013) (p. 65). Then, we analyzed and compared the transcriptomic profiles of R99 strain and that of its derivative mutant Δ*fur* (Pajuelo, 2013) in a minimal medium with and without free iron, conditions that simulate the infection process in terms of variations in iron concentration: from tank water to a fish (the bacterium would sense a decrease in iron concentration) and from a diseased fish to a human wound from a risk patient (the bacterium would sense an increase in iron concentration). Finally, the transcriptomic results that we detected as relevant for bacterial survival inside and outside the animal and human hosts were confirmed by performing a series of phenotypic *in vivo* and *in vitro* experiments specifically designed for each gene or group of genes.

TABLE 1 | Characteristics of the strains used in this study and its virulence for eels and mice.

Strain	Description	Virulence (LD_{50})[1]				
		Mice (i.p.)		Eel		
		normal	iron-overloaded	Bath		i.p.
				normal	iron-overloaded	
R99	*V. vulnificus* zoonotic clonal-complex representative strain. Isolated from a diseased eel in Spain (Roig *et al.*, 2018)	$2.6x10^4$	<5x10	$1.2x10^6$	$7.6x10^5$	$1x10^2$
Δfur	R99 *fur* defective mutant (Pajuelo, 2013)	$9x10^4$	$1x10^2$	$7.2x10^6$	$1.6x10^6$	$3x10^3$
cfur	Δ*fur* complemented strain (Pajuelo, 2013)	$2x10^4$	NT	$7.1x10^6$	NT	$1.3x10^2$

NT, non tested

[1]Virulence was expressed as LD_{50} in CFU/fish or mouse in case of i.p. infection and CFU/ml in case of bath infection.

2. Material and methods

Bacterial strains, bacterial counting and growth conditions

Bacterial strains (**TABLE 1**) were routinely grown in CM9/CM9A (M9 broth/agar (Miller, 1972) supplemented with 0.2% casamino acids) or on TSA-1 plates (TSA [tryptone soy agar], 1% NaCl) at 28ºC. To analyze the effect of exogenous iron on growth, the following culture media were used: CM9/CM9A-$Fe_{(D)}$ (media supplemented with 100 µM of the iron chelator 2,2'-bipyridyl [Sigma-Aldrich]), CM9/CM9A+Fe (media supplemented with 100 µM $FeCl_3$) and CM9+Tf (media supplemented with 10 µM of the iron chelator human apo-transferrin [Sigma-Aldrich]). In case of liquid cultures and unless clearly specified, 5 ml of medium were inoculated with overnight bacteria (18 h cultures) at a ratio 1:100 (v/v) and incubated with shaking (60 rpm, New Brunswick Scientific Agitator). For bacterial counting, the drop plate method on TSA-1 was used (Hoben and Somasegaran, 1982). All the strains were stored in LB-1 (Luria Bertani broth 1% NaCl) plus 20% glycerol at -80ºC.

Microarray analysis

The experimental design for microarray analysis as well as the performed transcriptomic comparisons are shown in **FIGURE 1**. The R99-microarray platform was used (accession number GPL19040). *Sample preparation*. Total RNA from mid-log phase cultures (6 h; Abs_{625} 0.3) was extracted, labelled and hybridized on microarray as detailed in p. 65. *Data analysis*. The following comparisons were performed: R99 in CM9+Tf vs CM9+Fe (iron stimulon) and Δ*fur* vs R99 both in CM9 (Fur regulon). The data were analyzed using the GeneSpring 14.5 GX software as described in p. 65. *Microarray validation by RT-qPCR.* The same RNA samples used for the microarray analysis were analyzed by RT-qPCR to calculate the expression of selected genes (primers listed in **TABLE 2**). To this end, cDNA was produced from 1 µg of RNA using Maxima Reverse Transcriptase (Thermo Scientific) as described by the manufacturer. qPCRs were carried out using Power SYBR® Green PCR Master Mix (Applied Biosystems) and the StepOne Plus RT-PCR System (Applied Biosystems). Reactions were carried out in a final volume of 10 µl (5 µl 2x Master Mix, 2 µl DEPC H_2O, 1 µl cDNA, 1 µl forward primer, 1 µl reverse primer) and the settings consist of 10 min of denaturalization at 95ºC followed by 40 cucles of 15 sec of denaturalization at 95ºC and 1 min of annealing and extension at 62ºC. The *recA* gene was used as standard and the fold induction ($2^{-\Delta\Delta Ct}$) for each gene was calculated according to Livak and Schmittgen (2001).

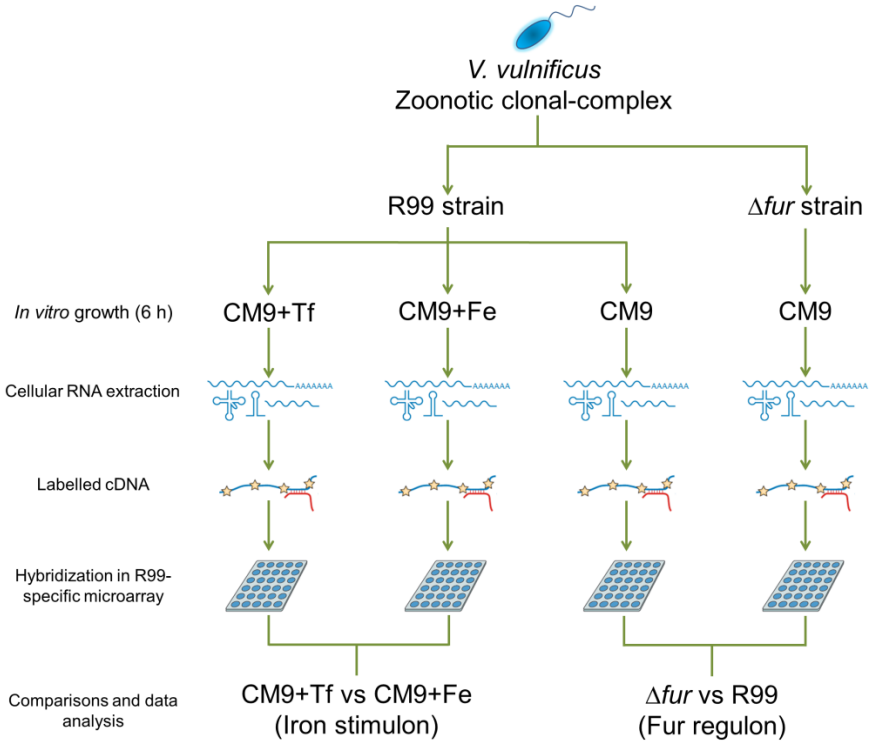

FIGURE 1 | Experimental design.

***In vivo* assays**

Animal maintenance and extraction of blood and serum. Mice (6- to 8-week-old female BALB/c, Charles River, France) and eels (*Anguilla anguilla;* from a local farm) of around 20 g of body weight were maintained and handled in the facilities of the SCSIE of the University of Valencia. Blood and serum were obtained from eels as previously described (Lee *et al.*, 2013). Briefly, eels were anaesthetized with 0.025 mg/ml MS222 (Tricaine methanesulfonate [Sigma-Aldrich]) and 1 ml of blood from the caudal vein was extracted with heparinized (50 mg/ml heparin [Sigma-Aldrich] in PBS) syringes. The collected blood was centrifuged at 3,000 rpm for 5 min in order to separate the cells from the serum. Serum was stored at -80ºC until use.

Virulence, colonization and invasion assays. Virulence for mice and eels of each strain was determined as LD_{50} (Reed and Muench, 1938) after infecting the animals with serial bacterial ten-fold dilutions. Eels were infected by both bath-immersion and i.p. (intra-peritoneal) injection (Amaro *et al.*, 1995) while mice were only i.p. infected (Amaro *et al.*, 1994). The effect of iron-overload in virulence was determined by comparing the LD_{50} values for normal and iron-overloaded animals (pre-injected with $FeCl_3$ [9 µg/g of animal] 2 h before challenge). Mortalities were only considered if the inoculated strain was recovered as a pure culture from internal organs.

TABLE 2 | Primers used in the study and microarray validation. Comparison of fold change values obtained by microarray and RT-qPCR with the *V. vulnificus* R99 and Δ*fur* strains. In case of RT-qPCR, results were obtained using *recA* as the reference gene and the fold induction ($2^{-\Delta\Delta Ct}$) for each gene was calculated.

Gene	Primer sequence	Sample	FC[1]	
			Microarray	RT-qPCR
2,3-DHBA-AMP ligase	Fw: AACGCCTTCCCCAATGC Rv: CAATCAAGCCTTCCGCCATA	Δ*fur* vs R99 in CM9	21.9 (++)	13.92 (++)
ABCt, ATP-binding protein	Fw: ACCGAGTGCTGGAGTTGTTC Rv: TGTATACGCCTGTTGCGGATT		11.9 (++)	15.03 (++)
54K polar flagellar sheath protein A	Fw: AGCAGCAACAAATGGCGATA Rv: CCTGCAGTCGCGATCGTT		- 34.2 (---)	-5 (-)
Carbon storage regulator	Fw: CGCGTAGGCGAAACACTGAT Rv: CCTTTAACACCCAGTACCGTTA		- 24.7 (--)	-2.7 (-)
Transketolase	Fw: AATCCGCGCACTCAGCAT Rv: GCCTGGATGGCCTGAGTTT		1.05 (=)	1.13 (=)
Pyruvate formate-lyase	Fw: ATCTGGGCAACAGAATCTATG Rv: GAACGCGTTACTAGCGTACGA		1.04 (=)	1.14 (=)
Bacterioferritin	Fw: AAGGCATCCCAAATCTGCAA Rv: TTTCTTGGGTATCTTCGCCAAT	CM9+Tf vs CM9+Fe in R99	45.19 (+++)	24.33 (++)
Catechol ABC transporter	Fw: TTTGCCGCCATCAAACAA Rv: GATGGTGAGCGCATCCACTT		41.18 (+++)	7.51 (+)
33 kDa chaperonin	Fw: TCGCTGGGAAGGCCATATT Rv: CTTTGCCCATCATGTCGTGTA		- 17.36 (--)	-2.63 (-)
54K polar flagellar sheath protein A	Fw: AGCAGCAACAAATGGCGATA Rv: CCTGCAGTCGCGATCGTT		- 55.3 (---)	-11.11 (--)
DNA-directed RNA polymerase, beta' subunit	Fw: CAAAACGCAAAAGTGAACAAG Rv: CCCGGCGTATTGCTGTTG		1.3 (=)	1.18 (=)
tcuB	Fw: TCTCTTCTTTTGGCTCAACGTTT Rv: TCCAATCCTCCCCCTTCCT		1.19 (=)	1.16 (=)
VBNC experiment				
aphC	Fw: CCCAGGTCAAGGTCTTGCA Rv: GATAACACCTTGTGGGTCGAT			
KatG	Fw: CCGTCAACAGCCCGAAAA Rv: TGCTTGGGCCATCTTGGT			
Reference gene				
recA	Fw: CGCCAAAGGCAGAAATCG Rv: ACGAGCTTGAAGACCCATGTG			

[1]Qualitative classification of fold change (FC): =, -2<X<2; +, 2≤X<10; ++, 10≤X<25; +++, 25≤X; -, -10<X≤-2; --, -25<X≤-10; ---, X≤-25.

Ethical statement. All assays involving animals were approved by the Institutional Animal Care and Use Committee and the local authority (Generalitat Valenciana), following European Directive 2010/63/EU and the Spanish law 'Real Decreto' 53/2013 and were performed in the SCSIE facilities by using the protocols 2016-USC-PEA-00033 type 2 (virulence in eels) and 2014-VSC-PEA-00195 type 2 (virulence in mice). We also have a permission from Generalitat Valenciana to use eel for scientific research purposes.

***In vitro* assays**

Induction of the VBNC state and resuscitation. These experiments were performed by growing bacteria in MSWYE (marine seawater supplemented with yeast extract) (Biosca *et al.*, 1996), MSWYE+Fe (MSWYE plus 100 µM $FeCl_3$) and MSWYE-$Fe_{(D)}$ (MSWYE plus 100 µM 2,2'-bipyridyl). To induce the VBNC state, bacteria previously grown at 28ºC for 18 h were additionally incubated at 4ºC until no culturable bacterium was recovered by the drop plate method. To induce resuscitation, cultures with no detectable culturable bacteria were additionally incubated at 22ºC and the resuscitation dynamic was monitored again by the drop plate method. Selected genes from the microarray results were quantified by RT-qPCR during the induction of the VBNC state (**TABLE 2**).

Motility. Motility was assayed on MA (motility agar: CM9-agar [0.3% wt/v]), MA+Fe (MA plus 100 µM $FeCl_3$) and MA-$Fe_{(D)}$ (plus 100 µM of 2,2'-bipyridyl) by inoculating 5 µl from a mid-log phase culture in CM9. Plates were incubated at 28ºC for 24 h and the surface of each colony in mm^2 (SC) as well as the number of bacteria forming the colony in CFU (NB) were determined. Then, the motility rate was calculated as SC/log NB. In parallel, microscopic observations of bacterial suspensions were made in a Nikon Phase-Contrast Microscope.

Chemotaxis towards blood components. Human serum was purchased from Sigma-Aldrich. Eel serum was obtained as previously detailed (p. 75) and hemolytic eel serum was obtained by centrifuging eel blood at 13,000 rpm at 4ºC for 5 min. The chemotactic response towards serum was determined by using the capillary assay as described by Larsen *et al.*, (2001). To this end, bacteria were recovered from 6 h cultures in CM9, washed twice in PBS and diluted in CB (chemotaxis buffer; PBS plus 0.01 mM EDTA) at 10^7 CFU/ml (Larsen *et al.*, 2001). Then, volumes of 0.5 ml of bacterial suspension were dispensed in 1.5 ml eppendorfs that were put into contact with each serum or CB (control) contained in capillary tubes (5-µl pre-calibrated pipettes [Vitrex]) for 35 min at room temperature. The number of bacteria inside the capillaries was determined by the drop plate method and the chemotaxis response towards

each serum was expressed as the ratio between bacterial numbers in the corresponding capillaries vs control capillaries.

Biofilm production. Bacteria were grown in 96-well plates containing 200 µl of CM9, CM9+Fe and CM9-$Fe_{(D)}$ and biofilm production was quantified by the crystal violet method (Jones *et al.*, 2008) at 24 h of growth. Incubations were performed at 28ºC.

Growth in iron restriction with holo-transferrin as the sole iron source. Growth in CM9 supplemented with 10 µM holo-transferrin (Sigma-Aldrich) was monitored according to Pajuelo *et al.*, (2014). Bacteria were grown at 28ºC with shaking in 96-well plates containing 200 µl of medium and Abs_{625} was measured at 1 h intervals for 10 h.

MIC (Minimal inhibitory concentration) for microcide peptides. MICs for polymyxin B sulfate (Sigma-Aldrich), lysozyme (Sigma-Aldrich) and SDC (sodium deoxycholate [Sigma-Aldrich]) were determined in CM9A, CM9A+Fe and CM9A-$Fe_{(D)}$ plates. Plates were inoculated with mid-log phase cultures in CM9, CM9+Fe or CM9-$Fe_{(D)}$ and sterile disks impregnated with different concentrations of polymyxin B sulfate (1-10^3 µg/ml), lysozyme (1-10^3 µg/ml) or SDC (10^3-10^6 µg/ml) were added. The MIC was defined as the lowest substrate concentration at which there was not growth.

Resistance to acid, oxidative and nitrosative stresses. Washed bacteria from overnight cultures in CM9, CM9+Fe or CM9-$Fe_{(D)}$ at 28ºC were inoculated in tubes containing 5 ml of MSWYE (control), MSWYE-pH5 (acid stress) or PBS+H_2O_2 (0.1% vol/vol) (oxidative stress), supplemented or not with 100 µM $FeCl_3$ or 100 µM 2,2'-bipyridyl, at a concentration of 10^5 CFU/ml. Tubes were incubated at 28ºC with shaking for 180 min. Culturable bacteria were estimated by the drop plate method at 30 min intervals. To test resistance to nitrosative stress, bacteria from overnight cultures in CM9, CM9+Fe or CM9+Tf at 28ºC were washed in PBS and inoculated in the respective fresh medium supplemented or not with 400 µM (Z)-1-[N-(3-aminopropyl)-N-(3-ammoniopropyl)amino]diazen-1-ium-1,2-diolate (DPTA NONOate [NO [nitric oxide] donor, Cayman chemicals]). DPTA NONOate was decayed for 3 h in the medium in order to achieve a constant NO release (Henares *et al.*, 2012). Growth was followed by measuring Abs_{625} on a spectrophotometer at 1 h intervals for 8 h.

Hemolytic activity. The ECPs (extracellular products) from each strain were obtained from overnight cultures on CM9A+Fe or CM9A-$Fe_{(D)}$ as previously described (Biosca and Amaro, 1996). The hemolytic activity of ECPs and live bacteria was estimated by measuring Abs_{540} of

released hemoglobin of infected RBC (bovine erythrocytes from Sigma-Aldrich) (Shinoda *et al.*, 1985).

Envelope analysis. Crude fractions of surface cell-associated polysaccharides (LPS plus capsule) were obtained from overnight cultures in CM9, CM9+Fe or CM9+Tf according to Hitchcock and Brown (1983). 10 µg of cell-associated polysaccharides, quantified using the Total Carbohydrate Assay Kit (BioVision), were separated by SDS-PAGE (Laemmli, 1970) in discontinuous gels (4% stacking gel, 10% separating gel), transferred onto a PVDF membrane and subjected to immunoblot analysis. The membranes were probed with anti-serE specific serum (Amaro *et al.*, 1992) diluted 1:3,000 and were developed following incubation with anti-rabbit IgG HRP (Horseradish Peroxidase-conjugated secondary antibody diluted 1:10,000 (Sigma-Aldrich), using Immobilon Western Chemiluminescent HRP Substrate.

Statistical analysis. Presented data represent the averages ± standard error of at least three independent experiments. Statistical analysis was performed using SPSS 19.0. The significance of the differences between averages was tested by using the unpaired Student´s t-test with a $P< 0.05$. When the effects of more than two independent variables were taken into account an ANOVA analysis was performed. Virulence assays were only performed twice because no differences were found between the two replicates that justify killing more animals.

3. Results

Virulence for mice and eels

The role of iron and Fur in virulence was tested by comparing the virulence of R99 strain and their derivative mutants, Δ*fur* and c*fur*, for normal and iron-overloaded animals (**TABLE 1**). Iron pretreatment significantly increased the susceptibility to vibriosis of i.p. infected mice, regardless of the inoculated strain, whereas it did not affect virulence for eels (**TABLE 1**) (note that iron-overloaded eels were not i.p. infected due to the high virulence of the pathogen when using this route). In addition, *fur* deletion slightly reduced virulence for both mice and eels, regardless of the route of infection, and the full virulence was restored when the complete gene was introduced by conjugation in the mutant (**TABLE 1**).

Differentially expressed genes

A high percentage of genes in the genome of R99 strain were detected as DEGs (differentially expressed genes) in response to changes in exogenous iron concentrations

(25.35%) and presence or absence of Fur (38.96%) (**FIGURE 2**). Therefore, iron stimulon, defined as the set of genes whose transcription changes with exogenous iron levels, would be formed by 1,154 genes, while Fur regulon, defined as the set of genes whose transcription changes when *fur* is deleted, would be formed by 1,774 genes (**FIGURE 2**).

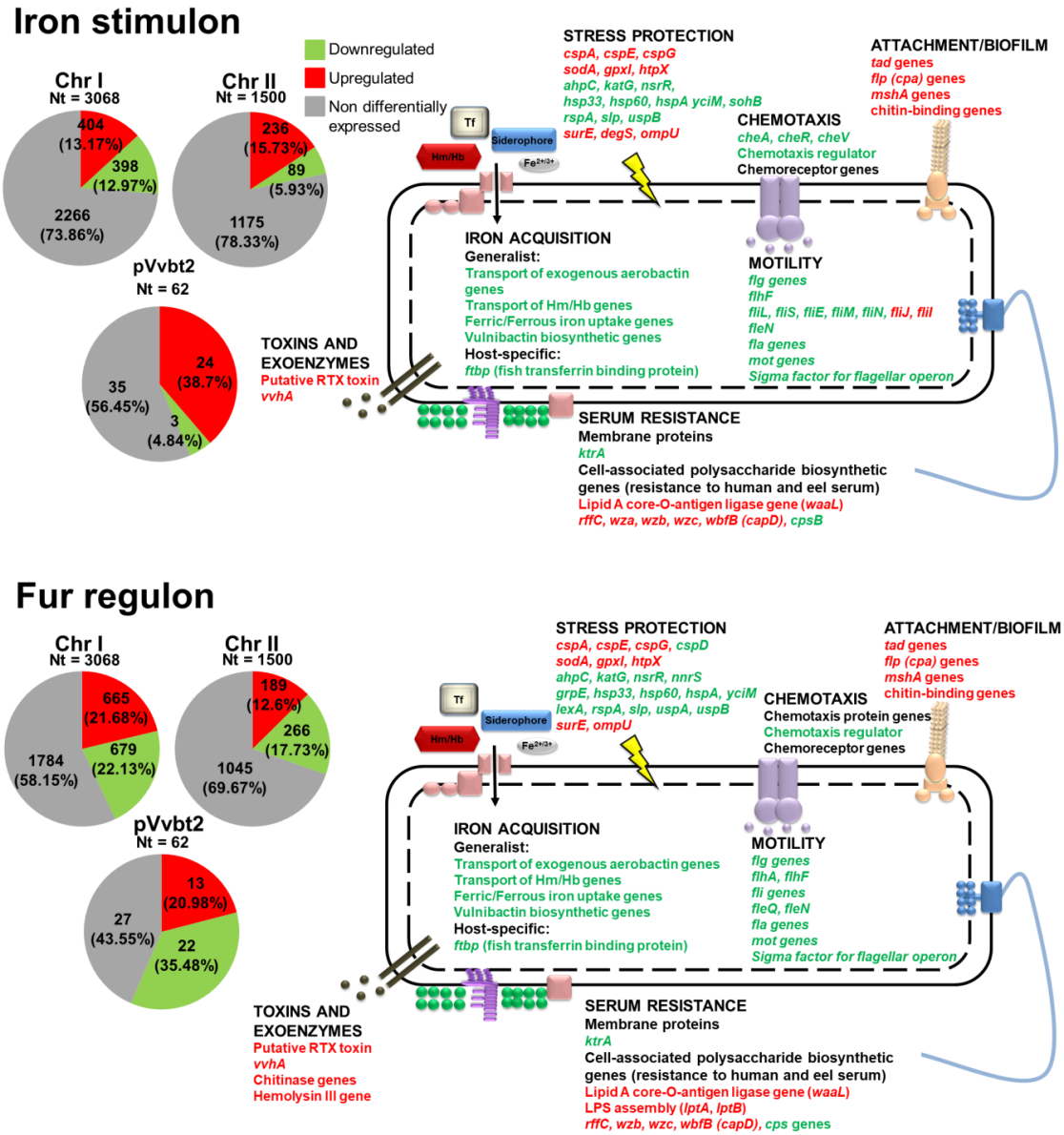

FIGURE 2 | DEGs by *V. vulnificus* in iron stimulon (CM9+Tf vs CM9+Fe) and Fur regulon (Δ*fur* vs R99). Genes which exhibited a value of fold change -2≤X≤2 with a p-value cut-off of *0.05* (averages from three independent biological samples) were considered as DEGs. Left: distribution of the DEGs per regulation category (down/upregulated or non-differentially expressed) and replicon (two chromosomes and one plasmid). The categories are represented with a color code. Right: main differentially affected virulence- and survival-related processes. Red color: upregulated genes; green color: downregulated genes; black color: a group of related genes for the same biological process, some up- and other downregulated**.**

TABLE 3 shows a selection of DEGs in iron stimulon and Fur regulon. Among the most strongly up- or downregulated genes under iron starvation, we found most of the plasmid genes (upregulated) and among the chromosomal ones those related with iron uptake (upregulated), cold shock resistance (upregulated), DNA sulfur modification (*dnd;* upregulated), flagellum biogenesis (downregulated), chemotaxis (downregulated) and drug resistance (downregulated) (**FIGURE 2** and **TABLE 3**). Interestingly, this pattern was highly similar to that found in Δ*fur* (**FIGURE 2** and **TABLE 3**). We highlight that most genes encoding response to different stressors, nutrient uptake and metabolism pathways were found to be under putative control by Fur and iron (**TABLE 3**).

Around 250 virulence and survival-related genes were clearly identified as putatively controlled by iron and/or Fur (**FIGURE 2** and **TABLE 3**), among them, genes encoding global transcriptional regulators (SmcR and HlyU) as well as the Fur protein (positively auto-regulated, as previously published (Lee *et al.*, 2007)) (**TABLE 3**). We found an acceptable correlation between microarray and RT-qPCR data corresponding to the genes selected for validation (**TABLE 2**).

TABLE 3 | Selected DEGs in *V. vulnificus* iron stimulon and Fur regulon.

Gene(s)[1]	FC[2]		Putative function/process[3]
	Iron stimulon	Fur regulon	
Iron uptake			
Aerobactin transport	73.3-3.3	46.1-12.9	Aerobactin biosynthesis and transport
Ferrous iron ABC transporters	67.1-8.5	63.3-6.8	Ferrous iron transport
Vulnibactin biosynthetic genes	39.7-8.8	36-8.9	Vulnibactin biosynthesis and transport
Ferric iron ABC transporters	32.3-10.1	28.2-11.1	Ferric iron transport
ftbp (or vep20)	12.9	29.4	Fish transferrin binding
Heme/Hemin related genes	12.2-4.2	67.9-4.5	Heme/hemin receptors and transport
vuuA	-2.2	-2.9	Ferric vulnibactin receptor
Nutrient uptake and metabolism (including regulators)			
potD	15.9	25.9	Polyamine transport
nupC	2.1	8.4	Permease for nucleoside uptake
fruR (cra)	-14.7	-6.8	Catabolite repressor

TABLE 3 | Continued.

Gene(s)[1]	FC[2]		Putative function/process[3]
	Iron stimulon	Fur regulon	
phoR,phoB	-(27.4-45.3)	--/-64.8	PhoR (histidine kinase/phosphatase for PhoB) and PhoB (positive transcriptional factor for Pho regulon) involved in phosphate starvation
fabR	-28.1	-3.3	Repressor for unsaturated fatty acid biosynthesis
N-acetylglucosamine-6-phosphate deacetylase	-39.7	-31.3	Chitin related metabolism
kdgR	-41.9	-29.6	Repressor for oligogalacturonide metabolism (Nieckarz *et al.*, 2017)
uxuR	-47.8	-16.3	Repressor for oligoglucuronide metabolism (Rodionov *et al.*, 2000)
arcA	--	26.9	Repressor for aerobic metabolism
Cyn operon transcriptional activator	--	10.7	Activator of cyanide metabolism, a subproduct from urea
Chitinase genes	--	-(2.5-74.9)	Chitin related metabolism
aer	--	-36.6	Aerotaxis sensor receptor protein
Lps and capsule			
rffC, wza,wzb,wzc	18.4-15.7	52-4	LPS biosynthesis
waaL	4.1	3.3	Lipid A core-O antigen ligase
wbfB (capB/D)	3.2	8.8	Capsule biosynthesis
cps genes	-35.7	-(2.9-58.2)	Capsule biosynthesis
msbA	NP	2.1	Lipid A export ATP-binding/permease protein
lptA, lptB	NP	60-48.2	LPS biosynthesis
Stress protection			
dndB, dndD, dndE	72.1	38.5-2.5	DNA protection from both H_2O_2 and hydroxyl radicals *in vivo*
cspA, cspE, cspG, cspD	62.4-6.5	49.8-(-8.6)	Cold shock proteins, involved in stress caused by membrane damage
ompU	42.9	51.8	Resistance to microcidal peptides (Mathur *et al.*, 2007)
sodA	23.5	8.7	Oxidative stress resistance
degS	25.3	--	Outer membrane integrity
nnrS	15.5	-3.4	Resistance to nitrosative stress

TABLE 3 | Continued.

Gene(s)[1]	FC[2]		Putative function/process[3]
	Iron stimulon	Fur regulon	
***hsp* genes**	-(7.7-17.5)	-22.2	Heat shock proteins, involved in stress caused by membrane damage
aphC	-8.9	-3.2	Oxidative stress resistance (VBNC state)
katG	-27.8	-5.3	Oxidative stress resistance (VBNC state)
nsrR	-27.4	-18.9	Repressor for resistance to nitrosative stress
uspA, uspB	--/-27.3	-(3.6-14.4)	Resistance to oxidative stress
Flagellum, pili and chemotaxis			
***msha* genes**	32.9-2.5	36.2-2.6	Pili MSHA biosynthesis
***flp* (*cpa*) genes**	28.8-3.2	28.7-7.4	Pilus assembly
***fli* genes**	25.9-(-62)	-(2.6-55.3)	Flagellar rotation
Chemoreceptor genes	25.9-(34.2)	29.2-(-24.7)	Methyl-accepting chemotaxis protein
***tad* genes**	12.7-7.4	7.3	Pilus assembly
Chitin-binding protein	8.1	9.9	Adherence to chitin surfaces
***che* genes**	-(2.3-48.3)	-28-3.3	Chemotaxis related
***flg* genes**	-(5.3-65.8)	-(2.7-74.4)	Flagellar hook-associated protein
Sigma factor for flagellar operon	-6.9	-60	Flagellar biosynthesis
fleN	-7.6	-6.8	Flagellar synthesis regulator
Chemotaxis regulator	-8.3	-42.5	Transmits chemoreceptor signals to flagelllar motor
***mot* genes**	-(9.8-59.8)	-(13.8-59.5)	Flagellar motor rotation protein
***fla* genes**	-(10.7-44.7)	-(2.6-65.1)	Flagellin proteins
flhA, flhF	--/-4.4	-(36.8-66.4)	Flagellar biosynthesis protein
Virulence factors and related regulators			
vvhAB	57.8-11.5	--	Hemolysin (vulnificolysin) and transport protein
hlyU	--	-4.1	*rtxA1* activator
smcR	--	21.5	Master regulator of *quorum sensing*. It down-regulates *hlyU* (Kim *et al.*, 2013)
fur	--	-45.6	Regulator of iron uptake mainly acting as a repressor

[1]Identified DEGs are indicated.
[2]FC: fold change value or range of fold change values for each individual gene or for a group of related genes, respectively.
[3]Putative function for the gene and related process.
--: not detected as differentially expressed.

Phenotypic assays

A series of phenotypic experiments were designed and performed to ascertain if the virulence and survival related processes identified by the transcriptomic study responded to exogenous iron levels and/or could be directly or indirectly controlled by Fur.

VBNC state. The entrance into the VBNC state by R99 strain was faster when *fur* was deleted (20 d vs 35 d) and returned to the R99 pattern when *fur* was introduced in the mutant by conjugation (**FIGURE 3A**). Interestingly, iron content altered the entry into the VBNC state in the mutant (10 d in MSWYE+Fe vs 21 d in MSWYE-$Fe_{(D)}$) but not in R99 strain (**FIGURE 3A**). No differences were observed among strains and conditions in resuscitation kinetic from the VBNC state (**FIGURE 3A**). These results are compatible with the hypothesis that the entrance into the VBNC state in *V. vulnificus* would be directly or indirectly controlled by Fur in an iron independent manner. Entry into the VBNC state in some *Vibrio* species has been previously related to a cold induced loss of antioxidative activity due to catalase (KatG) and/or alkyl hydroperoxide reductase protein C (AhpC) (Oliver, 2010; Wang *et al.*, 2013; Rao *et al.*, 2014). Precisely the gene transcripts for both enzymes were revealed as significantly downregulated in iron restriction (**TABLE 3**). Our experimental assays confirmed that both genes were upregulated in the wild-type strain during the entry into VBNC state (after 3, 7 and 16 d post-inoculation at 4ºC) and that *ahpC* but not *katG* was significantly less expressed when *fur* was deleted (**FIGURE 3B**). Finally, the faster entrance into VBNC state under iron excess conditions when *fur* is deleted could be explained by the combination of two detrimental factors, a higher susceptibility to oxidative stress due to the reduction in *ahpC* transcription and the presence of highly reactive hydroxyl radicals that are usually formed in minimal media under iron excess conditions (Becker and Skaar, 2014).

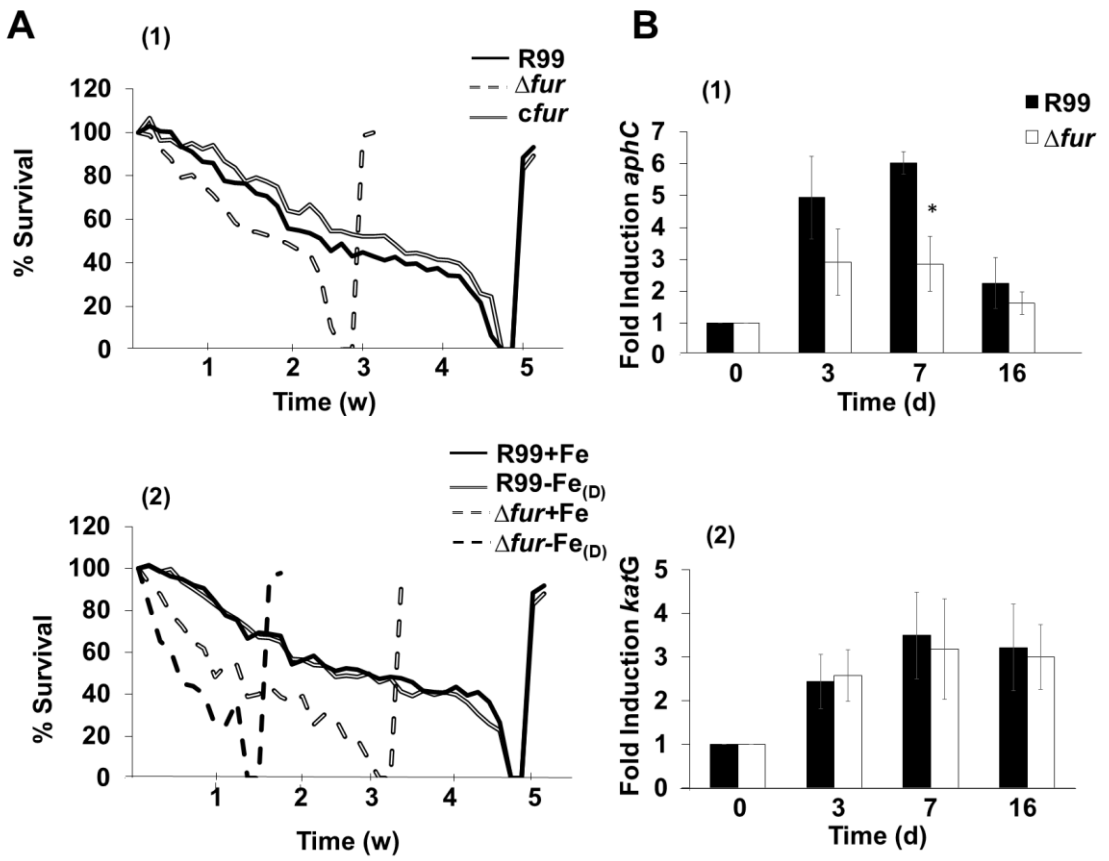

FIGURE 3 | Induction of VBNC state and resuscitation in *V. vulnificus* and transcription levels of *aphC* and *katG* during the entry into VBNC state. (A). Survival curves: overnight cultures in MSWYE (1), MSWYE+Fe (2) or MSWYE-$Fe_{(D)}$ (2) were maintained at 4ºC with shaking until no bacteria was recovered on TSA-1 plates (VBNC state) and then the VBNC cultures were placed at 22ºC with shaking and resuscitation was monitored by plate counting on TSA-1. % Survival: ratio of bacterial counts at selected time intervals vs 0 d. All values of % survival for Δ*fur* were significantly lower than those corresponding to R99 and c*fur* (*P<0.05*) from day 2 untill the entry into VBNC state. (B) Transcription levels of *aphC* (1) and *katG* (2) determined as fold induction by RT-qPCR at 0, 3, 7 and 10 d of bacteria incubation in MSWYE at 4ºC. Results are presented as average ± standard error of three independent biological experiments.*: significant differences (*P<0.05*) found in Δ*fur* vs R99.

Chemotaxis and motility. According to our transcriptomic results both iron and Fur could control positively and negatively the transcription of motility and chemotaxis related genes (**FIGURE 2** and **TABLE 3**). In case of motility, almost all of the genes involved in flagellum biosynthesis together with different regulators and a specific sigma factor were revealed to be putatively downregulated in iron restriction and Fur absence (**FIGURE 2** and **TABLE 3**). We phenotypically confirm that motility of the wild-type strain in all tested conditions was significantly reduced when *fur* was deleted, coming back to the original values when *fur* was introduced in the mutant by conjugation (**FIGURE 4A**). Furthermore, motility of the wild-type strain but not that of Δ*fur*, was significantly enhanced by adding iron to the medium (**FIGURE**

4A). Unexpectedly, motility of both strains, R99 and Δ*fur*, significantly decreased when iron was removed from the medium (**FIGURE 4A**). This last result suggests that other regulators apart from Fur could be involved in the motile response to variable iron conditions. Moreover, the microarray results revealed that iron and Fur could also control the transcription of chemotaxis-related genes (**FIGURE 2** and **TABLE 3**). Since motile *Vibrio* cells are positively chemo-attracted by blood liberated by eel skin wounds (Valiente *et al.*, 2008), the chemotactic response towards eel and human serum was tested under iron excess and iron poor conditions (**FIGURE 4B**). Serum and hemolytic serum positively attracted the wild-type strain, and this attraction was significantly enhanced by iron while *fur* deletion decreased chemo-attraction towards serum that was restored by complementation *in trans* of the mutant **(FIGURE 4B**).

Interestingly, Δ*fur* was repelled by human serum, which could also mask a higher sensitivity of the mutant to the bactericidal action of human serum. Together, our results show that both chemotaxis towards blood and motility in *V. vulnificus* would be controlled directly or indirectly by Fur in an iron dependent manner, although motility seems to be a more complex phenotype that would respond to other signals and be controlled by other regulator(s).

Attachment and biofilm production on abiotic surfaces. Among the genes involved in attachment putatively regulated by Fur and/or iron we identified some of those encoding a putative tight adherence (Tad) system (the machinery required for the assembly of an adhesive Flp [fimbrial low-molecular-weight protein] pilus) together with the *flp* (*cpa*) genes as well as those putatively encoding a MSHA pilus (**TABLE 3**). Interestingly, *tad*, *flp* (*cpa*) and *msha* genes were mostly upregulated in iron restriction conditions and in absence of Fur (**FIGURE 2** and **TABLE 3**). We analyzed biofilm production on a polystyrene hydrophobic surface and found that it decreased with an increase in iron concentration (**TABLE 4**). These results suggest that biofilm production and/or its dispersion is an iron dependent but Fur independent process.

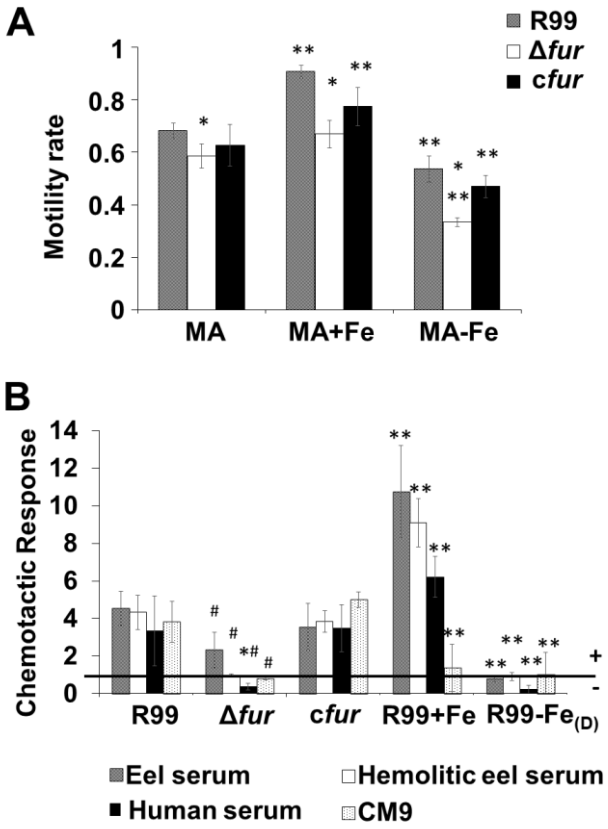

FIGURE 4 | Motility and chemotaxis in *V. vulnificus*. (A) Motility on MA measured as motility rate (colony surface in mm^2/log of colony bacterial number in CFU). Results are presented as average ± standard error of three independent biological experiments.*: significant differences in motility rate between strains (Δ*fur* or c*fur* vs R99) (*P<0.05*); **: significant differences between conditions (with [MA+Fe] or without iron [MA-$Fe_{(D)}$)] vs MA)] for the same strain (*P<0.05*). (B) Chemotaxis towards eel serum, hemolytic eel serum, human serum and CM9 was measured as chemotactic response (ratio of bacterial numbers in tested attractant-capillaries vs control-capillaries [containing CB]). Results are presented as average ± standard error of three independent biological experiments.*: significant differences in chemotactic response towards serum vs CM9 per strain (*P<0.05*); #: significant differences between strains (Δ*fur* or c*fur* vs R99) per tested attractant (*P<0.05*); **: significant differences in function of iron content in the CB (CB+Fe or CB-Fe vs CB) per tested attractant for R99 strain (*P<0.05*).

Toxins. A few genes for putative hemolysins were identified to be putatively under iron and/or Fur control, including the major hemolysin of the species (VvhA) (Yamanaka *et al.*, 1990) (**FIGURE 2** and **TABLE 3d**). We did not find significant differences in cell-associated or extracellular hemolytic activities among strains and conditions (**TABLE 4**).

TABLE 4 | Biofilm production and hemolytic activity of *V. vulnificus*.

	R99			Δ*fur*
	CM9-Fe	CM9	CM9+Fe	CM9
Biofilm (Abs_{540})[1]	0.63±0.02	0.66±0.04	0.45±0.04*	0.67±0.04
Hemolysis Cells (Abs_{520})[2]	0.41±0.04	0.45±0.01	0.43±0.01	0.46±0.02
Hemolysis ECPs (Abs_{520})[3]	0.55±0.02	0.55±0.02	0.52±0.01	0.5±0.02

[1]For biofilm quantification bacteria were grown in polystyrene wells, planktonic bacteria were eliminated and biofilm was quantified after staining with crystal violet by measuring Abs_{540} at 24 h post-incubation. *: significant differences between conditions (CM9-Fe vs CM9+Fe) for strain R99 (*P <0.05*).
[2/3]Hemolytic activity of bacterial cells[2]/ECPs[3] was quantified by measuring Abs_{520} after 90 min post-infection of a suspension of 1% bovine erythrocytes (Sigma-Aldrich).

Resistance to stressing conditions. A series of genes related to innate defenses that are associated with resistance to various stressors were identified to be putatively controlled by iron and/or Fur (**FIGURE 2** and **TABLE 3**). First, resistance to the antimicrobial compounds polymyxin B, lysozyme, and SDC (a bile salt) did not change with either iron concentration or *fur* deletion (polymyxin B: 250 µg/ml for all strains and conditions; lysozyme: 500 µg/ml for all strains and conditions; SDC: 12,500 µg/ml for all strains and conditions) while bacterial survival under acidic or oxidative conditions as well as the effect of NO on growth varied according to iron levels and/or presence/absence of *fur*. Thus, R99 strain was significantly more resistant to acid pH (pH 5) and to NO, and more sensitive to H_2O_2 when *fur* was deleted and the phenotype was reverted by complementation *in trans* of the mutant (**FIGURE 5A**, **B** and **C**). These results supported the microarray data where *sodA,* encoding an enzyme for resistance to acid stress (Kim *et al.*, 2005), *nsrR*, a repressor of the response to NO (Bodenmiller and Spiro, 2006) and *ahpC*/*katG,* related to resistance to oxidative stress, appeared up-, down- and downregulated, respectively, in Δ*fur*.

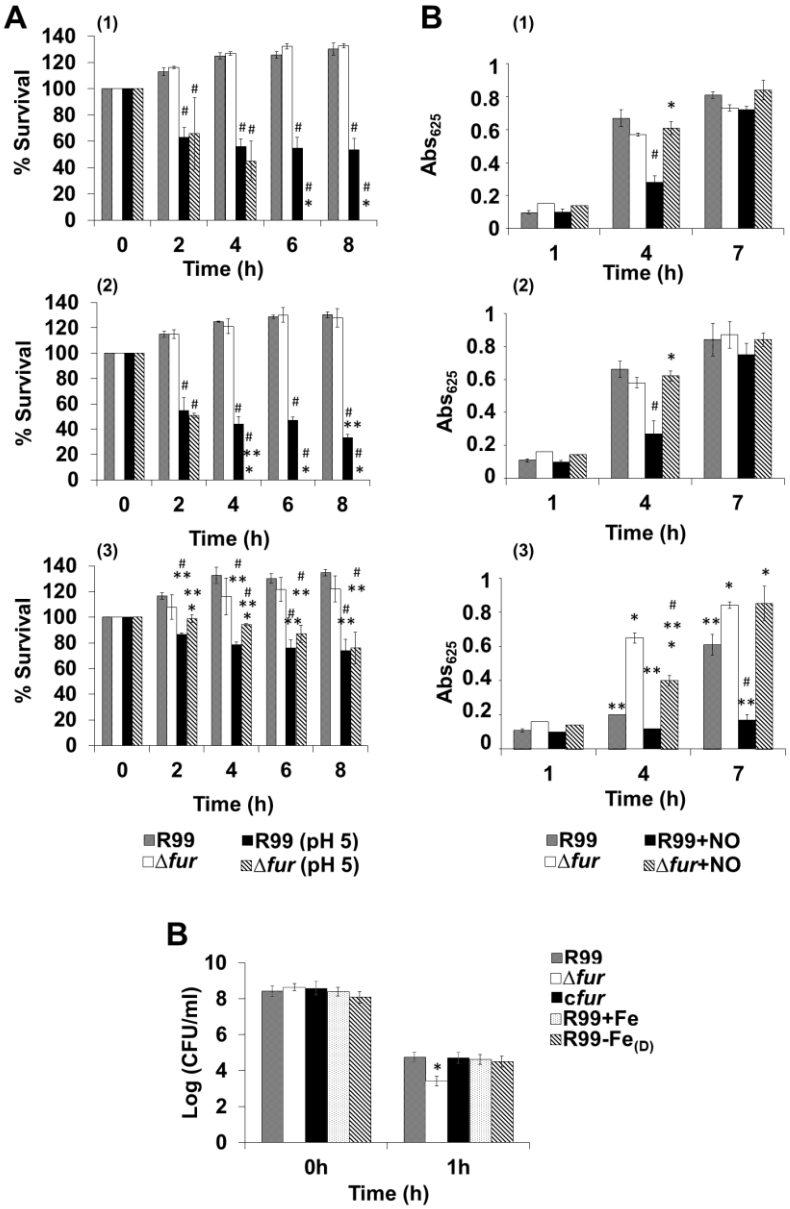

FIGURE 5 | Sensitivity to acid, oxidative and nitrosative stress in *V. vulnificus*. (A) Resistance to acid stress was tested by incubating bacteria in MSWYE (1), MSWYE+Fe (2) or MSWYE+Tf (3) in normal or acid medium (pH 5). % Survival: ratio of bacterial counts at selected time intervals vs 0 h. *: significant differences between strains (Δ*fur* vs R99) for the same culture medium and pH condition (normal or acid medium); **: significant differences between culture media (MSWYE+Fe/MSWYE+Fe vs MSWYE) for the same strain and pH condition; #: significant differences between pH conditions (normal vs acid medium (pH 5)) for the same strain and culture medium (*P<0.05*). (B) Resistance to H_2O_2 was tested by incubating bacteria in PBS-H_2O_2 (0.1%), respectively. Results are presented as bacterial counts (CFU/ml) at selected time intervals. *: significant differences between strains (Δ*fur* or c*fur* vs R99) (*P<0.05*). (C) Resistance to nitrosative stress was tested by following growth in CM9 (C1), CM9+Fe (C2) or CM9-$Fe_{(Tf)}$ (C3) with and without NO by measuring Abs_{625} at 1 h intervals for 7 h. *: significant differences between strains (Δ*fur* vs R99) for the same culture medium and NO condition (with or without NO); **: significant differences between culture media (CM9+Fe/CM9+Fe vs CM9) for the same strain and NO condition; #: significant differences between NO conditions (with NO vs without NO) for the same strain and culture medium (*P<0.05*). In all cases results are presented as average ± standard error of three independent biological experiments.

Regarding iron, sensitivity of the wild-type strain to H_2O_2 and to an acid pH was independent and dependent on this metal, respectively. Interestingly the wild-type strain was more resistant to acid pH under iron restriction conditions (**FIGURE 5A** and **B**) and more sensitive under iron excess conditions when *fur* was deleted. This sensitivity could be explained by a higher concentration of radical peroxide that is usually induced at acid pH (Teranishi *et al.*, 2016) (**FIGURE 5A(2)**). Although NO resistance is not altered by an increase in iron concentration, R99 strain is more sensitive to NO when grown in iron poor conditions (**FIGURE 5C**). The main mechanism by which NO inhibits bacterial growth is by binding iron and forming dinitrosyl iron complexes bound to iron-sulfur bacterial proteins, inhibiting their functions (Toledo *et al.*, 2008). In CM9+Tf, a medium with practically no free iron, all NO would bind to bacterial proteins and the bactericidal effect would be stronger than in an iron rich medium, thus explaining the higher sensitivity to NO of R99 strain. In conclusion, resistance to oxidative stress could be directly controlled by Fur in an iron independent manner; resistance to acid stress could be also controlled by Fur but in an iron dependent way and, finally, resistance to nitrosative stress should be a process indirectly depending on Fur.

Growth in iron restriction. Genes involved in iron acquisition were upregulated both in iron restriction and in absence of Fur (**FIGURE 2** and **TABLE 3**). Among them, the plasmid gene *ftbp* stands out due to the key role it plays in eel virulence (Pajuelo *et al.*, 2015). As expected, R99 strain under iron restriction grown faster when *fur* was deleted, wild-type strain growth was and reverted when *fur* was introduced in the mutant by conjugation (**FIGURE 6**).

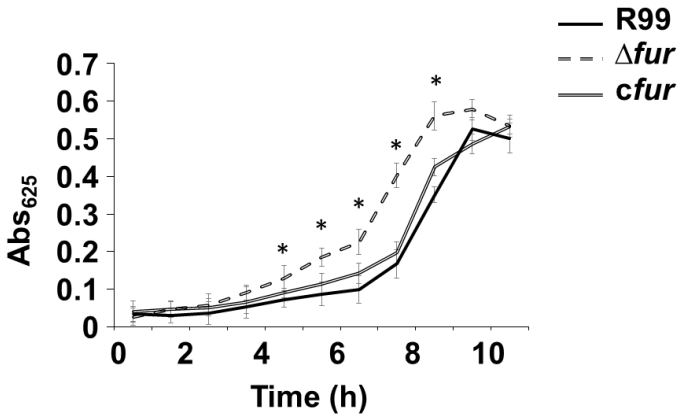

FIGURE 6 | Role of iron and Fur in bacterial growth in the presence of holo-transferrin as the sole iron source. The three strains of *V. vulnificus* were inoculated in CM9 supplemented with 10 µM holo-transferrin (Sigma-Aldrich) and growth was followed by measuring the Abs_{625} at regular time intervals. Results are presented as average ± standard error of three independent biological experiments. *: significant differences in values of Abs_{625} between the Δ*fur* vs R99 or c*fur* strains (*P<0.05*).

External envelope and serum resistance. A series of genes involved in core-lipid A, O-antigen, capsular and extracellular polysaccharide biosynthesis were differentially expressed under the assayed conditions (**FIGURE 2** and **TABLE 3**). Capsular polysaccharides have been previously related to resistance to the bactericidal effect of human serum but not with resistance to eel serum (Wright *et al.*, 1990; Biosca *et al.*, 1993). Most of the genes involved in core-lipid A and O-antigen biosynthesis were putatively upregulated in absence of Fur, with or without iron dependence, whereas those involved in capsule and extracellular polysaccharide biosynthesis were mostly downregulated in Fur absence in an iron dependent manner (**TABLE 3**). The cell-associated polysaccharides from the R99 grown in iron rich and iron poor conditions and from the Δ*fur* strains were extracted, quantified and analyzed. As predicted by microarray results, the quantity of polysaccharides in R99 strain (µg per 10^8 cells) i) significantly increased with iron concentration, ii) decreased when *fur* was deleted, and iii) returned to the wild-type level when *fur* was introduced in the mutant by conjugation (**TABLE 5**). Furthermore, this quantity did not significantly change in Δ*fur* with iron concentration (**TABLE 5**). Finally, the cell-associated polysaccharide pattern varied among strains and conditions: i.e., the core-lipid A increased with *fur* deletion, while the capsule increased concomitantly with a decrease in O-antigen when the wild-type strain was incubated under iron excess conditions (**FIGURE 7**).

TABLE 5 | Effect of iron concentration and *fur* deletion on the quantity of cellular-associated polysaccharides (µg/10^8 cells).

R99			Δ*fur*		
CM9+Tf	CM9	CM9+Fe	CM9+Tf	CM9	CM9+Fe
219.8±9.7#	235.2± 6.8**	298.8±18	178.6±22*	187.1± 3.6*	196.9±10*

*: significant differences between strains (Δ*fur* vs R99) for the same condition (*P<0.05*). **: significant differences between conditions (CM9 vs CM9+Fe) for the same strain (*P<0.05*). #: significant differences between conditions (CM9+Tf vs CM9+Fe) for the same strain (*P<0.05*).

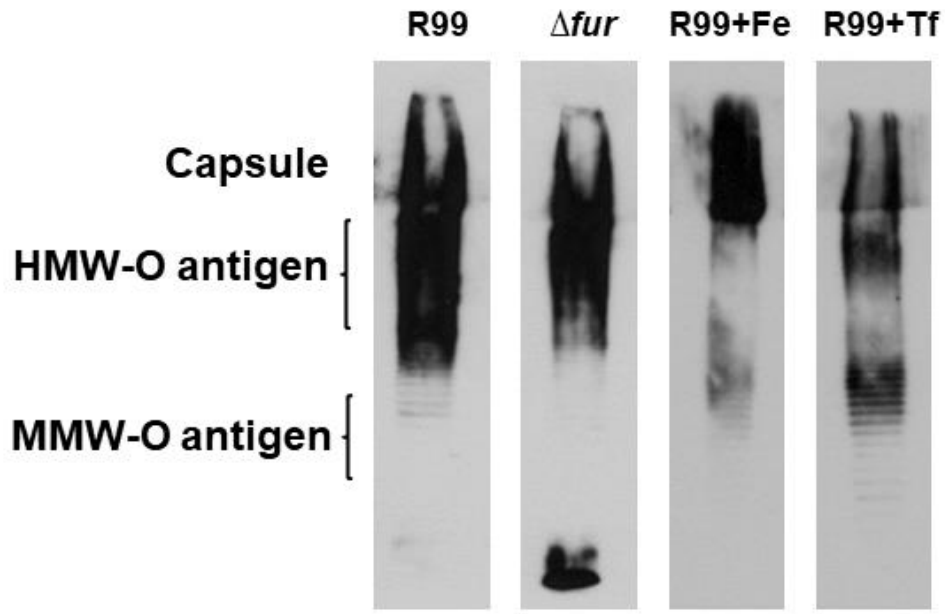

FIGURE 7 | Cell-associated polysaccharides of *V. vulnificus*. Cell-associated polysaccharides (LPS + capsule) were extracted, separated by SDS-PAGE and immunostained with rabbit primary antibody anti-SerE and secondary anti-rabbit HRP-conjugated. HMW, high molecular weight. MMW, medium molecular weight.

4. Discussion

The results obtained in this study support the hypothesis that iron and Fur have a key role in controlling the life cycle of *V. vulnificus*. First, iron stimulon involves 1 out of 4 genes present in the genome and Fur regulon 1 out of 3 genes, which is not surprising given that *V. vulnificus* is a septicemic microorganism and blood is an iron restrictive medium due to nutritional immunity. Similarly, around 20% of the gonococcal genome is regulated in response to iron both dependently and independently of Fur (Ducey *et al.*, 2005; Jackson *et al.*, 2010). Furthermore, most of the genes in pR99 were upregulated in iron restriction conditions which would ensure the expression of the host-specific resistance system to the innate immunity in the eel blood (Lee *et al.*, 2008).

Second, we also found strong evidences that Fur could repress as well as activate genes both independently and dependently of iron, which suggests that Fur protein in *V. vulnificus* is as versatile as in *V. cholerae* (Mey *et al.*, 2005). Although there are several mechanisms described that explain how Fur can act as an activator, the repression of other repressors (anti-repressor activation model) could be the major mechanism for Fur dependent activation (Troxell and Hassan, 2013). Accordingly, we found that Fur seems to repress, directly or

indirectly, the transcription of *smcR* and *hlyU*, which would affect all the processes controlled by these global regulators. Thus, the repression of *smcR* by Fur, already demonstrated in *V. vulnificus* by Kim *et al.*, (2013), could result in the transcription of genes repressed by this global regulator.

Third, our results also highlight that iron and Fur can control much more genes than those related to iron acquisition, including genes essential for resistance to acid and oxidative stress, for resistance and growth in human and fish serum as well as genes involved in attachment and biofilm formation among others.

FIGURE 8 summarizes our main results and proposes a model regarding the role of Fur and exogenous iron levels in each one of the different stages of the life cycle of *V. vulnificus*.

Entrance into the VBNC state and resuscitation. As a free living form, the pathogen switches between a VBNC and a vegetative state depending on nutrient availability as well as on water temperature and salinity (Wolf and Oliver, 1992; Biosca *et al.*, 1996; Whitesides *et al.*, 1997; Marco-Noales *et al.*, 1999). The results obtained in this work clearly show that the entry of this species into the VBNC state is controlled by Fur independently of iron and suggest a role in this process for AphA, which confers resistance to oxidative stress (**FIGURE 8**). This relation between loss of bacterial viability in parallel to loss of resistance to oxidative stress had been already highlighted in this and other *Vibrio* species (Nowakowska and Oliver, 2013; Li *et al.*, 2014).

V. vulnificus resuscitates from the VBNC state with an increase in temperature and/or in presence of nutrients (Wolf and Oliver, 1992; Biosca *et al.*, 1996; Whitesides *et al.*, 1997; Marco-Noales *et al.*, 1999). Nutrients for bacterial growth are abundant in the coastal regions, especially in estuarine waters, as well as in fish farms, being estuarine waters and farms natural and artificial habitats, respectively, for *V. vulnificus* and their animal hosts (Aarestrup *et al.*, 2009; Oliver, 2015). For this reason, temperature is probably the main factor that controls entry into the VBNC state and resuscitation in the environment in *V. vulnificus*. The results obtained in this work suggest that neither Fur nor iron have a role in the resuscitation process, at least in the conditions used in the present work (**FIGURE 8**).

Free vs attached lifestyle. According to our results, iron and Fur could have a role in determining the lifestyle of *V. vulnificus* in the aquatic environment. Thus, in presence of free iron, bacteria would mostly survive as free-living forms while in absence of free iron they would survive mostly attached to biotic and abiotic surfaces (**FIGURE 8**). In addition, in presence

of free iron, bacteria would produce a capsule and would be motile by a polar flagellum. Capsule and flagellum formation are controlled by Fur and, probably, other regulators (**FIGURE 8**). Previous studies have demonstrated that flagellum biosynthesis in *V. vulnificus* is regulated by quorum sensing through SmcR, which binds directly to the promoter of *flhF*, a gene driving activation of flagellum biogenesis (Kim *et al.*, 2012). In this study, *smcR* was upregulated in Δ*fur*, suggesting an additional indirect activation of flagellum biosynthetic genes by Fur. The precise regulatory role of Fur in flagellum biosynthesis remains to be investigated in further studies.

Our results also suggest that under iron starvation, bacteria would produce Flp (Cpa) and MSHA pili, a process directly or indirectly controlled by Fur. Both pili probably favor the attachment process, as it has been demonstrated for *Pseudomonas* and *V. cholerae* (Tomich *et al.*, 2007; Utada *et al.*, 2014). Our study also provides evidence suggesting that iron starvation could activate biofilm formation independently of Fur, as biofilm production by R99 strain decreases in iron excess conditions (**FIGURE 8**). In parallel, we detected a decrease in capsule production under iron restriction in direct agreement with the reported inverse correlation between capsule and biofilm production in *V. vulnificus* (Joseph and Wright, 2004). Finally, our results suggest that an iron excess would promote bacteria dispersion from the biofilms as capsulated motile bacteria.

Host colonization and septicemia. Motile or non-motile bacteria could be taken up passively by filtering organisms, the main reservoir for human infections acquired by the oral route (**FIGURE 8**). In addition, motile bacteria could be chemo-attracted by blood from their susceptible hosts (humans with high iron levels in the blood [risk patients] and healthy eels), a process also controlled by Fur and iron, according to our results (**FIGURE 8**). Once in the tissues, resistance to common animal and human stressors related to host innate immunity such as NO, oxidative stress, and acid pH would also be controlled by Fur. Thus, our results suggest that Fur would activate resistance to oxidative stress and repress resistance to acid and nitrosative stress, in both cases directly or indirectly and regardless of the host.

Human septicemia. Humans can be infected either by contact of a wound with contaminated water or with a carrier or diseased fish (zoonosis). After contact, the pathogen colonizes the wound and after ingestion, the intestine. From both locations the pathogen can invade the bloodstream. We have found that *V. vulnificus* would only survive in the blood under iron excess conditions, those that, according to our results, allow it to produce a protective capsule against complement and phagocytosis (Yoshida *et al.*, 1985; Wright *et al.*,

1990, 2001; Kashimoto *et al.*, 2003). Then, capsulated bacteria would uptake free iron in order to multiply in blood, and would secrete the toxins $RtxA1_3$ and VvhA, which, in turn, would cause the death of the risk patient by a toxic sepsis as it has been demonstrated by Murciano *et al.*, (2017) in a mice model. The toxin production is a complex process in which we have not been able to demonstrate the implication of Fur and iron, although we found transcriptomic evidences that Fur could repress the transcription of HlyU, the main regulator of VvhA and $RtxA1_3$ transcription (Liu *et al.*, 2011).

Fish septicemia. After wound colonization, some bacterial cells would invade the bloodstream and detect iron restriction, producing a protective envelope enriched in O-antigen that partially protects them against innate immunity in the blood (Amaro *et al.*, 1997). We found evidence suggesting that Fur directly or indirectly controls the expression of some genes related to O-antigen and core-lipid A biosynthesis. Thus, the Δ*fur* presents an altered LPS pattern without a clear relationship with iron concentration. Only those isolates possessing the virulence plasmid would express Vep07, a protein putatively involved in resistance to innate immunity by an unknown mechanism (Lee *et al.*, 2008), and Ftbp, a protein that binds fish transferrin specifically (Pajuelo *et al.*, 2015). In addition, the pathogen could also produce two additional iron uptake systems, those depending on siderophores and heme proteins, allowing it to optimally multiply in blood (Pajuelo *et al.*, 2014, 2015). The production of all of these iron uptake mechanisms is controlled by iron and Fur according to our results and the literature (Mey *et al.*, 2005; Pajuelo *et al.*, 2014, 2015). Afterwards, the pathogen would secrete $RtxA1_3$ and VvhA, which, in turn, would cause the death of the fishes by a toxic sepsis, hypothesis that remains to be demonstrated. Although we found that VvhA is highly transcribed under iron restriction, we could not relate iron and Fur with a change in hemolytic activity.

In summary, our results support the hypothesis that iron, not always through Fur, is one of the main signals acting as a niche marker for *V. vulnificus*. Iron impacts the entire life cycle of the pathogen from its survival in the marine environment, including motility and chemotaxis, to its survival in blood of its hosts. In blood, iron concentration would be the key signal for this septicemic bacterium, triggering the expression of genes involved in survival and resistance to the innate immune response allowing the bacterium to multiply and persist inside their hosts. Finally, this is the first time that the biogenesis of important bacterial appendices such as pili and flagellum as well as capsule and LPS biosynthesis have been related to iron and Fur in *Vibrio*.

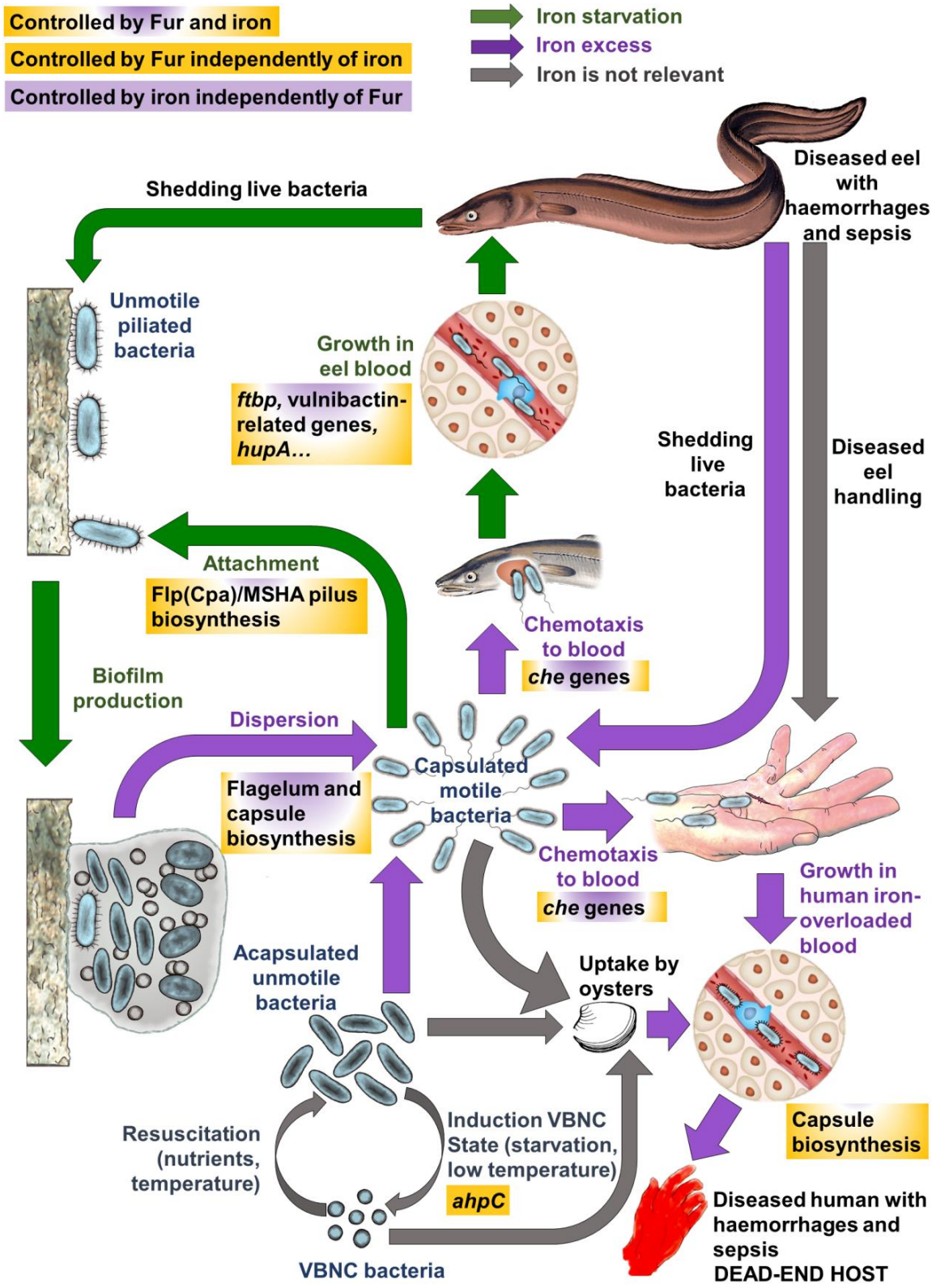

FIGURE 8 | Iron and Fur in the life cycle of *V. vulnificus*.

5. References

Aarestrup, K., Okland, F., Hansen, M.M., Righton, D., Gargan, P., Castonguay, M., et al. (2009) Oceanic spawning migration of the European Eel (*Anguilla anguilla*). *Science* **325**: 1660.

Alice, A.F., Naka, H., and Crosa, J.H. (2008) Global gene expression as a function of the iron status of the bacterial cell: influence of differentially expressed genes in the virulence of the human pathogen *Vibrio vulnificus*. *Infect Immun* **76**: 4019–4037.

Amaro, C., Biosca, E.G., Fouz, B., Alcaide, E., and Esteve, C. (1995) Evidence that water transmits *Vibrio vulnificus* biotype-2 infections to eels. *Appl Environ Microbiol* **61**: 1133–1137.

Amaro, C., Biosca, E.G., Fouz, B., and Garay, E. (1992) Electrophoretic analysis of heterogeneous lipopolysaccharides from various strains of *Vibrio vulnificus* biotypes 1 and 2 by silver staining and immunoblotting. *Curr Microbiol* **25**: 99–104.

Amaro, C., Biosca, E.G., Fouz, B., Toranzo, A.E., and Garay, E. (1994) Role of iron, capsule, and oxins in the pathogenicity of *Vibrio vulnificus* biotype-2 for mice. *Infect Immun* **62**: 759–763.

Amaro, C., Fouz, B., Biosca, E.G., Marco-Noales, E., and Collado, R. (1997) The lipopolysaccharide o side chain of *Vibrio vulnificus* serogroup E is a virulence determinant for eels. *Infect Immun* **65**: 2475–2479.

Becker, K.W. and Skaar, E.P. (2014) Metal limitation and toxicity at the interface between host and pathogen. *FEMS Microbiol Rev* **38**: 1235–1249.

Biosca, E.G. and Amaro, C. (1996) Toxic and enzymatic activities of *Vibrio vulnificus* biotype 2 with respect to host specificity. *Appl Environ Microbiol* **62**: 2331–2337.

Biosca, E.G., Amaro, C., Marco-Noales, E., and Oliver, J.D. (1996) Effect of low temperature on starvation-survival of the eel pathogen *Vibrio vulnificus* biotype 2. *Appl Environ Microbiol* **62**: 450–455.

Biosca, E.G., Llorens, H., Garay, E., and Amaro, C. (1993) Presence of a capsule in *Vibrio vulnificus* biotype 2 and its relationship to virulence for eels. *Infect Immun* **61**: 1611–1618.

Bodenmiller, D.M. and Spiro, S. (2006) The *yjeB* (*nsrR*) gene of *Escherichia coli* encodes a nitric

oxide-sensitive transcriptional regulator. *J Bacteriol* **188**: 874–881.

Ducey, T.F., Carson, M.B., Orvis, J., Stintzi, A.P., and Dyer, D.W. (2005) Identification of the iron-responsive genes of *Neisseria gonorrhoeae* by microarray analysis in defined medium. **187**: 4865–4874.

Hantke, K. (2001) Iron and metal regulation in bacteria. *Curr Opin Microbiol* **4**: 172–177.

Henares, B.M., Higgins, K.E., and Boon, E.M. (2012) Discovery of a nitric oxide responsive quorum sensing circuit in *Vibrio harveyi*. *ACS Chem Biol* **7**: 1331–1336.

Hitchcock, P.J. and Brown, T.M. (1983) Morphological heterogeneity among *Salmonella* lipopolysaccharide chemotypes in silver-stained polyacrylamide gels. *J Bacteriol* **154**: 269–277.

Hoben, H.J. and Somasegaran, P. (1982) Comparison of the pour, spread, and drop plate methods for enumeration of *Rhizobium spp.* in inoculants made from presterilized peat. *Appl Environ Microbiol* **44**: 1246–1247.

Hood, M.I. and Skaar, E.P. (2012) Nutritional immunity: transition metals at the pathogen-host interface. *Nat Rev Microbiol* **10**: 525–537.

Horseman, M.A. and Surani, S. (2011) A comprehensive review of *Vibrio vulnificus*: an important cause of severe sepsis and skin and soft-tissue infection. *Int J Infect Dis* **15**: e157–e166.

Jackson, L.A., Ducey, T.F., Day, M.W., Zaitshik, J.B., Orvis, J., and Dyer, D.W. (2010) Transcriptional and functional analysis of the *Neisseria gonorrhoeae* Fur regulon. *J Bacteriol* **192**: 77–85.

Jones, M.K., Warner, E.B., and Oliver, J.D. (2008) *csrA* inhibits the formation of biofilms by *Vibrio vulnificus*. *Appl Environ Microbiol* **74**: 7064–7066.

Joseph, L.A. and Wright, A.C. (2004) Expression of *Vibrio vulnificus* capsular polysaccharide inhibits biofilm formation. *J Bacteriol* **186**: 889–893.

Kashimoto, T., Ueno, S., Hanajima, M., Hayashi, H., Akeda, Y., Miyoshi, S., et al. (2003) *Vibrio vulnificus* induces macrophage apoptosis *in vitro* and *in vivo*. *Infect Immun* **71**: 533–535.

Kim, I.H., Wen, Y., Son, J.S., Lee, K.H., and Kim, K.S. (2013) The fur-iron complex modulates expression of the quorum sensing master regulator, *smcr*, to control expression of

virulence factors in *Vibrio vulnificus*. *Infect Immun* **81**: 2888–2898.

Kim, J.S., Sung, M.H., Kho, D.H., and Lee, J.K. (2005) Induction of manganese-containing superoxide dismutase is required for acid tolerance in *Vibrio vulnificus*. *J Bacteriol* **187**: 5984–5995.

Kim, S.M., Lee, D.H., and Choi, S.H. (2012) Evidence that the *Vibrio vulnificus* flagellar regulator FlhF is regulated by a quorum sensing master regulator SmcR. *Microbiology* **158**: 2017–2025.

Laemmli, U. (1970) Cleavage of structural proteins during the assembly of the head of bacteriophage T4. *Nature* **227**: 680–685.

Larsen, M., Larsen, J., and Olsen, J. (2001) Chemotaxis of *Vibrio anguillarum* to fish mucus: role of the origin of the fish mucus, the fish species and the serogroup of the pathogen. *FEMS Microbiol Ecol* **38**: 77–80.

Lee, C.T., Amaro, C., Wu, K.M., Valiente, E., Chang, Y.F., Tsai, S.F., et al. (2008) A common virulence plasmid in biotype 2 *Vibrio vulnificus* and its dissemination aided by a conjugal plasmid. *J Bacteriol* **190**: 1638–1648.

Lee, C.T., Pajuelo, D., Llorens, A., Chen, Y.H., Leiro, J.M., Padrós, F., et al. (2013) MARTX of *Vibrio vulnificus* biotype 2 is a virulence and survival factor. *Environ Microbiol* **15**: 419–432.

Lee, H., Bang, S.H., Lee, K., and Park, S. (2007) Positive Regulation of *fur* Gene Expression via Direct Interaction of Fur in a Pathogenic Bacterium, *Vibrio vulnificus*. *J Bacteriol* **189**: 2629–2636.

Lee, H.J., Park, K.J., Lee, A.Y., Park, S.G., Park, B.C., Lee, K.H., et al. (2003) Regulation of *fur* expression by RpoS and Fur in *Vibrio vulnificus*. *J Bacteriol* **185**: 5891–5896.

Li, L., Mendis, N., Trigui, H., Oliver, J.D., and Faucher, S.P. (2014) The importance of the viable but non-culturable state in human bacterial pathogens. *Front Microbiol* **5**: 258.

Liu, M., Rose, M., and Crosa, J.H. (2011) Homodimerization and binding of specific domains to the target DNA are essential requirements for HlyU to regulate expression of the virulence gene *rtxA1*, encoding the repeat-in-toxin protein in the human pathogen *Vibrio vulnificus*. *J Bacteriol* **193**: 6895–6901.

Livak, K.J. and Schmittgen, T.D. (2001) Analysis of relative gene expression data using real-time quantitative PCR and the 2−ΔΔCT method. *Methods* **25**: 402–408.

Marco-Noales, E., Biosca, E.G., and Amaro, C. (1999) Effects of Salinity and Temperature on Long-Term Survival of the Eel Pathogen *Vibrio vulnificus* Biotype 2 (Serovar E). *Appl Environ Microbiol* **65**: 1117–1126.

Mathur, J., Davis, B.M., and Waldor, M.K. (2007) Antimicrobial peptides activate the *Vibrio cholerae* σE regulon through an OmpU-dependent signalling pathway. *Mol Microbiol* **63**: 848–858.

Mey, A.R., Wyckoff, E.E., Kanukurthy, V., Fisher, C.R., and Payne, S.M. (2005) Iron and fur regulation in *Vibrio cholerae* and the role of *fur* in virulence. *Infect Immun* **73**: 8167–8178.

Miller, J.H. (1972) Experiments in Molecular Genetics. Cold Spring Harbor, NY: Cold Spring Harbor Laboratory Press.

Murciano, C., Lee, C.T., Fernández-Bravo, A., Hsieh, T.H., Fouz, B., Hor, L.I., et al. (2017) MARTX toxin in the zoonotic serovar of *Vibrio vulnificus* triggers an early cytokine storm in mice. *Front Cell Infect Microbiol* **7**: 1–19.

Nieckarz, M., Raczkowska, A., Jaworska, K., Stefańska, E., Skorek, K., Stosio, D., et al. (2017) The role of OmpR in the expression of genes of the KdgR regulon involved in the uptake and depolymerization of oligogalacturonides in *Yersinia enterocolitica*. *Front Cell Infect Microbiol* **7**: 1–25.

Nowakowska, J. and Oliver, J.D. (2013) Resistance to environmental stresses by *Vibrio vulnificus* in the viable but nonculturable state. *FEMS Microbiol Ecol* **84**: 213–222.

Oliver, J.D. (2010) Recent findings on the viable but nonculturable state in pathogenic bacteria. *FEMS Microbiol Rev* **34**: 415–425.

Oliver, J.D. (2015) The Biology of *Vibrio vulnificus*. *Microbiol Spectr* **3**: 1–10.

Pajuelo, D. (2013) Iron and virulence in the zoonotic pathogen *Vibrio vulnificus*. PhD Thesis. Universitat de València.

Pajuelo, D., Lee, C.T., Roig, F.J., Hor, L.I., and Amaro, C. (2015) Novel host-specific iron acquisition system in the zoonotic pathogen *Vibrio vulnificus*. *Environ Microbiol* **17**: 2076–2089.

Pajuelo, D., Lee, C.T., Roig, F.J., Lemos, M.L., Hor, L.I., and Amaro, C. (2014) Host-nonspecific iron acquisition systems and virulence in the zoonotic serovar of *Vibrio vulnificus*. *Infect Immun* **82**: 731–744.

Rao, N. V, Shashidhar, R., and Bandekar, J.R. (2014) Induction, resuscitation and quantitative real-time polymerase chain reaction analyses of viable but nonculturable *Vibrio vulnificus* in artificial sea water. *World J Microbiol Biotechnol* **30**: 2205–2212.

Reed, L.J. and Muench, H. (1938) A simple method of estimating fifty percent endpoints. *Am J Epidemiol* **27**: 493–497.

Rodionov, D.A., Mironov, A.A., Rakhmaninova, A.B., and Gelfand, M.S. (2000) Transcriptional regulation of transport and utilization systems for hexuronides, hexuronates and hexonates in gamma purple bacteria. *Mol Microbiol* **38**: 673–683.

Roig, F.J., González-Candelas, F., Sanjuán, E., Fouz, B., Feil, E.J., Llorens, C., et al. (2018) Phylogeny of *Vibrio vulnificus* from the analysis of the core-genome: Implications for intra-species taxonomy. *Front Microbiol* **8**: 1–13.

Shinoda, S., Miyoshi, S., Yamanaka, H., and Miyoshi-Nakahara, N. (1985) Some properties of *Vibrio vulnificus* hemolysin. *Microbiol Immunol* **29**: 583–590.

Teranishi, M., Naya, S., and Tada, H. (2016) Temperature- and pH-dependence of hydrogen peroxide formation from molecular oxygen by gold nanoparticle-loaded titanium(IV) oxide photocatalyst. *Phys Chem C* **120**: 1083–1088.

Toledo, J.C.J., Bosworth, C.A., Hennon, S.W., Mahtani, H.A., Bergonia, H.A., and Lancaster, J.R.J. (2008) Nitric oxide-induced conversion of cellular chelatable iron into macromolecule-bound paramagnetic dinitrosyliron complexes. *J Biol Chem* **283**: 28926–28933.

Tomich, M., Planet, P.J., and Figurski, D.H. (2007) The *tad* locus: postcards from the widespread colonization island. *Nat Rev Microbiol* **5**: 363–375.

Troxell, B. and Hassan, H.M. (2013) Transcriptional regulation by Ferric Uptake Regulator (Fur) in pathogenic bacteria. *Front Cell Infect Microbiol* **3**: 59.

Utada, A.S., Bennett, R.R., Fong, J.C.N., Gibiansky, M.L., Yildiz, F.H., Golestanian, R., et al. (2014) *Vibrio cholerae* use pili and flagella synergistically to effect motility switching and conditional surface attachment. *Nat Commun* **5**: 4913.

Valiente, E., Lee, C.T., Lamas, J., Hor, L.I, and Amaro, C. (2008) Role of the virulence plasmid pR99 and the metalloprotease Vvp in resistance of *Vibrio vulnificus* serovar E to eel innate immunity. *Fish Shellfish Immunol* **24**: 134–141.

Wang, H.W., Chung, C.H., Ma, T.Y., and Wong, H. (2013) Roles of alkyl hydroperoxide reductase subunit C (AhpC) in viable but nonculturable *Vibrio parahaemolyticus*. *Appl Environ Microbiol* **79**: 3734–3743.

Weinberg, E.D. (2009) Iron availability and infection. *Biochim Biophys Acta Gen Subj* **1790**: 600–605.

Whitesides, M.D., Oliver, J.D., and Carolina, N. (1997) Resuscitation of *Vibrio vulnificus* from the Viable but Nonculturable State. *Biochim Biophys Acta Gen Subj* **63**: 1002–1005.

Wolf, P.W. and Oliver, J.D. (1992) Temperature effects on the viable but non-culturable state of *Vibrio vulnificus*. *FEMS Microbiol Lett* **101**: 33–39.

Wright, A.C., Powell, J.L., Kaper, J.B., and Morris, J.G.J. (2001) Identification of a group 1-like capsular polysaccharide operon for *Vibrio vulnificus*. *Infect Immun* **69**: 6893–6901.

Wright, A.C., Simpson, L.M., Oliver, J.D., and Morris, J.G. (1990) Phenotypic evaluation of acapsular transposon mutants of *Vibrio vulnificus*. *Infect Immun* **58**: 1769–1773.

Yamanaka, H., Sugiyama, K., Furuta, H., Miyoshi, S., and Shinoda, S. (1990) Cytolytic action of *Vibrio vulnificus* haemolysin on mast cells from rat peritoneal cavity. *J Med Microbiol* **32**: 39–43.

Yoshida, S., Ogawa, M., and Mizuguchi, Y. (1985) Relation of capsular materials and colony opacity to virulence of *Vibrio vulnificus*. *Infect Immun* **47**: 446–451.

CHAPTER 2

Host-adaptation strategies in *Vibrio vulnificus*

Hernández-Cabanyero, C., Lee, C.T., Tolosa-Enguis, V., Sanjuán, E., Pajuelo, D., Reyes-López, F., Tort, L. and Amaro, C. (2019) Adaptation to host in *Vibrio vulnificus*, a zoonotic pathogen that causes septicemia in fish and humans. Environmental Microbiology. 21: 3118–3139.

1. Introduction

As a zoonotic pathogen, *V. vulnificus* infects humans or fish (especially farmed fish species) causing a variety of diseases called vibriosis (Amaro *et al.*, 2015; Oliver, 2015). If the infected host is a human risk patient or a farmed eel, the pathogen can invade the bloodstream, resist the innate immunity and cause death by sepsis (Horseman and Surani, 2011; Oliver, 2015). Epidemiological studies suggest that the main risk factor predisposing to sepsis caused by *V. vulnificus* in humans is a high iron concentration in blood due to various pathologies (Horseman and Surani, 2011; Oliver, 2015) while septicemia in eels occurs even in healthy specimens (Amaro *et al.*, 2015).

In the previous chapter, we have described the iron stimulon and the Fur regulon in *V. vulnificus* using a strain representative of the species that belongs to the zoonotic clonal-complex and, consequently, is able to infect humans and fish. We demonstrated that iron triggers the expression of genes involved in survival and resistance to the innate immune such as capsular antigen or O-antigen.

The aim of this chapter is to gain insights into the mechanisms that *V. vulnificus* uses to cause sepsis in hosts as evolutionarily distant as humans and fish. To this end, we have analyzed the transcriptome of R99 strain in serum from each host (*ex vivo* model of septicemia (Sanjuán and Amaro, 2004)) and validated the results by genetic (RT-qPCR) and phenotypic assays with selected mutants.

2. Materials and methods

Strains, media and bacterial growth

Bacterial strains (**TABLE 1**) were grown in TSA-1, CM9, CM9+Tf, CM9-$Fe_{(D)}$ (200, 400 or 800 µM 2,2'-bipyridyl [Sigma-Aldrich]), CM9+Fe, eel serum, eel serum plus 2.5, 5 or 100 µM $FeCl_3$ (iron-overloaded eel serum), human serum (Sigma-Aldrich) and human serum plus 100 µM $FeCl_3$ (iron-overloaded human serum) (Murciano *et al.*, 2017). Unless clearly specified, 2.5 ml of each serum/broth were inoculated with washed bacteria (10^5 CFU/ml) and incubated with agitation (60 rpm) at 28ºC (eels) or 37ºC (humans). Bacterial growth was monitored as CFU/ml at regular time intervals by the drop plate method. All the strains were stored in LB-1 plus 20% glycerol at -80ºC.

TABLE 1 | Virulence and resistance to innate immunity in blood of the strains used in this study.

Strain	Description	Virulence (LD_{50})[1]			Resistance to innate immunity in blood				
		Mice (i.p.)	Eel		Eel			Human	
			i.p.	bath	Blood	Phagocytes	Serum	Blood	Serum
R99	*V. vulnificus* zoonotic clonal-complex representative strain. Isolated from a diseased eel in Spain (Roig *et al.*, 2018)	4×10^5	1.7×10^2	2×10^6	+++	+	+++	+/-	+/-
Δvep07	R99 *vep07* defective mutant. Putative involved in fish innate immunity resistance (Lee *et al.*, 2008). The specific role is demonstrated in the present work	6×10^5	5.2×10^5*	$>10^8$*	+*	+/-*	+*	+/-	+/-
cvep07	Δ*vep07* complemented strain (Lee *et al.*, 2008)	7×10^5	1.4×10^2	6×10^6	+++	+	+++	+/-	+/-
ΔvvhA	R99 Δ*vvhA* (major *V. vulnificus* hemolysin) (Murciano *et al.*, 2017)	NT	3.3×10^2	1.4×10^7	+++	NT	+++	NT	NT
ΔrtxA1₃	R99 Δ*rtxA1₃*. Lacks both plasmidic and chromosomic copies of $RtxA1_3$ (Lee *et al.*, 2013)	NT	NT	NT	NT	NT	NT	NT	NT
ΔvvhAΔrtxA1₃	R99 Δ*vvhA* and Δ*rtxA1₃* (Murciano *et al.*, 2017)	NT	NT	NT	NT	NT	NT	NT	NT

NT, non tested

[1]Virulence was expressed as LD_{50} in CFU/fish or mouse in case of i.p. infection and CFU/ml in case of bath infection.

[2]Resistance to innate immunity in blood was measured as the ratio between bacterial counts at 4 h and 0 h of incubation in blood, phagocyte suspension and serum (SI_{4h}): -, no survival; -/+, $0 < SI_{4h} < 1$; +, $1 < SI_{4h} < 10$; ++, $10 < SI_{4h} < 25$; +++>25. *: significant differences in SI_{4h} ($P<0.05$) between R99 and the derivative mutant strains.

Microarray analysis

Bacterial transcriptome of R99 strain was analyzed in serum vs CM9 using the R99-specific microarray platform (**FIGURE 1**). *Sample preparation*. Total RNA from 6 h cultures (Abs_{625} 0.3) (serum complement starts to be significantly inactivated from 6 h of incubation) was extracted, labelled and hybridized on microarray according to previously specified in p. 65. *Data analysis*. The data were analyzed with Genespring 14.5 GX software as described in p. 65. The following comparisons were performed: eel serum vs CM9, human serum vs CM9 and iron-overloaded human serum vs CM9. *Microarray validation by RT-qPCR.* The same RNA samples used for the microarray analysis as well as the samples from eel tissues were analyzed by RT-qPCR to calculate the expression of the selected genes (primers listed in **TABLE 2**) as specified in p. 74.

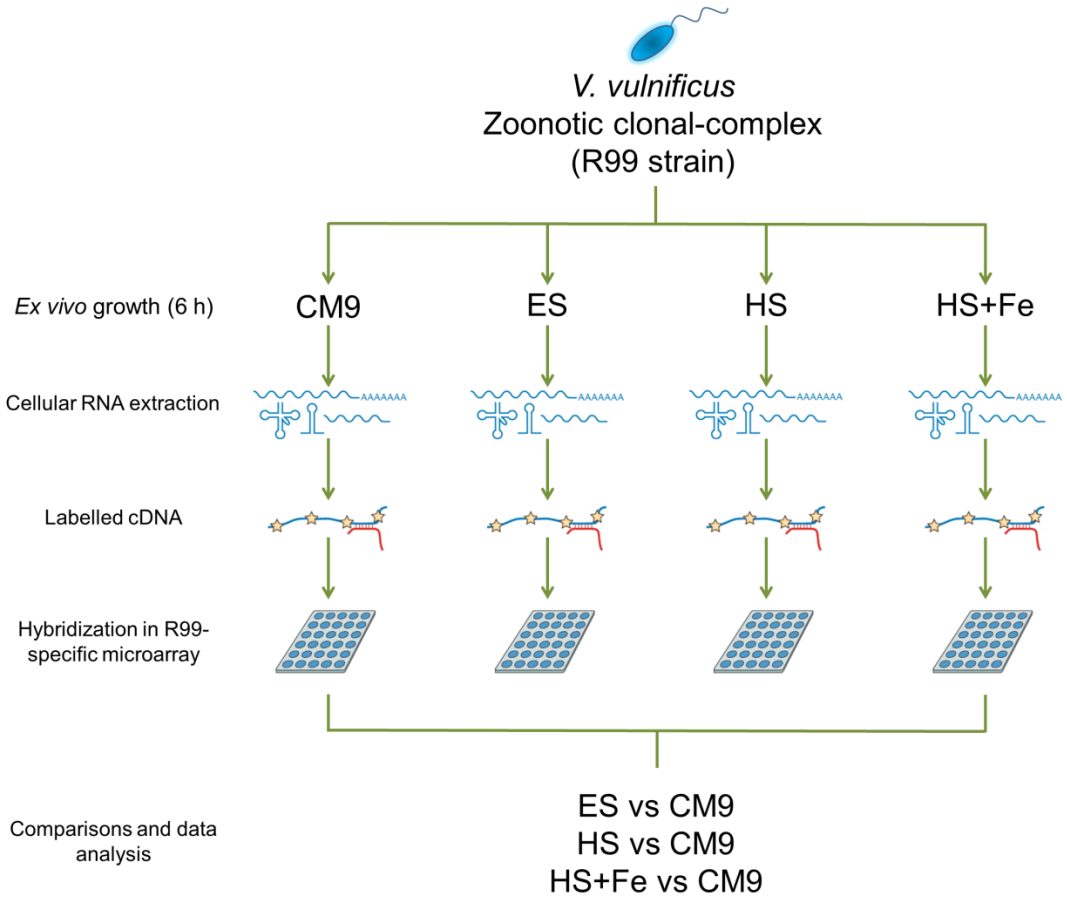

FIGURE 1 | Experimental design. Eel serum (ES), human serum (HS) and iron-overloaded human serum (HS+Fe).

TABLE 2 | Primers used in the study and microarray validation. Comparison of fold change values obtained by microarray and RT-qPCR with the *V. vulnificus* R99 strain. In case of RT-qPCR, results were obtained using *recA* as the reference gene and the fold induction ($2^{-\Delta\Delta Ct}$) for each gene was calculated.

Gene	Primer sequence	Sample	FC[1]	
			Microarray	RT-qPCR
cspE	Fw: CGGCCCGGACGTTTTT Rv: AAGAGTGCGGAAGCCATCAC	Eel serum vs CM9	8.49 (+)	2.51 (+)
rfbC	Fw: CATATTGCGTGGGCTGCAT Rv: AACCACTCGCACAAGCTTACC		2.47 (+)	1.26 (=)
rtxA	Fw: GAGTGATGATGGGCGCTTTAC Rv: CAGCCGCGATGGATGCT		-2.62 (-)	-7.03 (-)
vvhA	Fw: TGTTTATGGTGAGAACGGTGAC Rv: TTCTTTATCTAGGCCCCAAACTT		30.92 (+++)	6.36 (+)
vvhB	Fw: TGACGACGCAAGGCTTGA Rv: CAGGAGCTGACAGTCCTAAACCA		118.28 (+++)	5.21 (+)
cpsC	Fw: CCGTTCAGGCTCGACTTTG Rv: GGTTCACAGGGTGCGTGAGT		-1.59 (=)	-5.62 (-)
vep07	Fw: ATTTTGGAAGCAGCATTTCTGTT Rv: ATGTGTAAACTCCTCCCTTCTTAC		5.67 (+)	7.29 (+)
ksdC	Fw: GGCGTCAAAGCGCTTATGAA Rv: TTGTGACTGACGACCGGTAATAA		-2.25 (-)	-0.71(=)
lpxA	Fw: ACGCTTTACCGCAGTGGTTT Rv: CCGTCTCTTTCGCGATTTCT		2.09 (+)	2.88 (+)
lpxD	Fw: CGCGCAAGCCTTAGACACA Rv: GCCGACGACGCAATGC		--	2.57 (+)
lpxK	Fw: TGGTGGTTGTGGATGGTCAA Rv: GGCCGAGCGGGATCA		--	2.72 (+)
waaL	Fw: CGCCGCCATCTTGGTATT Rv: CCAAACGCGTGCCTTTCT		2.44 (+)	4.95 (+)
ompU	Fw: CGTACAACAACGCAGAAACGA Rv: CGTCAACGGCGAAGTTATCA		1.97 (=)	2.31 (+)
hlyU	Fw: AACCGTTTGTGCTTCTTTGC Rv: ATGAAAGACGCCTGCAAATC		-4.64 (-)	-2.89 (-)
qorA	Fw: GGCAAACGGCAGCACAA Rv: GCACTCTCTCCCCTTCTTTCAC	Human serum vs CM9	1.92 (=)	1.51 (=)
rtxA	See above		--	-0.72 (=)
vvhA	See above		--	2.47 (+)
lpxA	See above		--	1.01 (=)
lpxD	See above		--	1.09 (=)
lpxK	See above		--	1.73 (+)
waaL	See above		--	2.43 (+)
sypJ	Fw: CGCGCTGCCATTGGTATC Rv: TGCGAGCGGATGTGATCA		--	3.67 (+)
pygL	Fw: GGGCCGTGCGTTAGCA Rv: TTGTCTGTCTCTGTTGCAAGCA	Iron-overloaded human serum vs CM9	27.5 (+++)	2.73 (+)
rtxA	See above		6.08 (+)	40.79 (+++)
vvhA	See above		4.16 (+)	4.28 (+)
vvhB	See above		--	-4.79 (-)

TABLE 2 | Continued.

Gene	Primer sequence	Sample	FC[1]	
			Microarray	RT-qPCR
sypJ	See above	Iron-overloaded human serum vs CM9	5.32 (+)	3.13 (+)
cpsD	Fw: ATTTTGGAATCGCTTTGACG Rv: CGACCTTCGCTAGAAAAACG		3.75 (+)	8.73 (+)
ktrB	Fw: GCCACGGTCGGTTTAACG Rv: TTGCCCGGTTCCGAAA		6.18 (+)	3.16 (+)
malG	Fw: CCAGAATCCACGTCCAACGT Rv: GAGTGCCGATGCGGATGT		3.80 (+)	10.32 (++)
vieB	Fw: GGCCAAAAGAGAGGGAAATC Rv: CGACCTGATATTGCTGCTCA		-4.26 (-)	-1.95 (=)
qseB	Fw: GCAGGTGCCGATGATTACTT Rv: GACCCTGCCACATCACTTTT		11.46 (++)	3.59 (+)
hlyU	See above		2 (+)	1.83 (=)
cpsA	Fw: GCAGCTCATCGAGTGACGTA Rv: GCAGCTCATCGAGTGACGTA		-5.57 (-)	-5.92 (-)
cpsB	Fw: GCGGAACTGGTAATCCAAAA Rv: CCAAGCAAGAAGCTGAATCC		--	5.14 (+)
cpsH	Fw: AACAGTGGCAATCGGATCTC Rv: GGGGAAAGTCGGATCTTCTT		--	3.48 (+)
Fur	Fw: ACCCTTCCAAGGCTGAAAAT Rv: CAAAGTGGTGGCGAGTAACA		--	5.12 (+)
fruR	Fw: TCTGGCAATGCAAAAGTCAG Rv: AATATTCAACTCGGGCAACG		--	2.88 (+)
Reference gene				
recA	Fw: CGCCAAAGGCAGAAATCG Rv: ACGAGCTTGAAGACCCATGTG			

[1]Qualitative classification: =, -2<X<2; +, 2≤X<10; ++, 10≤X<25; +++, 25≤X; -, -10<X≤-2; --, -25<X≤-10; ---, X≤-25. --: this gene was not detected as differentially expressed by microarray hybridization.

***In vivo* assays**

Animal maintenance and extraction of blood, serum, RBC and phagocytes. Mice (6- to 8-week-old female BALB/c mice, Charles River, France) and farmed European eels (purchased from a local eel farm that does not vaccinate against *V. vulnificus*) were maintained and handled in the facilities of the SCSIE of the University of Valencia. Blood, serum, RBC and phagocytes were obtained from eels as previously described (Lee *et al.*, 2013). Human blood was obtained from healthy volunteers at the University of Valencia. Assays were approved by the Institutional Committee on Human Research (project license H1487946643442) following the Declaration of Helsinki.

Virulence, colonization and invasion assays. Virulence for normal mice and eels was determined as detailed in chapter 1 (p. 75). Eel colonization and invasion assays were

performed by immersion of groups of 24 eels (around 50 gr) per strain in an infective bath adjusted at the LD_{50} for R99 strain (Amaro *et al.*, 1995). Three live eels per group were randomly captured at 0, 9, 24 and 72 h, sacrificed and sampled (blood, head kidney, liver, spleen and gills) for bacterial counts in TSA-1 (CFU/ml for blood and CFU/g for tissues) and for quantification of selected genes by RT-qPCR according to Pajuelo *et al.*, (2015). In all cases, an extra group was infected with sterile PBS as a control (Amaro *et al.*, 1995).

All assays involving animals were approved by the Institutional Animal Care and Use Committee and the local authority (Generalitat Valenciana), following European Directive 2010/63/EU and the Spanish law 'Real Decreto' 53/2013 and were performed in the SCSIE facilities by using the protocols 2016-USC-PEA-00033 type 2 (virulence in eels), 2014-VSC-PEA-00195 type 2 (virulence in mice) and 2016-USC-PEA-00033 type 2 (colonization and invasion in eels). We also have a permission from Generalitat Valenciana to use eel for scientific research purposes.

***In vitro* assays**

Resistance to innate immunity in serum and blood. Bacteria were incubated (10^3 CFU/ml) in 96-well plates containing 200 µl of each sample (serum/blood) for 4 h. The effect of iron or complement inactivation on bacterial survival ability was determined by comparing the bacterial growth in fresh vs treated serum. Serum plus iron and inactivated serum were obtained as previously published (Sunyer and Tort, 1995; Pajuelo *et al.*, 2015; Murciano *et al.*, 2017). The SI_{4h} (survival index after 4 h of incubation) was determined according to Lee *et al.*, (2013).

Resistance to phagocytosis. Blood eel phagocytes were seeded in poly-L-lysine treated 96-well plates (10^5 cells/well). Bacteria were added at a moi (multiplicity of infection) of 10 in a final volume of 200 µl/well. Bacterial counts were performed at 0 and 90 min to calculate the percentage of bacteria that survived after phagocytosis (Lee *et al.*, 2013).

Hemolysis. Artificial blood was prepared by adding eel or human RBC (10^6 cells/ml) to serum (eel or iron-overloaded human serum, respectively). Artificial blood was seeded in 96-well plates and bacteria were added at a moi of 0.5 in a final volume of 200 µl/well. RBC counts were performed at 0, 1.30, 3 and 6 h post-infection to calculate the percentage of cell lysis. In parallel, samples for RNA extraction and quantification of *vvhA* and *rtxA1*$_3$ were taken.

Motility. Motility was assayed on CM9, eel serum, human serum and iron-overloaded human serum, 0.3% agar (wt/vol) as previously described in chapter 1 (p. 77). In parallel,

microscopic observations of bacterial suspensions were made in a Nikon Phase-Contrast Microscope.

Metabolism. The ability to respire nitrate/nitrite was determined in R99 strain grown for 6 h in 96-well plates containing 200 µl of CM9, eel serum or iron-overloaded human serum by adding NIT1 and NIT2 reagents (API®, BioMérieux) to each well. The ability to grow from exogenous maltose added to CM9, human serum and iron-overloaded human serum was determined by growing R99 in glass tubes and after 6 h of growth 0.2% (wt/v) maltose was added. Growth was measured as bacterial counts (CFU/ml) at 0 and 30 min after the addition of maltose.

Envelope analysis. Crude fractions of surface cell-associated polysaccharides (LPS plus capsule) of R99 in CM9, eel serum, human serum and iron-overloaded human serum were obtained and analyzed as described in chapter 1 (p. 79).

Biofilm production. Biofilm production by R99 strain in CM9 and iron-overloaded human serum was quantified as detailed in chapter 1 (p. 78).

Generation of anti-rVEP07 serum and immunoblots. A 17 kDa partial recombinant Vep07 (rVep07) with a C-terminal six-histidine tag was overexpressed by inducing *E. coli* BL21 strain containing partial *vep07* gene cloned into pE30a with 1 mM IPTG for 16 h at 30 ºC. Bacterial pellets disrupted by sonication and rVep07 were purified by affinity binding with the Ni^{2+} chelating sepharose (Chelating Sepharose™ Fast Flow, GE Healthcare Life Sciences). Six week-old female mice were immunized by subcutaneous injection with the 6xhistagged partial rVep07 according to Pajuelo *et al.*, (2015). For the *vep07* gene translation studies, R99 was cultured in different iron concentration conditions. 5 µg of the insoluble fraction of each total cell lysate (quantified using the Pierce BCA Protein Assay Kit [Thermo Scientific]) were fractionated by SDS-PAGE and then transferred onto a PVDF membrane. The membranes were probed with mouse anti-Vep07 serum. The blots were developed as described in chapter 1 (p. 79).

Statistical analysis. Data are presented as averages ± standard error of at least three independent experiments. Statistical analysis was performed using SPSS 19.0. The significance of the differences between averages was tested by using the unpaired Student´s t-test with a $P<0.05$. When the effects of more than two independent variables were taken into account an ANOVA analysis was performed. Virulence assays were only performed twice because no differences were found between the two replicates that justify killing more animals.

3. Results

Transcriptome in serum and phenotypic validation

We analyzed the DEGs of R99 strain in eel serum, human serum and iron-overloaded human serum (to mimic the bloodstream of a risk patient affected from haemochromatosis (Murciano *et al.*, 2017)). Remarkably, the affected cellular processes were the same than those revealed by the transcriptomic study performed in chapter 1. **FIGURE 2** shows the number of DEGs in serum which are in common with iron stimulon and/or Fur regulon, **FIGURE 3** shows the DEGs by *V. vulnificus* in serum and **TABLE 2** provides a comparison between fold change values obtained by hybridization with the R99-specific microarray and by RT-qPCR.

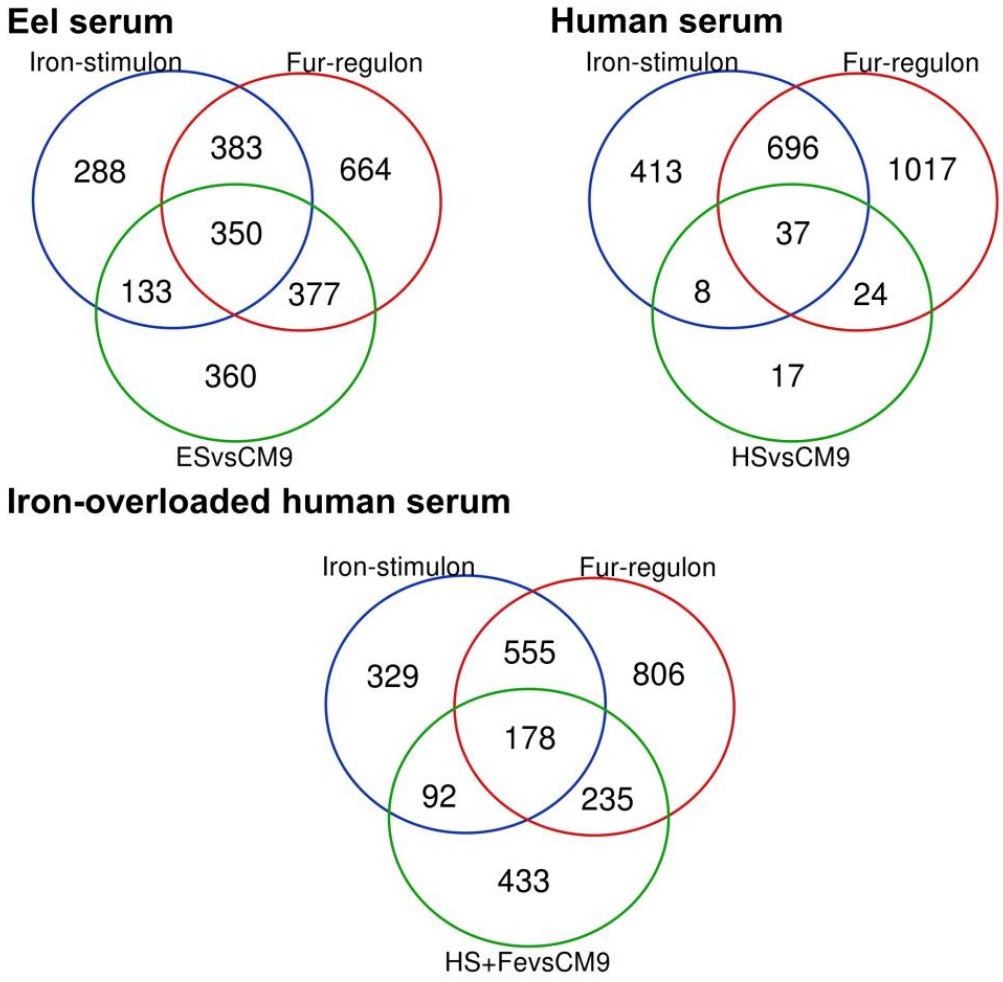

FIGURE 2 | Number of DEGs in serum in common with iron stimulon and/or Fur regulon (previously described in chapter 1)) represented as Venn diagrams. ES (eel serum), HS (human serum), HS+Fe (iron-overloaded human serum).

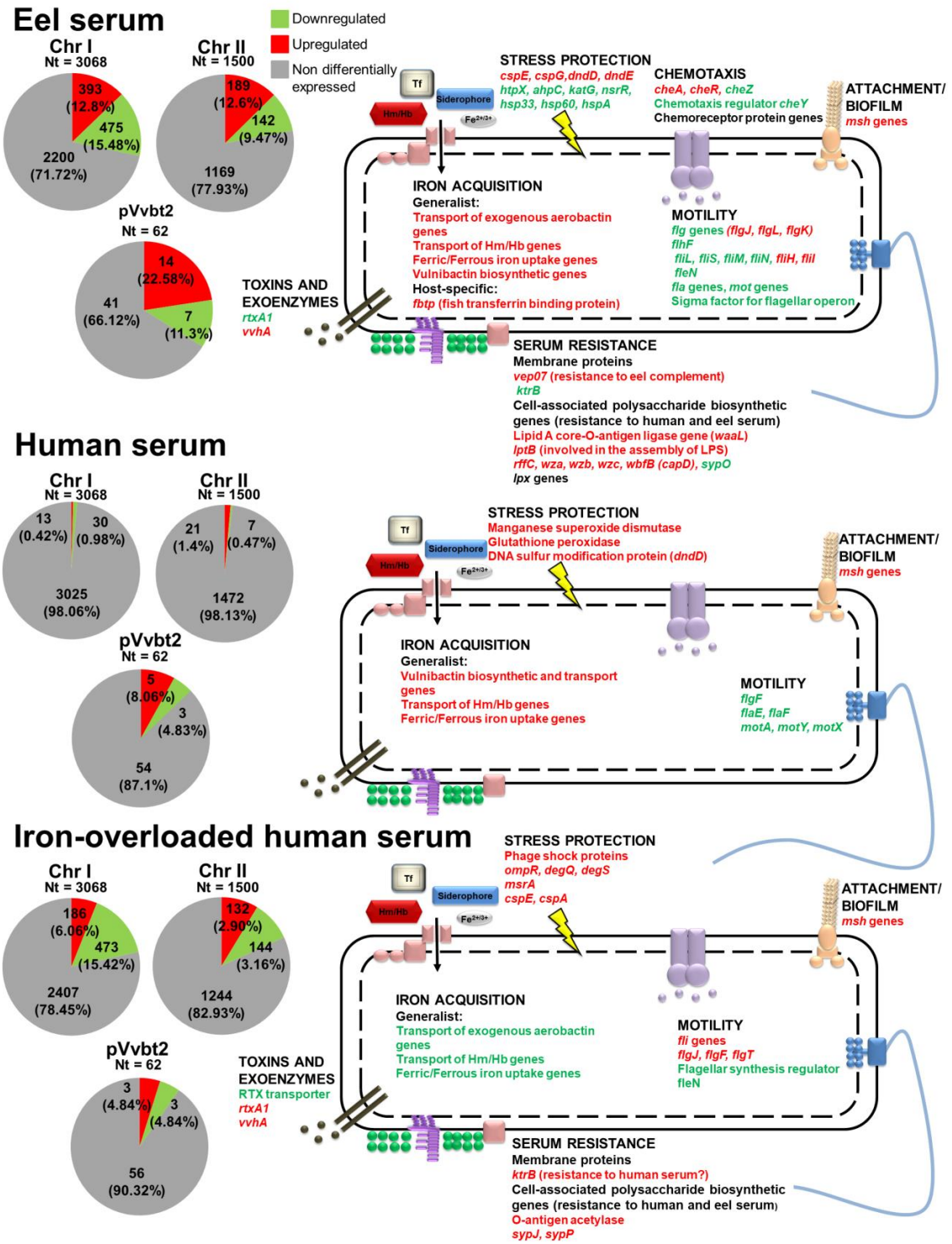

FIGURE 3 | DEGs by *V. vulnificus* R99 in serum vs CM9. Genes which exhibited a value of fold change -2≤X≤2 with a p-value cut-off of *0.05* (averages from three independent biological samples) were considered as DEGs. Left: distribution of the DEGs per regulation category (down/upregulated or non-differentially expressed) and replicon (two chromosomes and one plasmid). The categories are represented with a color code. Right: main DEGs affected virulence- and survival-related processes. Red color: upregulated genes; green color: downregulated genes; black color: a group of related genes for the same biological process, some up- and other downregulated**.**

Eel serum. We obtained strong evidence of a switch from aerobic to anaerobic metabolism in eel serum vs CM9, mainly highlighted by the upregulation of *arcA* (anaerobic metabolism repressor) together with most of the genes for nitrate/nitrite respiration (**TABLE 3**). This result was phenotypically confirmed by a dissimilatory reduction of nitrate/nitrite in eel serum but not in CM9 at 6 h post-inoculation (**FIGURE 4A**). Accordingly, the pathogen upregulated *lrp*, encoding a master regulator for N-compound metabolism, plus multiple genes for organic nitrogen compound uptake/transport/metabolism (**TABLE 3**) (Brinkman *et al.*, 2003; Ho *et al.*, 2017). In parallel, genes for regulators/sensors related to nitrogen, phosphorus and nucleoside starvation (*cytR*) were also differentially expressed in eel serum vs CM9 (**TABLE 3**). Regarding CytR, it has also been described to regulate competence (Antonova *et al.*, 2012), which is activated in *V. cholerae* by chitin or their derivative amino sugars (e.g. N-acetyl- glucosamine) (Meibom *et al.*, 2005). Accordingly, the main competence regulator TfoX (Metzger and Blokesch, 2016), and genes for specific N-acetyl-glucosamine uptake/transport were also upregulated concomitantly with the downregulation of two genes for amino sugar metabolism repressors (*uxuR* and *kdgR*) (Nieckarz *et al.*, 2017) (**TABLE 3**). R99 strain also downregulated *fur* and upregulated most of the genes for vulnibactin biosynthesis/uptake/transport, as well as for transport/utilization of the host's heme compounds and fish transferrin (**TABLE 3**).

We obtained strong evidence of cell damage and stress response in eel serum, since multiple genes related to membrane regeneration were highly upregulated as well as genes for different stress-related protective proteins (Mathur and Waldor, 2004; Mathur *et al.*, 2007; Phadtare and Severinov, 2010; Manganelli and Gennaro, 2017) (**TABLE 3**). Remarkably, R99 strain seemed to respond specifically against oxidative/nitrosative stress by downregulating genes for two repressors, *ohr* and *nsr*, and upregulating an activator, *norR*, together with genes for various hydroperoxidases, a glutathione synthetase (*glnA*) and a hydroxylamine reductase (Fuangthong *et al.*, 2001; Rodionov *et al.*, 2005) (**TABLE 3**). In addition, a significant proportion of the genes involved in flagellum biosynthesis were downregulated in eel serum (**TABLE 3**). This result was also phenotypically confirmed as R99 strain was non-motile on eel serum supplemented with 0.3% agar, while it was motile on CM9-agar (**FIGURE 4B**). Finally, some genes for capsule/O-antigen biosynthesis, *vvhA*, *rtxA1*$_3$ plus genes for regulators involved in toxin production, quorum sensing and a gene for a DNA-binding H-NS protein (silencing protein mainly for mobile genetic elements transcription) were also differentially expressed (**TABLE 3**).

Interestingly, more than 90% of the mentioned genes belong to iron stimulon and/or Fur regulon (**TABLE 3** and **FIGURE 2**).

TABLE 3 | Selected DEGs in eel serum vs CM9.

Gene(s)[1]	FC[2]	Iron stimulon	Fur regulon	Putative function/process[3]
Metabolic regulators and sensors				
cytR	14.3	No	Yes	Repressor (response to nucleoside starvation, competence) (Antonova *et al.*, 2012)
arcA	3.5	No	Yes	Repressor for aerobic metabolism
Cyn operon transcriptional activator	3	No	Yes	Activator of cyanide metabolism, a subproduct from urea
fabR	-2.5	Yes	Yes	Repressor for unsaturated fatty acid biosynthesis
fur	-2.3	No	Yes	Regulator of iron uptake mainly acting as a repressor
aer	-2.7	No	Yes	Aerotaxis sensor receptor protein
phoR, phoB	-(2.7-3.8)	Yes	No/Yes	PhoR (histidine kinase/phosphatase for PhoB) and PhoB (positive transcriptional factor for Pho regulon) involved in phosphate starvation
Nitrogen regulatory protein P-II	-6.8	Yes	Yes	Nitrogen starvation
kdgR	-8.2	Yes	Yes	Repressor for oligogalacturonide metabolism (Nieckarz *et al.*, 2017)
uxuR	-9.4	Yes	Yes	Repressor for oligoglucuronide metabolism (Rodionov *et al.*, 2000)
fruR (cra)	-89.1	Yes	Yes	Catabolite repressor/activator (Cra) protein
Anaerobic respiration				
Nitrate reductase cytochrome c550-type subunit	13	Yes	No	Nitrate reductase complex subunit
napA, napC, napD, napF, napG, napH	11.4-3.7	Some	Some	Subunits of the periplasmic nitrate reductase,
ccoN	11	No	Yes	Cytochrome c oxidase subunit
nrfBCD	5.9-4.6	No	No	Formate-dependent nitrite reductase complex
Peptide/amino acid/ammonium metabolism (including transporters)				
nupC	13.7	Yes	Yes	Permease for nucleoside uptake
rbsBD	8.9-4.2	No	No	Ribose ABC transport system

TABLE 3 | Continued.

Gene(s)[1]	FC[2]	Iron stimulon	Fur regulon	Putative function/process[3]
PTS system, N-acetylglucosamine-specific IIB component	8.7	Yes	No	Amino sugar transport
Serine transporter	7.6	Yes	No	Amino acid transport
Tail-specific protease precursor	3.5	Yes	Yes	Protein degradation
Peptide ABC transporters	4.2-2.2	No	Yes	Peptide transport
glnA	2.3	No	Yes	Ammonia assimilation cycle
N-Acetyl-D-glucosamine ABC transport system	2.2	No	No	Amino sugar transport
potD	2	Yes	Yes	Polyamine transport
Iron uptake				
Vulnibactin biosynthetic genes	8.4-2	Yes	Yes	Vulnibactin biosynthesis and transport
Heme/Hemin transport	5.4-3.1	Yes	Yes	Heme/Hemin transport and utilization
Ferric iron ABC transporters	4.3-2.7	Yes	Yes	Ferric iron transport
Aerobactin transport	3-2	Yes	Yes	Aerobactin transport
***ftbp* (or *vep20*)**	3	Yes	No	Eel transferrin binding
LPS and capsule				
rffC, wzbc, waaL, rfbD	4.2-2.1	Yes	Yes	LPS biosynthesis
wza, lptB	2.3	No	Yes	LPS biosynthesis
cpsC	-2	No	Yes	Capsule biosynthesis
sypO	-2.9	Yes	Yes	Capsule biosynthesis
yciS	-3.8	Yes	Yes	LPS (core) biosynthesis
SOS response, DNA repair and competence				
tfoX	3.1	Yes	Yes	Positive regulator of competence
uvrC	2.2	Yes	No	Excinuclease ABC subunit C for DNA repair
lexA	-3.1	No	Yes	Repressor of SOS response
dns	-5.8	Yes	Yes	Competence related: degradation of DNA for nutrient uptake
Stress protection related genes				
glpABC	33-22	No	No	Anaerobic glycerol-3-phosphate dehydrogenase, phospholipid biosynthesis/membrane regeneration
hcp	13.8	No	No	Hydroxylamine reductase, a scavenger of potentially toxic byproducts of nitrate metabolism

TABLE 3 | Continued.

Gene(s)[1]	FC[2]	Iron stimulon	Fur regulon	Putative function/process[3]
aphC	10.3	Yes	Yes	Resistance to oxidative stress
cspE, cspG	8.5-6.3	Yes	Yes	Cold shock proteins, involved in stress caused by membrane damage
Formate efflux transporter	6	Yes	Yes	Resistance to microcidal peptides
madN	6	No	Yes	Resistance to microcidal peptides
usp8	5.3	No	Yes	Universal stress protein family 8, related to resistance to oxidative stress
Glutathione synthetase	3.8	No	No	Resistance to oxidative stress
pspABC	3.5-2.6	No	Some	Phage shock proteins involved in resistance to different stresses (Manganelli and Gennaro, 2017)
Cold-shock DEAD-box protein A (helicase of RNA)	3.1	No	Yes	Resistance to different stresses
norR	2.8	No	No	Anaerobic nitric oxide reductase transcription regulator
dndDE	2	No	Yes	DNA modification, DNA protection from H_2O_2 and hydroxyl radicals *in vivo*
ompU	2	Yes	Yes	Resistance to microcidal peptides (Mathur *et al.*, 2007)
rseABC	-(2.6-5.4)	*Yes*	Some	Negative regulatory proteins for RpoE, a sigma factor for envelope stress response
ohr	-2.9	No	Yes	Repressor for organic hydroperoxide resistance
rpoD	-7	No	No	Nitric oxide-sensitive repressor of genes involved in protecting the cell against nitrosative stress
nsrR	-7.2	Yes	Yes	Repressor for resistance to nitrosative stress
Flagellum and pili				
MSHA cluster	4.8-2.8	Some	Some	Pili MSHA biosynthesis
flaDEF	-(2-3.9)	Some	Yes	Flagellin proteins
fliL	-2.2	Yes	Yes	Controls the rotational direction of flagella during chemotaxis
fliS	-2.2	Yes	Yes	Flagellar secretion chaperone
flgABCDE, flgG	-(2.4-5)	Some	Some	Flagellar basal-body rod proteins
flhF	-2.5	Yes	Yes	Flagellar biosynthesis protein
fleN	-4.9	Yes	Yes	Flagellar synthesis regulator

TABLE 3 | Continued.

Gene(s)[1]	FC[2]	Iron stimulon	Fur regulon	Putative function/process[3]
RNA polymerase sigma factor for flagellar operon	-4.9	Yes	Yes	Flagellar biosynthesis
motX	-5.2	Yes	Yes	Sodium-type polar flagellar protein
flgN	-6.1	No	Yes	Flagellar biosynthesis protein
flgM	-6.7	Yes	Yes	Hook associated protein
motA	-12.1	Yes	Yes	Flagellar motor rotation protein
Virulence factors and related regulators				
vvhAB	118-31	Yes	No	Hemolysin (vulnificolysin) and transport protein
lrp	2.4	Yes	Yes	Global regulator involved in virulence that is up-regulated under nutrient starvation (Ho *et al.*, 2017)
smcR	2	No	Yes	Master regulator of quorum sensing. It downregulates *hlyU* (Kim *et al.*, 2013)
luxU	-2	Yes	Yes	Phosphorelay protein LuxU involved in quorum sensing
rtxA1$_3$	-2.6	No	No	Toxin involved in cytokine storm in mice (Murciano *et al.*, 2017)
luxO	-3	Yes	Yes	Indirectly represses *smcR* transcription
csrA	-3	Yes	Yes	Carbon storage regulator, a global repressor of multiple virulence factors
hlyU	-4.6	No	Yes	*rtxA1$_3$* activator
rtxC	-5	No	Yes	Cytolysin-activating lysine-acyltransferase, *rtxA1$_3$* activator
DNA-binding protein H-NS	-10.2	Yes	Yes	Transcriptional repression (silencing) of mobile genetic element transcription

[1]Identified DEGs are indicated.
[2]FC: fold change value or range of fold change values for each individual gene or for a group of related genes, respectively.
[3]Putative function for the gene and related process.

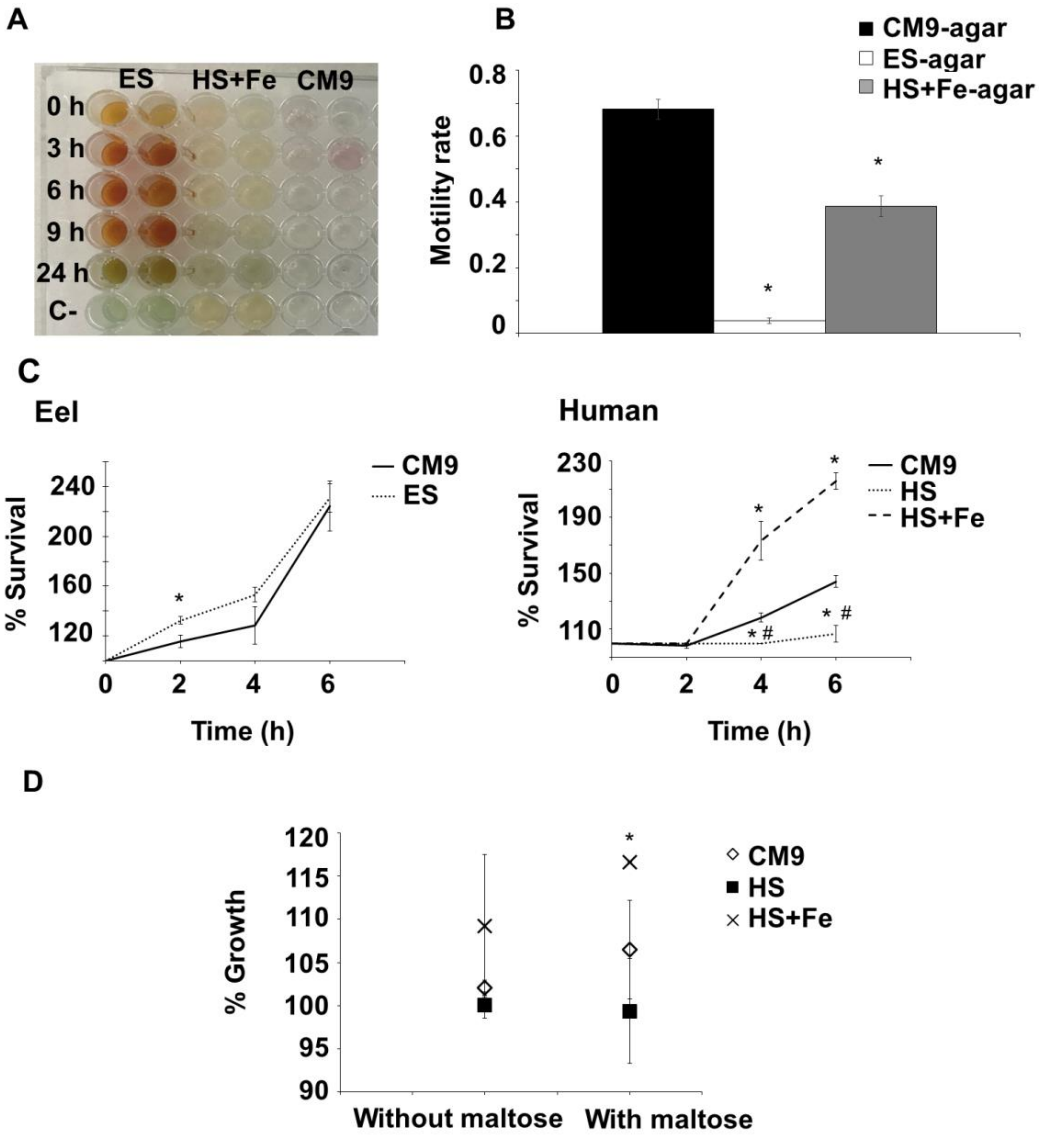

FIGURE 4 | Phenotypic assays to validate microarray data in serum. (A) Nitrate and nitrite respiration. Nitrate and nitrite respiration were measured with the API20E™ kit (Biomerieux, Spain) after incubation of R99 strain in eel serum (ES), iron-overloaded human serum (HS+Fe) and CM9. Positive results (red colored wells) were obtained for eel serum at 3, 6 and 9 h post-incubation. (B) Motility was measured as motility rate (colony surface in mm^2/log of colony bacterial number in CFU/ml). The assay was performed on plates of CM9- or serum-agar (0.3%). ES-agar plates were incubated at 28ºC and HS+Fe-agar plates at 37ºC. CM9-agar column and bar present the average and standard error corresponding to 6 plates (3 incubated at 28ºC and 3 at 37ºC). *: significant differences (*P<0.05*) in serum-agar vs CM9-agar. (C) Survival in serum: R99 strain was inoculated in CM9 and serum (ES, human serum [HS] or HS+Fe and incubated for 6 h at 28ºC (CM9/ES) or 37ºC (CM9/HS/HS+Fe). % Survival: ratio of bacterial counts at selected time intervals vs 0 h. Points and bars show the average and standard error from three independent experiments. *: significant differences (*P<0.05*) in serum vs CM9; #: significant differences (*P<0.05*) in HS vs HS+Fe. (D) Growth from exogenous maltose. R99 was grown in tubes containing CM9, HS and HS+Fe for 6 h at 37ºC. Maltose (0.2% wt/v) was added to half of the tubes and all the tubes were incubated for additional 30 min. % Growth: ratio of bacterial counts at 30 min vs 0 min post maltose addition. Data are presented using a dot plot graph. Points and bars correspond to average and standard error from three independent experiments. *: significant differences found with ANOVA analysis (*P<0.05*) in HS/HS+Fe vs CM9.

Human serum. R99 strain was unable to multiply efficiently in human serum, inability that was reversed by adding iron to serum (**FIGURE 4C**). Consequently, few DEGs were upregulated in human serum vs CM9, specifically only those related to siderophore biosynthesis/uptake, resistance/protection against oxidative stress, and MSHA biosynthesis, most of which were also overexpressed in eel serum (**TABLE 4**). In contrast, a more diverse transcriptomic response was observed in iron-overloaded human serum vs CM9 (**TABLE 5**), where most of the DEGs were oppositely regulated to what we observed in eel serum, i.e., genes for nitrite/nitrate respiration, siderophore biosynthesis/uptake, flagellum biosynthesis and motility (**TABLES 3** and **5**). We phenotypically confirmed most of these transcriptomic evidence as R99 strain was unable to respire nitrate/nitrite and was more motile in iron-overloaded human serum supplemented with 0.3% agar than in CM9-agar (or eel serum supplemented with 0.3% agar) (**FIGURE 4B**). As in eel serum, R99 seemed to present an anaerobic respiratory metabolism in iron-overloaded human serum, probably based on organic compounds (i.e., fumarate) and using glycogen/glucan and derived sugars (i.e., maltose) as the main energy and carbon sources (**TABLE 5**). This result was confirmed by a significant positive result for increased growth after exogenous maltose addition in iron-overloaded human serum but not in CM9 (or human serum) (**FIGURE 4D**). The pathogen also upregulated genes for protection against different stresses, regeneration of damaged proteins, lipids, and membranes in iron-overloaded human serum, many of which differed from those found in eel serum (**TABLES 3** and **5**). As in eel serum, *vvhA* and *rtxA1*$_3$ were also differentially expressed in iron-overloaded human serum, as were some genes for LPS/capsule biosynthesis (**TABLE 5**). Finally, genes encoding for different transcriptional regulators, most of them not found in eel serum, were also differentially expressed in iron-overloaded human serum (i.e., HlyU, the main activator of *rtxA1*$_3$ (Liu *et al.*, 2011), VieB, a repressor for the virulence activator VieA (Lee *et al.*, 1998; Mitchell *et al.*, 2015), SmcR, the main quorum sensing regulator (Kim *et al.*, 2013), QseB, a regulator that responds to iron and quorum sensing signals (Weigel *et al.*, 2015) and VpsT, a biofilm formation activator (Krasteva *et al.*, 2010)) (**TABLE 5**).

Approximately, 90% of all the above genes belong to iron stimulon and/or Fur regulon (**TABLE 5** and **FIGURE 2**).

TABLE 4 | Selected DEGs in human serum vs CM9.

Gene(s)[1]	FC[2]	Iron stimulon	Fur regulon	Putative function/process[3]
Protection against oxidative stress				
sodA	9.4	Yes	Yes	Oxidative stress
frmA	5.6	No	No	Oxidative stress
Glutathione peroxidase	3.7	Yes	Yes	Oxidative stress
dndD	2.9	No	Yes	DNA sulfur modification
Metabolism				
fruR	-8	Yes	Yes	Catabolite repressor/activator (Cra) protein
Iron uptake				
Vulnibactin biosynthetic genes	34.4-4.3	Yes	Yes	Vulnibactin biosynthesis and transport
Flagellum and pili				
MSHA cluster	8.9-3.5	Some	Some	Pili MSHA biosynthesis
flgF	-3.1	No	Yes	Flagellar basal-body rod protein
flaEF	-(3.7-4.7)	Yes/No	Yes	Flagellin proteins
motY	-4.2	Yes	Yes	Sodium-type flagellar protein
motX	-5.1	Yes	Yes	Sodium-type polar flagellar protein
motA	-8.7	Yes	Yes	Flagellar motor rotation protein

[1]Identified DEGs are indicated.
[2]FC: fold change value or range of fold change values for each individual gene or for a group of related genes, respectively.
[3]Putative function for the gene and related process.

TABLE 5 | Selected DEGs in iron-overloaded human serum vs CM9.

Gene(s)[1]	FC[2]	Iron stimulon	Fur regulon	Putative function/process[3]
Metabolic regulators				
fabR	-2.4	Yes	Yes	Repressor for unsaturated fatty acid biosynthesis
trpR	-4	Yes	Yes	Amino acid (Trp) biosynthesis
metJ	-4.4	No	Yes	Amino acid (Met) biosynthesis (repressor)
yvoA	-4.5	No	No	2-aminoethylphosphonate uptake and metabolism regulator (phosphonate metabolism)
kdgR	-6.2	Yes	Yes	Repressor for amino sugars metabolism (Nieckarz *et al.*, 2017)
Metabolic and nutrient transport genes (including iron)				
nirB	63.5	No	Yes	Assimilatory nitrite reductase
malQ	44.9	No	Yes	4-alpha-glucanotransferase (amylomaltase)
Nitrate ABC transporter, nitrate-binding protein	22.2	No	No	Nitrogen metabolism
malK, malG, malI	19.4-3.8	No	Yes	Maltose/maltodextrin ABC transporter
glgB, glgX	6.4-15.3	No	Yes	Glycogen branching and debranching enzymes
Amine oxidase, flavin-containing	11.6	No	Yes	Nitrogen metabolism
amtB	11	No	No	Ammonium transporter
dctM, dctQ	6.5-5.4	No	No	TRAP dicarboxylate transporters
murP	6.4	No	No	Amino sugar transport (PST system)
ABC-type phosphate transport system	5.7	No	No	Phosphate transport
artI, artQ	5.5-3.1	No	No	Arginine ABC transporters
C4-dicarboxylate like transporter	5	No	No	Dicarboxylate transport
sapB	4.7	No	Yes	Peptide transport system permease
Predicted ferric reductase	4.1	No	Yes	Ferric reductase
N-Acetyl-D-glucosamine ABC transport system	3.6	No	No	Amino sugar transport
vuuA	-5	Yes	Yes	Ferric vulnibactin receptor

TABLE 5 | Continued.

Gene(s)[1]	FC[2]	Iron stimulon	Fur regulon	Putative function/process[3]
Stress protection related genes				
pspABC	69-59	No	Some	Phage shock proteins involved in resistance to different stresses
Phosphoglycerol transferase I	27.2	Yes	Yes	Phospholipid biosynthesis/membrane regeneration
Anaerobic glycerol-3-phosphate dehydrogenase subunits (B, C)	10-8	No	No	Phospholipid biosynthesis/membrane regeneration
S-(hydroxymethyl)glutathione dehydrogenase	9	No	No	Peroxilipid detoxification
Glutathione S-transferase	8.9	No	Yes	Peroxilipid detoxification
Thiol peroxidase, Bcp-type	4.4	Yes	Yes	Resistance to oxidative stress
glnA	3.8	No	No	Resistance to oxidative stress
msrA	3.8	No	No	Peptide methionine sulfoxide reductase involved in reparation of oxidized proteins
YfgC precursor	3.8	Yes	Yes	Outer membrane integrity
degQ, degS	3.3-2.7	No/Yes	No	Outer membrane integrity
cspA, cspE	2.6	Yes	Yes/No	Cold shock proteins involved in resistance to different stresses
Flagellum and pili				
rpoN	7.6	Yes	No	RNA polymerase sigma factor
mshE, mshJ, mshQ	4.5-2.8	No	Some	Pili MSHA
Von Willebrand factor type A domain protein	4.2	No	No	Pili MSHA
fliH, fliLMNO	3.6-2.6	Some	Some	Flagellar biosynthesis proteins
flgF, flgJ, flgT	2.6-2	Some	Some	Flagellar proteins
Probable type IV pilus assembly FimV-related	2.8	No	No	Pili MSHA
LPS and capsule				
O-antigen acetylase	10.2	No	Yes	LPS modification
sypJP	3.3-5.3	No	No	Capsule biosynthesis
cpsD	3.8	No	No	Capsule biosynthesis

TABLE 5 | Continued.

Gene(s)[1]	FC[2]	Iron stimulon	Fur regulon	Putative function/process[3]
Virulence factors and related regulators				
qseB	11.5	No	No	Positive regulation of flagella and motility
ktrB	6.2	No	No	Potassium uptake protein involved in serum resistance
rtxA1	6.1	No	No	Toxin involved in cytokine storm in mice (Murciano *et al.*, 2017)
vvhA	4.2	Yes	No	Hemolysin (vulnificolysin)
ompR	3.1	No	Yes	Virulence regulator that responds to osmotic pressure
RTX toxin transporter	2.3	No	Yes	MARTX transporter
hlyU	2	No	Yes	*rtxA1*$_3$ activator
vpsT	-4	Yes	No	Repressor of biofilm and biofilm related polysaccharide formation (Krasteva *et al.*, 2010)
vieB	-4.3	No	Yes	Controls VieA, that activates virulence genes (Mitchell *et al.*, 2015)
fleN	-4.3	No	No	Repressor of flagellum biosynthesis
smcR	-6.2	No	No	Master regulator of quorum sensing. It downregulates *hlyU* (Kim *et al.*, 2013)

[1]Identified DEGs are indicated.
[2]FC: fold change value or range of fold change values for each individual gene or for a group of related genes, respectively.
[3]Putative function for the gene and related process.

Virulence factors differentially expressed in serum

Toxins. *vvhA* and *vvhB* (encoding a secretory protein for VvhA (Yamamoto *et al.*, 1990)), were the most strongly upregulated genes in eel serum, while *rtxA1*$_3$ and *rtxC* (encoding an enzyme for RtxA1$_3$ post-transcriptional modification (Satchell, 2011)) were downregulated (**TABLE 3d**). We demonstrated that *vvhA* is involved in virulence and *in vivo* survival in blood since both LD_{50} as well as bacterial counts in blood from bath-infected eels were significantly impaired in a mutant strain deficient in *vvhA* (**TABLE 1** and **FIGURE 5A**). To uncover the role of VvhA in survival in blood, we evaluated the hemolysis produced by R99 vs Δ*vvhA* strain in artificial eel blood (eel serum supplemented with RBC) as well as the transcription of *vvhA* by

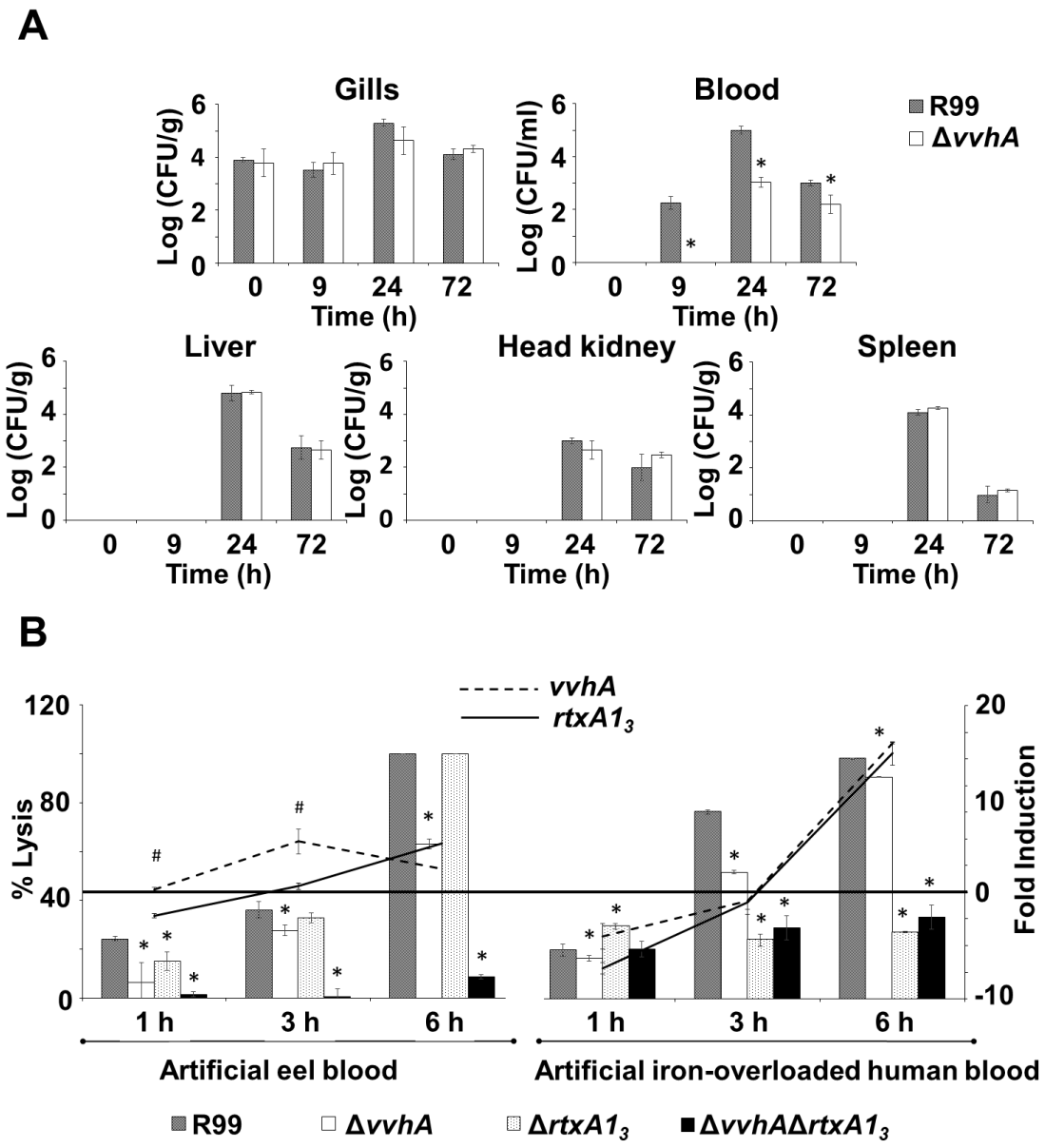

FIGURE 5 | Role of *vvhA* in eel colonization and hemolysis. (A) Eel colonization and invasion. Groups of 24 eels per strain (3 animals per sampling point) were bath-infected with either R99 or Δ*vvhA* strains at the same dose (2x10^6 CFU/ml) and gills, blood, liver, head kidney and spleen were sampled for bacterial counting on TSA-1 at 0, 9, 24 and 72 h post-infection. *: significant differences in bacterial counts from R99 vs Δ*vvhA* infected eels using the unpaired Student´s t-test (*P< 0.05*). (B) Hemolysis and gene expression in artificial blood. Artificial eel and iron-overloaded human blood were prepared by adding RBC to their respective sera (1x10^6 cells/ml). Then, artificial blood samples were infected with either R99 or each one of its derivative mutants (Δ*vvhA*, Δ*rtxA1$_3$* and Δ*vvhA*Δ*rtxA1$_3$*) at a moi of 0.5. Hemolysis (percentage of lysed cells [% lysis]) and *vvhA*/*rtxA1$_3$* transcription (fold induction in artificial blood vs serum) were determined at 1, 3 and 6 h post-infection. *: significant differences in % lysis between R99 and each mutant strain were determined using the unpaired Student´s t-test (*P<0.05*); #: significant differences between *rtxA1$_3$* and *vvhA* fold induction were determined using the unpaired Student´s t-test (*P<0.05*). All results are presented as average ± standard error of three independent biological experiments.

R99 strain for 6 h post-infection. In these experiments we also included the Δ*rtxA1₃* and Δ*vvhA*Δ*rtxA1₃* mutants as controls, as RtxA1$_3$ also cause hemolysis *in vitro* (Wright and Morris, 1991; Kim *et al.*, 2008). First, we found that *rtxA1₃* was upregulated when RBC were added to eel serum (fold change value changing from -2.6 in eel serum to 5.8 in artificial eel blood at 6 h post-infection), which correlated with previous results obtained *in vivo* (Lee *et al.*, 2013). Second, *vvhA* was transcribed before *rtxA1₃* and appeared to be mainly responsible for hemolysis at 6 h post-infection (**FIGURE 5B**). This result correlated well with those obtained *in vivo*, as *vvhA* and *rtxA1₃* were upregulated in blood of bath-infected eels (*vvhA* at 3 h and *rtxA1₃* at 9 h post-infection with fold induction values of 8.7±0.5 and 3±0.2, respectively). We repeated the experiments with artificial iron-overloaded human blood (iron-overloaded serum supplemented with RBC) and observed that *rtxA1₃* and *vvhA* were transcribed in parallel from the beginning of the experiment, achieving a similar fold induction value at 6 h post-infection, however in this case, the hemolysis at 6 h seemed to be mainly due to RtxA1$_3$ (**FIGURE 5B**).

Envelope polysaccharides. Capsule and O-antigen are involved in resistance to human and fish innate immunity (Amaro *et al.*, 1994, 1997). Transcriptomic results showed that multiple genes related to both LPS and capsule biosynthesis were differentially expressed in serum (**TABLES 3** and **5**). Therefore, we analyzed the polysaccharide profile from R99 strain grown in eel serum, human serum and iron-overloaded human serum. The pathogen changed the proportion of capsule vs O-antigen in human serum, producing more capsule in iron-overloaded human serum (**FIGURE 6**). In case of eel serum, the pathogen seemed to produce an intermediate pattern with similar amounts of capsule and O-antigen, without major differences to those seen in CM9 (**FIGURE 6**). Remarkably, the O-antigen contained the high/medium molecular weight bands previously described to be involved in resistance to eel complement (Amaro *et al.*, 1997). Although we could not estimate free iron in serum, we determined the total iron (free and protein associated) and found that eel serum contains more iron (1.1 mg/l) than human serum (0.75 mg/ml), suggesting that eel serum is less restrictive.

Vep07. One of the most upregulated genes in both eel serum and human serum was *vep07*, a gene encoding a hypothetical protein involved in virulence (by unknown mechanisms) for eels but not for mice (Lee *et al.*, 2008). An *in silico* analysis of this protein (using two bacterial lipoprotein prediction programs, LipoP (Juncker and Willenbrock, 2003) and DOLOP (Madan Babu, and Sankaran, 2002)) revealed that Vep07 is probably an OM (outer membrane) lipoprotein. Therefore, we analyzed the presence of Vep07 in different bacterial fractions by

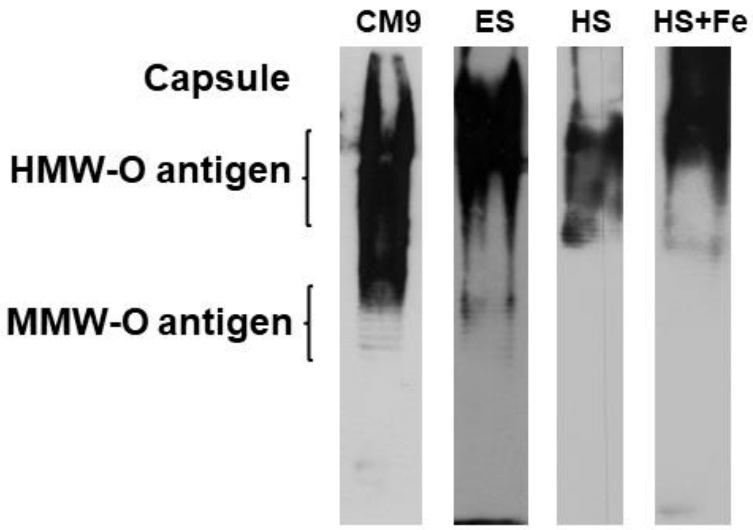

FIGURE 6 | LPS and capsule of *V. vulnificus* in serum. Bacteria were grown for 6 h in CM9, eel serum (ES), human serum (HS) and iron-overloaded human serum (HS+Fe). Then, cell-associated polysaccharides (LPS plus capsule) were extracted, separated by SDS-PAGE and subjected to immunoblot analysis with antibodies against cell-envelopes of R99 (diluted 1:3000) and developed following incubation with anti-rabbit IgG HRP-conjugated secondary antibody (diluted 1:10000 [Sigma-Aldrich]) using Immobilon Western Chemiluminescent HRP Substrate (Millipore). HMW, high molecular weight. MMW, medium molecular weight.

immunostaining with the antibody anti-rVep07 and confirmed that Vep07 is an OMP (outer membrane protein) of 55 kDa that is regulated by iron as it was only expressed under iron restricted conditions, imposed by an iron chelator or by eel serum (**FIGURE 7A**). Additional *in vitro* and *ex vivo* experiments showed that *vep07* was mainly transcribed during the first hours of growth both in eel serum and CM9+Tf (**FIGURE 7B**). To determine the role of Vep07 in virulence, we used R99, Δ*vep07* and c*vep07* strains in a series of *in vivo* and *ex vivo* assays. Similar to Δ*ftbp* (Pajuelo *et al.*, 2015), Δ*vep07* was severely impaired in virulence for eels, growth in eel blood and resistance to eel serum, and did not show changes in virulence for mice and resistance to human serum (**TABLE 1**). The inhibitory effect of eel serum on Δ*vep07* was reversed by the inactivation of both the alternative and classical pathways of complement or by the inactivation of the alternative pathway alone, but was not reversed when iron was added or when the classical pathway alone was inactivated (**TABLE 6**). Additionally, Δ*vep07* was sensitive to phagocytosis (**TABLE 1**). The sensitivity to complement and phagocytosis was reversed by the complemented strain (**TABLES 1** and **6**). Finally, *in vivo* experiments of colonization and invasion showed that Δ*vep07* was impaired in internal colonization not only for blood but also for the other internal organs (**FIGURE 7C**).

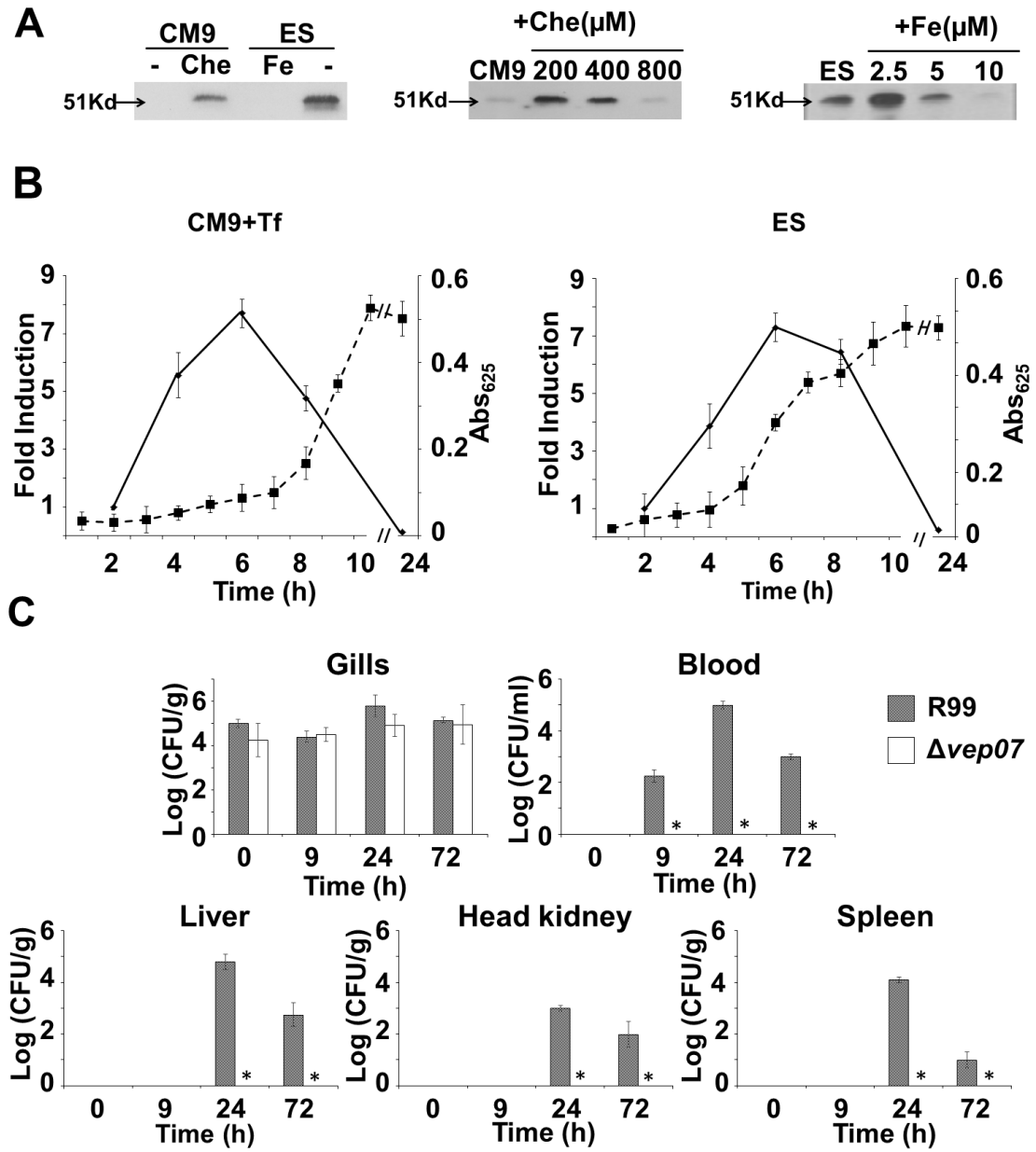

FIGURE 7 | *vep07*: protein characterization, gene transcription, role in virulence and phylogeny. (A) Translation vs iron concentration. R99 was cultured in CM9 (without [-] or with the iron-chelator 2,2'-bipyridyl [Che]) or eel serum (ES) (without [-] or with added iron as $FeCl_3$ [Fe]) for 18 h. The cells were lysed, and 5 µg of the insoluble protein fraction were separated by SDS-PAGE on discontinuous gels (4% stacking gel, 10% separating gel) and immunostained with anti-rVep07 serum. (B) Transcription vs growth. *vep07* transcription levels (solid line) vs bacterial growth (dotted line) in CM9+Tf or ES. Each point represents the average of the fold induction (compared with CM9) or the Abs_{625} values of three independent biological samples ± standard error that were statistically analyzed using the unpaired Student´s t-test (*P<0.05*). (C) Eel colonization and invasion. Groups of 24 eels per strain (3 animals per sampling point) were bath-infected with either the R99 or the mutant strain at the same dose ($2x10^6$ CFU/ml) and gills, blood, liver, head kidney and spleen were sampled for bacterial counting on TSA-1 at 0, 9, 24 and 72 h post-infection. Results are presented as average ± standard error of three independent biological experiments. *: significant differences between the R99 and Δ*vep07* (*P<0.05*).

TABLE 6 | Resistance to human and eel serum of R99 and Δ*vep07* strains: effect of iron and complement inactivation.

Strain	Human serum			Eel serum				
	Fresh	Iron overloaded	Complement inactivation[1]	Fresh	Iron overloaded	Complement inactivation[1]		
						All pathways	Alternative-lectin pathway	Classical pathway
R99	+/-	+	+	+++	+++	+++	+++	+++
Δ*vep07*	+/-	+	+	+*	+*	+++	+++	+*
c*vep07*	+/-	+	+	+++	+++	+++	+++	+++

[1]Complement activity was completely abolished by heating eel and human serum at 56ºC for 30 min and 1 h respectively. Alternative-lectin pathway was inactivated by heating at 47ºC for 20 min and classical pathway by incubating with EGTA-$MgCl_3$ (Sunyer and Tort, 1995; Amaro *et al.*, 1997).

4. Discussion

In this chapter, we aimed to characterize the strategies used by *V. vulnificus* to survive within hosts as evolutionarily distant as human and fish. Our main conclusions from the transcriptomic study performed in serum plus the complementary phenotypic assays are summarized in the models presented in **FIGURE 8** (predicted regulatory networks, external stimuli and phenotype presented by *V. vulnificus* growing in serum) and **FIGURE 9** (main virulence factors that the pathogen would express in blood per susceptible host, as well as its putative role in virulence). Because approximately one out of every two DEGs in serum belong to the previously described Fur regulon and/or iron stimulon (chapter 1), we selected the most relevant DEGs encoding regulators, sensors and virulence factors, all of which (with very few exceptions) belong to one or both regulatory systems.

V. vulnificus activates an anaerobic metabolism to survive and grow in blood regardless of the host and iron levels (**FIGURE 8**) and even oxygen levels, since the dissolved oxygen was similar in all the inoculated sera and control media (1-2 mg/l O_2). This anaerobic metabolism would probably be based on N-compound utilization and nitrate/nitrite respiration in eels or glycogen (i.e. maltose) compounds utilization and organic compounds respiration (i.e. fumarate) in high risk human patients. Although the external signals triggering this metabolic switch are unclear, it seems reasonable to hypothesize that membrane attack by complement and microcidal peptides (common to fish and human sera) would disrupt proton motive force, thus activating the *pspABC* system (belonging to Fur regulon and upregulated in both sera, especially in iron-overloaded human serum [**TABLES 3** and **5**]). This in turn would activate the anaerobic metabolism as it has been described for *E. coli* (Jovanovic *et al.*, 2006) (**FIGURE 8**). In addition, the upregulation of *arcA* in eel serum (linked to the upregulation of *pspABC* (Manganelli and Gennaro, 2017)), as well as the upregulation of *qseB* in iron-overloaded human serum, could also contribute to anaerobic metabolism activation. Indeed, QseB has been described as an activator of anaerobic metabolism in iron-overloaded media in response to catechol amines (Weigel *et al.*, 2015) as well as an activator of motility (Weigel and Demuth, 2016), a phenotype that is induced in iron-overloaded human serum (**TABLE 5** and **FIGURE 4B**). The transcriptomic results also suggest that Fur would play a central role in determining the preferable nutrient to be used, either as apo-Fur through Lrp (Ho *et al.*, 2017) in eel serum, or as holo-Fur through unknown pathways in iron-overloaded human serum as all the glycogen metabolism-related DEGs belong to Fur regulon (**TABLE 5** and **FIGURE 8**). The ability to respire nitrate/nitrite in eel blood provides the pathogen with an additional advantage as the protective mechanisms against NO (a respiration byproduct) that are concomitantly activated

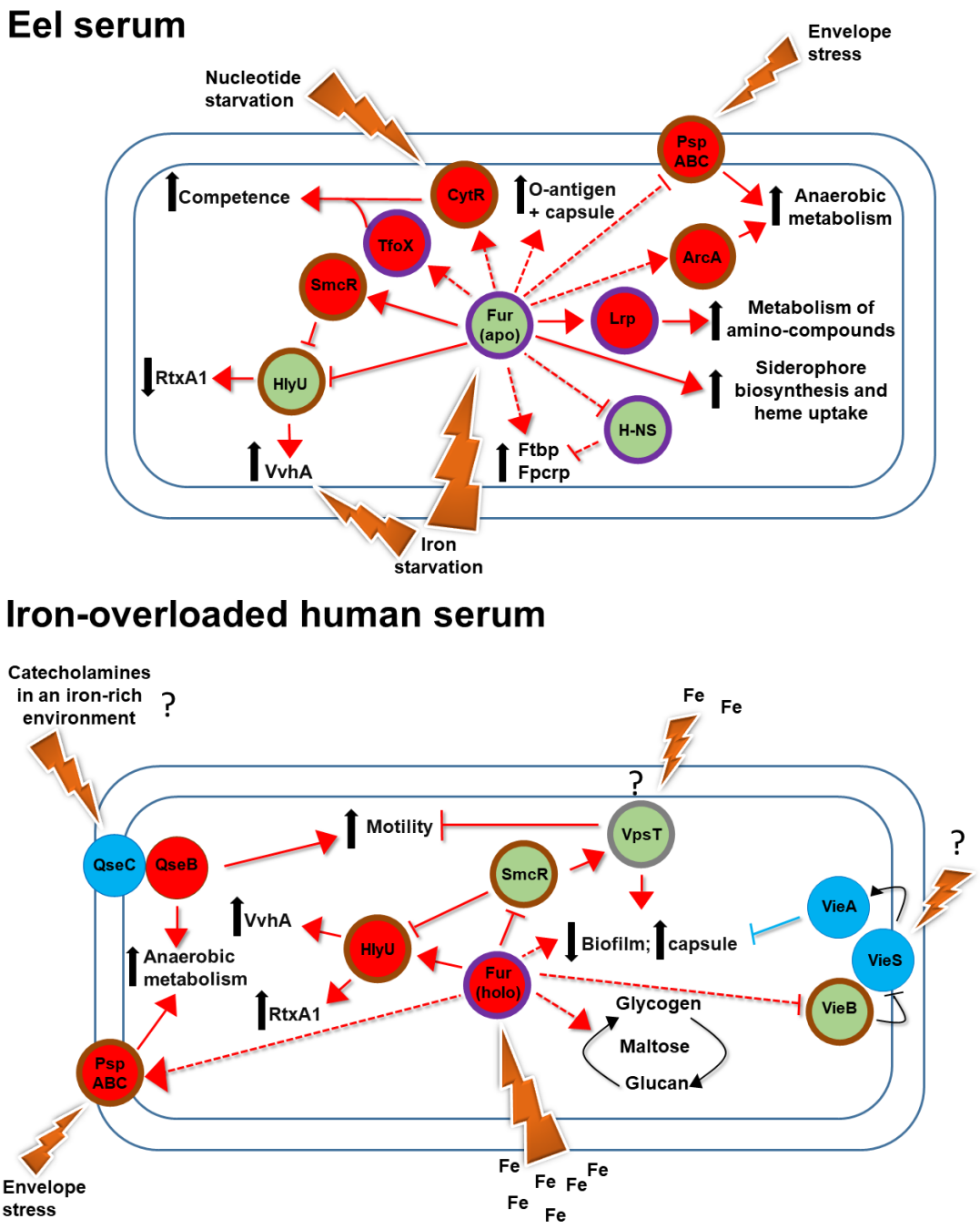

FIGURE 8 | Regulatory network, external stimulus and phenotype presented by *V. vulnificus* growing in serum: a holistic model per susceptible host. The models show the main regulators and sensors that would respond to the putative external signals in serum as well as the resultant phenotype, and are based on our results as well as on data from the literature (Brinkman *et al.*, 2003; Meibom *et al.*, 2005; Krasteva *et al.*, 2010; Shao *et al.*, 2011; Antonova *et al.*, 2012; Kim *et al.*, 2013; Weigel *et al.*, 2015; Ho *et al.*, 2017). The regulators and sensors are presented as bubbles in red (upregulated in our transcriptome), green (downregulated in our transcriptome) and blue (predicted according to the literature but not found in our transcriptome) surrounded by a purple line (belongs to both iron stimulon and Fur regulon), brown line (belongs to the Fur regulon) or grey line (belongs to the iron stimulon) (chapter 1). Direct/indirect interaction between regulators and the predicted bacterial phenotype are shown as lines (confirmed results supported by this work and the literature) or dotted lines (proposed in this work but without previous evidences in the literature).

(**TABLE 3**) would protect it against this important microcidal molecule produced by the host, contributing to the high virulence of the pathogen for eels.

Besides this metabolic adaptation, our transcriptomic results also suggest that *V. vulnificus* responds to more signals of nutrient starvation in eel serum than in iron-overloaded human serum (**TABLES 3** and **5**). We highlight that *V. vulnificus* would respond in eel serum to iron and nucleotide starvation, which would involve Fur and CytR (belonging to Fur regulon), respectively, resulting in the upregulation of different genes involved in the uptake of both kinds of nutrients (i.e., vulnibactin biosynthesis, receptors for different exogenous iron sources, nucleoside transporters, etc.). As a secondary consequence of *cytR* upregulation, competence could be activated, at least partially, in eel serum, which is supported by the upregulation of *tfoX* (**FIGURE 8**). We hypothesize that this putative competence activation could indicate that *V. vulnificus* might activate this state in its natural habitat, i.e., fish mucosae (Carda-Diéguez *et al.*, 2017), as *V. cholerae* does (Metzger and Blokesch, 2016), and that iron starvation could play a role in the process as both eel serum and fish mucosae are iron restricted environments (Pajuelo *et al.*, 2015; Carda-Diéguez *et al.*, 2017).

V. vulnificus expresses a toxic phenotype based on VvhA plus $RtxA1_3$ production when it is growing in the blood of its susceptible hosts. Our transcriptomic and phenotypic results suggest that iron, Fur, SmcR and HlyU could play a significant role in the activation of this toxic phenotype (**FIGURE 8**). In case of high risk patients, $RtxA1_3$ and VvhA could act additively in blood as both genes were upregulated in iron-overloaded human serum and were transcribed in parallel and exponentially in artificial iron-overloaded human blood during the 6 h of incubation we analyzed. A role for this additive function in blood invasion from the intestine has already been suggested for *V. vulnificus* strains, other than the zoonotic ones (Jeong and Satchell, 2012). In addition, the regulation of *smcR*, *fur*, and *hlyU* in iron-overloaded human serum was as expected according to both the observed toxin gene transcription and the published literature (Shao *et al.*, 2011; Kim *et al.*, 2013) (**FIGURE 8**). In consequence, a highly toxic phenotype would be induced in *V. vulnificus* when infecting high risk patients, which agrees with clinical data on human septicemia (Horseman and Surani, 2011; Oliver, 2015).

The scenario was different in the case of eels, as the results were unexpected. First, $rtxA1_3$, a gene essential for eel death by sepsis (Lee *et al.*, 2013), was downregulated in eel serum, while *vvhA*, a gene with an unknown role in eel virulence, was one of the most strongly upregulated (**FIGURE 8**). The complementary experiments performed in artificial eel blood and *in vivo* demonstrated that the $rtxA1_3$transcription requires contact of the bacteria with host

cells as previously suggested for the function of this toxin (Kim *et al.*, 2008; Lee *et al.*, 2013). Second, *hlyU* was downregulated which correlated with *rtxA1*$_3$ transcription but not with *vvhA* transcription, suggesting that iron starvation, in absence of HlyU, could trigger *vvhA* transcription through an unknown regulatory pathway (**FIGURE 8**). Additional experiments to unravel the role of *vvhA* in eel virulence by using a mutant and the corresponding complemented strain demonstrated that *vvhA* is a virulence gene probably involved in early fitness in eel blood. Interestingly, *vvhA* was transcribed before *rtxA1*$_3$, both in artificial eel blood and *in vivo*, and in both cases the fold change/induction value was much lower than that observed in eel serum at 6 h post-infection. All these results highlight a new hypothesis on hemolysin transcription *in vivo*: the temporality in the transcription of *rtxA1*$_3$ and *vvhA* could depend on changes in iron concentration in the bacteria's surrounding environment. A model summarizing the role of both toxins per host is shown in **FIGURE 9**. This model incorporates the hypothesis that VvhA (transcribed first in eel serum) would lyse RBC and create an iron (heme) rich microenvironment that would favor the transcription of *rtxA1*$_3$ in eel blood. More studies are necessary to prove these.

V. vulnificus produces a protective envelope in blood against complement from each susceptible host in terms of capsule vs O-antigen ratio. Our transcriptomic and phenotypic results suggest that iron and Fur would have a role in the production of this protective envelope as the entire identified capsule and LPS biosynthetic DEGs belonged to Fur regulon and most of them also to iron stimulon (**FIGURE 8**). Accordingly, the selected strain produced a capsule-enriched envelope in iron-overloaded human serum and an envelope without capsule but O-antigen-enriched in human serum (**FIGURE 5**), which supports the results obtained in chapter 1 regarding the role of iron in capsule and O-antigen production. The fact that *V. vulnificus* is unable to produce the capsule in human serum would by itself explain why this pathogen does not cause septicemia in healthy patients as the invading bacteria would be destroyed by human complement (Amaro *et al.*, 1994). In partial accordance, the envelope produced in eel serum by the analyzed strain contained both capsule and high/medium molecular weight O-antigen, both participating in protection against eel complement (Biosca *et al.*, 1993; Amaro *et al.*, 1997).

Capsule production is inversely linked to biofilm formation in *V. vulnificus* (Casper-Lindley and Yildiz, 2004; Joseph and Wright, 2004). Accordingly, we found that biofilm formation was significantly higher (*P<0.05*) in CM9 than in iron-overloaded human serum (values of Abs_{540} after crystal violet staining of 0.29±0.04 and 0.01±0.001, respectively) confirming that biofilm production is downregulated in iron-overloaded human serum (**FIGURE 8**). We also found

transcriptomic evidences: i.e., the downregulation of *smcR*, linked to the downregulation of *vpsT*, an activator of biofilm formation (Krasteva *et al.*, 2010) plus the upregulation of *fur* linked to the downregulation of *vieB*, a repressor of VieA, which forms with VieS a two-component system that represses biofilm formation (Mitchell *et al.*, 2015).

The external envelope of *V. vulnificus* growing in blood from susceptible fish species contains two plasmid-encoded IROMPs (iron regulated OMPs) that confer specific ability to resist fish innate immunity. These two proteins are Ftbp, a recently described receptor for eel transferrin that can bind transferrin from sea bass as well (Pajuelo *et al.*, 2015; unpublished results), and *vep07*, encoding a multifunctional OMP (probably a lipoprotein) conferring resistance to eel complement, activated by the alternative pathway, and phagocytosis (**FIGURE 7** and **TABLE 6**). We propose Fpcrp (Fish Phagocytosis and Complement Resistance Protein) as the name for this protein. Both proteins would constitute a "survival in fish blood kit" conferring both specific adaptation to resist the fish innate immunity and high virulence for healthy eels (**FIGURE 9**). Our hypothesis is that Fpcrp binds an unknown fish complement inhibitor, thus preventing bacterial killing and efficient opsonization and phagocytosis. Incubation of purified rVep07 with albumin-free eel serum and further identification of the ligand by LC–MS/MS (liquid chromatography and tandem mass spectrometry) (Pajuelo *et al.*, 2015) were unsuccessful, probably because the eel protein targeted has not been sequenced yet (results not shown). Future analysis of the eel serum proteome is needed in order to identify the Fpcrp ligand.

In summary, we have unraveled some of the mechanisms that enable *V. vulnificus* to cause septicemia in hosts as evolutionary distant as humans and fish and clarified the link between virulence and iron content in the blood. First, *V. vulnificu*s would only be able to cause septicemia in humans with elevated iron levels in blood because it is only under iron excess that it would be able to produce a capsule-enriched envelope that would allow it to multiply efficiently in the blood and to express the highly toxic phenotype responsible for patient death by sepsis. Second, *V. vulnificus* encodes a "survival in fish blood kit" that allows it to resist fish innate immunity and multiply in the blood expressing a toxic phenotype responsible for animal death by sepsis. In conclusion, our results highlight the risk that the aquaculture industry poses to public health, especially in the case of such zoonotic pathogens as *V. vulnificus* whose multiplication and spreading to new areas is being favored by global warming.

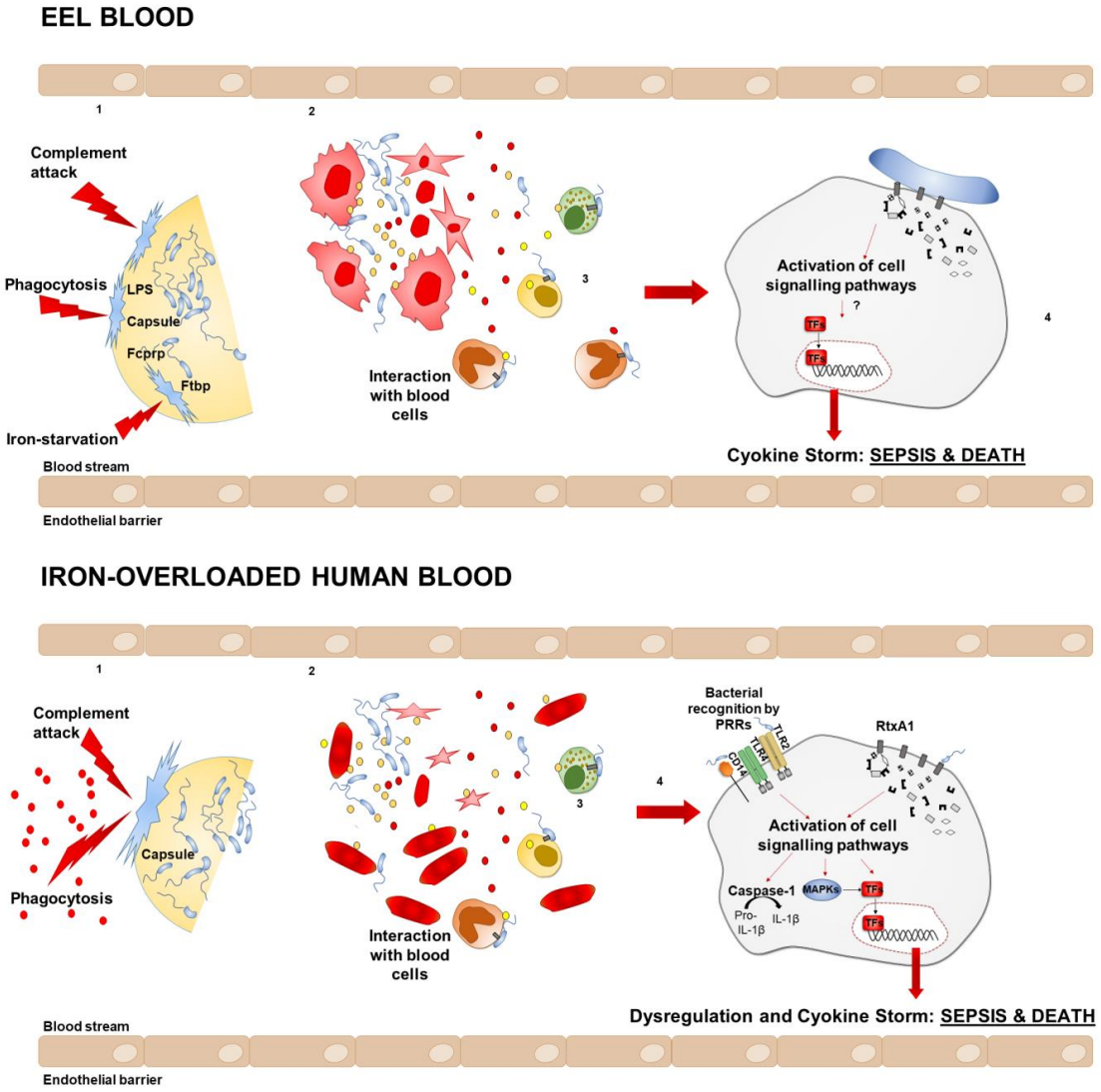

FIGURE 9 | Main virulence- and survival-related factors expressed by *V. vulnificus* in host blood and their predicted function in septicemia. Model in eel. In eel blood, *V. vulnificus* cells detect iron starvation and express an adapted external envelope that contains two plasmid OMPs, a receptor for eel transferrin (Ftbp) and a protective protein against eel complement and phagocytosis (Fpcrp), embedded in an LPS enriched in the high/medium molecular weight part of the O-antigen and surrounded by a capsule (1). As a consequence, the bacteria resist in serum and multiply, secreting VvhA (yellow balls), a cytotoxin that lyses erythrocytes, which are very abundant in eel blood (approximately 10^9 cell per ml), which in turn, liberate hemoglobin creating a microenvironment rich in heme iron (2). In these conditions, and after contact with blood cells, the RtxA1$_3$ (in grey) is produced and secreted, entering into the eukaryotic cell (3) and causing a hypothetic cytokine storm, by unknown signaling cascades (4). Model in an iron-overloaded human. In the blood from a risk patient, *V. vulnificus* cells detect iron excess (red balls) and express an adapted external envelope enriched in a capsule that protects them against both complement and phagocytosis (1). The protected bacteria multiply and produce both VvhA (yellow ball) and RtxA1$_3$ (grey bars), which collaborate in cellular destruction (3). When RtxA1$_3$ interacts with the appropriate immune cell, it triggers a cytokine storm by inducing the overexpression of inflammation mediators as described by Murciano *et al.*, (2017). Figure modified from Murciano *et al.*, (2017).

5. References

Amaro, C., Biosca, E.G., Fouz, B., Alcaide, E., and Esteve, C. (1995) Evidence That Water Transmits *Vibrio vulnificus* Biotype-2 Infections To Eels. *Appl Environ Microbiol* **61**: 1133–1137.

Amaro, C., Biosca, E.G., Fouz, B., Toranzo, A.E., and Garay, E. (1994) Role of Iron, Capsule, and Toxins in the Pathogenicity of *Vibrio vulnificus* Biotype-2 for Mice. *Infect Immun* **62**: 759–763.

Amaro, C., Fouz, B., Biosca, E.G., Marco-Noales, E., and Collado, R. (1997) The lipopolysaccharide o side chain of *Vibrio vulnificus* serogroup E is a virulence determinant for eels. *Infect Immun* **65**: 2475–2479.

Amaro, C., Sanjuán, E., Fouz, B., Pajuelo, D., Lee, C.T., Hor, L., et al. (2015) The fish pathogen *Vibrio vulnificus* biotype 2: epidemiology , phylogeny , and virulence factors involved in warm-water vibriosis. *Microbiol Spectr* **3**.

Antonova, E.S., Bernardy, E.E., and Hammer, B.K. (2012) Natural competence in *Vibrio cholerae* is controlled by a nucleoside scavenging response that requires CytR-dependent anti-activation. *Mol Microbiol* **86**: 1215–1231.

Biosca, E.G., Garay, E., Toranzo, A.E., and Amaro, C. (1993) Comparison of outer membrane protein profiles of *Vibrio vulnificus* biotypes 1 and 2. *FEMS Microbiol Lett* **107**: 217–222.

Brinkman, A.B., Ettema, T.J.G., De Vos, W.M., and Van Der Oost, J. (2003) The Lrp family of transcriptional regulators. *Mol Microbiol* **48**: 287–294.

Carda-Diéguez, M., Ghai, R., Rodríguez-Valera, F., and Amaro, C. (2017) Wild eel microbiome reveals that skin mucus of fish could be a natural niche for aquatic mucosal pathogen evolution. *Microbiome* **5**: 162.

Casper-Lindley, C. and Yildiz, F.H. (2004) VpsT is a transcriptional regulator required for expression of *vps* biosynthesis genes and the development of rugose colonial morphology in *Vibrio cholerae* O1 El Tor. *J Bacteriol* **186**: 1574–1578.

Fuangthong, M., Atichartpongkul, S., Mongkolsuk, S., and Helmann, J.D. (2001) OhrR is a repressor of *ohrA*, a key organic hydroperoxide resistance determinant in *Bacillus subtilis*. *J Bacteriol* **183**: 4134–4141.

Ho, Y.C., Hung, F.R., Weng, C.H., Li, W.T., Chuang, T.H., Liu, T.L., et al. (2017) Lrp, a global regulator, regulates the virulence of *Vibrio vulnificus*. *J Biomed Sci* **24**: 54.

Horseman, M.A. and Surani, S. (2011) A comprehensive review of *Vibrio vulnificus*: An important cause of severe sepsis and skin and soft-tissue infection. *Int J Infect Dis* **15**: 157–166.

Jeong, H.G. and Satchell, K.J.F. (2012) Additive function of *Vibrio vulnificus* MARTXVv and VvhA cytolysins promotes rapid growth and epithelial tissue necrosis during intestinal infection. *PLoS Pathog* **8**: e1002581.

Joseph, L.A. and Wright, A.C. (2004) Expression of *Vibrio vulnificus* capsular polysaccharide inhibits biofilm formation. *J Bacteriol* **186**: 889–893.

Jovanovic, G., Lloyd, L.J., Stumpf, M.P.H., Mayhew, A.J., and Buck, M. (2006) Induction and function of the phage shock protein extracytoplasmic stress response in *Escherichia coli*. *J Biol Chem* **281**: 21147–21161.

Juncker, A. and Willenbrock, H. (2003) Prediction of lipoprotein signal peptides in Gram negative bacteria. *Protein Sci* **12**: 1652–1662.

Kim, I.H., Wen, Y., Son, J.S., Lee, K.H., and Kim, K.S. (2013) The fur-iron complex modulates expression of the quorum-sensing master regulator, *smcr*, to control expression of virulence factors in *Vibrio vulnificus*. *Infect Immun* **81**: 2888–2898.

Kim, Y.R., Lee, S.E., Kook, H., Yeom, J.A., Na, H.S., Kim, S.Y., et al. (2008) *Vibrio vulnificus* RTX toxin kills host cells only after contact of the bacteria with host cells. *Cell Microbiol* **10**: 848–862.

Krasteva, P.V., Jiunn, J.C., Shikuma, N.J., Beyhan, S., Navarro, M.V.A.S., Yildiz, F.H., et al. (2010) *Vibrio cholerae vpsT* regulates matrix production and motility by directly sensing cyclic di-GMP. *Science* **327**: 866–868.

Lee, C.T., Amaro, C., Wu, K.M., Valiente, E., Chang, Y.F., Tsai, S.F., et al. (2008) A common virulence plasmid in biotype 2 *Vibrio vulnificus* and its dissemination aided by a conjugal plasmid. *J Bacteriol* **190**: 1638–1648.

Lee, C.T., Pajuelo, D., Llorens, A., Chen, Y.H., Leiro, J.M., Padrós, F., et al. (2013) MARTX of *Vibrio vulnificus* biotype 2 is a virulence and survival factor. *Environ Microbiol* **15**: 419–432.

Lee, S.H., Angelichio, M.J., Mekalanos, J.J., and Camilli, A. (1998) Nucleotide sequence and spatiotemporal expression of the *Vibrio cholerae vieSAB* genes during infection. *J Bacteriol* **180**: 2298–2305.

Liu, M., Rose, M., and Crosa, J.H. (2011) Homodimerization and binding of specific domains to the target DNA are essential requirements for HlyU to regulate expression of the virulence gene *rtxA1*, encoding the repeat-in-toxin protein in the human pathogen *Vibrio vulnificus*. *J Bacteriol* **193**: 6895–6901.

Madan Babu, M. and Sankaran, K. (2002) DOLOP - database of bacterial lipoproteins. *Bioinformatics* **18**: 641–643.

Manganelli, R. and Gennaro, M.L. (2017) Protecting from envelope stress: variations on the phage-shock-protein theme. *Trends Microbiol* **25**: 205–216.

Mathur, J., Davis, B.M., and Waldor, M.K. (2007) Antimicrobial peptides activate the *Vibrio cholerae* σE regulon through an OmpU-dependent signalling pathway. *Mol Microbiol* **63**: 848–858.

Mathur, J. and Waldor, M.K. (2004) The *Vibrio cholerae* ToxR-regulated porin OmpU confers resistance to antimicrobial peptides. *Infect Immun* **72**: 3577–3583.

Meibom, K.L., Blokesch, M., Dolganov, N.A., Wu, C.Y., and Schoolnik, G.K. (2005) Microbiology: chitin induces natural competence in *Vibrio cholerae*. *Science* **310**: 1824–1827.

Metzger, L.C. and Blokesch, M. (2016) Regulation of competence-mediated horizontal gene transfer in the natural habitat of *Vibrio cholerae*. *Curr Opin Microbiol* **30**: 1–7.

Mitchell, S.L., Ismail, A.M., Kenrick, S.A., and Camilli, A. (2015) The VieB auxiliary protein negatively regulates the VieSA signal transduction system in *Vibrio cholerae* signaling and cellular microbiology. *BMC Microbiol* **15**: 1–16.

Murciano, C., Lee, C.T., Fernández-Bravo, A., Hsieh, T.H., Fouz, B., Hor, L.I., et al. (2017) MARTX toxin in the zoonotic serovar of *Vibrio vulnificus* triggers an early cytokine storm in mice. *Front Cell Infect Microbiol* **7**: 1–19.

Nieckarz, M., Raczkowska, A., Jaworska, K., Stefańska, E., Skorek, K., Stosio, D., et al. (2017) The role of OmpR in the expression of genes of the KdgR regulon involved in the uptake and depolymerization of oligogalacturonides in *Yersinia enterocolitica*. *Front Cell Infect Microbiol* **7**: 1–25.

Oliver, J.D. (2015) The Biology of *Vibrio vulnificus*. *Microbiol Spectr* **3**: 1–10.

Pajuelo, D., Lee, C.T., Roig, F.J., Hor, L.I., and Amaro, C. (2015) Novel host-specific iron acquisition system in the zoonotic pathogen *Vibrio vulnificus*. *Environ Microbiol* **17**: 2076–2089.

Phadtare, S. and Severinov, K. (2010) RNA remodeling and gene regulation by cold shock proteins. *RNA Biol* **7**: 788–795.

Rodionov, D.A., Dubchak, I.L., Arkin, A.P., Alm, E.J., and Gelfand, M.S. (2005) Dissimilatory metabolism of nitrogen oxides in bacteria: comparative reconstruction of transcriptional networks. *PLoS Comput Biol* **1**: 0415–0431.

Rodionov, D.A., Mironov, A.A., Rakhmaninova, A.B., and Gelfand, M.S. (2000) Transcriptional regulation of transport and utilization systems for hexuronides, hexuronates and hexonates in gamma purple bacteria. *Mol Microbiol* **38**: 673–683.

Roig, F.J., González-Candelas, F., Sanjuán, E., Fouz, B., Feil, E.J., Llorens, C., et al. (2018) Phylogeny of *Vibrio vulnificus* from the analysis of the core-genome: implications for intra-species taxonomy. *Front Microbiol* **8**: 1–13.

Sanjuán, E. and Amaro, C. (2004) Protocol for specific isolation of virulent strains of *Vibrio vulnificus* serovar E (Biotype 2) from environmental samples. *Appl Environ Microbiol* **70**: 7024–7032.

Satchell, K.J.F. (2011) Structure and function of MARTX toxins and other large repetitive RTX proteins. *Annu Rev Microbiol* **65**: 71–90.

Shao, C.P., Lo, H.R., Lin, J.H., and Hor, L.I. (2011) Regulation of cytotoxicity by quorum-sensing signaling in *Vibrio vulnificus* is mediated by SmcR, a repressor of *hlyU*. *J Bacteriol* **193**: 2557–2565.

Sunyer, O. and Tort, L. (1995) Natural hemolytic and bactericidal activities of sea bream *Sparus aurata* serum are affected by the alternative complement pathway. *Vet Immunol Immunopathol* **2427**: 333–345.

Weigel, W.A. and Demuth, D.R. (2016) QseBC, a two-component bacterial adrenergic receptor and global regulator of virulence in Enterobacteriaceae and Pasteurellaceae. *Mol Oral Microbiol* **31**: 379–397.

Weigel, W.A., Demuth, D.R., Torres-Escobar, A., and Juárez-Rodríguez, M.D. (2015) *Aggregatibacter actinomycetemcomitans* QseBC is activated by catecholamines and iron and regulates genes encoding proteins associated with anaerobic respiration and metabolism. *Mol Oral Microbiol* **30**: 384–398.

Wright, A.C. and Morris, J.G. (1991) The extracellular cytolysin of *Vibrio vulnificus*: inactivation and relationship to virulence in mice. *Infect Immun* **59**: 192–198.

Yamamoto, K., Wright, A.C., Kaper, J.B., and Morris, J.G. (1990) The cytolysin gene of *Vibrio vulnificus*: sequence and relationship to the *Vibrio cholerae* El Tor hemolysin gene. *Infect Immun* **58**: 2706–2709.

CHAPTER 3

The effect of environmental temperature on the host-adaptation in *Vibrio vulnificus*

1. Introduction

V. vulnificus is a worldwide-distributed aquatic pathogen that inhabits waters of salinity between 0.3 and 2.5% located in tropical, subtropical and temperate areas. The species can be isolated from coastal ecosystems when water temperature is between 10 and 30ºC (Baker-Austin and Oliver, 2018). In fact, environmental temperature determines the life strategy of *V. vulnificus* in the aquatic ecosystem as this species enters into the VBNC state below 4 ºC and multiplies in the water column (if nutrients are available) above 18ºC with an optimum above 25ºC (Oliver, 2015). There is strong scientific evidence that global warming is increasing the sea surface temperature, which is about 1ºC higher than 100 years ago (https://www.epa.gov/climate-indicators/climate-change-indicators-sea-surfacetemperature). It is also predicted that the melting of the ice at the poles will also produce a decrease in the salinity of seawater around the world. Since *V. vulnificus* grows preferentially in warm brackish water (1-2%) at temperatures above 18ºC, the warming of marine waters together with the reduction in salinity will result in larger populations of these bacteria and, therefore will increase the risk of *Vibrio* infections (Le Roux *et al.*, 2015).

V. vulnificus is pathogenic for multiple hosts, both poikilothermic (fish and shrimps) and homoeothermic (humans), and it is able to cause death by hemorrhagic septicemia with similar clinical signs in all of them (Amaro *et al.*, 2015; Oliver, 2015). The human disease can be acquired either by contact with seawater or fish or by ingestion of raw seafood. In the first case, the pathogen causes severe wound infections, and in the second one gastroenteritis, both pathologies converging in sepsis and death in risk patients (mainly those that present high levels of free iron in blood due to different predisposing underlying diseases such as hemochromatosis) (Horseman and Surani, 2011; Oliver, 2015). The disease caused in fish is known as warm-water vibriosis because the most serious outbreaks always occur at temperatures above 25ºC (Amaro *et al.*, 2015). Warm-water vibriosis is an acute hemorrhagic septicemia, that occurs in farms of eels and tilapia as epizootic or outbreaks of high and medium mortalities depending on water temperature (Fouz and Amaro, 2002; Fouz *et al.*, 2006; Amaro *et al.*, 2015). Epizootiological studies performed at laboratory scale confirmed that the pathogen virulence for eels is dependent on water temperature: maximal at 28ºC (the maximum tested temperature) and minimal (no virulence at all) at 20 ºC and bellow (Amaro *et al.*, 1995).

In the previous chapters, we performed transcriptomic studies that confirmed that iron is one of the external signals triggering a host-adapted virulent phenotype in the pathogen. This

iron-dependent and host-adapted response includes the production of a generalist but host-specific protective envelope to resist the host innate immunity (capsule for humans and O-antigen for eels) together with a toxic phenotype depending on the $RtxA1_3$ and VvhA toxins.

In this chapter, we hypothesized that environmental temperature (water and/or host) could also contribute to the generation of this host-adapted virulent phenotype. In fact, *V. vulnificus* is able to cause severe septicemia at both 28ºC (in fish species) and 37ºC (in humans). Although temperature-dependent gene expression has been widely studied in other bacterial species (Gao *et al.*, 2006; Wang *et al.*, 2017; Matanza and Osorio, 2018), to our knowledge this is the first time that the global transcriptomic response to temperature is analyzed in *V. vulnificus*. Nevertheless, it is well known that temperature impacts *V. vulnificus* growth (Kim *et al.*, 2016) and the expression of some virulence factors such as the major protease Vvp, iron uptake systems (HupA and VuuA) and quorum sensing (McDougald *et al.*, 2001; Oh *et al.*, 2009; Kim *et al.*, 2012, 2016; Elgaml and Miyoshi, 2017).

Taken all together, the aim of this chapter was to find out the role of temperature in the generation of the host-adapted virulent phenotype, using a transcriptomic and phenotypic approach. To this end, we analyzed the transcriptome of R99 strain grown in a minimal medium incubated at different temperatures according to the those at which the outbreaks of fish vibriosis are produced in farms (20ºC [no outbreak is registered in fish farms, thus selected as control condition]), 25ºC (outbreaks of medium mortality), 28ºC (outbreaks of high mortality) as well as at 37ºC, the human host body temperature (Amaro *et al.*, 2015; Oliver, 2015). Then, the bacterial transcriptome at each infective temperature was obtained by microarray hybridization followed by the bioinformatics analysis. The results were compared with those obtained in the previous chapters (in iron stimulon and fur regulon [chapter 1] and in eel and human serum [chapter 2]). Finally, the transcriptomic results were confirmed by RT-qPCR and phenotypic tests.

2. Materials and methods

Bacterial strains and growth conditions

R99 strain, a representative strain of the zoonotic clonal-complex (Roig *et al.*, 2018) was routinely grown on TSA-1 and CM9/CM9A. The inoculum for assays was prepared by inoculating 5 ml of media with bacteria from overnight cultures in a ratio 1:100 (v/v) and incubated with agitation (60 rpm) at 20, 25, 28 and 37ºC. Bacterial growth was followed as bacterial counts by the drop plate method and by Abs_{625} measurements.

Microarray analysis

The experimental design for microarray analysis as well as the performed transcriptomic comparisons are shown in **FIGURE 1**. *Sample preparation*. Total RNA from mid-log phase cultures ($1x10^8$ CFU/ml, Abs_{625} 0.3: 19 h cultures grown at 20ºC, 7 h cultures grown at 25ºC and 6 h cultures grown at 28 and 37ºC) was extracted, labelled and hybridized on microarray according to what was described in p. 65. *Data analysis*. The data were analyzed with Genespring 14.5 GX software as described in p. 65. The following comparisons were performed: 25ºC vs 20ºC, 28ºC vs 20ºC and 37ºC vs 20ºC. *Microarray validation by RT-qPCR.* The same samples used for the microarray analysis were analyzed by RT-qPCR to calculate the expression of selected genes (**TABLE 2**). The *recA* gene was used as standard and the fold induction ($2^{-\Delta\Delta Ct}$) for each gene was calculated according to Livak and Schmittgen, (2001).

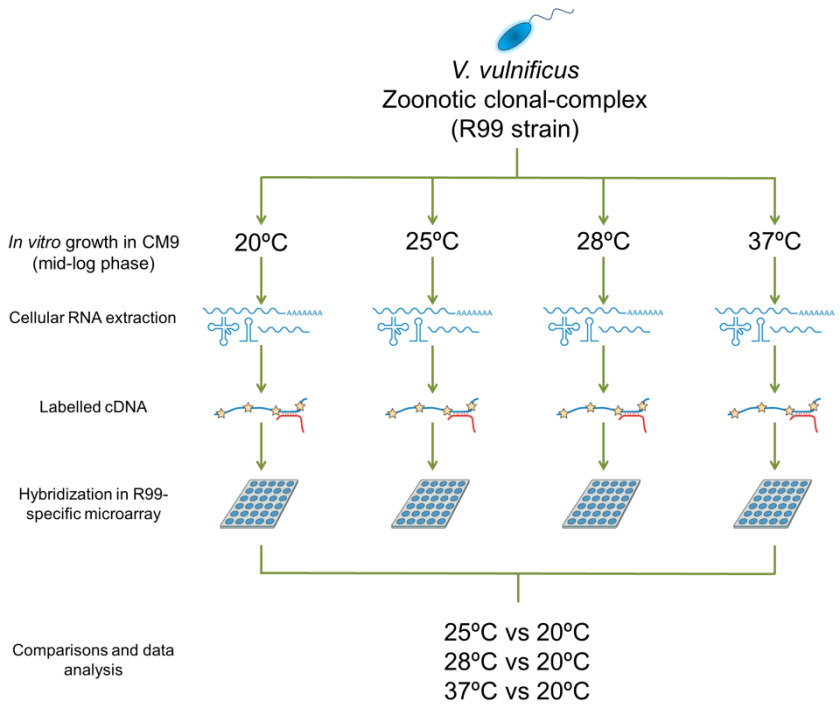

FIGURE 1 | Experimental design.

TABLE 1 | Primers used in the study and microarray validation. Comparison of fold change values obtained by array and RT-qPCR with the *V. vulnificus* R99 strain. In case of RT-qPCR, results were obtained using *recA* as the reference gene and the fold induction ($2^{-\Delta\Delta Ct}$) for each gene was calculated.

Gene	Primer sequence	Sample	FC[1]	
			Array	RT-qPCR
Microarray validation by RT-qPCR				
ftbp	Fw: CACTCGCCTCTTTGGTTTCG Rv: GGGACTGATTCTCTCTTC	25ºC vs 20ºC	2 (+)	1.3 (=)
cpsA	Fw: GCAGCTCATCGAGTGACGTA Rv: GCAGCTCATCGAGTGACGTA		2 (+)	4.9 (+)
vvp	Fw: TTGCCGCAGTCGTGTGTT Rv: CGGAGACGGACACCATTTCT		--	1.5 (=)
vvhA	Fw: TGTTTATGGTGAGAACGGTGACA Rv: TTCTTTATCTAGGCCCCAAACTTG		--	1.6 (=)
rtxA1$_3$	Fw: GAGTGATGATGGGCGCTTTAC Rv: CAGCCGCGATGGATGCT		--	1.9 (=)
flp	Fw: TGGTGTTAGCCATAGGAACTCTCTT Rv: CCACCTGCCTCTCCTTCCA	28ºC vs 20ºC	14 (++)	3.6 (+)
malG	Fw: CCAGAATCCACGTCCAACGT Rv: GAGTGCCGATGCGGATGT		-3.1 (-)	-1.2 (=)
vvp	See above		--	1.7 (=)
vvhA	See above		--	1.3 (=)
rtxA1$_3$	See above		--	1.9 (=)
vpsT	Fw: GAAGGAAGAACCGCAGTTAGA Rv: ATCGTCTCGGTGATAAA	37ºC vs 20ºC	5.1 (+)	3.6 (+)
ktrA	Fw: ATCGGCGCAGACCACATC Rv: TCGCCACGCGGATCA		3.4 (+)	1.6 (=)
vvp	See above		--	1.9 (=)
vvhA	See above		--	1.7 (=)
rtxA1$_3$	See above		--	1.4 (=)
Reference gene				
recA	Fw: CGCCAAAGGCAGAAATCG Rv: ACGAGCTTGAAGACCCATGTG			

[1]Qualitative classification of FC (fold change): =, -2<X<2; +, 2≤X<10; ++, 10≤X<25; -, -10<X≤-2.
--: this gene was not detected as differentially expressed by microarray hybridization.

***In vitro* assays**

Biofilm production. R99 was grown in CM9 at 20, 25, 28 and 37ºC for 24 h and biofilm production was quantified by staining with crystal violet as specified in chapter 1 p. 79.

Motility. Motility was assayed on MA at 20, 25, 28 and 37ºC and the motility rate was calculated as previously defined in chapter 1 p. 77.

Proteolytic activity. The ECPs from R99 strain were obtained from 24 h cultures on CM9A at 20, 25, 28 and 37ºC according to Biosca and Amaro, (1996). Proteolytic activity in ECPs was evaluated as previously described by Valiente *et al.*, (2008), using azocasein (Sigma-Aldrich) as substratum. Proteolytic activity was calculated as PU (proteolytic units) produced in each condition as described by Miyoshi *et al.*, (1987).

Chemotaxis. Eel skin mucus was collected by placing non-anaesthetized eels in empty sterile flasks, and the secreted material was recovered and filtered through 0.8 and 0.45 µm pore-size membranes (Millipore) (Esteve-Gassent *et al.*, 2003). The chemotaxis towards eel skin mucus was determined at 20, 25, 28 and 37ºC by using the capillary assay as described in chapter 1 (p. 77).

Envelope analysis. Crude fractions of cell-associated polysaccharides (LPS plus capsule) from mid-log phase cultures of R99 strain in CM9 at 20, 25, 28 and 37ºC were obtained and analyzed as specified in chapter 1 (p. 79).

Statistical analysis. All the results presented represent the averages ± standard error of three independent biological experiments. The significance of the differences between means was tested with SPSS 19.0 software by using one-way ANOVA with a $P<0.05$.

3. Results

Bacterial growth

The effect of temperature on bacterial growth was determined in CM9 at 20, 25, 28 and 37ºC. **FIGURE 2** shows the growth curves obtained at the different tested temperatures. The pathogen presented growth patterns statistically different at 20 vs 25ºC, 20 vs 28ºC and 25 vs 28ºC but not at 28 vs 37ºC. Temperature mainly affected the lag phase, whose duration was longer at 20ºC (14 h) followed by 25ºC (5 h), and shorter and similar at 28ºC and 37ºC (around 2 h). The bacterial numbers achieved at 24 h post-incubation were around $1x10^9$ CFU/ml at 20, 25 and 28ºC, and around $1x10^8$ CFU/ml at 37ºC, suggesting that the death phase is accelerated at this temperature. Interestingly the maximum population size was similar regardless the incubation temperature (around 10^9 CFU/ml).

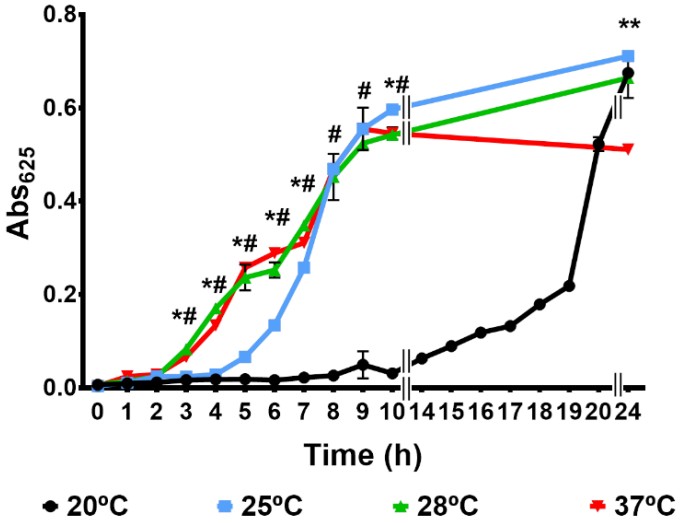

FIGURE 2 | Growth of *V. vulnificus* in a minimal medium at different incubation temperatures. R99 strain was inoculated in CM9 and incubated with agitation at 20, 25, 28 and 37ºC. Growth was followed by measuring the Abs_{625} at regular time intervals. #: significant differences (*P<0.05*) in Abs_{625} between 20 vs 28ºC. *: significant differences (*P<0.05*) in Abs_{625} between 25 vs 28ºC. **: significant differences (*P<0.05*) in Abs_{625} between 37 vs 28ºC.

Transcriptomic results

We obtained the bacterial transcriptome of R99 strain in CM9 at 20, 25, 28 and 37ºC and analyzed the DEGs at infective temperatures (25, 28 and 37ºC) vs non-infective (20ºC). **FIGURE 3** shows the number and distribution in the genome of the DEGs at each temperature, **TABLE 1** provides a comparison between fold change values obtained by hybridization with the R99-specific microarray and by RT-qPCR and **TABLE 2** shows relevant selected DEGs at each temperature.

The temperature stimulon, defined as the set of DEGs at the analyzed temperatures, is formed by 1,375 genes (30.2% of genes in the genome). This value was similar to that found in the iron stimulon (25.78%), Fur regulon (35.91%) and host-serum stimulons (26.35% [eel serum] and 20.32% [serum from a risk patient]) (chapters 1 and 2) (**FIGURE 3**). In addition, around 40% of the genes that belonged to temperature stimulon were also found in the rests of stimulons and/or regulons (**FIGURE 4**), mostly presenting a contrary regulation (results not shown). This was not the case of the plasmid genes since less than 1% of the plasmid DEGs in the temperature stimulon belonged also to another stimulon/regulon (results not shown), which suggests that globally the plasmid genes involved in response to temperature neither are controlled by Fur nor belong to the bacterial networks involved in response to iron or serum.

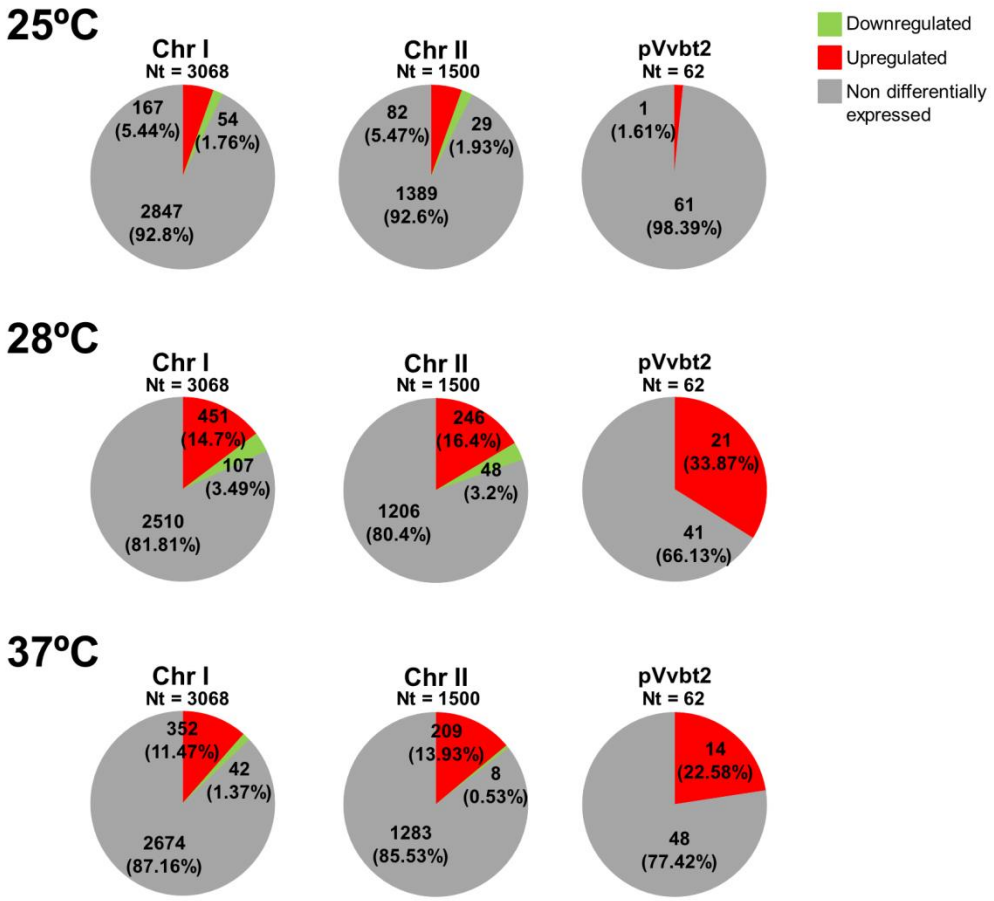

FIGURE 3 | Graphical representation of DEGs distribution among *V. vulnificus* genome in response to temperature. Figure shows the distribution of the DEGs per regulation category (upregulated, downregulated or nonregulated) and replicon (two chromosomes and one plasmid). The categories are represented with a color code.

The PCA (principal component analysis) showed the transcriptomic samples clearly separated by temperatures (**FIGURE 5**), being those obtained at 20 and 25ºC more similar to each other than those obtained at 28 and 37ºC. In addition, the PCA showed that i) biological replicates obtained at each temperature were very similar to each other, with the exception of those obtained at 37 ºC, which showed greater variability, and ii) the samples obtained at 28ºC were the furthest from the rest. Precisely, the highest number of DEGs was obtained at 28ºC (**FIGURES 4A** and **5**), temperature at which the highest number of plasmid DEGs was detected with 21 genes upregulated (including *ftbp* [encoding a fish transferrin binding protein essential for fish virulence (Pajuelo *et al.*, 2015)]) and none downregulated (**FIGURE 2**). pVvBt2 is a plasmid essential for virulence because it confers resistance to the innate immunity of teleost fish (Lee *et al.*, 2008). Therefore, this difference in plasmid gene expression could explain, partially, why the pathogen is more virulent for fish at 28 ºC than at 25 or 20ºC (Amaro *et al.*, 2015).

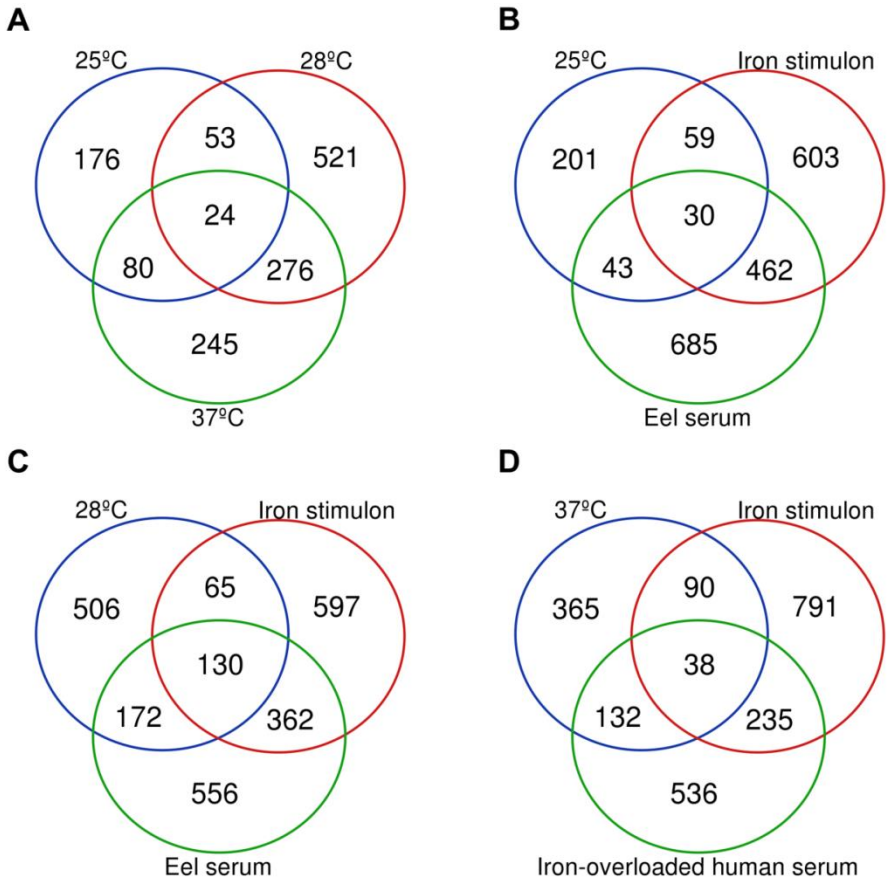

FIGURE 4 | Graphical representation of number of DEGs at each temperature in common with iron stimulon and host serum (previously described in chapters 1 and 2). A) Number of DEGs in common between the three temperatures assayed. B) Number of DEGs at 25ºC in common with iron stimulon and eel serum. C) Number of DEGs at 28ºC in common with iron stimulon and eel serum. D) Number of DEGs at 37ºC in common with iron stimulon and iron-overloaded human serum.

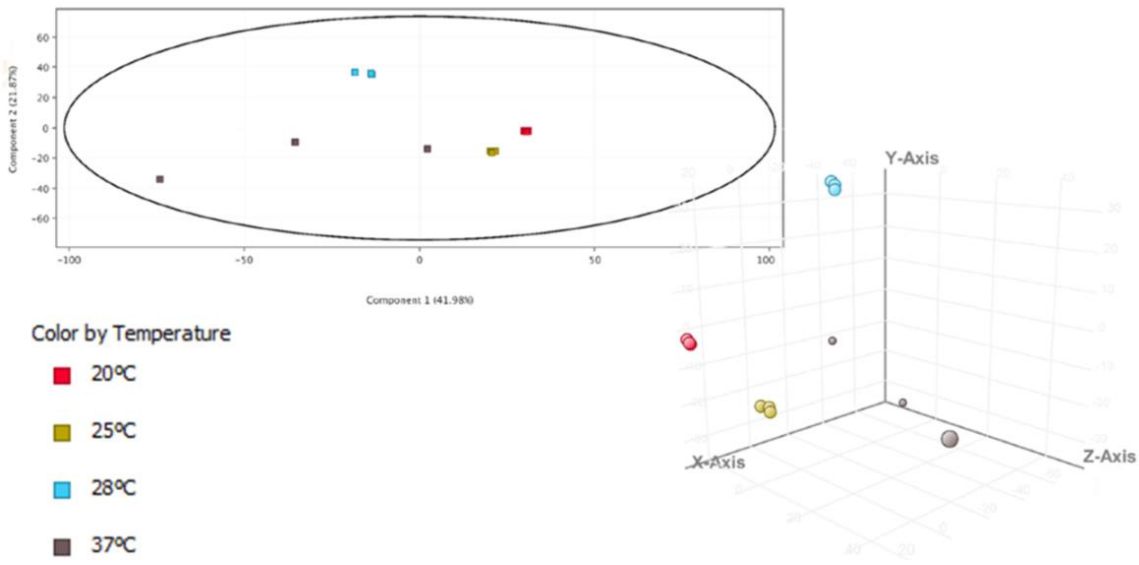

FIGURE 5 | PCA 3-D plot of temperature samples.

Most of the genes that responded to an increase in temperature were related to nutrient uptake and metabolism, two cellular processes that were among the most strongly activated when increasing temperature (**TABLE 2**). For example, *dns*, encoding an extracellular nuclease (Blokesch and Schoolnik, 2008), together with *nupC*, which encodes a nucleoside uptake protein involved in *V. choleare* fitness in nutrient limited environments (Gumpenberger *et al.*, 2016), and multiple genes related to amino acid biosynthesis and transport (including genes for oligopeptide transport [*opp* genes]) as well as lipid and fatty acid metabolism and transport were upregulated at infective temperatures (**TABLE 2**). Accordingly, *fabR*, a repressor of unsaturated fatty acid metabolism was downregulated at 37ºC. Finally, we found some genes involved in vulnibactin siderophore biosynthesis and iron transport (either ferrous or ferric iron), including the plasmid gene *ftbp*, upregulated at all the assayed temperatures (**TABLE 2**). In accordance, *crp*, encoding c-AMP (cyclic AMP) receptor protein, a regulator reported to be responsible for positive control of iron uptake systems (Choi *et al.*, 2006; Oh *et al.*, 2009; Kim *et al.*, 2016) was upregulated at 28 and 37ºC. Altogether, our results suggest that an increase in temperature leads to a transcriptomic upregulation of multiple genes involved in biosynthesis, degradation and transport of amino acids, fatty acids, lipids and iron, which would ensure growth of *V. vulnificus* at host physiological temperature during the infection. Curiously, and as an exception, we found transcriptomic evidence of maltose/maltodextrin transport downregulation at 25 and 28ºC (a process previously found upregulated by iron and when the bacterium was grown in iron-overloaded human serum at 37ºC [chapters 1 and 2]), together with the upregulation of maltose regulon repressor (*malI*) (**TABLE 2**).

Transcriptomic signs of stress response activated by *V. vulnificus* were obtained at all the assayed temperatures (**TABLE 2**). Although the DEGs involved in the stress response were not exactly the same at each of the assayed temperatures, the global response was very similar and mostly enhanced at 28ºC (**TABLE 2**). This stress response included the upregulation of defense mechanisms such as membrane protection and regeneration (phospholipid biosynthesis), resistance to oxidative and nitrosative environments (*aphF*, superoxide dismutase, glutathione-related genes and nitrate reductase-related genes), together with the repression of *ohr* (encoding a repressor for oxidative stress resistance) as well as genes involved in resistance to microcidal compounds (**TABLE 2**). All these processes together comprise bacterial ability to resist inside the host during the infection (Kaufmann and Dorhoi, 2016; Lim *et al.*, 2017; Uribe-Querol and Rosales, 2017).

Motility and chemotaxis are bacterial virulence factors required for host colonization (Lee *et al.*, 2004). Our transcriptomic results showed several flagella-related genes (including genes

encoding flagellar hook proteins, flagellar basal-body proteins and flagellar motor activity proteins) and chemotaxis-related genes upregulated in all the assayed conditions (**TABLE 2**). Curiously, all the motility related genes found upregulated by an increase in temperature were previously found downregulated in iron stimulon and eel serum, but upregulated in iron-overloaded human serum (chapters 1 and 2). Concerning biofilm, our transcriptomic results showed that bacterial MSHA and Flp pilus (*msh* and *tad* genes), involved in biofilm formation (Watnick *et al.*, 1999; Pu and Rowe-Magnus, 2018) were upregulated when temperature rises, as they were in iron deficiency and in serum of its hosts (**TABLE 2**). Contrary, *vpsT*, encoding a repressor for biofilm production (Krasteva *et al.*, 2010) was upregulated by temperature.

Finally, we also found that multiple external envelope biosynthesis genes (LPS and capsule production), involved in resistance to host innate immunity (Amaro *et al.*, 1994, 1997), were upregulated by temperature (**TABLE 2**), although not as many as those regulated by iron and host serum (chapters 1 and 2). Curiously, we did not find any of the genes for the major toxins or the virulence master regulators differentially expressed in any of the comparisons performed, with the exception of the upregulation of quorum sensing regulators (*luxU* and *luxO* at 28ºC and *smcR* at 37ºC) and *tetR*, encoding a master regulator involved in transcriptional regulation of multidrug efflux pumps, antibiotics biosynthesis, response to osmotic stress, control of catabolic pathways, and pathogenicity (Ramos *et al.*, 2005), at 25 and 28ºC (**TABLE 2**).

TABLE 2 | Selected DEGs at 25, 28 and 37ºC vs 20ºC.

Gene(s)[1]	FC[2]			Putative function/process[3]
	25ºC	28ºC	37ºC	
Metabolic and nutrient transport and utilization genes (including iron)				
fadH	11.3	--	2.3	Unsatturated fatty acids metabolism
Peptide ABC transporters#	10.4-2.4	--	3.9	Peptide transport
ilvE, ilvG, ilvI	7.8-2.5	--	2.1	Amino acid biosynthesis
trpCD	6.1-4	--	2.8	Amino acid biosynthesis (tryptophan)
C4-dicarboxylate transporters#	6-2.4	--	20.7-2.9	Dicarboxylate transport
argG, argI	5-2.1	2.1	--	Amino acid metabolism
Ferric iron ABC transporter*#	3.7	3.4-2.3	2.6	Ferric iron transport
Long-chain fatty acid transport protein	3.3	--	--	Fatty acids transport

TABLE 2 | Continued.

Gene(s)[1]	FC[2]			Putative function/process[3]
	25ºC	28ºC	37ºC	
Vulnibactin biosynthetic genes*#	3-2.3	2.9-2.5	2.3	Vulnibactin biosynthesis and transport
hisBD	2.7	-2.1	--	Amino acid biosynthesis
fabGH	2.4	--	2.4	Fatty acids metabolism
Amino acid ABC transporter*	2.3	5.5-2.8	13.8-6.2	Amino acid transport
metB,metK, metL	2.3-2.1	8.5	2.8	Amino acid biosynthesis
L-serine dehydratase	2.3	--	--	Amino acid metabolism
potB, potD*#	2.2	2	--	Polyamine transport
PTS system, N-acetylglucosamine-specific IIB, IID components*#	2.1	--	3.5	Aminosugar transport
Nitrate ABC transporter	2.1	--	--	Nitrogen metabolism
ftbp*#	2	2	2.8	Fish transferrin binding protein
rbsABCD#	-2.6	-(3.4-3.7)	6.6-3.4	Ribose ABC transport system
Short chain fatty acids transporter	-2.7	-2.4	--	Fatty acids transport
malG	-2.9	-3.1	--	Maltose/maltodextrin ABC transporter
prsA	-3.1	-2.6	--	Ribose metabolism
Chitinase proteins	--	22.3-2.5	8.8	Chitinase activity
serB	--	10.6	9.8	Amino acid biosynthesis
pflA	--	8.4	--	Glucose metabolism
Succinate-semialdehyde dehydrogenase [NADP+]	--	8.4	--	Amino acid degradation
nupC*#	--	6.7	8.1	Permease for nucleoside uptake
dns*#	--	5.7	--	Degradation of DNA for nutrient uptake (competence related)
Zinc ABC transporter	--	4.5-3.5	--	Zinc transport
Lipase-related proteins	--	4.2-2.7	8-5.3	Extracellular lipid utilization
Phosphate ABC transporter#	--	3.8-2.6	6.6	Phosphate transport
trkA, trkH	--	3.1	3.9-2.4	Potassium uptake
oppBCD, oppF	--	3-2.7	7.9-2.1	Oligopeptide transport system permease
ktrA#	--	2.8	3.4	Potassium uptake
thrC	--	2.7	--	Amino acid iosynthesis

TABLE 2 | Continued.

Gene(s)[1]	FC[2]			Putative function/process[3]
	25ºC	28ºC	37ºC	
dctQ#	--	2.3	6.5	TRAP dicarboxylate transporters
proA	--	2.3	--	Amino acid biosynthesis
Ferrous iron transporter B	--	2	--	Ferrous iron transport
acp12	--	-(2.6-3.7)	--	Fatty acids biosynthesis
glgX#	--	--	12.8	Glycogen debranching enzyme
hmgA	--	--	10-4	Amino acid degradation
citAB	--	--	8.3-2.8	Citrate metabolism
Anaerobic respiration				
Nitrate reductase cytochrome c550-type subunit*	2.7	--	3	Nitrite reductase complex subunit
napC, napE, napGH*#	--	22.5-6.7	3.9-2.2	Subunit of the periplasmic nitrite reductase complex
Nitrite reductase subunits	--	3.5-2.8	--	Nitrite reductase complex
nrfF	--	--	23.3	Formate-dependent nitrite reductase complex
LPS and capsule				
cpsABC#	2	5.5-3.3	--	Capsule biosynthesis
sypAB, sypR	--	5.1-2.3	15.8-5.2	Capsule biosynthesis
wza#	--	-2.8	--	LPS biosynthesis
galE	--	--	4.7	O-antigen biosynthesis
lptA	--	--	2.3	LPS biosynthesis
Stress response and defense mechanisms				
Anaerobic glycerol-3-phosphate dehydrogenase subunits (B, C)#	4.6-2.2	--	4.4-3.7	Phospholipid biosynthesis/membrane regeneration
S-(hydroxymethyl)glutathione dehydrogenase#	3	2.3	--	Resistance to oxidative stress
aphF	2.8	--	--	Resistance to oxidative stress
Glutathione S-transferase#	2.7	4.5	--	Resistance to oxidative stress
uspA	2.7	--	--	Universal stress protein A, involved in damage resistance
mutS*	2.5	--	--	DNA mismatch repair protein
Superoxide dismutase [Cu-Zn] precursor	2.3	--	--	Resistance to oxidative stress
plsXY#	2.2	4.9	3.3	Phospholipid biosynthesis/membrane regeneration

TABLE 2 | Continued.

Gene(s)[1]	FC[2]			Putative function/process[3]
	25ºC	28ºC	37ºC	
Phosphoglycerol transferase I*#	2.2	4.2	--	Phospholipid biosynthesis/membrane regeneration
YfgC precursor*	2.1	--	--	Outer membrane integrity
cydD	2.1	--	--	Glutahione transport
Permease of the drug/metabolite transporters (DMT)#	2	4.8-2.1	11.5-2.3	Resistance to microcidal compounds
Glycerophosphoryl diester phosphodiesterase#	2	--	3.1	Phospholipid biosynthesis/membrane regeneration
sspAB	-(2-2.3)	-2.1	--	Stringent starvation proteins
rseABC*#	--	9.5-6.2	--	Negative regulatory proteins for RpoE, a sigma factor for envelope stress response
nsrR*#	--	8.2	--	Repressor for resistance to nitrosative stress
cmeB	--	7.2	--	Drug efflux system
clpB*#	--	5.7	--	Stress-induced chaperone
Formate efflux transporter*#	--	4.8	--	Resistance to microcidal peptides
cspD*	--	3.7	--	Cold shock proteins, involved in stress caused by membrane damage
Manganese superoxide dismutase	--	3.5	11	Resistance to oxidative stress
norR*	--	3.4	--	Anaerobic nitric oxide reductase transcription regulator
uvrC*#	--	3.2	4.5	Excinuclease ABC subunit C for DNA repair
marR	--	3	6.6	Multiple antibiotic resistance protein
htpG	--	3	--	Chaperone protein
msrAB#	--	2.7	2.3	Peptide methionine sulfoxide reductase involved in reparation of oxidized proteins
ohr*	--	-2.6	-3.65	Repressor for organic hydroperoxidase resistance
degQ#	--	--	2.1	Outer membrane integrity
Flagellum, pili and chemotaxis				
Methyl-accepting chemotaxis protein*#	8.5-2.4	12.8-2.5	15.5-2	Chemotaxis
mshH, mshJK, mshOP*#	2.7	3.2-2.1	4.2-2.1	Pili MSHA biosynthesis
fleQ, fleS	2.4-2.2	2	4.1-3.1	Flagellar regulatory protein

TABLE 2 | Continued.

Gene(s)[1]	FC[2]			Putative function/process[3]
	25ºC	28ºC	37ºC	
flgA, flgHI, flgL, flgT*#	2.2-2.1	4.1	11.9-3.2	Flagellar basal-body rod proteins
tadBCD, tadZ*	2.2-2	14.1-3.2	10	Flp pili assembly
fliF, fliM*#	2	2.2-2.1	3.6-2.6	Flagellar motor activity
Probable type IV pilus assembly FimV-related	-2.4	-2.4	--	Pili MSHA
rpoN*#	--	27.1	3.8	RNA polymerase sigma factor
flgN	--	8.7	2.1	Flagellar biosynthesis protein
flgK, flgM*#	--	8.5	16	Hook associated protein
motAB*#	--	7.5-2.8	3.6	Flagellar motor rotation protein
fleN*#	--	5.8	2.1	Flagellar synthesis regulator
RNA polymerase sigma factor for flagellar operon	--	5.4	--	Flagellar biosynthesis
acfD	--	4	--	Accessory colonization factor, putatively involved in motility
fliL	--	3.7	--	Controls rotational direction of flagella during chemotaxis
flaD. flaFG*#	--	3.6-2.3	6.5-4	Flagellin protein
cheD	--	3.3	--	Chemotaxis protein
Chemotaxis regulator#	--	3.1	5.8	Transmits chemoreceptor signals to flagellar motor
Transcriptional regulators				
Nitrogen regulation protein NR(I)*	3.1	-2.7	--	Nitrogen starvation
tetR*#	2.6	7.9	--	Involved in transcriptional control of multidrug efflux pumps, pathways for the biosynthesis of antibiotics, response to osmotic stress and toxic chemicals, control of catabolic pathways, differentiation processes and pathogenicity
rpoS	2.5	--	--	Stress and metabolism management
arcA#	-2.4	-2.6	--	Repressor for aerobic metabolism
uxuR*#	--	9	--	Repressor for oligogalacturonide metabolism
malI*#	--	4.3	--	Maltose regulon repressor protein
deoR	--	4	--	Repressor of deoxyribose operon

TABLE 2 | Continued.

Gene(s)[1]	FC[2]			Putative function/process[3]
	25ºC	28ºC	37ºC	
***vpsT**#*	--	3.7	5.1	Repressor of biofilm and biofilm related polysaccharide formation
***luxO**#*	--	3.6	--	Involved in quorum sensing pathways
***phoR**#*	--	2.9	--	Histidine kinase for PhoB, involved in phosphate metabolism
***luxU**#*	--	2.9	--	Phosphorelay protein involved in quorum sensing
crp*	--	2.9	5	cAMP receptor protein, regulatory protein
argR	--	2.5	--	Repressor of arginine metabolism
smcR#	--	--	2.2	Involved in quorum sensing pathways
***fabR**#*	--	--	-2.7	Repressor for unsaturated fatty acid biosynthesis

[1]Identified DEGs are indicated.

[2]FC: fold change value or range of values for each identified gene or group of related genes at 25ºC, 28ºC and 37ºC.

[3]Putative function for selected genes and related process.

*Differentially expressed in iron stimulon (chapter 1).

#Differentially expressed in eel or iron-overloaded human serum (chapter 2).

--: not detected as differentially expressed.

Phenotypic results

Biofilm production. Our transcriptomic results suggested changes in biofilm formation (**TABLE 2**). Therefore, we phenotypically tested the bacterial ability to form biofilm by staining biofilms with crystal violet after 24 h of growth and measuring Abs_{540}. No significant differences were found for biofilm production between conditions although a slight increase in biofilm quantity with temperature was observed (**TABLE 3**).

Motility. Flagella-related genes were the most abundant DEGs in our transcriptomic study, upregulated when incubation temperature rises up (**TABLE 2**). We performed a motility assay and confirmed that the motility rate of *V. vulnificus* significantly increases when the environmental temperature increases, being non-motile at 20ºC, intermediate-motile at 25 and 28ºC (without significant differences between these two temperatures) and high-motile at 37ºC (**TABLE 3**).

Proteolytic activity. Vvp, the major metalloprotease of *V. vulnificus*, is involved in adhesion and mucosal colonization and, therefore, is considered an important virulence factor for both fish and humans (Paranjpye and Strom, 2005; Valiente *et al.*, 2008; Jones and Oliver, 2009). Although we did not find *vvp* differentially expressed in any of the transcriptomic comparisons performed, we found upregulated at optimal temperatures for eel and human vibriosis (28 and 37ºC, respectively) several minor putative proteases, as well as, *crp*, encoding c-AMP receptor protein, and quorum sensing regulators, both described as inducers of Vvp activity (Elgaml and Miyoshi, 2017) (**TABLE 2**). Therefore, we checked the effect of temperature on protease production by *V. vulnificus* by measuring azocasein proteolysis at 20, 25, 28 and 37ºC. Our results revealed that at 20ºC there was no proteolytic activity and that this activity increased with temperature, achieving the major point of activity at 28ºC and again decreasing at 37ºC (**TABLE 3**). Our results are in accordance with previous studies of temperature-dependent regulation of Vvp, which is described to be efficient at 26ºC (Elgaml and Miyoshi, 2017).

Chemotaxis. Among the most upregulated genes in response to temperature were those related to chemotactic response (**TABLE 2**). Given that both motility and proteolytic activity are temperature-dependent (**TABLES 2** and **3**), and motile *V. vulnificus* cells which produce Vvp are positively chemo-attracted by eel mucus (Valiente *et al.*, 2008), we tested *V. vulnificus* chemo-attraction towards eel skin mucus at 20, 25, 28 and 37ºC. Interestingly, the pathogen only exhibits positive attraction to eel mucus at 28 and 37ºC but not at 20 or 25ºC (**FIGURE 5**), which agrees with the efficient temperatures for protease activity (28ºC) and motility (37ºC) (**TABLE 3**).

TABLE 3 | Phenotypic assays performed to validate microarray data in response to temperature.

Sample	Biofilm[1]	Motility rate[2]	Cellular-associated polysaccharides[3]	Proteolytic activity[4]
20ºC	0.027±0.002	0.24±0.02*	87.67±0.37*	12.09±6.65*
25ºC	0.034±0.005	1.56±0.08#	95.37±1.32*#	6216.17±250.55#
28ºC	0.035±0.016	1.40±0.31#	103.55±2.77#	6498.76±210.18#
37ºC	0.066±0.048	2.46±0.60*#	108.68±5.92#	4021.47±181.49*#

[1]Biofilm from 24 h cultures was quantified after staining with crystal violet by measuring Abs_{540}.
[2]Motility measured as motility rate on MA (colony surface in mm2/log of colony CFU).
[3]Total polysaccharide concentration is expressed as μg/10^8 cells.
[4]Proteolytic activity in ECPs expressed as PU determined using azocasein as substratum.
Results are presented as the averages ± standard deviation of three independent experiments. *: significant differences (*P<0.05*) temperature vs 28ºC. #: significant differences (*P<0.05*) temperature vs 20ºC.

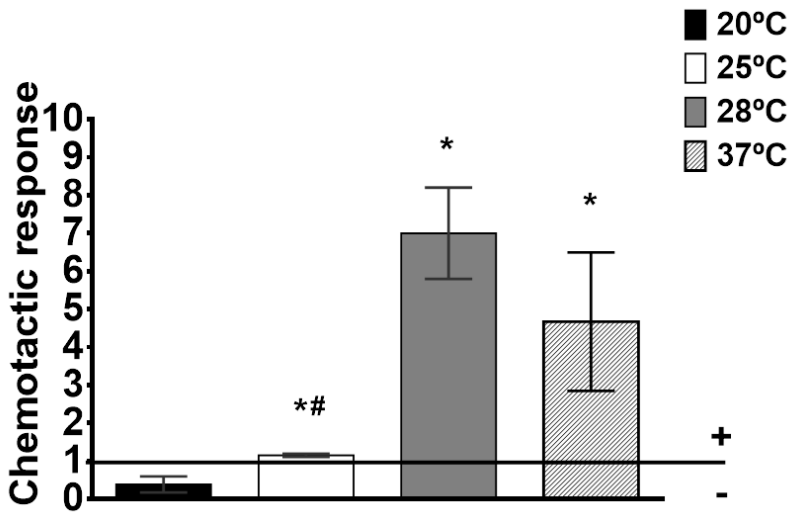

FIGURE 6 | Chemotaxis towards eel skin mucus in *V. vulnificus*. Chemotaxis was measured as chemotactic response (ratio of bacterial numbers in eel skin mucus-capillaries vs control-capillaries [containing chemotaxis buffer]). The horizontal line marks the borderline between positive and negative chemotaxis. *: significant differences in chemotactic response towards eel skin mucus at each temperature vs 20ºC (*P<0.05*). #: significant differences between each temperature and 28ºC (*P<0.05*).

Surface cell-associated polysaccharides. We determined in chapters 1 and 2 that the external envelope of *V. vulnificus* is regulated by iron concentration and seems to confer resistance to innate immunity in a host-dependent manner. A few genes related to O-antigen (*galE*) and capsule biosynthesis (*cps* and *syp* genes) were upregulated in response to an increase in temperature, albeit they did not correspond to those previously obtained in response to iron and/or host sera (**TABLE 2**). In order to better understand how temperature could influence external envelope formation, cell-associated polysaccharides of *V. vulnificus* grown at 20, 25, 28 and 37ºC were extracted, quantified and analyzed. The quantity of cellular-associated polysaccharides (μg per 10^8 cells) significantly increased with temperature until 28ºC and from that on (37ºC) the increase in temperature did not produce significant changes in polysaccharide concentration (**TABLE 3**). Accordingly, the cell-associated polysaccharide pattern also showed changes with temperature. This pattern can be only visualized by immunoblotting because neither the LPS nor the capsule are stained with silver (Biosca *et al.*, 1993). Given that the quantity of polysaccharide per well was the same, the immunogenicity of external polysaccharides seems to change with temperature (i.e., no band was immunostained at 20ºC). In addition, the O-antigen pattern was different at 25, 28 and 37ºC, being the portion of the O-antigen involved in resistance to eel innate immunity (MMW O-antigen, (Amaro *et al.*, 1997)) clearly increased at 28ºC (**FIGURE 7**). The same changes affecting O-antigen pattern

were also observed when the LPS from cells grown in eel serum (28ºC) was compared with that obtained in iron-overloaded human serum (37ºC), while the change observed in capsule production was not reproduced by changes in temperature. Altogether these results suggest that temperature influences the LPS biosynthesis while capsule production is mainly controlled by iron in *V. vulnificus*.

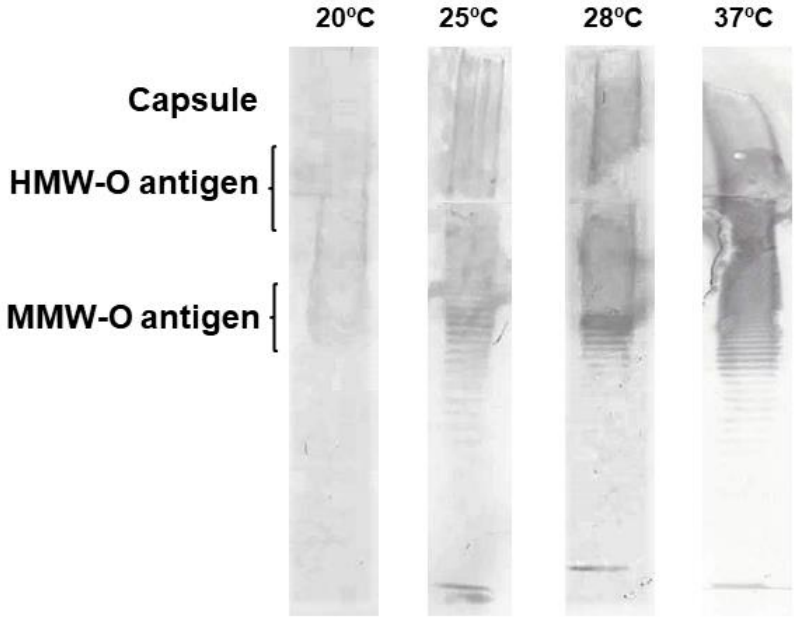

FIGURE 7 | *V. vulnificus* LPS and capsule profiles in response to temperature. 10 µg of cell-associated polysaccharides (LPS + capsule) from R99 mid-log phase cultures in CM9 at 20, 25, 28 and 37ºC were separated by SDS-PAGE, transferred to a PVDF membrane and subjected to immunoblot analysis with antibodies against R99-cell-envelopes as specified in chapter 1 (p. 79).

4. Discussion

V. vulnificus is an accidental pathogen from brackish water ecosystems located in tropical, subtropical and temperate areas that is spreading to traditionally colder areas, such as the Baltic sea or Greenland, due to the global warming (Motes *et al.*, 1998; Oliver, 2015). This expansion is responsible of an unusually high number of infections affecting humans and fish that has been registered in these new areas in the last years (Baker-Austin and Oliver, 2018). There are numerous field data that relate water temperature with outbreak severity of vibriosis in fish farms (Rodolfo Barrera, personal communication), data that have been probed at laboratory scale by infecting eels at different water temperatures (Amaro *et al.*, 1995). These experiments demonstrated that the pathogen was avirulent at 20ºC (or below) and caused septicemia in fish maintained over 22ºC being moderately virulent at 25ºC and highly

at 28ºC (Amaro *et al.*, 1995). Moreover, *V. vulnificus,* as a multi-host pathogen, is also able to infect humans and cause septicemia at 37ºC (Horseman and Surani, 2011).

In this work, we hypothesized that temperature is one of the external signals which trigger virulence in *V. vulnificus*. In fact, an increase in environmental temperature activates virulence factors expression in other bacteria that are also accidental pathogens (Konkel and Tilly, 2000). To test our hypothesis, we analyzed the global transcriptome of *V. vulnificus* grown at infective vs non-infective temperature and confirmed the results by phenotypic assays.

Temperature controls bacterial motility and chemotaxis, which were clearly increased with temperature. *V. vulnificus* infects fish and humans trough water and its infection capability is dependent on motility and chemo-attraction towards fish mucus or host blood (Valiente *et al.*, 2008). Therefore, as motility and chemotaxis increases, the host colonization and virulence also increases. Similar results were reported in *Photobacterium damselae* subsp. *piscicida* (*Pdp*) and *V. harveyi* (Matanza and Osorio, 2018; Montánchez *et al.*, 2019), two multi-host pathogens like *V. vulnificus*, which suggests a general role of temperature on bacterial colonization in Vibrionaceae.

Host colonization by *V. vulnificus* is dependent on *vvp*, a gene encoding the main exoprotease of this species, as mutants deficient in this gene are unable to be attracted by mucine (the main component of mucus) or human blood (Valiente *et al.*, 2008). Vvp is also involved in fish virulence since mutants deficient in the protease are also deficient in gill colonization and, therefore, in virulence when using water as transmission route for the bacterial infection (Valiente *et al.*, 2008). Protease is involved in mucine degradation (Miyoshi *et al.*, 1997; Valiente *et al.*, 2008) and, therefore, facilitates chemo-attraction towards mucosal surfaces. Although Vvp was not detected as belonging to the temperature stimulon, we phenotypically confirmed that protease activity was increased with temperature with a maximum at 28ºC, followed by 37ºC. Therefore, during host infection at warm temperatures *V. vulnificus* could produce more protease, which would favor colonization of mucosal epithelial tissues, and consequently, the infection. This, together with the chemo-attraction to mucus at 28ºC but not at 20 neither at 25ºC would explain in part the high virulent phenotype for eels expressed by *V. vulnificus* only at 28ºC.

Several regulators related to motility, chemotaxis and protease production were found to belong to the temperature stimulon and were regulated accordingly with the observed phenotype: i.e., *vpsT*, encoding a repressor of biofilm formation, that promotes motility from biofilm dispersion (Krasteva *et al.*, 2010); *crp*, which encodes for a global regulator involved in

the activation of Vvp (the main *V. vulnificus* protease) (Elgaml and Miyoshi, 2017); and several quorum sensing-related regulators that activate the expression of *vvp* (Kim *et al.*, 2013; Elgaml and Miyoshi, 2017).

Interestingly, temperature influenced the entrance of *V. vulnificus* in the log phase of growth, which was slower at lower temperatures (20 and 25ºC) as well as the entrance in the death phase, which was faster at 37ºC. However, temperature did not seem to affect the maximum population size, which was similar at all the assayed temperatures. Therefore, all these results suggest that *V. vulnificus* once established on the host tissues could be easily eliminated by the innate immunity before achieving the population size needed to produce vibriosis when fish are kept at 20ºC while could multiply and achieve blood before being attacked by innate defenses when fish are kept over 28ºC. In case of humans, the bacterial survival in a wound could also be favored at 28ºC.

When we analyzed the global transcriptome from cells obtained in the mid log phase of growth, we found that most of the DEGs in response to temperature were involved in metabolism and transport of nutrients. Thus, an increase in temperature upregulated genes related to amino acids, lipids, fatty acids, nucleoside and iron metabolism and/or transport. Similar results were previously reported in other gramnegative species such as *Pdp* and *Pseudomonas putida* (Fonseca *et al.*, 2011; Matanza and Osorio, 2018) including *V. vulnificus* (Kim *et al.*, 2016). In agreement, *crp*, which is also a positive regulator for iron uptake (Kim *et al.*, 2016) was also upregulated at 28 and 37ºC. Remarkably, and contrarily to previous data in other Vibrionaceae species (Liu *et al.*, 2017; Matanza and Osorio, 2018), oligopeptide uptake and metabolism (*opp* operon) was also activated by temperature suggesting a putative role of this kind of metabolism in bacterial fitness in serum, a medium particularly rich in oligopeptides (Samant *et al.*, 2008).

Temperature also enhanced bacterial ability to cope with stress since an upregulation of membrane regeneration, oxidative and nitrosative resistance-related genes was found when temperature raised. Therefore, temperature could indirectly enhance *V. vulnificus* virulence, preparing the bacterium for resisting the toxic byproducts of its own metabolism as well as ROS and/or NO produced by host phagocytes and neutrophils (Kaufmann and Dorhoi, 2016; Uribe-Querol and Rosales, 2017).

V. vulnificus needs to overcome host innate defenses in blood to cause septicemia. In previous chapters, we demonstrated that iron controls the production of a protective envelope, either rich in capsule in iron-overloaded human blood or rich in HMW/MMW O-

antigen of LPS together with two plasmid IROMPs in eel blood. We found transcriptomic and phenotypic evidences that temperature could control the LPS production, in particular, the O-antigen production, and contribute to the highly virulent phenotype in case of fish infections.

Notably, neither the major toxins of the species nor virulence-related transcriptional regulators were found as controlled by temperature in our study. This result is in accordance with previous studies that suggest that virulence-related genes are controlled, directly or indirectly, by other external signals such as iron and/or presence of eukaryotic cells in the environment (Lee *et al.*, 2013; chapters 1 and 2 of the present thesis). Considering the importance of the toxins $RtxA1_3$ and VvhA in *V. vulnificus* virulence, we expected to find them upregulated at 28 and 37ºC. Contrarily, we did not find any of them differentially expressed at the assayed conditions (neither by microarray, nor by RT-qPCR), an observation supported by previous studies in *Pdp* (Matanza and Osorio, 2018).

Finally, our results highlight the importance of pVvBt2 in the virulent phenotype of *V. vulnificus* for fish, as the most numerous response of plasmid genes was at 28ºC, with the majority of those genes upregulated. In a similar way, Matanza and Osorio have recently described that most of the genes encoded by *Pdp* virulence plasmid are upregulated with an increase in temperature, including Ftbp- and Fpcrp-like genes (Matanza and Osorio, 2018). Our results only show Ftbp but not Fpcrp as regulated by temperature, but this could be explained since in *V. vulnificus* the two genes are located in different operons while in *Pdp* they belong to the same operon (results not shown).

In conclusion, our results reveal that the environmental temperature acts as an external signal that controls virulence and host adaptation mechanisms in the pathogen *V. vulnificus.* Thus, temperature over 28ºC activates motility, chemotaxis and protease production, shorten the lag phase, activates metabolism, iron uptake, and the production of a partially protective external envelope (at least against fish innate immunity), all these processes being involved in host colonization. Although most of the genes belonging to temperature stimulon do not belong to iron stimulon, those related to flagella biogenesis and chemotaxis do belong to iron stimulon (chapter 1), meaning that temperature and iron could act synergistically to control *V. vulnificus* dissemination inside its hosts. However, the main virulence factors for this pathogen, the toxin $RtxA1_3$ and the hemolysin VvhA, are not controlled by temperature. According to these results, in iron rich environments, like those found in fish farms, and at infective temperatures, *V. vulnificus* would be motile, which in turn would result in attraction to mucus and colonization of the fish host. In the same way, in seawater the bacterium would increase

motility with temperature (in summer, or warm months) being able to be attracted by the blood human and colonize wounds. From gills and human wounds, the pathogen would enter occasionally to the bloodstream where it should produce some of the factors involved in resistance to complement and phagocytosis. From that point, other signals such as iron and contact with eukaryotic cells would trigger the formation of a truly protective barrier together with the expression of a toxic phenotype involved in septicemia.

5. References

Amaro, C., Biosca, E.G., Fouz, B., Alcaide, E., and Esteve, C. (1995) Evidence that water transmits *Vibrio vulnificus* Biotype 2 infections to eels. *Appl Environ Microbiol* **61**: 1133–1137.

Amaro, C., Biosca, E.G., Fouz, B., Toranzo, A.E., and Garay, E. (1994) Role of iron, capsule and toxins in the pathogenicity of *Vibrio vulnificus* Biotype 2 for mice. *Infect Immun* **62**: 759–763.

Amaro, C., Fouz, B., Biosca, E.G., Marco-Noales, E., and Collado, R. (1997) The lipopolysaccharide o side chain of *Vibrio vulnificus* serogroup E is a virulence determinant for eels. *Infect Immun* **65**: 2475–2479.

Amaro, C., Sanjuán, E., Fouz, B., Pajuelo, D., Lee, C.T., Hor, L., et al. (2015) The fish pathogen *Vibrio vulnificus* Biotype 2: epidemiology, phylogeny and virulence factors involved in warm-water vibriosis. *Microbiol Spectr* **3**.

Baker-Austin, C. and Oliver, J.D. (2018) *Vibrio vulnificus*: new insights into a deadly opportunistic pathogen. *Environ Microbiol* **20**: 423–430.

Biosca, E.G. and Amaro, C. (1996) Toxic and enzymatic activities of *Vibrio vulnificus* biotype 2 with respect to host specificity. *Appl Environ Microbiol* **62**: 2331–2337.

Biosca, E.G., Garay, E., Toranzo, A.E., and Amaro, C. (1993) Comparison of outer membrane protein profiles of *Vibrio vulnificus* biotypes 1 and 2. *FEMS Microbiol Lett* **107**: 217–222.

Blokesch, M. and Schoolnik, G.K. (2008) The extracellular nuclease Dns and its role in natural transformation of *Vibrio cholerae*. *J Bacteriol* **190**: 7232–7240.

Choi, M.H., Sun, H.Y., Park, R.Y., Kim, C.M., Bai, Y.H., Kim, Y.R., et al. (2006) Effect of the *crp*

mutation on the utilization of transferrin-bound iron by *Vibrio vulnificus*. *FEMS Microbiol Lett* **257**: 285–292.

Elgaml, A. and Miyoshi, S.I. (2017) Regulation systems of protease and hemolysin production in *Vibrio vulnificus*. *Microbiol Immunol* **61**: 1–11.

Esteve-Gassent, M.D., Nielsen, M.E., and Amaro, C. (2003) The kinetics of antibody production in mucus and serum of European eel (*Anguilla anguilla* L.) after vaccination against *Vibrio vulnificus*: Development of a new method for antibody quantification in skin mucus. *Fish Shellfish Immunol* **15**: 51–61.

Fonseca, P., Moreno, R., and Rojo, F. (2011) Growth of *Pseudomonas putida* at low temperature: Global transcriptomic and proteomic analyses. *Environ Microbiol Rep* **3**: 329–339.

Fouz, B. and Amaro, C. (2002) Isolation of a new serovar of *Vibrio vulnificus* pathogenic for eels cultured in freshwater farms. *Aquaculture* **217**: 677–682.

Fouz, B., Larsen, J.L., and Amaro, C. (2006) *Vibrio vulnificus* serovar A: an emerging pathogen in European anguilliculture. *J Fish Dis* **29**: 285–291.

Gao, H., Yang, Z.K., Wu, L., Thompson, D.K., and Zhou, J. (2006) Global transcriptome analysis of the cold shock response of *Shewanella oneidensis* MR-1 and mutational analysis of its classical cold shock proteins. *J Bacteriol* **188**: 4560–4569.

Gumpenberger, T., Vorkapic, D., Zingl, F.G., Pressler, K., Lackner, S., Seper, A., et al. (2016) Nucleoside uptake in *Vibrio cholerae* and its role in the transition fitness from host to environment. *Mol Microbiol* **99**: 470–483.

Hoben, H.J. and Somasegaran, P. (1982) Comparison of the pour, spread, and drop plate methods for enumeration of *Rhizobium spp.* in inoculants made from presterilized peat. *Appl Environ Microbiol* **44**: 1246–1247.

Horseman, M.A. and Surani, S. (2011) A comprehensive review of *Vibrio vulnificus*: An important cause of severe sepsis and skin and soft-tissue infection. *Int J Infect Dis* **15**: e157–e166.

Jones, M.K. and Oliver, J.D. (2009) *Vibrio vulnificus*: disease and pathogenesis. *Infect Immun* **77**: 1723–1733.

Kaufmann, S.H.E. and Dorhoi, A. (2016) Molecular Determinants in Phagocyte-Bacteria Interactions. *Immunity* **44**: 476–491.

Kim, C.M., Ahn, Y.J., Kim, S.J., Yoon, D.H., and Shin, S.H. (2016) Temperature change induces the expression of *vuuA* encoding Vulnibactin receptor and *crp* encoding cyclic AMP receptor protein in *Vibrio vulnificus*. *Curr Microbiol* **73**: 54–64.

Kim, I.H., Wen, Y., Son, J.S., Lee, K.H., and Kim, K.S. (2013) The fur-iron complex modulates expression of the quorum-sensing master regulator, *smcr*, to control expression of virulence factors in *Vibrio vulnificus*. *Infect Immun* **81**: 2888–2898.

Kim, Y.W., Lee, S.H., Hwang, I.G., and Yoon, K.S. (2012) Effect of temperature on growth of *Vibrio paraphemolyticus* and *Vibrio vulnificus* in flounder, salmon sashimi and oyster meat. *Int J Environ Res Public Health* **9**: 4662–4675.

Konkel, M.E. and Tilly, K. (2000) Temperature-regulated expression of bacterial virulence genes. *Microbes Infect* **2**: 157–166.

Krasteva, P.V., Jiunn, J.C., Shikuma, N.J., Beyhan, S., Navarro, M.V.A.S., Yildiz, F.H., et al. (2010) *Vibrio cholerae vpst* regulates matrix production and motility by directly sensing cyclic di-GMP. *Science* **327**: 866–868.

Le Roux, F., Wegner, K.M., Baker-Austin, C., Vezzulli, L., Osorio, C.R., Amaro, C., et al. (2015) The emergence of *Vibrio* pathogens in Europe: Ecology, evolution and pathogenesis (Paris, 11-12 March 2015). *Front Microbiol* **6**.

Lee, C.T., Amaro, C., Wu, K.M., Valiente, E., Chang, Y.F., Tsai, S.F., et al. (2008) A common virulence plasmid in biotype 2 *Vibrio vulnificus* and its dissemination aided by a conjugal plasmid. *J Bacteriol* **190**: 1638–1648.

Lee, C.T., Pajuelo, D., Llorens, A., Chen, Y.H., Leiro, J.M., Padrós, F., et al. (2013) MARTX of *Vibrio vulnificus* biotype 2 is a virulence and survival factor. *Environ Microbiol* **15**: 419–432.

Lee, J.H., Rho, J.B., Park, K.J., Kim, C.B., Han, Y.S., Choi, S.H., et al. (2004) Role of flagellum and motility in pathogenesis of *Vibrio vulnificus*. *Infect Immun* **72**: 4905–4910.

Lim, J.J., Grinstein, S., and Roth, Z. (2017) Diversity and versatility of phagocytosis: Roles in innate immunity, tissue remodeling, and homeostasis. *Front Cell Infect Microbiol* **7**: 1–12.

Liu, W., Huang, L., Su, Y., Qin, Y., Zhao, L., and Yan, Q. (2017) Contributions of the oligopeptide permeases in multistep of *Vibrio alginolyticus* pathogenesis. *Microbiologyopen* **6**: e511.

Livak, K.J. and Schmittgen, T.D. (2001) Analysis of relative gene expression data using real-time quantitative PCR and. *Methods* **25**: 402–408.

Matanza, X.M. and Osorio, C.R. (2018) Transcriptome changes in response to temperature in the fish pathogen *Photobacterium damselae* subsp. *damselae*: Clues to understand the emergence of disease outbreaks at increased seawater temperatures. *PLoS One* **13**: e0210118.

McDougald, D., Rice, S.A., and Kjelleberg, S. (2001) SmcR-dependent regulation of adaptive phenotypes in *Vibrio vulnificus*. *J Bacteriol* **183**: 758–762.

Miyoshi, N., Shimizu, C., Miyoshi, S.I., and Shinoda, S. (1987) Purification and characterization of *Vibrio vulnificus* protease. *Microbiol Immunol* **31**: 13–25.

Miyoshi, S., Wakae, H., Tomochika, K., and Shinoda, S. (1997) Functional domains of a zinc metalloprotease from *Vibrio vulnificus*. *J Bacteriol* **179**: 7606–7609.

Montánchez, I., Ogayar, E., Plágaro, A.H., Esteve-Codina, A., Gómez-Garrido, J., Orruño, M., et al. (2019) Analysis of *Vibrio harveyi* adaptation in sea water microcosms at elevated temperature provides insights into the putative mechanisms of its persistence and spread in the time of global warming. *Sci Rep* **9**.

Motes, M.L., DePaola, A., Cook, D.W., Veazey, J.E., Hunsucker, J.C., Garthright, W.E., et al. (1998) Influence of water temperature and salinity on *Vibrio vulnificus* in Northern Gulf and Atlantic Coast oysters (*Crassostrea virginica*). *Appl Environ Microbiol* **64**: 1459–1465.

Oh, M.H., Lee, S.M., Lee, D.H., and Choi, S.H. (2009) Regulation of the *Vibrio vulnificus hupA* gene by temperature alteration and cyclic AMP receptor protein and evaluation of its role in virulence. *Infect Immun* **77**: 1208–1215.

Oliver, J.D. (2015) The biology of *Vibrio vulnificus*. *Microbiol Spectr* **3**: 1–10.

Pajuelo, D., Lee, C.T., Roig, F.J., Hor, L.I., and Amaro, C. (2015) Novel host-specific iron acquisition system in the zoonotic pathogen *Vibrio vulnificus*. *Environ Microbiol* **17**: 2076–2089.

Paranjpye, R.N. and Strom, M.S. (2005) A *Vibrio vulnificus* type IV pilin contributes to biofilm

formation, adherence to epithelial cells and virulence. *Infect Immun* **73**: 1411–1422.

Pu, M. and Rowe-Magnus, D.A. (2018) A Tad pilus promotes the establishment and resistance of *Vibrio vulnificus* biofilms to mechanical clearance. *npj Biofilms Microbiomes* **10**.

Ramos, J.L., Martı, M., Molina-henares, A.J., Tera, W., Brennan, R., and Tobes, R. (2005) The TetR family of transcriptional. *Microbiol Mol Biol Rev* **69**: 326–356.

Roig, F.J., González-Candelas, F., Sanjuán, E., Fouz, B., Feil, E.J., Llorens, C., et al. (2018) Phylogeny of *Vibrio vulnificus* from the analysis of the core-genome: Implications for intra-species taxonomy. *Front Microbiol* **8**.

Samant, S., Lee, H., Ghassemi, M., Chen, J., Cook, J.L., Mankin, A.S., et al. (2008) Nucleotide biosynthesis is critical for growth of bacteria in human blood. *PLoS Pathog* **4**.

Uribe-Querol, E. and Rosales, C. (2017) Control of phagocytosis by microbial pathogens. *Front Immunol* **8**: 1–23.

Valiente, E., Lee, C., Hor, L.I, Fouz, B., and Amaro, C. (2008) Role of the metalloprotease Vvp and the virulence plasmid pR99 of *Vibrio vulnificus* serovar E in surface colonization and fish virulence. *Environ Microbiol* **10**: 328–338.

Wang, Z., Li, Y., and Lin, X. (2017) Transcriptome analysis of the Antarctic psychrotrophic bacterium P*sychrobacter* sp. in response to temperature stress. *Acta Oceanol Sin* **36**: 78–87.

Watnick, P.I., Fullner, K.J., and Kolter, R. (1999) A role for the mannose-sensitive hemagglutinin in biofilm formation by *Vibrio cholerae* El Tor. *J Bacteriol* **181**: 3606–3609.

CHAPTER 4

Cross-talk between *Vibrio vulnificus* and eel blood cells

1. Introduction

V. vulnificus is a pathogen that infects the eel through water, colonizes the gills, invades the bloodstream and internal organs and, eventually, causes death by sepsis, all this process in less than 24-48 h (Amaro *et al.*, 1995; Marco-Noales *et al.*, 2001). Among the *V. vulnificus* virulence factors, the toxin $RtxA1_3$ is considered the most relevant one, as animals infected either i.p. or by immersion with a mutant strain defective in the toxin (Δ*rtxA1*$_3$) suffer from septicemia but do not die (Lee *et al.*, 2013). This toxin belongs to the MARTX family proteins. They are secreted proteins with conserved external modules that bind to eukaryotic cell membranes and form a pore that allows the central module to be exposed to the cytosol. The formed pore is used to translocate the central module of the toxin, which harbors the effector domains that are responsible for the cytotoxicity. There are different types of MARTX that differ in number and function of their internal domains. In *V. vulnificus* seven types of MARTX and nine functional domains have been described so far (Satchell, 2011, 2015; Agarwal *et al.*, 2015). Those seven types of MARTX seem to act as cytolysins *in vitro* but differ in the mechanism of cell destruction, which probably relys on the precise domain combination (Satchell, 2015). Interestingly, *rtxA1*$_3$ (encoding the RtxA of *V. vulnificus* pv. *piscis*) is an early expressed gene with cytolytic activity on RBC and WBC (white blood cells) both *ex vivo* and *in vivo* (Valiente *et al.*, 2008a; Lee *et al.*, 2013). *Ex vivo* experiments of infection of eel blood cells at short term (3 h of incubation, moi of 1), demonstrated that Δ*rtxA1*$_3$ strain either agglutinates in presence of RBC or is phagocyted in the presence of WBC (Lee *et al.*, 2013). These results associate the toxin with protection against phagocytosis and suggest that RBC could secrete some lectin that would cause bacterial agglutination or, alternatively, a signal that would activate changes in bacterial surface and aggregation. Interestingly, *V. vulnificus* aggregates in a similar way in presence of eukaryotic bacterial predators (i.e., amoeba) as a putative mechanism of defense against phagocytosis (Marco-Noales *et al.*, 2004).

RBC from fish are nucleated cells and, therefore, they should be transcriptionally active (Glomski *et al.*, 1992; Morera and MacKenzie, 2011; Morera *et al.*, 2011). Recently, it has been suggested that RBC of several teleost fish species could have a role against certain pathogens, and therefore, be a part of the innate defenses (Morera and MacKenzie, 2011; Morera *et al.*, 2011; Pereiro *et al.*, 2017). In fact, it has already been demonstrated in rainbow trout that fish RBC are able to develop specific responses to different PAMPs and modulate an anti-viral WBC response (Morera *et al.*, 2011), a role that has also been proven in Atlantic salmon RBC (Workenhe *et al.*, 2008; Morera *et al.*, 2011). Atlantic salmon and rainbow trout RBC can also act as phagocytes and antigen presenting cells and produce and secrete cytokine-related

factors upon viral infection (Workenhe *et al.*, 2008; Dahle *et al.*, 2015; Nombela *et al.*, 2017; Nombela and Ortega-villaizan, 2018). Nevertheless, to our knowledge, fish RBC response upon bacterial infection has not been studied yet.

Interestingly, eels (European eels) stand out among other teleost fish because they contain an extraordinarily high number of RBC per ml of blood (5-8x10^9 RBC/ml in eels vs 0.5-4x10^9 RBC/ml in common carp and rainbow trout) (Morera and MacKenzie, 2011; Witeska, 2013), a number that does not diminish when eels are under stress (i.e., starvation) while it does in common carp and rainbow trout (Witeska, 2013). Taken all this into account, our first hypothesis in the present chapter was that eel RBC would participate in the immune response against *V. vulnificus*, and probably against other bacterial pathogens. Our second hypothesis was that RBC and/or WBC would respond against the aggression of $RtxA1_3$ by generating an anomalous immune response that would lead to the animal death.

To test these hypotheses, we used a transcriptomic approach known as dual-RNAseq. Basically, this approach differs from traditional approaches, such as microarray or RNAseq, in that RNA samples come from two organisms that are interacting and the discrimination of bacterial and eukaryotic transcriptomes is carried out *in silico*, mapping the sequenced reads against reference genomes, during the data analysis step (Westermann *et al.*, 2012). Although this procedure is extraordinarily powerful, it has an important restriction: the very low bacterial vs eukaryotic RNA ratio found in most of bacterial diseases makes the bacterial transcripts during the *in silico* processing of samples undetectable (taken from *in vivo* infections) unless hundreds of millions of reads are performed, which makes the *in vivo* study of host-pathogen interaction unaffordable by dual-RNAseq (Westermann *et al.*, 2012). This constraint is especially true for *V. vulnificus* as very few bacterial cells (less than 100 per animal) are needed to cause septicemia and death in eels (Valiente and Amaro, 2006; Valiente *et al.*, 2008b). Taking into account these limitations, we have set up an *ex vivo* approximation to analyze the transcriptome of both organisms in parallel by dual-RNAseq: to infect eel RBC and WBC separately, both suspended in eel serum with the wild-type strain (R99) and its derivative mutant Δ*rtxA1*$_3$, and analyze the transcriptome of both, host and pathogen, at 3 h post infection, the time at which the toxin is expressed *ex vivo* and *in vivo* (Lee *et al.*, 2013). We expected to demonstrate that RBC are innate immune cells that respond to bacterial infections and relate $RtxA1_3$ with an early and atypical immune response in which RBC and/or WBC would be involved.

2. Materials and methods

Strains, media and bacterial growth

Bacterial strains (**TABLE 1**) were routinely grown in TSA-1 and CM9. Unless clearly specified, 5 ml of media were inoculated with washed bacteria (10^5 CFU/ml) and incubated with agitation (60 rpm) at 28ºC. All the strains were stored in LB-1 plus 20% glycerol at -80ºC.

TABLE 1 | Strains and plasmids used in this study.

Strain	Description
R99	*V. vulnificus* strain isolated from a diseased eel in Spain (Roig *et al.*, 2018). This strain was selected as representative of the zoonotic clonal-complex
Δ*vvhA*	R99 Δ*vvhA* (major *V. vulnificus* hemolysin) (Murciano *et al.*, 2017)
Δ*rtxA1*$_3$	R99 Δ*rtxA1*$_3$ lacks both plasmidic and chromosomic copies of RtxA1$_3$ (Lee *et al.*, 2013)
Δ*vvhA*Δ*rtxA1*$_3$	R99 Δ*vvhA* and Δ*rtxA1*$_3$ (Murciano *et al.*, 2017)
Δ*vgrG*	R99 Δ*vgrG* (toxin associated to T6SS) (This study)
Δ*vvhA*Δ*rtxA1*$_3$Δ*vgrG*	R99 Δ*vvhA,* Δ*rtxA1*$_3$ and Δ*vgrG* (This study)
Strains and plasmids used for mutant strains construction	
pTfoX	IPTG-inducible expression plasmid pC2x6HT carrying TfoX (master regulator of *Vibrio* natural competence)
R99pTfoX	R99 carrying pTfoX plasmid (This study)
Δ*vvhA*Δ*rtxA1*$_3$pTfoX	R99 Δ*vvhA*Δ*rtxA1*$_3$ carrying pTfoX plasmid (This study)

Animal maintenance and sample collection

Eels purchased from a local farm were maintained and handled in the facilities of the SCSIE of the University of Valencia. Blood was obtained and separated into serum, RBC and WBC according to Lee *et al.*, (2013) and Callol *et al.*, (2013). Briefly, eels were anaesthetized with 0.025 mg/ml MS222 and blood from the caudal vein was extracted with heparinized syringes. Blood was centrifuged at 3,000 rpm at 4ºC for 5 min and serum and cells were separated in the supernatant and pellet, respectively (Lee *et al.*, 2013). For RBC and WBC separation, cells were washed with 1 ml of PBS and centrifuged at 3,000 rpm for 5 min and then cells were recovered and suspended in the same volume of PBS. The suspension was added to 2 ml of Ficoll®-Paque Premium (Sigma-Aldrich) and density gradient separation was carried out by centrifugation at 2,760 rpm for 30 min. Finally, RBC and WBC layers were identified by eye, collected, washed in PBS and suspended in the appropriate volume of serum (Callol *et al.*, 2013).

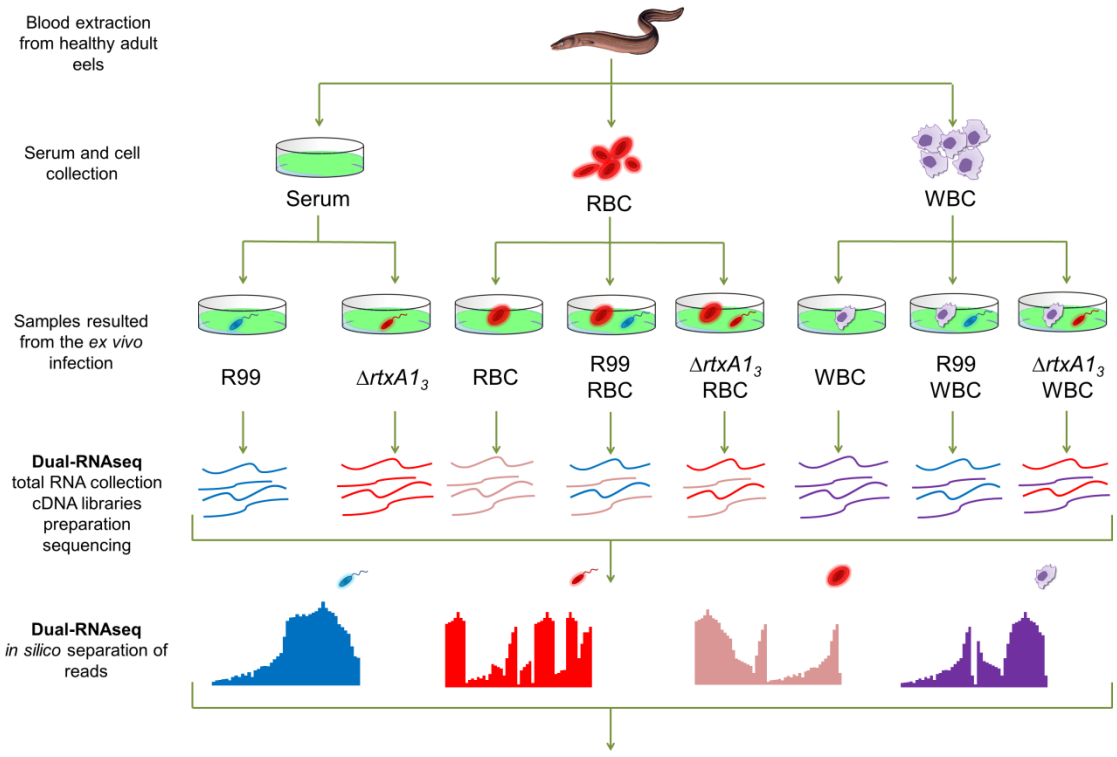

Comparisons for differential gene expression analysis

V. vulnificus	Eel
R99 vs Δ*rtxA1*$_3$	-
WBC R99 vs R99	RBC R99 vs RBC
RBC Δ*rtxA1*$_3$ vs Δ*rtxA1*$_3$	RBC Δ*rtxA1*$_3$ vs RBC
RBC R99 vs RBC Δ*rtxA1*$_3$	RBC R99 vs RBC Δ*rtxA1*$_3$
WBC R99 vs R99	WBC R99 vs WBC
WBC Δ*rtxA1*$_3$ vs Δ*rtxA1*$_3$	WBC Δ*rtxA1*$_3$ vs WBC
WBC R99 vs WBC Δ*rtxA1*$_3$	WBC R99 vs WBC Δ*rtxA1*$_3$

FIGURE 1 | Experimental design.

Dual-RNAseq analysis

The eel and *V. vulnificus* transcriptomes were analyzed in parallel following the *ex vivo* approach that is summarized in **FIGURE 1**. Briefly, a volume of 490 µl of a suspension of RBC ($1x10^7$ cells/ml) or 400 µl of a suspension of WBC ($3x10^6$ cells/ml) in fresh eel serum were seeded in 24-wells plates and infected with 10 or 100 µl, respectively, of exponentially growing *V. vulnificus* cells (R99 or Δ*rtxA1*$_3$) at a moi of 1. Co-cultures were incubated for 3 h at 28ºC. *Sample preparation*. Total RNA from 3 h co-cultures (final moi of 100, **FIGURE 1**) was purified (using RNeasy MinElute Cleanup kit [Qiagen], TURBO™ DNase [Ambion], RNeasy MinElute Cleanup kit [Qiagen] and Ribo-Zero™ Gold Removal KIt [Illumina]) and sequenced (between 1 and 30 million reads depending on the sample using NextSeq500 technology). The obtained

reads were filtered, aligned with reference genomes and differential expression analysis was performed using EdgeR packages. For further information on the data analysis see p. 66. The comparisons performed to unravel differential gene expression are summarized in **FIGURE 1**.

Bacterial genetic modification for mutant strain construction

The Δ*vgrG* and Δ*vvhA*Δ*rtxA1*$_3$Δ*vgrG* mutant strains derived from R99 strain were obtained by allelic exchange as schematized in **FIGURE 2**. *vgrG*, encoding a putative actin-cross linking toxin, was selected to be further studied because of its differential expression in one of the comparative assays performed in this chapter (see p. 180) while the triple mutant was obtained to abolish any hemolytic activity of *V. vulnificus* as VgrG, RtxA1$_3$ and VvhA can lyse RBC (Wright and Morris, 1991; Kim *et al.*, 2008; Lee *et al.*, 2013, chapter 2). To this end, 1.2 kb DNA fragments up- and downstream *vgrG* from R99 genome and trimethoprim cassette were amplified by PCR with primers vgrG-1 and vgrG-2, vgrG-3 and vgrG-4, and tp-1 and tp-2, respectively (**TABLE 2**). The resultant amplicons were purified with GeneJET Gel Extraction and DNA Cleanup Micro Kit (Thermo Scientific) and used in a nested PCR with primers vgrG-1 and vgrG-4. As primers vgrG-2 and tp-1 and tp-2 and vgrG-3 were designed containing complementary regions which allow them to hybridize between them, we obtained a DNA construction with *vgrG* deleted and trimethoprim cassette inserted (**FIGURE 2**). The resultant 2.7 kb DNA fragment from nested PCR was used to transform R99pTfoX (for Δ*vgrG* generation) or Δ*vvhA*Δ*rtxA1*$_3$pTfoX (for Δ*vvhA*Δ*rtxA1*$_3$Δ*vgrG* generation) strains. This double mutant in VvhA and RtxA1$_3$ was previously obtained by Murciano *et al.*, (2017). Transformation was performed using 10 μl of an overnight culture of R99pTfoX/Δ*vvhA*Δ*rtxA1*$_3$pTfoX and 50 μl of the nested PCR product in 500 μl of instant ocean sea salts (Thermo Scientific) supplemented with 50 mM $MgCl_2$ and 0.5 M IPTG. Transformation mixtures were incubated overnight at 28ºC in static. Then, 1 ml LB-1 was added to the mixture and, after 6 h of incubation with gentle agitation (100 rpm) at 28ºC, the mixtures were placed on LB-1 plates with trimethoprim for isolation of mutants. The isolated mutants were checked for *vgrG* deletion by PCR. Δ*vgrG*pTfoX and Δ*vvhA*Δ*rtxA1*$_3$Δ*vgrG*pToX strains were cured from pTfoX plasmid by eight consecutive passes on TSA-1 plates at 38ºC (limiting temperature) and loss of plasmid was confirmed by PCR with primers pTfoX-1 and pTfoX-2. The resultant Δ*vgrG* and Δ*vvhA*Δ*rtxA1*$_3$Δ*vgrG* strains were tested for normal growth on CM9 (results not shown).

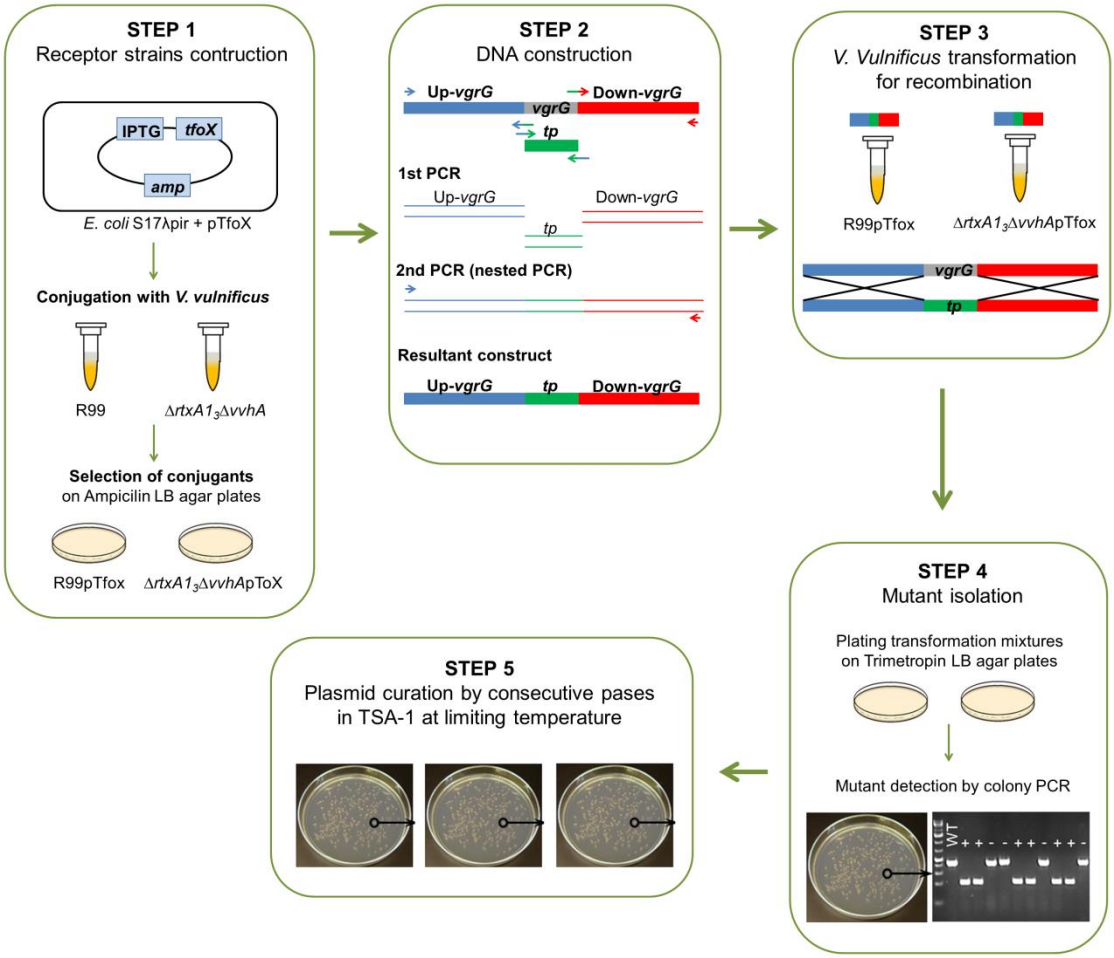

FIGURE 2 | Mutant construction protocol.

In vitro assays for T6SS characterization

Amoeba infection assays. *Dictyostelium discoideum* Ax2 Ka Vpsa-GFP strain was routinely grown on HL5c medium (Formedium, Switzerland). Infections were performed in 35 mm µ-Dish devices (IBIDI, Switzerland) containing $1x10^6$ amoeba/ml of HL5c (diluted from non-confluent amoeba cultures). After 3 h of static incubation at 30ºC, adherent amoeba were washed three times with the infection medium SorC (Sor medium (Gerisch *et al.*, 1967), supplemented with 50 µM Ca^{2+}) and infected with mid-log or stationary-phase growing (with or without iron [100 µM $FeCl_3$) bacteria (three times washed in the infection medium) at a moi of 500 in a final volume of 1 ml. Co-cultures were immediately observed with a confocal microscopy to follow amoeba toxicity due to bacterial infection. Confocal lasers scanning microscope imaging was done using a Zeiss LSM 700 inverted microscope (Zeiss, Feldbach, Switzerland). *D. discoideum* killing was assessed using short frame intervals and/or a reduced

scanning speed. In parallel, samples for RNA extraction and quantification of *vvhA, rtxA1*$_3$ and *vgrG* were taken.

Interbacterial predation assay. T6SS (type 6 secretion system)-mediated killing of *E. coli* TOP10 (kanamycin resistant) and *V. cholerae* A1552 (rifampicin resistant) preys by *V. vulnificus* was performed by co-incubation on solid LB agar surfaces. Briefly, overnight cultures were dilute 1:100 into fresh CM9 (supplemented or not with 100 µM $FeCl_3$) and grown until exponential growth phase. Then, cultures of predator (*V. vulnificus*) and prey (*V. cholerae*/*E. coli*) were mixed in a ratio 10:1. 5 µl of the mixture were place onto 0.2 sterile membrane filters on pre-warmed LB agar plates. Plates with membranes were incubated 4 h at 37ºC and then filters were removed and placed in 1 ml PBS tubes where bacterial cells were separated from filter by vortexing. Recovered preys were counted by drop plate on selective media (LB agar + 40 µM kanamycin for *E. coli* TOP10 and LB agar + 50 µM rifampicin for *V. cholerae* A1552) (Borgeaud *et al.*, 2015).

TABLE 2 | Primers used in this study.

Gene	Primer sequence	Primer
Mutant strains isolation		
1.2 Kb upstream *vgrG*	Fw: GTGCTGGAGAACAAATAGCTT Rv: GAAGCAGCTCCAGCCTACATAAACTGAACTAGGAAGAACACAT	vgrG-1 vgrG-2
1.2 Kb downstream *vgrG*	Fw: GTCGACGGATCCCCGGAATCAAAGGAGGGCACTTTCGAAC Rv: TGTTTTGGAGAAAATCACCGC	vgrG-3 vgrG-4
trimethoprim	Fw: ATTCCGGGGATCCGTCGAC Rv: TGTAGGCTGGAGCTGCTTC	tp-1 tp-2
pTfoX fragment	Fw: TGTGTGGAATTGTGAGCGGATAACA Rv: CAGGCAAATTCTGTTTTATCAG	pTfox-1 pToX-2
RT-qPCR		
vvhA	Fw: TGTTTATGGTGAGAACGGTGACA Rv: TTCTTTATCTAGGCCCCAAACTTG	
***rtxA1*$_3$**	Fw: GAGTGATGATGGGCGCTTTAC Rv: CAGCCGCGATGGATGCT	
vgrG	Fw: CAGGCAAATTCTGTTTTATCAG Rv: CATCGTCCGGCGGTTAAC	
RT-qPCR reference gene		
recA	Fw: CGCCAAAGGCAGAAATCG Rv: ACGAGCTTGAAGACCCATGTG	

Hemolysis. Eel RBC lysis was assayed as previously detailed in chapter 2 p. 110). In parallel samples for RNA extraction and quantification of *vgrG* were taken.

RT-qPCR. Samples from experiments were analyzed by RT-qPCR to calculate the expression of the selected genes (**TABLE 2**) as described in chapter 1 (p. 74). The *recA* gene was used as standard and the fold induction ($2^{-\Delta\Delta Ct}$) for each gene was calculated according to Livak and Schmittgen, (2001).

Statistical analysis. The presented data represent averages ± standard error of at least three independent experiments. Statistical analysis was performed using SPSS 19.0. The significance of the differences between averages was tested by using the unpaired Student´s t-test with a $P<0.05$. When the effects of more than two independent variables were taken into account an ANOVA analysis was performed.

3. Results

Transcriptomic results

To study host-pathogen interaction by dual-RNAseq, we mimicked the eel blood by suspending RBC or WBC in fresh serum (serum+RBC, serum+WBC) and simulated the early septicemia by infecting the blood cells samples with the pathogen (*V. vulnificus* R99 strain). We also analyzed the role of $RtxA1_3$ in this early interaction by infecting blood cell suspensions with a mutant deficient in the toxin derived from R99 (Δ*rtxA1*$_3$ (Lee *et al.*, 2013)). **FIGURE 1** summarizes all the comparisons performed to obtain the bacterial and host DEGs and **FIGURE 3** shows the number of DEGs obtained in each comparison.

Bacterial transcriptome

The effect of the deletion of *rtxA1*$_3$ in the bacterial transcriptome was analyzed by comparing R99 vs Δ*rtxA1*$_3$ transcriptomes in serum. Out of a total of 4,516 predicted ORFs (https://www.ncbi.nlm.nih.gov/genome/189?genomeassemblyid=323426), only two sugar metabolism-related genes were differentially expressed in R99 compared to Δ*rtxA1*$_3$ (**FIGURE 3**). This result confirms that the transcriptomic profiles of both strains are practically identical and that the toxin deletion does not affect the pathogen's physiology, which supports previous results (Lee *et al.*, 2013).

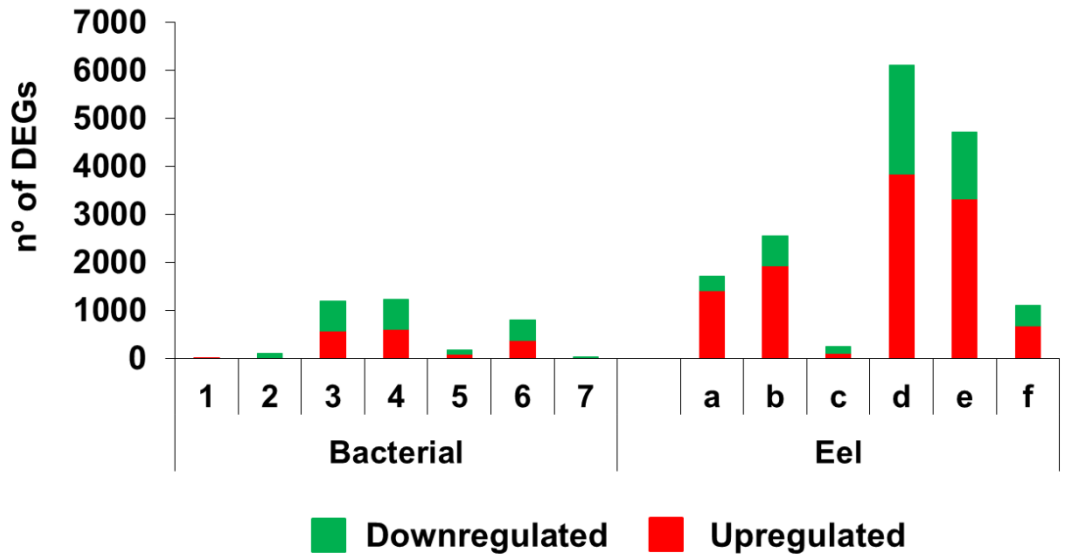

FIGURE 3 | Magnitude of response. The number of DEGs (down- and upregulated) found in each comparison is represented. Bacterial comparisons. 1: R99 vs Δ*rtxA1*$_3$ both in serum, 2: R99 in serum+RBC vs R99 in serum, 3: Δ*rtxA1*$_3$ in serum+RBC vs Δ*rtxA1*$_3$ in serum, 4: R99 in serum+RBC vs Δ*rtxA1*$_3$ in serum+RBC, 5: R99 in serum+WBC vs R99 in serum, 6: Δ*rtxA1*$_3$ in serum+WBC vs WBC in serum, 7: R99 in serum+WBC vs Δ*rtxA1*$_3$ in serum+WBC. Eel comparisons: a: R99 in serum+RBC vs serum+RBC, b: Δ*rtxA1*$_3$ in serum+RBC vs serum+RBC, c: R99 in serum+RBC vs Δ*rtxA1*$_3$ in serum+RBC, d: R99 in serum+WBC vs serum+WBC, e: Δ*rtxA1*$_3$ in serum+WBC vs serum+WBC, f: R99 in serum+WBC vs Δ*rtxA1*$_3$ in serum+WBC,

Effect of RBC on bacterial transcriptome. When RBC were added to serum, R99 strain differentially expressed *rtxA1*$_3$ (**TABLE 3**; confirmed by RT-qPCR with a fold induction of 4.03±0.96) as well as a series of genes related to LPS modification, motility, capsule biosynthesis and Flp pilus biogenesis (**TABLE 3**). Interestingly, all these DEGs belong to the bacterium iron stimulon (chapter 2) and, with the exception of those related to capsule, all of them were upregulated. This result is compatible with an increase in free iron levels (mainly as heme compounds) as a consequence of RBC lysis caused by the bacteria (percentage of eel RBC lysis in presence of *V. vulnficus*: 40±3% at 3 h post-infection). This hypothesis is strongly supported by the repression of *hutA* (**TABLE 3**), a gene encoding a heme transporter that belongs to iron stimulon and that is used as gold standard control (Pajuelo *et al.*, 2014). The amount of DEGs in presence of RBC increased even more when the comparison R99 vs Δ*rtxA1*$_3$ was performed (**FIGURE 3** and **TABLE 3**), reflecting not only a change in iron content due to RBC lysis caused by RtxA1$_3$ (percentage of RBC lysis caused by the mutant: 28±2% at 3 h post-infection) but also additional changes due to the response of RBC against non-toxic bacteria.

TABLE 3 | Effect of eel RBC and the deletion of *rtxA1$_3$* on *V. vulnificus* transcriptome. List of selected transcripts differentially expressed by *V. vulnificus* during RBC infection. *: relevant mRNAs with FC<2, however with statistically significant difference (*P<0.05*).

Gene (s)[1]	FC[2]	Putative function/process[3]
RBC[4]		
vvhA	699.4	Hemolysin (vulnificolysin)
rtxA1$_3$	491.1	RtxA1$_3$ toxin
O-antigen acetylase	2.4	LPS modification
motB	2.3	Flagellar motor rotation protein
Nitrite reductase	1.9(*)	Anaerobic respiration. NO protection
cpsA	-3.1	Capsule biosynthesis
hutA	-4.4	Heme transporter (Pajuelo *et al.*, 2014)
tadZ	-5.3	Pilus assembly
oppB	-8.2	Oligopeptide permease (Jones *et al.*, 2014)
RBC + gene deletion[5]		
vgrG	2.8	VgrG$_1$ toxin from T6SS (Pukatzki *et al.*, 2006)
***nrf* genes**	2.8-2.5	Nitrite reductase complex assembly
***flg* genes**	2.8-1.5(*)	Flagellar basal-body rod proteins
hflC	2	Stress-related response
rtxA1$_3$	1.9(*)	RtxA1$_3$ toxin
hflK	1.9(*)	Stress-related response
pndR	1.8(*)	Pyridine nucleotide disulfide oxidoreductase
hutA	1.7(*)	Heme transporter (Pajuelo *et al.*, 2014)
wzc	1.6(*)	Capsule biosynthesis (Chatzidaki-Livanis *et al.*, 2006)
sypF	1.4(*)	Capsule biosiynthesis
pilA	1.7(*)	Fimbrial protein, involved in cell adhesion
sypO	1.6(*)	Capsule biosiynthesis
katG	1.3(*)	Catalase, involved in oxidative stress resistance
smcR	1.3(*)	Master regulator of *quorum sensing*
pilP	1.3(*)	Type IV pilus biogenesis
vvhA	1.3(*)	Hemolysin (vulnificolysin)
vuuA	-1.4(*)	Vulnibactin
mshE	-1.4(*)	Pili MSHA biosynthesis
fpcrp	-1.4(*)	Fish phagocytosis and complement resistance protein (chapter 3)

[1]Identified DEGs are indicated.
[2]FC: fold change value or range of fold change values for each individual gene or for a group of related genes, respectively.
[3]Putative function for the gene and related process.
[4]Comparative R99 in serum+RBC vs R99 in serum.
[5]Comparative R99 vs Δ*rtxA1$_3$* both in serum+RBC.

Among the genes whose expression levels were higher in the wild-type strain, we highlight *vgrG* (**TABLE 3**). This gene encodes a putative toxin whose role in virulence of *V. vulnificus* has not been studied. $VgrG_1$ is an effector toxin of the T6SS in *V. cholerae* (and other gramnegative bacteria) that is secreted to destroy its main predators (aquatic amoeba in the natural environment and phagocytes in the human host) (Pukatzki *et al.*, 2006; Dong *et al.*, 2013). Therefore, *V. vulnificus* could use $VgrG_1$ together with $RtxA1_3$ and VvhA (also upregulated in presence of RBC [**TABLE 3**]) in a coordinated way to optimally attack RBC. Other genes differentially expressed by R99 (compared with Δ*rtxA1*$_3$) (**TABLE 3**) were genes involved in nitrite reductase assembly (*nrf* genes) (upregulated), a protective enzyme against NO; capsule biosynthesis (upregulated); flagellum biogenesis (upregulated); siderophore production (downregulated) and protection against complement in eel blood (*fpcrp* [chapter 2]) (downregulated) (**TABLE 3**). Again, all these genes belong to iron stimulon and its regulation was according to the results expected when two media that differ in iron content are compared (RBC high lysis vs low lysis). Summarizing, with the exception of *vgrG,* whose regulation could be more complex, given that it is only detected in the comparison R99 vs mutant strain, the rest of DEGs by *V. vulnificus* in presence of RBC are mostly controlled by iron.

Effect of WBC on the bacterial transcriptome. As expected (Lee *et al.*, 2013), R99 strain upregulated *rtxA1*$_3$ in the presence of WBC (**TABLE 4**; confirmed by RT-qPCR with a fold induction of 2.8±0.23). R99 also upregulated a series of genes clearly related to bacterial protection against oxidative stress and microcidal peptides, including several genes for DNA reparation and membrane regeneration (**TABLE 4**). All these results suggest that *V. vulnificus* detects antibacterial products secreted by WBC (ROS [reactive oxygen species] and microcidal peptides) and activates mechanisms of protection against them. Besides, R99 strain also upregulated a series of genes for sugar, iron, and magnesium transport and metabolism, a part of which is probably involved in capsular polysaccharide biosynthesis (**TABLE 4**). Among the genes downregulated a negative regulator of NO resistance together with genes related to flagellum biogenesis and *vgrG* should be highlighted. These last results suggest that WBC should produce NO and that the regulation process of the flagellum biogenesis as well as $VgrG_1$ production is a complex process that probably depends on additional factors apart from iron/heme, as WBC do not liberate hemoglobin when they are lysed (eel WBC lysis values in presence of *V. vulnficus*: 50±15% at 3 h post-infection). Accordingly, the bacterial genes upregulated in presence of WBC were not the same as those upregulated in presence of RBC (**TABLES 3** and **4**).

TABLE 4 |Effect of eel WBC and the deletion of *rtxA1₃* on *V. vulnificus* transcriptome. List of selected transcripts differentially expressed by *V. vulnificus* during WBC infection. *: relevant mRNAs with FC<2, however with statistically significant difference (*P<0.05*).

Gene[1]	FC[2]	Putative function/process[3]
WBC[4]		
rtxA1₃	3327	RtxA1$_3$ toxin
gstA	237.2	Glutathine-S transferase; resistance to oxidative stress
Permease of the drug	148.1	Resistance to microcidal peptides
recA	28.3	DNA reparation
rtxC	11.2	Cytolysin-activating lysine-acyltransferase, *rtxA1₃* activator
phhA	9	Phenylalanine-4-hydroxylase, resistance to oxidative stress
ptsN	5.6	Phosphotransferase system mannitol/fructose-specific
manA	5.6	Mannose-6-phosphate isomerase
hppD	5.6	4-hydroxyphenylpyruvate dioxygenase, resistance to oxidative stress
wecA	4.8	Undecaprenyl-phosphate N-acetylglucosaminyl 1-phosphate transferase
freA	3.7	PTS system, fructose-specific IIBC component
malI	3.6	Maltose regulon regulatory protein, repressor for maltose operon
ABC transporter	2.8	ABC-type sugar transport system, periplasmic component
rpoN	2.7	Stress related R polymerase sigma-54 factor RpoN
acrA	2.6	Acriflavin resistance, resistance to microcidal peptides
mgtA	2.5	Magnesium transporter
hsp60	2.5	Stress-related response
dsbA	2.4	Thiol:disulfide interchange protein, involved in stress response
Glycerol uptake facilitator protein	2.3	Glycerol uptake facilitator protein
Iron binding protein	2.1	(Fe-S)-binding protein
rfaG	-2	Lipopolysaccharide biosynthesis glycosyltransferase
norR	-2.3	Anaerobic nitric oxide reductase transcription regulator (repressor)
flgH	-2.3	Flagellar L-ring protein
flgN	-3.9	Flagellar biosynthesis protein
vgrG	-4.3	VgrG$_1$ toxin from T6SS (Pukatzki *et al.*, 2006)
WBC + gene deletion[5]		
rtxA1₃	2.6	RtxA1$_3$ toxin
tehA	2.5	Tellurite resistance protein, involved in stress response
phhB	1.9(*)	pterin-4-alpha-carbinolamine, resistance to oxidative stress

[1]Identified DEGs are indicated.
[2]FC: fold change value for each individual gene.
[3]Putative function for the gene and related process.
[4]Comparative R99 in serum+WBC vs R99 in serum.
[5]Comparative R99 vs Δ*rtxA1₃* both in serum+WBC.

Finally, certain stress resistance genes together with *rtxA1*$_3$ were the only ones detected in the comparison R99 vs Δ*rtxA1*$_3$. The number of DEGs found in R99 vs Δ*rtxA1*$_3$ was lower than that observed in presence of RBC, which is in accordance with the minor changes in iron levels that are produced when WBC instead of RBC are lysed (**TABLE 4**). Summarizing, *V. vulnificus* in presence of WBC activates defensive mechanisms against NO, ROS and microcidal peptides that seem to respond to other signals different from iron concentration.

Host transcriptome

Red blood cells. Transcriptomic results obtained from RBC infected with *V. vulnificus* confirm that they are transcriptionally active cells that respond to bacterial aggression (**FIGURE 3** and **TABLE 5**). First, we found transcriptomic evidence that RBC were attacked by RtxA1$_3$ as several genes related with actin rearrangements, endosomal traffic, autophagy and apoptosis activation (the toxin contains an ACD domain with actin-cross linking activity (Satchell, 2011), an ABH domain involved in autophagy and endosomal traffic and a MCF domain involved in apoptosis mediated by mitochondria (Agarwal *et al.*, 2015)) as well as a series of cellular stress-related genes were strongly activated in the presence of the wild-type strain (**TABLE 5**).

We also found evidence suggesting that RBC could participate in the eel response against *V. vulnificus* with the following roles:

i) *Antigen presenting cells*. RBC upregulated genes for several PRRs (pattern-recognition receptors) such as Tlr1 and Tlr2, both cooperating in the recognition and binding to bacterial polysaccharides (Oliveira-Nascimento *et al.*, 2012) as well as MhcI, which is involved in intracellular antigen presentation (**TABLE 5**).

ii) *Cells that respond to cytokines and active interferon production*. We found numerous evidence that RBC could participate in the innate immunity and inflammation (**TABLE 5**). Thus, multiple genes related to signaling pathways (i.e., *mapks*, *jak*/*stat*) through the activation or repression of transcriptional factors (i.e., *klf2*, *klf13*, *bcl2*) were strongly activated in presence of the wild-type strain (**TABLE 5**) (Shuai and Liu, 2003; Arthur and Ley, 2013). As a consequence of this overexpression, RBC would also be involved in production of inflammatory cytokines and related proteins. In agreement, numerous genes related to detection of the cytokines Tnf, Il18, and Il1 as well as transcriptional factors involved in the induction of the production of Infα and Infβ were upregulated, the ones related to Tnf being very strongly upregulated (**TABLE 5**). Interestingly a gene for Tnfa-type was strongly upregulated (**TABLE 5**).

iii) *Cells that regulate the innate immunity*. Some genes related to innate immunity regulation were also upregulated by RBC (i.e. *mlec*, *cd84*) with one of them, *nlrc3*, encoding an inhibitor of innate immunity, strongly upregulated (**TABLE 5**). In addition, we also found some genes involved in epigenetic modifications, such us the histone methyltransferases encoded by *carm1* and *kmt2d*, that could also contribute to modulate the immune response by silencing of genes through methylation (Medzhitov and Horng, 2009; Shakespear *et al.*, 2011).

iv) *Effector cells*. RBC strongly upregulated galectin, a soluble lectin that binds gangliosides, as well as a receptor for transferrin involved in transferrin recycling while downregulated and genes involved in coagulation (**TABLE 5**). Finally, RBC also upregulated several genes related to prostaglandin biosynthesis, which is involved in inflammation. Prostaglandins are powerful locally acting vasodilators and inhibit the aggregation of blood platelets also contributing to an inhibition of coagulation (Ricciotti *et al.*, 2011).

Curiously, although *V. vulnificus* is an extracellular pathogen, some genes related to defense against intracellular pathogens were found upregulated by RBC (i.e., *mhcI* and *irf5*) (**TABLE 5**).

TABLE 5 | Effect of *V. vulnificus* infection on eel RBC transcriptome. List of selected transcripts differentially expressed by eel RBC during R99 infection (R99 in serum+RBC vs serum+RBC). *: relevant mRNAs with FC<2, however with statistically significant difference (*P<0.05*).

Gene[1]	FC[2]	Putative function/process[3]
Stress-related genes		
stip1	784.6	Stress-induced-phosphoprotein 1
hsp40 (dnajb1)	263.2	DnaJ homolog subfamily B member 1
Cytoskeleton rearrangements		
mhcA	3411.1	Myosin-2 heavy chain. Involved in cell motility and F actin localization in eukaryotic microorganisms (Heid *et al.*, 2004)
cct8	873.1	T-complex protein 1 subunit theta. Involved in actin and tubulin folding
arhgap24	519.2	Rho GTPase-activating protein 24
git2	508.5	ARF GTPase-activating protein Git2
tbcc	504.3	Tubulin-specific chaperone C, tubulin folding pathway
lrrc16A	5	F-actin uncapping protein
exoc4	2.8	Exocyst complex component 4, actin cytoskeletal remodeling
chp1	2.4	Calcineurin B homologous protein 1, calcium-binding protein involved in different processes such as cytoplasmic microtubule organization

TABLE 5 | Continued

Gene[1]	FC[2]	Putative function/process[3]
Endosomal traffic		
unc13D	1024	Protein unc-13 homolog D. Plays a role in cytotoxic granule exocytosis
bin1	786.9	Myc box-dependent-interacting protein 1
PRRs		
tlr2-2	174.1	Toll-like receptor 2 type 2, participates in the innate immune response to microbial agents. The wide array of TLR2 ligands includes molecules with diacyl and triacylglycerol moieties, proteins and polysaccharides (Oliveira-Nascimento *et al.*, 2012)
tlr1	2.8	Receptor Toll-like receptor 1, specifically recognizes diacylated and triacylated lipopeptides. Cooperates with TLR2 to mediate the innate immune response to bacterial lipoproteins or lipopeptides
Antigen presentation		
mhcI	656.2	Major histocompatibility complex class I
ap1m1	52.7	AP-1 complex subunit mu-1. Related to MhcII
Signal transducers and transcriptional factors		
irak3	1112.8	Interleukin-1 receptor-associated kinase 3. Activates apoptosis
jak2	716.6	Tyrosine-protein kinase
traf2	696	Tnf receptor-associated factor 2, regulates activation of NF-Kβ and Jnk and plays a central role in the regulation of cell survival and apoptosis
nfkb2	431.1	Nuclear factor NF-Kβ p100 subunit, related to many biological processes such as inflammation, immunity, differentiation, cell growth, tumorigenesis and apoptosis
mapk6	175	Mitogen-activated protein kinase 6, involved in intracellular signal transduction
matk	55.7	Megakaryocyte-associated tyrosine-protein kinase, signal transduction of hematopoietic cells
stat1	21.2	Signal transducer and activator of transcription 1-alpha/beta, mediates cellular responses to interferon and cytokines
map3k8	13.9	Mitogen-activated protein kinase kinase kinase 8, Il1-mediated signaling pathway
mapk8	12	Mitogen-activated protein kinase 8
klf2	2.3	Krueppel-like factor 2
klf13	1.7	Krueppel-like factor 13
bcl2	-11.8	Inhibitor of cell death
Migration		
vash1	643.6	Vasohibin-1. Negative regulator of migration
cd97	125.6	Promotes adhesion and migration to sites of inflammation
Inflammatory cytokines and related proteins		
tnfaip3	728.6	Tnfα-induced protein 3, Involved in immune and inflammatory responses signaled by cytokines. Negative regulator of cell death
tnfrsf14	588.1	TNF receptor superfamily member 14
tnip1	331.8	Tnfaip3-interacting protein 1, involved in leukocyte integrin activation during inflammation

TABLE 5 | Continued.

Gene[1]	FC[2]	Putative function/process[3]
card11	106.9	Caspase recruitment domain-containing protein. It activates Il12
litaf	22	Lipopolysaccharide-induced Tnfα factor homolog
tnfrsf1a	17.3	Tnf receptor superfamily member 1A, cytokine-mediated signaling pathway
il18r1	14.7	Il18 receptor 1, contributes to Il18-induced cytokine production and inflammatory response
irak4	2.5	Interleukin-1 receptor-associated kinase 4, plays a critical role in initiating innate immune response against foreign pathogens in a cytokine-mediated way
irf5	2.2	Interferon regulatory factor 5, transcription factor involved in the induction of interferons InfA and InfB and inflammatory cytokines upon virus infection
tnf	-1.2(*)	Tumor necrosis factor, related to cytokine activity
Cell death		
lamp1	861.1	Lysosome-associated membrane glycoprotein 1. Involved in autophagy
traf2	694.6	Tnf receptor-associated factor 2. Involved in apoptosis
prkcbb	401.7	Protein kinase C beta type. Involved in apoptosis
rhot1a	337.8	Mitochondrial Rho GTPase 1-A. Involved in apoptosis
Regulation innate immunity		
nlrc3	508.9	Inhibition of innate immunity. Negative regulator of the innate immune response. Attenuates signaling pathways activated by TLRs and the DNA sensor Sting/Tmem173 in response to pathogen-associated molecular patterns, such as intracellular poly(dA:dT), but not poly(I:C), or in response to DNA virus infection, including that of Herpes simplex virus 1 (HSV1)
mlec	31.6	Malectin, carbohydrate-binding protein that prime innate immunity in scallops (Wang *et al.*, 2019)
cd84	4.3	SLAM family member 5, involved in the regulation and interconnection of both innate and adaptive immune response
sart1	3.5	snRNP-associated protein 1, positive regulation of cytotoxic T cell differentiation
cd276	1.6(*)	CD276 antigen, modulates T-cell-mediated immune responses
Histone modifications (epigenetics)		
sap30L	1377.7	Histone deacetylase complex subunit
carm1	718.1	Histone-arginine methyltransferase
kat7	78.5	Histone acetyltransferase
bcl6	-2.3	B-cell lymphoma 6 protein, forms complexes with different co-repressors and histone deacetylases to repress the transcriptional expression of different subsets of target genes
kmt2d	-3.2	Histone-lysine N-methyltransferase 2D
Effectors		
tactr	809	Clotting factor B. Involved in coagulation
tfr2	627.3	Transferrin receptor protein 2. Transferrin recycling
lgals3	557.6	Galectin-3. Secreted lectin in *Danio renio* (zebrafish) that binds galactosides

TABLE 5 | Continued.

Gene[1]	FC[2]	Putative function/process[3]
igf2r	508.5	Cation-independent mannose-6-phosphate receptor. Lectin
fn1	427.6	Fibronectin. Fibronectin plays a crucial role in wound healing (Lenselink, 2015). Along with fibrin, plasma fibronectin is deposited at the site of injury, forming a blood clot that stops bleeding and protects the underlying tissue.
ptgs2	301.7	Prostaglandin G/H synthase 2. Involved in inflammatory response
mmp14	3.9	Matrix metalloproteinase-14
ptges3	1.4(*)	Prostaglandin E synthase 3
f13a1	-3	Coagulation factor XIII A chain
muc5ac	-9.1	Mucin-5AC, gel-forming glycoprotein that protects the mucosa from infection and chemical damage by binding to microorganisms and particles that are subsequently removed by the mucociliary system

[1]Identified DEGs are indicated.
[2]FC: fold change value for each individual gene.
[3]Putative function for the gene and related process.

White blood cells. Although our transcriptomic results suggest that RBC contribute to the eel immune response against *V. vulnificus*, the major role in defense is probably carried out by WBC, as can be concluded by the amount and expression level of genes upregulated by this cell type in presence of the wild-type strain (**FIGURE 3** and **TABLE 6**). First, we found transcriptomic evidences that WBC were also attacked by $RtxA1_3$ since important genes related to actin rearrangements, endosomal traffic and apoptosis activation as well as a series of cellular stress-related genes and cell death were upregulated in the presence of the wild-type strain (**TABLE 6**).

Our transcriptomic results also suggest that WBC should have the following roles in the eel's response against *V. vulnificus*:

i) *Antigen presenting cells*. WBC as RBC, also upregulated *tlr2-2*, *tlr1, mhc1*, and more importantly and specifically, *mhcII* as well as *tlr7* and *tlr13* genes, encoding intracellular PRRs that usually recognize RNA (Lund *et al.*, 2004; Signorino *et al.*, 2014) (**TABLE 6**).

ii) *Cells that secrete cytokines and active interferon production*. As RBC, multiple genes related to signaling pathways (i.e., different *mapks*, *jak*/*stat*, etc.) through the activation or repression of transcriptional factors (i.e., *traf2*, *nfkb2)* were strongly activated in the presence of the wild-type strain (**TABLE 6**). These activations could be related to the upregulation of

genes for early pro-inflammatory cytokine and chemokine production such as Tnfα, Il1β, Il8, and Il17c , suggesting that WBC produce inflammatory cytokines in response to *V. vulnificus*.

iii) *Cells that regulate innate immunity*. Similarly to RBC, WBC upregulated a series of genes related to innate immunity regulation including genes involved in epigenetic modifications (**TABLE 6**). However, and in contrast to RBC, the most upregulated gene by WBC is involved in the inhibition of the inflammation process and inflammasome (*nlrc3*), suggesting that WBC are activating an unbalanced immune response (**TABLE 6**) (Martinon *et al.*, 2002; Guo *et al.*, 2015). In agreement, multiple negative regulators of Nf-Kβ (i.e. NF-Kβ inhibitor alpha, NF-Kβ repressing factor) were upregulated by WBC in the presence of the pathogen (**TABLE 6**).

iii) *Effector cells*. As RBC, WBC strongly upregulated *lgals3* as well as *tfr2* and, specifically, *vps50*, which promotes Tfr2 recycling, thus ensuring an iron restricted environment in eel blood in order to reduce the pathogen proliferation during the infection (**TABLE 6**) (Stafford and Belosevic, 2003; De Domenico *et al.*, 2008; Neves *et al.*, 2009; Liu *et al.*, 2012). Finally, WBC also upregulated *ptgs2* (**TABLE 6**).

We did not detect genes for NADPH oxidase (the major enzyme involved in the respiratory burst) and NO synthase among the DEGs by WBC, although pre-existing enzymes should be present and active as multiple bacterial genes of defenses against oxidative burst and even NO were upregulated by the pathogen (**TABLE 3**).

Curiously, although *V. vulnificus* is an extracellular pathogen, some genes related to defense against intracellular pathogens were found upregulated in common by RBC and WBC (*mhcI* and *irf5*) and only by WBC (*tlr7*). Together with *tlr7*, the overexpression of *isg20*, *irf2* and *wisp1* (Wnt-1-inducible) supports the hypothesis that $RtxA1_3$ internal domains could be recognized as a viral agent (Taniguchi *et al.*, 2001; Espert *et al.*, 2003; Chen and Lau, 2009). A plausible explanation for these results is that $RtxA1_3$, which enters into the cytoplasm of the eukaryotic cell (Satchell, 2011), may be detected in a similar way as viral proteins/RNA and, consequently, gene transcription response to intracellular infection would be activated.

Finally, the differential expression found in RBC and WBC related to *muc* genes is remarkable, encoding proteins secreted by mucosal-epithelial cells and involved in adhesion to bacteria for bacterial removal (McGuckin *et al.*, 2011; Brinchmann, 2016). Interestingly, *muc5b* was strongly upregulated by WBC while *muc5ac* was downregulated by both RBC and WBC. This result would suggest the existence of a link between mucosal and systemic immunity,

mediated mainly by WBC, which would migrate from blood to mucosal tissues. More studies are needed in order to prove this hypothesis.

TABLE 6 | Effect of *V. vulnificus* infection on eel WBC transcriptome. List of selected transcripts differentially expressed by eel WBC during R99 infection (R99 in serum+WBC vs serum+WBC). *: relevant mRNAs with FC<2, however with statistically significant difference (*P<0.05*).

Gene[1]	FC[2]	Putative function/process[3]
Stress-related genes		
hsp70	7.1	Heat shock 70 kDa protein, cellular response to stress
Cytoskeleton rearrangements		
actn4	93.4	Alpha-actinin-4, F-actin cross-linking protein which is thought to anchor actin to a variety of intracellular structures
ccdc53	2.9	WASH complex subunit 3, actin filament polymerization
Endosomal traffic		
unc13D	584.1	Protein unc-13 homolog D. Plays a role in cytotoxic granule exocytosis
bin1	1002.9	Myc box-dependent-interacting protein 1
PRRs		
tlr2-2	6.5	Toll-like receptor 2 type 2, participates in the innate immune response to microbial agents. Acts via MYD88 and TRAF6, leading to NF-Kβ activation, cytokine secretion and the inflammatory response
tlr7	4.9	Toll-like receptor 7, activated by single-stranded viral RNA. Acts via MYD88 and TRAF6, leading to NF-Kβ activation, cytokine secretion and the inflammatory response
tlr13	2	Toll-like receptor 13, an endosomal receptor that is not present in humans, is activated by an unmethylated motif present in the large ribosomal subunit of bacterial RNA (23S rRNA)
tlr1	1.5(*)	Receptor Toll-like receptor 1, specifically recognizes diacylated and triacylated lipopeptides. Cooperates with TLR2 to mediate the innate immune response to bacterial lipoproteins or lipopeptides
Antigen presentation		
mhcI	1530.7	Major histocompatibility complex class I
mhcII	1.6(*)	Major histocompatibility complex class II
Signal transducers and transcriptional factors		
jak2	2049.4	Tyrosine-protein kinase related to Il6, Il12 signaling pathways as well as IFN-alpha, IFN-beta, IFN-gamma
traf2	1616.9	Directly interacts with TNF receptors, and forms a heterodimeric complex with Traf1. This protein is required for TNF-alpha-mediated activation of MAPK8/JNK and NF-Kβ. The protein complex formed by this protein and TRAF1 interacts with the inhibitor-of-apoptosis proteins (IAPs), and functions as a mediator of the anti-apoptotic signals from TNF receptors.
nfkb2	1199.3	Nuclear factor NF-Kβ p100 subunit, related to many biological processes such as inflammation, immunity, differentiation, cell growth, tumorigenesis and apoptosis

TABLE 6 | Continued.

Gene[1]	FC[2]	Putative function/process[3]
mapk6	319.8	Mitogen-activated protein kinase 6, involved in intracellular signal transduction
isg20	131.7	Interferon-stimulated gene 20 kDa protein, interferon-induced antiviral exoribonuclease
mapk8	46.7	Mitogen-activated protein kinase 8
map3k8	28.6	Mitogen-activated protein kinase kinase kinase 8, interleukin-1-mediated signaling pathway
ptx3	18.2	Pentraxin-related protein Ptx3, plays a role in the regulation of innate resistance to pathogens and inflammatory reactions
stat1	18.2	Signal transducer and activator of transcription 1-alpha/beta, mediates cellular responses to interferon and cytokines
jun	14.9	Transcription factor AP-1, activating transcription factor
klf2	11.5	Krueppel-like factor 2
irf2	8.6	Interferon regulatory factor 2-binding protein 1, acts as a transcriptional corepressor
wisp1	6.6	Wnt1-inducible-signaling pathway protein 1, downstream regulator in the Wnt/Frizzled-signaling pathway
stat3	2.6	Signal transducer and activator of transcription
nlrc5	2.2	Nlrc5 protein, plays a role in homeostatic control of innate immunity and in antiviral defense mechanisms
klf13	-1.6(*)	Krueppel-like factor 13
Migration		
cd97	488.1	Cd97 is upregulated to promote adhesion and migration to sites of inflammation
Inflammatory cytokines and related proteins		
tnfaip3	4507.2	TNFα-induced protein 3. Involved in immune and inflammatory responses signaled by cytokines
tnfrsf14	1992	TNF receptor superfamily member 14
cxc9	26.7	C-X-C motif chemokine 9
ccl20	24.6	C-C motif chemokine 20. Acts as a ligand for Ccr. Signals through binding and activation of CCR6 and induces a strong chemotactic response and mobilization of intracellular calcium ions
tnf	18.2	Tumor necrosis factor
il8	15.2	Interleukin 8, chemokine activity. It is released in response to an inflammatory stimulus
il1β	11.6	Interleukin-1 beta, pro-inflammatory cytokine
il17c	7.5	Interleukin-17C, stimulates the production of antibacterial peptides and pro-inflammatory molecules for host defense by signaling through the NF-Kβ and MAPK pathways
irak4	4.3	Interleukin-1 receptor-associated kinase 4, plays a critical role in initiating innate immune response against foreign pathogens in a cytokine-mediated way
ccl4	3.9	C-C motif chemokine 4. It is a chemoattractant for natural killer cells, monocytes and a variety of other immune cells
tnfsf13	3.7	Tumor necrosis factor ligand superfamily member 13

TABLE 6 | Continued.

Gene[1]	FC[2]	Putative function/process[3]
irf5	3.3	Interferon regulatory factor 5, transcription factor involved in the induction of interferons IFNα and INFβ and inflammatory cytokines upon virus infection
fcrl5	3.3	Fc receptor-like protein
il18r1	3.1	Il18 receptor 1, contributes to IL18-induced cytokine production and inflammatory response
tnfrsf1a	3	Tnf receptor superfamily member 1A, cytokine-mediated signaling
cd40	2.7	Tnf receptor
tnfaip2	2.7	Tumor necrosis factor alpha-induced protein 2
il2r	2.5	Il2 receptor subunit, inflammatory response to antigenic stimulus
cxcr3	2.5	C-X-C chemokine receptor type 3
il21r	2.3	Il21 receptor, contributes to IL21-mediated positive regulation of inflammatory response
cxcr5	2.3	C-X-C chemokine receptor type 5
il6r	2	Il6 receptor, contributes to Il6 response in acute phase
tnfrsf11	2	Tumor necrosis factor receptor superfamily member 11
tnfrsf9	1.9(*)	Tumor necrosis factor receptor superfamily member 9
tnfrsf22	1.8(*)	Tumor necrosis factor receptor superfamily member 22
cxcr4	1.8(*)	C-X-C chemokine receptor type 4
il17ra	1.6(*)	Il17 receptor A, leads to induction of expression of inflammatory chemokines and cytokines
il12r	-2.4	Il12 receptor, anti-inflammatory response
il1r1	-4	Il1 receptor type 1, involved in inflammatory responses
il1r2	-5.2	Il1 receptor type 2, Reduces IL1β activities
Cell death		
dram2	2556.6	DNA damage-regulated autophagy modulator protein 2. Involved in autophagy
rnf185	729.1	E3 ubiquitin-protein ligase Rnf185. Involved in autophagy
gabarap	714.1	Gamma-aminobutyric acid receptor-associated protein. Involved in autophagy
lamp1	433.5	Lysosome-associated membrane glycoprotein 1. Involved in autophagy
ube2i	172.3	SUMO-conjugating enzyme UBC9, involved in the sumoylation of p53/TP53. Involved in apoptosis
perp	4.9	p53 apoptosis effector related to PMP-22. Involved in apoptosis
apaf1	4.2	Apoptotic protease-activating factor 1. Involved in apoptosis
cbx4	3.1	E3 SUMO-protein ligase Cbx4, involved in the sumoylation of Hnrnpk, a p53/Tp53 transcriptional coactivator. Involved in apoptosis
atg13	2.4	Autophagy-related protein 13. Involved in autophagy
aen	1.9(*)	Apoptosis-enhancing nuclease. Involved in apoptosis

TABLE 6 | Continued.

Gene[1]	FC[2]	Putative function/process[3]
Regulation innate immunity		
nlrc3	3392.2	Inhibition of innate immunity. Negative regulator of the innate immune response. Attenuates signaling pathways activated by TLRs and the DNA sensor Sting/Tmem173 in response to pathogen-associated molecular patterns, such as intracellular poly(dA:dT), but not poly(I:C), or in response to DNA virus infection, including that of Herpes simplex virus 1 (HSV1)
mlec	30.5	Malectin, carbohydrate-binding protein that prime innate immunity in scallops
cd84	11.5	SLAM family member 5, involved in the regulation and interconnection of both innate and adaptive immune response
sart1	3.9	snRNP-associated protein 1, positive regulation of cytotoxic T cell differentiation
cd276	2.4	Cd276 antigen, modulates T-cell-mediated immune responses
Histone modifications (epigenetics)		
carm1	1370	Histone-arginine methyltransferase
sap30L	1351.2	Histone deacetylase complex subunit
kat7	3.8	Histone acetyltransferase
RNA regulation		
Transposons	3956-2	More than 115 transposable-related transcripts
xrn1	14	5'-3' exoribonuclease 1
dis3l2	12.3	DIS3-like exonuclease 2
exosc3	3.2	Exosome complex component RRP40
Effectors		
tfr2	2352.5	Transferrin receptor protein 2. Transferrin recycling
lgals3	2452.4	Galectin-3, beta-galactoside-binding protein family that plays an important role in cell-cell adhesion, cell-matrix interactions, macrophage activation, angiogenesis, metastasis, apoptosis
muc5b	761.7	Mucin-5B, gel-forming glycoprotein that protects the mucosa from infection and chemical damage by binding to microorganisms and particles that are subsequently removed by the mucociliary system
ptgs2	449.8	Prostaglandin G/H synthase 2
vps50	2.9	Syndetin, promotes recycling of transferrin receptor
muc5ac	-10.5	Mucin-5AC, gel-forming glycoprotein that protects the mucosa from infection and chemical damage by binding to microorganisms and particles that are subsequently removed by the mucociliary system

[1]Identified DEGs are indicated.
[2]FC: fold change value for each individual gene.
[3]Putative function for the gene and related process.

Response of RBC and WBC against the toxin. To unravel the role of RtxA1$_3$ in triggering an atypical immune response in eels, we compared the transcriptomes of RBC and WBC infected with R99 and Δ*rtxA1$_3$* strains. Both RBC and WBC upregulated important genes for actin-cytoskeleton reparation, probably in response to the RtxA1$_3$ ACD domain activity (**TABLE 7**): *pfn1*, encoding profilin, an essential protein regulating actin polymerization in response to extracellular signals (Alkam *et al.*, 2017); *dmtn*, encoding dematin, involved in F-actin stabilization (Koshino *et al.*, 2012); *ran*, encoding a GTP-binding nuclear protein involved in actin-cytoskeleton organization (Moss *et al.*, 2009); and *actn4*, encoding α-actinin. According to what was expected, both RBC and WBC also upregulated genes related to stress protection (**TABLE 7**) as well as *mapk8*, which under stress conditions would induce the SAP/JNK signaling pathway, also upregulated, which in turn leads to programmed cell death (Dhanasekaran and Reddy, 2008). This relation between RtxA1$_3$ action and programmed cell death activation was also supported by the upregulation of *pdcd6* in WBC and *sqstm1* in RBC, both encoding proteins involved in intracellular signaling for apoptosis and autophagy (Dupont *et al.*, 2010). Moreover, we found upregulated chemokine receptors (*cmlkr1, cxcr4*) in the presence of RtxA1$_3$, which would favor a chemokine-mediated inflammatory response (*il8*), probably in a deregulated manner (**TABLE 7**). Specifically in RBC, we found upregulated *gtpbp*, encoding a signaling protein involved in the activation of degranulation, a process that can induce inflammation and impair immune cell recruitment in other pathogens (Yang *et al.*, 2019). But the most striking factor was that WBC, specifically upregulated a series of genes for transposable elements and/or retrotransposons which could be related to a specific response against RtxA1$_3$ (**TABLE 6**). Related to this, it has already been suggested that transposable elements could be activated by blood cells to interfere with antiviral immune responses in an RNAi-mediated process (Obbard *et al.*, 2009). We hypothesized that similar responses would be induced in eel blood cells by RtxA1$_3$ effector domains. Moreover, we found upregulated genes related to an antiviral response (*isg20*), which could indicate that eels initiate erroneous signaling processes directed to an antiviral immune response, which would end with animal death. Nevertheless, more studies are needed to test this hypothesis.

One interesting result was the strong upregulation of *muc5b.* MUC5B is significantly elevated in several important human pulmonary diseases such as chronic obstructive pulmonary disease and cystic fibrosis (Fahy and Dickey, 2010), as well as in idiopathic pulmonary fibrosis (Seibold *et al.*, 2011). In addition to associations with disease, human MUC5B regulates features of lung homeostasis, such as mucociliary clearance, suggesting it has a critical role in lung defense to pathogens (Roy *et al.*, 2014). This finding indicates a link

between mucosal and systemic immune response in fish as WBC are able to upregulate genes involved in mucosal immunity and suggests a relationship between Muc5B and toxin cytotoxicity that deserves to be explored in depth.

Finally, the differential response observed in cytokine production by WBC between R99 and Δ*rtxA1*$_3$ strain showed a higher expression of *il11*, *il18*, *il1β* and *il17c* in the presence of Δ*rtxA1*$_3$ strain (**TABLES 5-7**). This result is probably related to an immune-protective response against the atoxic mutant, which correlates with the survival of the eels infected with the mutant (Lee *et al.*, 2013) and suggests that the response against the toxin would be more related with a retrotransposon activation and/or antiviral mediators. *In vivo* experiments are needed to test this hypothesis.

TABLE 7 | Effect of RtxA1$_3$ deletion during *V. vulnificus* infection on eel blood cells transcriptome. List of selected transcripts differentially expressed by eel RBC and WBC during R99 infection compared to Δ*rtxA1*$_3$ infection (cells+R99 vs cells+Δ*rtxA1*$_3$). *: relevant mRNAs with FC<2, however with statistically significant difference (*P<0.05*).

Gene[1]	FC[2]	Putative function/process[3]
RBC		
tsc2	14.1	Tuberin, involved in autophagy
mapk8	3	Mitogen-activated protein kinase 8
rasal3	2.4	RAS protein activator like-3, T cell-specific Ras GTPase-activating
pfn1	2.2	Profilin-1, binds to actin and affects the structure of the cytoskeleton
cmlkr1	1.9(*)	Chemokine-like receptor 1, activation of intracellular signaling molecules affecting immune responses
gtpbp2	1.9(*)	GTP-binding protein 2, platelet degranulation
fhod3	1.8(*)	FH1/FH2 domain-containing protein 3, actin filament organization
snx12	1.6(*)	Sorting nexin 12, intracelular trafficking
dmtn	1.5(*)	Dematin, actin-cytoskeleton organization
cxcr4	1.4(*)	C-X-C chemokine receptor type 4-A, response to cytokine stimulus
sdf2	1.4(*)	Stromal cell-derived factor 2-like protein 1, regulation of apoptosis
sqstm1	1.4(*)	Sequestosome-1, regulation of apoptosis and autophagy
tspo	-1.6(*)	Translocator protein. Negative regulation of nitric oxide biosynthesis
sox4	-1.7(*)	Transcription factor SOX-4. DNA damage response, signal transduction by p53 class mediator resulting in cell cycle arresting
tnip2	-1.8(*)	Tnfaip3-interacting protein 2. Inhibitor of endothelial cell apoptosis

TABLE 7 | Continued.

Gene[1]	FC[2]	Putative function/process[3]
WBC		
muc5b	721.1	Mucin-5B, gel-forming glycoprotein that protects the mucosa from infection and chemical damage by binding to microorganisms and particles that are subsequently removed by the mucociliary system
cpne8	529.3	Copin-8, calcium mediated intracellular processes
ran	213.3	GTP-binding nuclear protein Ran, actin-cytoskeleton organization
sema4a	146.1	Semaphorin-4, regulation of cell migration
pdcd6	139.3	Programmed cell death protein 6, apoptotic signaling pathway
isg20	123.6	Interferon-stimulated gene 20 kDa protein, interferon-induced antiviral exoribonuclease
actn4	87.6	Alpha-actinin-4, F-actin cross-linking protein which is thought to anchor actin to a variety of intracellular structures
il8	5.2	Interleukin-8, chemokine released in response to inflammatory stimuli
macf1	2.3	Microtubule-actin cross-linking factor 1, plays a role in cross-linking actin to other cytoskeletal proteins
tlr7	1.7(*)	Toll-like receptor 7, activated by single-stranded viral RNA. Via MYD88 and TRAF6, leads to NF-Kβ activation and cytokine secretion
il17c	-2.5	Interleukin-17C, stimulates the production of antibacterial peptides and pro-inflammatory molecules for host defense via NF-Kβ and MAPKs
il1β	-2.6	Interleukin-1 beta, pro-inflammatory cytokine
il18	-3.3	Interleukin-18, pro-inflammatory cytokine
il11	-8	Interleukin-11, stimulates the proliferation of hematopoietic stem cells

[1]Identified DEGs (are indicated.
[2]FC: fold change value for each individual gene.
[3]Putative function for the gene and related process.

In vitro phenotypic assays for T6SS characterization

As *vgrG* was upregulated in the R99 strain when infecting eel RBC (**TABLE 3**), we hypothesized that the toxin encoded by this gene, and therefore T6SS, could be involved in cytotoxicity towards eukaryotic cells. In order to test this hypothesis, we constructed the R99 derivative strains Δ*vgrG* and Δ*vvhA*Δ*rtxA1*$_3$Δ*vgrG* and, together with mutants in the major toxins of species (Δ*rtxA1*$_3$, Δ*vvhA* and Δ*vvhA*Δ*rtxA1*$_3$), we used them in a series of *in vitro* phenotypic assays.

D. discoideum infections. Infection of the amoeba species *D. discoideum* (used as a model of eukaryotic phagocytic cell (Pukatzki *et al.*, 2006)) with R99 strain revealed that *V. vulnificus* was only able to kill amoeba when iron was present in the growing medium, independently of the growth phase (**FIGURE 4A**). Using R99 derivative mutant strains in the major toxins of the species (Δ*rtxA1*$_3$, Δ*vvhA*, Δ*vvhA*Δ*rtxA1*$_3$ and Δ*vgrG*) we determined that although RtxA1$_3$ and VvhA could have a minor role in amoeba killing, VgrG$_1$ seemed essential for toxicity towards eukaryotic cells since the Δ*vgrG* strain was highly impaired in killing when compared with the R99 strain (**FIGURE 4B**). Moreover, *vgrG* expression was upregulated under iron excess conditions during the infection of *D. discoideum* (**FIGURE 4C**), which is in accordance with the hypothesis that VgrG$_1$ and T6SS are involved in toxicity for eukaryotic cells.

Interbacterial predation. VgrG$_1$ and T6SS of *V. cholerae* and other bacterial species have been related to inter-species bacterial killing (Borgeaud *et al.*, 2015). Thus, we tested the ability of R99 and its derivative mutant strains (Δ*rtxA1*$_3$, Δ*vvhA*, Δ*vvhA*Δ*rtxA1*$_3$ and Δ*vgrG*) (grown with and without iron) to predate *V. cholerae* and *E. coli* strains (used as potential preys). In the experimental conditions we tested, *V. vulnificus* was unable to kill neither *V. cholerae* nor *E. coli* (**FIGURE 5**), and therefore we can conclude that *V. vulnificus* T6SS is not involved in interbacterial predation, at least towards the bacterial species and under the conditions we tested.

Hemolysis. *vgrG* expression is induced upon the lyses of eel RBC (apparently in a *rtxA1*$_3$ expression-dependent way, since *vgrG* expression was significantly decreased in Δ*rtxA1*$_3$ compared to the wild-type strain) and, together with RtxA1$_3$ and VvhA, VgrG$_1$ contributes to eel RBC lysis (**FIGURE 6**).

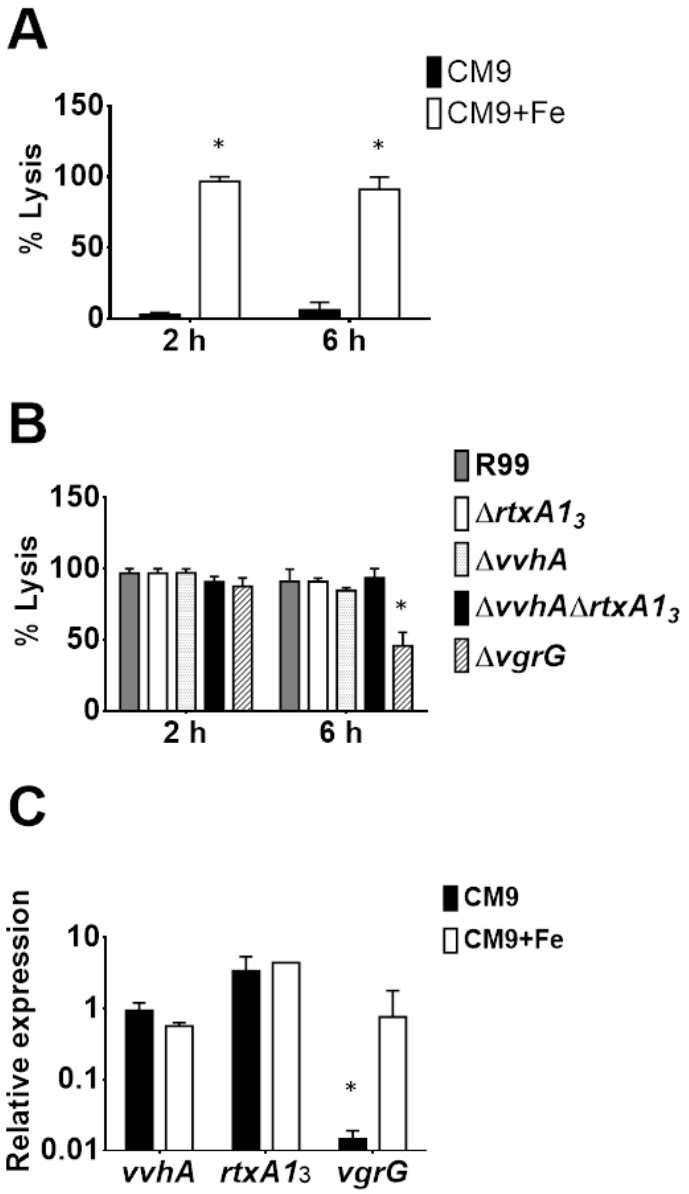

FIGURE 4 | *D. discoideum* relationship with *V. vulnificus*. A) *D. discoideum* (1x10^6 amoeba/ml) were infected with log-phase (2 h) and stationary phase (6 h) *V. vulnificus* R99 strain cultures grown without (CM9) or with iron (CM9+Fe) at a moi of 500. Percentage of lysed amoeba (% lysis) was determined at 2 h post-infection. *: significant differences in % lysis caused by R99 between growth with CM9+Fe vs in CM9 were determined using the unpaired Student´s t-test (*P<0.05*). B) *D. discoideum* (1x10^6 amoeba/ml) were infected with log-phase (2 h) and stationary phase (6 h) *V. vulnificus* R99 and its derivative mutant strains (Δ*rtxA1*$_3$, Δ*vvhA*, Δ*vvhA*Δ*rtxA1*$_3$ and Δ*vgrG*) cultures grown in CM9+Fe at a moi of 500. % lysis was determined at 2 h post-infection. *: significant differences in % lysis caused by each mutant strain vs R99 were determined using the unpaired Student´s t-test (*P<0.05*). C) *vvhA*/*rtxA1*$_3$/*vgrG* transcription (relative expression at 1 h post-infection) was determined in R99. *: significant differences between the expression when grown in CM9+Fe vs CM9 were determined for each gene using the unpaired Student´s t-test (*P<0.05*). All results are presented as average ± standard error of three independent biological experiments.

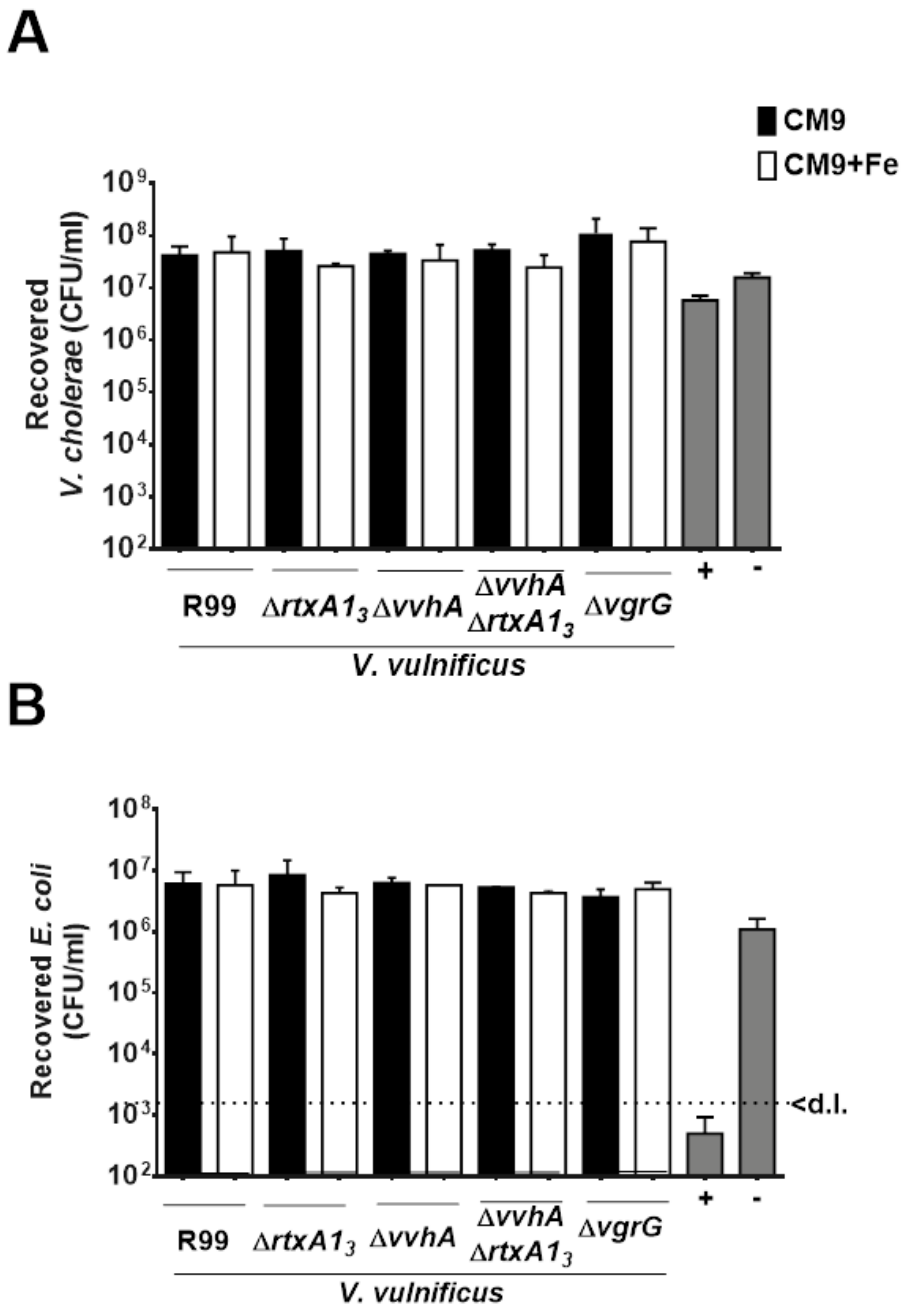

FIGURE 5 | *V. vulnificus* interbacterial predation. Interbacterial predation ability of *V. vulnificus* R99 strain and its derivative mutants (Δ*rtxA1*$_3$, Δ*vvhA*, Δ*vvhA*Δ*rtxA1*$_3$ and Δ*vgrG*) was determined towards *V. cholerae* (A) and *E. coli* (B) species. Positive (+) and negative (-) controls were included in the experiment.

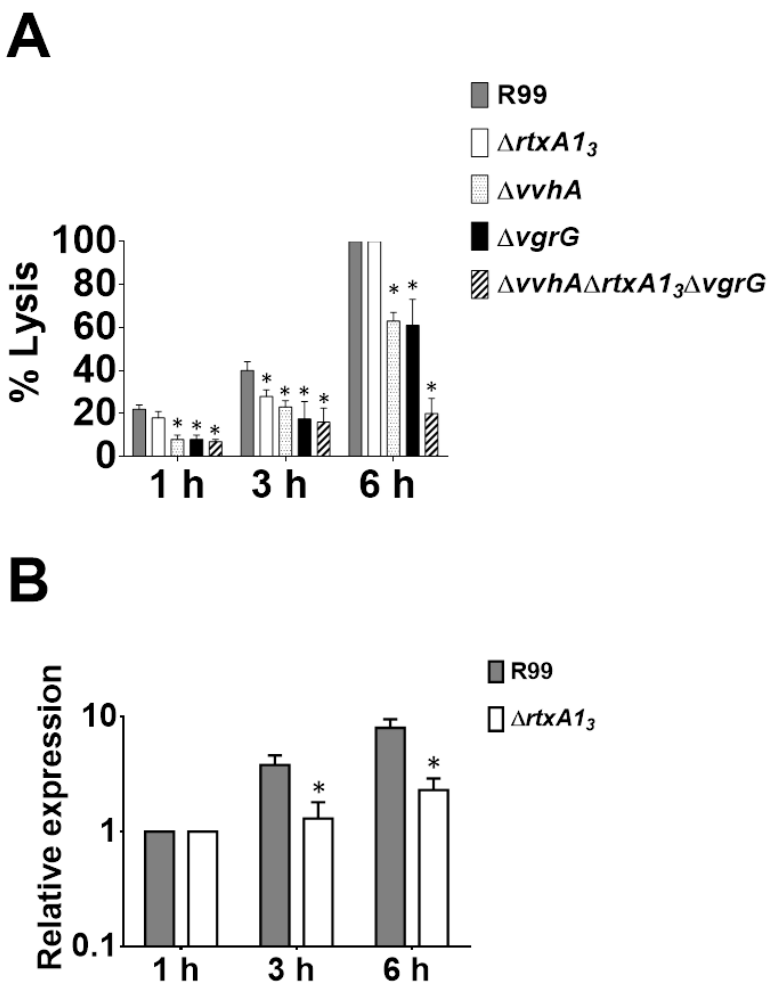

FIGURE 6 | Role of *vgrG* in hemolysis. (A) Hemolysis and (B) gene expression in artificial blood. Artificial eel blood was prepared by adding eel RBC to their respective sera ($1x10^6$ cells/ml). Then, artificial blood samples were infected with either R99 or each one of its derivative mutants (Δ*vvhA*, Δ*rtxA1*$_3$, Δ*vgrG* and Δ*vvhA*Δ*rtxA1*$_3$Δ*vgrG*) at a moi of 0.5. Hemolysis (percentage of lysed cells [% lysis]) and *vgrG* transcription (fold induction in artificial blood vs serum in R99 and Δ*rtxA1*$_3$ strains) were determined at 1, 3 and 6 h post-infection. *: significant differences in % lysis/*vgrG* expression between R99 and each mutant strain were determined using the unpaired Student´s t-test (*P<0.05*). All results are presented as average ± standard error of three independent biological experiments.

4. Discussion

The main objective of this chapter was to demonstrate that eel blood cells are involved in the generation of an atypical immune response against *V. vulnificus* in which RtxA1$_3$ would have a key role. A related objective was to demonstrate that RBC have a defensive role against bacteria. To this end, we developed an *ex vivo* model of infection that partially reproduces the cross talk between bacteria and blood cells during early septicemia, obtained the transcriptomes of host and pathogen and analyzed them by dual-RNAseq.

According to the published literature, *V. vulnificus* infects the eel through water, colonizes the gills and, almost immediately, arrives to the bloodstream, where it resists the bactericidal action of serum thanks to the production of the two proteins, Ftbp and Fpcrp, that confer resistance to the innate immunity mechanisms (Pajuelo *et al.*, 2015; chapter 2). In the early phase of vibriosis, *V. vulnificus* interacts with blood cells and attacks them by secreting $RtxA1_3$, a toxin whose production is activated by contact with eukaryotic cells (Kim *et al.*, 2008; Lee *et al.*, 2013). This toxin contains one domain with actin cross-linking activity (ADC domain) (Murciano *et al.*, 2017), two copies of a domain involved in autophagy and endosomal traffic (ABH domain), and a domain involved in apoptosis mediated by mitochondria (MCF domain) (Agarwal *et al.*, 2015). All these studies about the domain's function were performed by using mutants either derived from RtxA1 or RtxA2 (ABH and MCF) or from $RtxA1_3$ (ACD) and using culture cells from humans and/or mice (Agarwal *et al.*, 2015; Satchell, 2015; Murciano *et al.*, 2017). Our transcriptomic results revealed that eel RBC and WBC upregulated multiple genes related to cytoskeleton rearrangements, endosomal traffic and cell death by apoptosis and autophagy, thus confirming that the action of each one of the different domains is universal, regardless of the animal species affected (human or eel) or cell type (intestinal or blood), which could explain why this kind of toxins are so extended among fish and human pathogens (Satchell, 2015; Kim, 2018).

We also obtained strong evidence that eel RBC are transcriptionally active and act as immune cells in fish, not only against viral infections as it has been described (Workenhe *et al.*, 2008; Morera and MacKenzie, 2011; Morera *et al.*, 2011; Dahle *et al.*, 2015; Nombela *et al.*, 2017; Pereiro *et al.*, 2017; Nombela and Ortega-villaizan, 2018), but also against bacterial pathogens, since they upregulated multiple genes related to i) antigen recognition, processing and presentation, ii) Tnf production, and iii) cross talk with other immune cells, mainly T-lymphocytes and, probably, platelets and endothelial cells upon *V. vulnificus* infection. Our results also reveal that RBC could act as effector cells since they also upregulated genes related to lectin secretion (*lgals3*, encoding Galectin-3), prostaglandins, transferrin recycling, and blood clotting (including fibronectin). Galectin could be the lectin involved in bacterial recognition and aggregation (Baum *et al.*, 2014) as it was also highly upregulated when RBC were exposed to the mutant strain. Among the different genes related to cross talk with other immune cells we highlight the gene encoding a specific type of Tnfa that responds to LPS (*litnfa*). RBC concentration is so high in eel blood that probably small amounts of Litnfa could lead to important changes in cytokine/chemokine production. In fact, among the most highly upregulated transcripts by RBC there were also numerous genes related with response to Tnfa

(**TABLE 5**). However, this Tnf type was not revealed as differentially expressed when RBC were exposed to the toxin deficient mutant, so we cannot relate Tnfa production with toxin action. The only RBC genes that we could relate to $RtxA1_3$ activity were related to cellular toxicity, being the most strongly upregulated *tsc2*, a gene encoding a protein involved in autophagy (Tan *et al.*, 2014). This result suggests that the toxin mainly activates RBC death by autophagy and correlates with previous microscopic observation of tissues from eels infected with *V. vulnificus* (Lee *et al.*, 2013; Callol *et al.*, 2015).

On the other hand, our bacterial transcriptomic results suggest that *V. vulnificus* in turn is able to produce a change in the iron content of the environment, probably by lysing RBC and the consequent liberation of heme compounds. The resulting increase in iron concentration would explain the upregulation of the detected bacterial genes, almost all of them belonging to iron stimulon and involved in heme transport, envelope biosynthesis and pili production. Once again, and in accordance with our previous results (chapters 1 and 2), this result stresses the importance of iron as an external signal that activates bacterial processes related to survival, in this case, in the host blood. We did not detect upregulation of genes involved in bacterial defense against ROS but we detected a gene that would protect bacteria from NO (nitrite reductase), which in accordance with previous studies suggests that fish RBC do not produce ROS (Kaufmann and Dorhoi, 2016; Lim *et al.*, 2017; Uribe-Querol and Rosales, 2017), although they could produce NO, a possibility that remains to be demonstrated as we did not detect genes for NO biosynthesis among the upregulated genes by RBC.

The most relevant result found in the bacterial transcriptome was the overexpression of *vgrG*, encoding an effector toxin of T6SS (Pukatzki *et al.*, 2006), in R99 strain cultured in the presence of RBC. *V. cholerae* $VgrG_1$ has been related to cytotoxic effect towards bacterial and eukaryotic cells (phagocytes such as amoeba) (Pukatzki *et al.*, 2006, 2007; Ma *et al.*, 2009). Thus, we hypothesized that in a similar manner *V. vulnificus* $VgrG_1$ could be involved in eel RBC and amoeba lysis. To test this, we obtained the R99 derivative strain defective in *vgrG* (Δ*vgrG)* and used it in combination with mutants in the pathogen major hemolysis-related toxins (Δ*rtxA1*$_3$, Δ*vvhA*, Δ*vvhA*Δ*rtxA1*$_3$ and Δ*vvhA*Δ*rtxA1*$_3$Δ*vgrG*) in a series of experiments with RBC and amoeba. We found strong evidence that iron (among other putative signals) could activate *vgrG* transcription, and that $VgrG_1$ acts against protists and RBC but not against other bacterial cells. This result suggests that $VgrG_1$ could be involved both in resistance to *V. vulnificus* natural predators in the aquatic ecosystem and bacterial growth in blood. Therefore, $VgrG_1$ could be considered a survival factor for *V. vulnificus* both outside and inside the host. More

studies are needed to characterize the molecular action of this toxin and its relevance in vibriosis.

Regarding WBC, we found transcriptional evidences for ROS production and probably microcidal peptides to act against bacteria, but curiously, the evidence came from the bacterial transcriptome and not from WBC transcriptome as many bacterial genes related to protection against these bactericidal compounds were upregulated by *V. vulnificus* when it was incubated in the presence of WBC, regardless of wether or not the strain tested produced $RtxA1_3$. This result suggests that the genes related to ROS and microcidal peptides production are constitutively expressed by WBC and that its overexpression would require either longer incubation or the cooperation of other immune cells such as dendritic and endothelial cells or even RBC. As expected, we also found strong evidence for WBC, as we did for RBC, acting as antigen presenting cells, which is one of the functions attributed to these cell types (Miller *et al.*, 1998). In addition, WBC also upregulated *mchII* and *cd40*, confirming their role as professional antigen presenting cells. Concomitantly with the upregulation of genes encoding for TLRs and MHCs, multiple genes for cytokine production as well as response to cytokines were upregulated by WBC in the presence of *V. vulnificus*, regardless of the production or not of the toxin. Among the upregulated genes we highlight those encoding for inflammation mediators (Il1β and Il18) and interleukin receptors (Il1R, Il2R, Il6R, Il21R), TNF (Traf1, Cd40), IFN (IfnaR1) and immunoglobulins (Fc receptor like) as well as for multiple cytokines (Il8), all of them involved in inflammation. The gene encoding Il17c deserves a special mention. In humans this cytokine acts coordinately with IL6 by activating the production of the secreted mucins by epithelial and mucosal cells (Perrais *et al.*, 2002; Chen *et al.*, 2003). The role of these mucins is to trap bacteria collaborating in their clearance from mucosal tissues. Secreted mucins have a high homology degree with mucins of other animal species and, therefore, its role in innate immunity is probably the same (Brinchmann, 2016). We did not detect *il6* among the DEGs, so we analyzed the transcription of this gene in samples taken from the same experiments by RT-qPCR and found that *il6* was effectively upregulated by WBC independently from toxin action (fold induction values of 3.4±0.6 and 2.6±0.5 in wild-type and Δ$rtxA1_3$ strain, respectively). It has been demonstrated that Il6 and Il17 activate secreted mucin expression by epithelial cells through a series of pathways in which various cellular types are involved (Perrais *et al.*, 2002; Chen *et al.*, 2003; Adamo *et al.*, 2004). Interestingly, we found most of the genes involved in these pathways upregulated, suggesting that eel WBC present a similar pathway and, therefore, are able to secrete mucins in response to certain bacterial pathogens such as *V. vulnificus*.

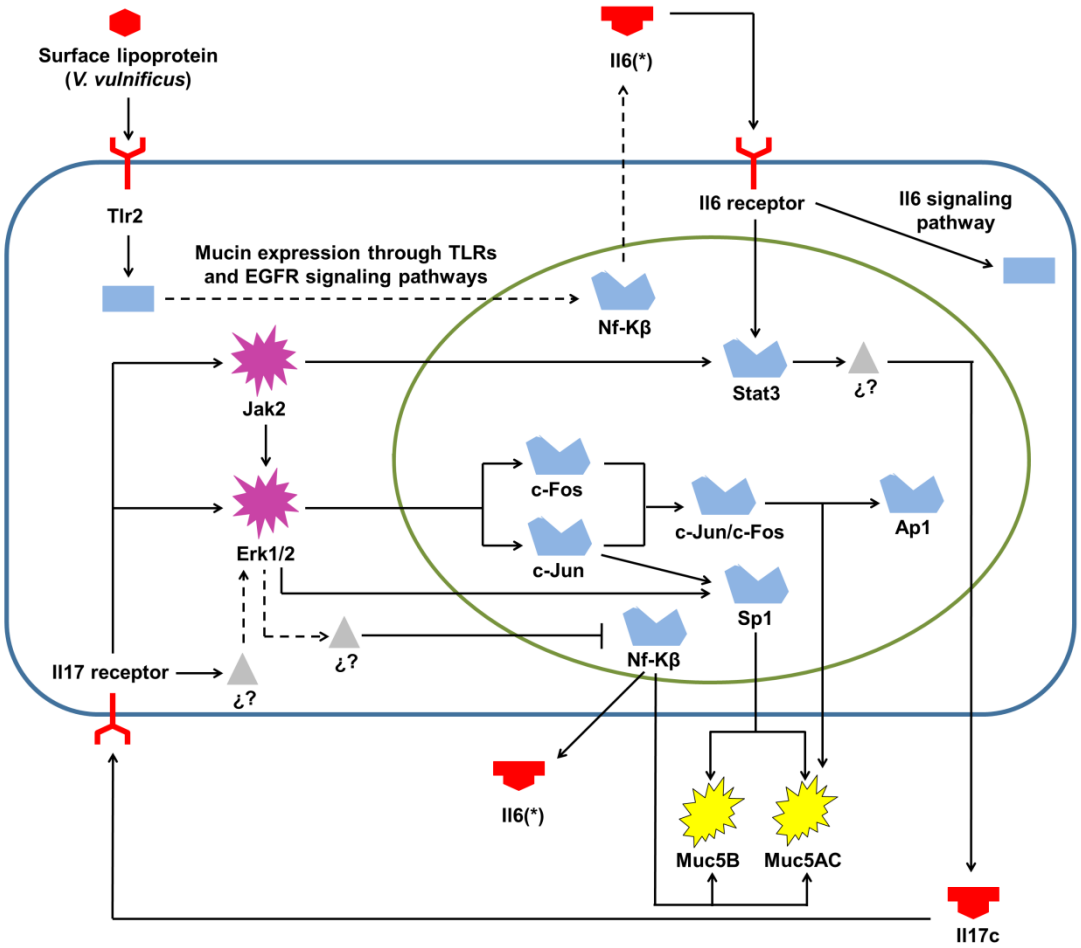

FIGURE 7 | Putative Il6 and Il17c-mediated mucin expression by eel WBC in response to *V. vulnificus* infection. *V. vulnificus* surface lipoprotein is recognized by Tlr2 in eel WBC, activating signal transduction mediated by Jak2 and Erk1/2 which in turn activate transcriptional factors such as c-Jun, c-Fos and Stat3. As a result, Muc5B and Muc5C are secreted as a defensive mechanism against the pathogen. *: *il6* expression was the only one of the represented genes that was not detected by dual-RNAseq but its transcription was confirmed by RT-qPCR. Figure adapted from Perrais *et al.*, (2002) and Chen *et al.*, (2003) based on our transcriptomic results.

FIGURE 7 schematizes this mucin production pathway as an eel WBC specific process activated in response to *V. vulnificus*. This pathway would connect mucosal with systemic immunity, a link that had already been phenotypically demonstrated in eels vaccinated against *V. vulnificus* (Esteve-Gassent *et al.*, 2003). In that study, eels vaccinated by i.p. injection were able to produce an early mucosal immunity localized in gills and intestine that protected the animals from vibriosis after *V. vulnificus* administration by water or orally, respectively (Esteve-Gassent *et al.*, 2003). Taken all this into account, this result suggests that WBC stimulated with the pathogen would be able to migrate to mucosal tissues and directly secrete mucins against the bacterium. An interesting finding related to mucins is that in our study we found that *muc5Ac* was downregulated by RBC and WBC, while *muc5B* was upregulated specifically by

WBC. MUC5AC and MUC5B gene products have been demonstrated to be the major components in human airway mucous secretions (Thai *et al.*, 2008; Bonser and Erle, 2017). In healthy adult human tissues, MUC5AC message is expressed in goblet cells of airway surface epithelium, whereas MUC5B is mainly expressed in mucous cells of submucosal gland regions (Bonser and Erle, 2017). Multiple reports have shown that MUC5B gene product is one of the major components in mucus obtained from subjects with asthma and cystic fibrosis (Chen *et al.*, 2003; Bonser and Erle, 2017). These results implicate the involvement of MUC5B in the pathogenesis of airway diseases. Precisely, *muc5B* was one of the genes whose upregulation could be associated with the toxin action (**TABLE 6d**). As a consequence, RtxA1$_3$ would induce WBC to overproduce this mucin type. The specific molecular mechanism and consequences of this activation are not known and deserve further research.

Finally, when the upregulated genes for TLRs were compared between WBC and RBC, we found that both cell types upregulate genes encoding for Tlr1 and Tlr2. Both TLRs act coordinately and recognize triacyl lipopeptides, heat-labile enterotoxins, lipomannan/lipoarabinomannan and porins (Hug *et al.*, 2018). It has been reported that Tlr2 can recognize an outer lipoprotein of *V. vulnificus* (Goo *et al.*, 2007), so probably this is the main target for the pathogen external recognition by both RBC and WBC. However, there was an important difference between RBC and WBC response against *V. vulnificus*: WBC, but not RBC, upregulated Tlrs for intracellular RNA recognition (*tlr7*). Furthermore, *tlr7* could be directly related to the toxin as it was upregulated by WBC infected with the wild-type strain but not with the mutant strain. TLR7 specifically recognizes single-stranded viral RNA in endosomes (Vidya *et al.*, 2018) and has been also related to the recognition of phagosomal, but not cytosolic, bacteria by the liberation of bacterial RNA (Eberle *et al.*, 2009; Mancuso *et al.*, 2009; Petzke *et al.*, 2009). Previous studies have demonstrated that *V. vulnificus* resists phagocytosis by macrophages because it is able to evade phagocytosis by attacking phagocytes using RtxA1$_3$ but none of the studies have reported that *V. vulnificus* can survive intracellularly in the phagosome or in the cytosol. Related to this surprising finding, we found multiple evidences for *V. vulnificus*-mediated strong activation of an immune response against RNA based on the production of exonucleases for RNA. Surprisingly, we also found a high number of transposable elements and retrotransposons upregulated in WBC infected with R99 strain. These observations lead us to speculate with the possibility of the involvement of RtxA1$_3$ in the generation of a retrotransposon storm which would favor the atypical immune response that lead to the rapid eel's death after *V. vulnificus* infection (Abubaker *et al.*, 2014; Dubnau, 2019). Nevertheless more studies are needed to prove this hypothesis.

In conclusion, our *ex vivo* study validates the transcriptomic dual-RNAseq approach to analyze host-pathogen interactions from both pathogen and host perspectives at the same time. In this sense, our results shed some light on the active role that nucleated RBC from teleost fish could play in the immune response against bacterial infections as well as the ability of an intracellular bacterial toxin, $RtxA1_3$, to induce a differential immune response in host cells in order to produce an atypical response, probably based on retrotransposon or RNAi rapid RNA regulation, which cause animal death. Moreover, we have identified that the recently described T6SS through $VgrG_1$ is putatively involved in eel RBC cytotoxicity. However, this kind of studies should be considered as exploratory experiments and should be combined with further *in vivo* or *in vitro* studies to confirm or better support the obtained results.

5. References

Abubaker, S., Abdalla, S., Mahmud, S., and Wilkie, B. (2014) Antiviral innate immune response of RNA interference. *J Infect Dev Ctries* **8**: 804–810.

Adamo, R., Sokol, S., Soong, G., Gomez, M.I., and Prince, A. (2004) *Pseudomonas aeruginosa* flagella activate airway epithelial cells through asialoGM1 and toll-like receptor 2 as well as toll-like receptor 5. *Am J Respir Cell Mol Biol* **30**: 627–634.

Agarwal, S., Kim, H., Chan, R.B., Williamson, R., Cho, W., et al. (2015) Autophagy and endosomal trafficking inhibition by *Vibrio cholerae* MARTX toxin phosphatidylinositol-3-phosphate-specific phospholipase A1 activity. *Nat Commun* **6**.

Alkam, D., Feldman, E.Z., Singh, A., and Kiaei, M. (2017) Profilin1 biology and its mutation, actin(g) in disease. *Cell Mol Life Sci* **74**: 967–981.

Amaro, C., Biosca, E.G., Fouz, B., Alcaide, E., and Esteve, C. (1995) Evidence that water transmits *Vibrio vulnificus* Biotype 2 infections to eels. *Appl Environ Microbiol* **61**: 1133–1137.

Arthur, J.S.C. and Ley, S.C. (2013) Mitogen-activated protein kinases in innate immunity. *Nat Rev Immunol* **13**: 679.

Baum, L.G., Garner, O.B., Schaefer, K., and Lee, B. (2014) Microbe-host interactions are positively and negatively regulated by galectin-glycan interactions. *Front Immunol* **5**: 1–8.

Bonser, L. and Erle, D. (2017) Airway mucus and asthma: The role of MUC5AC and MUC5B. *J Clin Med* **6**: 112.

Borgeaud, S., Metzger, L.C., Scrignari, T., and Blokesch, M. (2015) The type VI secretion system of *Vibrio cholerae* fosters horizontal gene transfer. *Science (80-)* **347**: 63–68.

Brinchmann, M.F. (2016) Immune relevant molecules identified in the skin mucus of fish using -omics technologies. *Mol Biosyst* **12**: 2056–2063.

Callol, A., Pajuelo, D., Ebbesson, L., Teles, M., MacKenzie, S., and Amaro, C. (2015) Early steps in the European eel (*Anguilla anguilla*)-*Vibrio vulnificus* interaction in the gills: role of the RtxA1{3} toxin. *Fish Shellfish Immunol* **43**: 502–509.

Callol, A., Roher, N., Amaro, C., and MacKenzie, S. (2013) Characterization of PAMP/PRR interactions in European eel (*Anguilla anguilla*) macrophage-like primary cell cultures. *Fish Shellfish Immunol* **35**: 1216–1223.

Chatzidaki-Livanis, M., Jones, M.K., and Wright, A.C. (2006) Genetic variation in the *Vibrio vulnificus* group 1 capsular polysaccharide operon. *J Bacteriol* **188**: 1987–1998.

Chen, C.C. and Lau, L.F. (2009) Functions and mechanisms of action of CCN matricellular proteins. *Int J Biochem Cell Biol*.

Chen, Y., Thai, P., Zhao, Y.H., Ho, Y.S., DeSouza, M.M., and Wu, R. (2003) Stimulation of airway mucin gene expression by interleukin (IL)-17 through IL-6 paracrine/autocrine loop. *J Biol Chem* **278**: 17036–17043.

Dahle, M.K., Wessel, Ø., Timmerhaus, G., Nyman, I.B., Jørgensen, S.M., Rimstad, E., et al. (2015) Transcriptome analyses of Atlantic salmon (*Salmo salar* L.) erythrocytes infected with piscine orthoreovirus (PRV). *Fish Shellfish Immunol* **45**: 780–790.

Dhanasekaran, D.N. and Reddy, E.P. (2008) JNK signaling in apoptosis. *Oncogene* **27**: 6245–6251.

De Domenico, I., McVey Ward, D., and Kaplan, J. (2008) Regulation of iron acquisition and storage: Consequences for iron-linked disorders. *Nat Rev Mol Cell Biol* **9**: 72–81.

Dong, T.G., Ho, B.T., Yoder-Himes, D.R., and Mekalanos, J.J. (2013) Identification of T6SS-dependent effector and immunity proteins by Tn-seq in *Vibrio cholerae*. *Proc Natl Acad*

Sci U S A **110**: 2623–2628.

Dubnau, J. (2019) The retrotransposon storm and the dangers of a Collyger´s genome. *Curr Opin Genet Dev* **49**: 95–105.

Dupont, N., Temime-Smaali, N., and Lafont, F. (2010) How ubiquitination and autophagy participate in the regulation of the cell response to bacterial infection. *Biol Cell* **102**: 621–634.

Eberle, F., Sirin, M., Binder, M., and Dalpke, A.H. (2009) Bacterial RNA is recognized by different sets of immunoreceptors. *Eur J Immunol* **39**: 2537–2547.

Espert, L., Degols, G., Gongora, C., Blondel, D., Williams, B.R., Silverman, R.H., et al. (2003) ISG20, a new interferon-induced RNase specific for single-stranded RNA, defines an alternative antiviral pathway against RNA genomic viruses. *J Biol Chem* **278**: 16151–16158.

Esteve-Gassent, M.D., Nielsen, M.E., and Amaro, C. (2003) The kinetics of antibody production in mucus and serum of European eel (*Anguilla anguilla* L.) after vaccination against *Vibrio vulnificus*: Development of a new method for antibody quantification in skin mucus. *Fish Shellfish Immunol* **15**: 51–61.

Fahy, J. V and Dickey, B.F. (2010) Airway mucus function and fysfunction. *N Engl J Med* **363**: 2233–2247.

Gerisch, G., Luderitz, O., and Ruschmann, E. (1967) Antibodies promoting phagocytosis of bacteria by amoebae. *Zeitschrift fur Naturforschung* **22**: 109.

Glomski, C.A., Tamburlin, J., and Chainani, M. (1992) The phylogenetic odyssey of the erythrocyte. III. Fish, the lower vertebrate experience. *Histol Histopathol* **7**: 501–528.

Goo, S.Y., Soo, H.Y., Kim, W.H., Lee, K.H., and Park, S.J. (2007) *Vibrio vulnificus* IlpA-induced cytokine production is mediated by toll-like receptor 2. *J Biol Chem* **282**: 27647–27658.

Guo, H., Callaway, J.B., and Ting, J.P.Y. (2015) Inflammasomes: Mechanism of action, role in disease and therapeutics. *Nat Med* **21**: 677–687.

Heid, P.J., Wessels, D., Daniels, K.J., Gibson, D.P., Zhang, H., Voss, E., et al. (2004) The role of myosin heavy chain phosphorylation in *Dictyostelium* motility, chemotaxis and F-actin

localization. *J Cell Sci* **117**: 4819–4835.

Hug, H., Mohajeri, M.H., and La Fata, G. (2018) Toll-like receptors: Regulators of the immune response in the human gut. *Nutrients* **10**: 11–13.

Jones, M.M., Johnson, A., Koszelak-Rosenblum, M., Kirkham, C., Brauer, A.L., Malkowski, M.G., et al. (2014) Role of the oligopeptide permease ABC transporter of *Moraxella catarrhalis* in nutrient acquisition and persistence in the respiratory tract. *Infect Immun* **82**: 4758–4766.

Kaufmann, S.H.E. and Dorhoi, A. (2016) Molecular Determinants in Phagocyte-Bacteria Interactions. *Immunity* **44**: 476-491.

Kim, B.S. (2018) The modes of action of MARTX toxin effector domains. *Toxins (Basel)* **10**.

Kim, Y.R., Lee, S.E., Kook, H., Yeom, J.A., Na, H.S., Kim, S.Y., et al. (2008) *Vibrio vulnificus* RTX toxin kills host cells only after contact of the bacteria with host cells. *Cell Microbiol* **10**: 848–862.

Koshino, I., Mohandas, N., and Takakuwa, Y. (2012) Identification of a novel role for dematin in regulating red cell membrane function by modulating spectrin-actin interaction. *J Biol Chem* **287**: 35244–35250.

Lee, C.T., Pajuelo, D., Llorens, A., Chen, Y.H., Leiro, J.M., Padrós, F., et al. (2013) MARTX of *Vibrio vulnificus* biotype 2 is a virulence and survival factor. *Environ Microbiol* **15**: 419–432.

Lenselink, E.A. (2015) Role of fibronectin in normal wound healing. *Int Wound J* **12**: 313–316.

Lim, J.J., Grinstein, S., and Roth, Z. (2017) Diversity and versatility of phagocytosis: Roles in innate immunity, tissue remodeling, and homeostasis. *Front Cell Infect Microbiol* **7**: 1–12.

Liu, Y., Yu, S., Chai, Y., and Zhu, Q. (2012) Transferrin gene expression in response to LPS challenge and heavy metal exposure in roughskin sculpin (*Trachidermus fasciatus*). *Fish Shellfish Immunol* **32:** 223–229.

Livak, K.J. and Schmittgen, T.D. (2001) Analysis of relative gene expression data using real-time quantitative PCR and. *Methods* **25**: 402–408.

Lund, J.M., Alexopoulou, L., Sato, A., Karow, M., Adams, N.C., Gale, N.W., et al. (2004) Recognition of single-stranded RNA viruses by Toll-like receptor 7. *Proc Natl Acad Sci U S A* **101**: 5598–5603.

Ma, A.T., McAuley, S., Pukatzki, S., and Mekalanos, J.J. (2009) Translocation of a *Vibrio cholerae* type VI secretion effector requires bacterial endocytosis by host cells. *Cell Host Microbe* **5**: 234–243.

Mancuso, G., Gambuzza, M., Midiri, A., Biondo, C., Papasergi, S., Akira, S., et al. (2009) Bacterial recognition by TLR7 in the lysosomes of conventional dendritic cells. *Nat Immunol* **10**: 587–594.

Marco-Noales, E., Biosca, E.G., Rojo, C., and Amaro, C. (2004) Influence of aquatic microbiota on the survival in water of the human and eel pathogen *Vibrio vulnificus* serovar E. *Environ Microbiol* **6**: 364–376.

Marco-Noales, E., Milán, M., Fouz, B., Sanjuán, E., and Amaro, C. (2001) Transmission to eels, portals of entry, and putative reservoirs of *Vibrio vulnificus* Serovar E (Bioype 2). *Appl Environ Microbiol* **67**: 4717–4725.

Martinon, F., Burns, K., and Tschopp, J. (2002) The Inflammasome: A molecular platform triggering activation of inflammatory caspases and processing of proIL-β. *Mol Cell* **10:** 417–426.

McGuckin, M.A., Lindén, S.K., Sutton, P., and Florin, T.H. (2011) Mucin dynamics and enteric pathogens. *Nat Rev Microbiol* **9**: 265–278.

Medzhitov, R. and Horng, T. (2009) Transcriptional control of the inflammatory response. *Nat Rev Immunol* **9**: 692–703.

Miller, N., Wilson, M., Bengtén, E., Stuge, T., Warr, G., and Clem, W. (1998) Functional and molecular characterization of teleost leukocytes. *Immunol Rev* **166**: 187–197.

Morera, D. and MacKenzie, S.A. (2011) Is there a direct role for erythrocytes in the immune response? *Vet Res* **42**: 89.

Morera, D., Roher, N., Ribas, L., Balasch, J.C., Doñate, C., Callol, A., et al. (2011) Rna-seq reveals an integrated immune response in nucleated erythrocytes. *PLoS One* **6**: e26998.

Moss, D.K., Wilde, A., and Lane, J.D. (2009) Dynamic release of nuclear RanGTP triggers TPX2-dependent microtubule assembly during the apoptotic execution phase. *J Cell Sci* **122**: 644–655.

Murciano, C., Lee, C.T., Fernández-Bravo, A., Hsieh, T.H., Fouz, B., Hor, L.I., et al. (2017) MARTX toxin in the zoonotic serovar of *Vibrio vulnificus* triggers an early cytokine storm in mice. *Front Cell Infect Microbiol* **7**: 1–19.

Neves, J.V., Wilson, J.M., and Rodrigues, P.N.S. (2009) Transferrin and ferritin response to bacterial infection: The role of the liver and brain in fish. *Dev Comp Immunol* **33**: 848–857.

Nombela, I., Carrion, A., Puente-Marin, S., Chico, V., Coll, J., Ortega-villaizan, M.M., et al. (2017) Infectious pancreatic necrosis virus triggers antiviral immune response in rainbow trout red blood cells , despite not being infective. *F1000Research* **6**: 1968.

Nombela, I. and Ortega-Villaizan, M.M. (2018) Nucleated red blood cells : Immune cell mediators of the antiviral response. *PLoS Pathog* **14**: e1006910.

Obbard, D.J., Gordon, K.H.J., Buck, A.H., and Jiggins, F.M. (2009) The evolution of RNAi as a defence against viruses and transposable elements. *Philos Trans R Soc B Biol Sci* **364**: 99–115.

Oliveira-Nascimento, L., Massari, P., and Wetzler, L.M. (2012) The role of TLR2 in infection and immunity. *Front Immunol* **3**.

Pajuelo, D., Lee, C.T., Roig, F.J., Hor, L.I., and Amaro, C. (2015) Novel host-specific iron acquisition system in the zoonotic pathogen *Vibrio vulnificus*. *Environ Microbiol* **17**: 2076–2089.

Pajuelo, D., Lee, C.T., Roig, F.J., Lemos, M.L., Hor, L.I., and Amaro, C. (2014) Host-nonspecific iron acquisition systems and virulence in the zoonotic serovar of *Vibrio vulnificus*. *Infect Immun* **82**: 731–744.

Pereiro, P., Romero, A., Díaz-Rosales, P., Estepa, A., Figueras, A., and Novoa, B. (2017) Nucleated teleost erythrocytes play an Nk-lysin- and autophagy-dependent role in antiviral immunity. *Front Immunol* **8**: 1–15.

Perrais, M., Pigny, P., Copin, M.C., Aubert, J.P., and Van Seuningen, I. (2002) Induction of MUC2 and MUC5AC mucins by factors of the epidermal growth factor (EGF) family is mediated

by EGF receptor/Ras/Raf/extracellular signal-regulated kinase cascade and Sp1. *J Biol Chem* **277**: 32258–32267.

Petzke, M.M., Brooks, A., Krupna, M.A., Mordue, D., and Schwartz, I. (2009) Recognition of *Borrelia burgdorferi*, the Lyme disease spirochete, by TLR7 and TLR9 induces a Type I IFN response by human immune cells. *J Immunol* **183**: 5279–5292.

Pukatzki, S., Ma, A.T., Revel, A.T., Sturtevant, D., and Mekalanos, J.J. (2007) Type VI secretion system translocates a phage tail spike-like protein into target cells where it cross-links actin. *Proc Natl Acad Sci U S A* **104**: 15508–15513.

Pukatzki, S., Ma, A.T., Sturtevant, D., Krastins, B., Sarracino, D., Nelson, W.C., et al. (2006) Identification of a conserved bacterial protein secretion system in *Vibrio cholerae* using the *Dictyostelium* host model system. *Proc Natl Acad Sci U S A* **103**: 1528–1533.

Ricciotti, E., A, G., and Fitzgerald (2011) Prostaglandins and inflammation. *Arter Thromb Vasc Biol* **31**: 986–1000.

Roig, F.J., González-Candelas, F., Sanjuán, E., Fouz, B., Feil, E.J., Llorens, C., et al. (2018) Phylogeny of *Vibrio vulnificus* from the analysis of the core-genome: Implications for intra-species taxonomy. *Front Microbiol* **8**: 1–13.

Roy, M.G., Livraghi-butrico, A., Fletcher, A.A., Melissa, M., Evans, S.E., Boerner, R.M., et al. (2014) Muc5b is required for airway defense. *Nature* **505**: 412–416.

Satchell, K.J.F. (2015) Multifunctional-autoprocessing repeats-in-toxin (MARTX) Toxins of *Vibrios*. *Microbiol Spectr* **3**.

Satchell, K.J.F. (2011) Structure and function of MARTX toxins and other large repetitive RTX proteins. *Annu Rev Microbiol* **65**: 71–90.

Seibold, M.A., Brown, K.K., Loyd, J.E., Fingerlin, T.E., Ph, D., Bois, R.M., et al. (2011) A common MUC5B promoter polymorphism and pulmonary fibrosis. *N Engl J Med* **364**: 1503–1512.

Shakespear, M.R., Halili, M.A., Irvine, K.M., Fairlie, D.P., and Sweet, M.J. (2011) Histone deacetylases as regulators of inflammation and immunity. *Trends Immunol* **32:** 335–343.

Shuai, K. and Liu, B. (2003) Regulation of JAK-STAT signalling in the immune system. *Nat Rev Immunol* **3**: 900–911.

Signorino, G., Mohammadi, N., Patanè, F., Buscetta, M., Venza, M., Venza, I., et al. (2014) Role

of toll-like receptor 13 in innate immune recognition of group B Streptococci. *Infect Immun* **82**: 5013–5022.

Stafford, J.L. and Belosevic, M. (2003) Transferrin and the innate immune response of fish: Identification of a novel mechanism of macrophage activation. *Dev Comp Immunol* **27**: 539–554.

Tan, S.H., Shui, G., Zhou, J., Shi, Y., Huang, J., Xia, D., et al. (2014) Critical role of SCD1 in autophagy regulation via lipogenesis and lipid rafts-coupled AKT-FOXO1 signaling pathway. *Autophagy* **10**: 226–242.

Taniguchi, T., Ogasawara, K., Takaoka, A., and Tanaka, N. (2001) IRF Family of transcription factors as regulators of host defens. *Annu Rev* **19**: 623–655.

Thai, P., Loukoianov, A., Wachi, S., and Wu, R. (2008) Regulation of airway mucin gene expression. *Annu Rev Physiol* **70**: 405–429.

Uribe-Querol, E. and Rosales, C. (2017) Control of phagocytosis by microbial pathogens. *Front Immunol* **8**: 1–23.

Valiente, E. and Amaro, C. (2006) A method to diagnose the carrier state of *Vibrio vulnificus* serovar E in eels: Development and field studies. *Aquaculture* **258**: 173–179.

Valiente, E., Lee, C.T, Hor, L.I, Fouz, B., and Amaro, C. (2008a) Role of the metalloprotease Vvp and the virulence plasmid pR99 of *Vibrio vulnificus* serovar E in surface colonization and fish virulence. *Environ Microbiol* **10**: 328–338.

Valiente, E., Lee, C.T., Lamas, J., Hor, L., and Amaro, C. (2008b) Role of the virulence plasmid pR99 and the metalloprotease Vvp in resistance of *Vibrio vulnificus* serovar E to eel innate immunity. *Fish Shellfish Immunol* **24**: 134–141.

Vidya, M.K., Kumar, V.G., Sejian, V., Bagath, M., Krishnan, G., and Bhatta, R. (2018) Toll-like receptors: Significance, ligands, signaling pathways, and functions in mammals. *Int Rev Immunol* **37**: 20–36.

Wang, M.Q., Wang, B.J., Liu, M., Jiang, K.Y., and Wang, L. (2019) The first identification of a malectin gene (CfMal) in scallop *Chlamys farreri*: Sequence features and expression profiles. *Invertebr Surviv J* **16**: 25–33.

Westermann, A.J., Gorski, S.A., and Vogel, J. (2012) Dual RNA-seq of pathogen and host. *Nat*

Rev Microbiol **10**: 618–630.

Witeska, M. (2013) Erythrocytes in teleost fishes: a review. *Zool Ecol* **23**: 275–281.

Workenhe, S.T., Kibenge, M.J.T., Wright, G.M., Wadowska, D.W., Groman, D.B., and Kibenge, F.S.B. (2008) Infectious salmon anaemia virus replication and induction of alpha interferon in Atlantic salmon erythrocytes. *Virol J* **5**.

Wright, A.C. and Morris, J.G. (1991) The extracellular cytolysin of *Vibrio vulnificus*: inactivation and relationship to virulence in mice. *Infect Immun* **59**: 192–198.

Yang, J., Wang, J., Zhang, X., Qiu, Y., Yan, J., Sun, S., et al. (2019) Mast cell degranulation impairs pneumococcus clearance in mice via IL-6 dependent and TNF-α independent mechanisms. *World Allergy Organ J* **12**.

CHAPTER 5

Transcriptomic study performed *in vivo*: eel vibriosis and the role RtxA1$_3$ of *Vibrio vulnificus* in eel virulence

1. Introduction

V. vulnificus pv. *piscis* is the etiological agent of the warm-water vibriosis, an acute hemorrhagic septicemia that occurs as outbreaks of high mortality rate in eel and tilapia farms cultured in brackish water over 22ºC (Biosca *et al.*, 1991; Amaro *et al.*, 1995, 2015). *V. vulnificus* has caused multiple closures of eel farms across Europe due to its high infectivity when fish are grown in the environmental conditions that favor the pathogen survival and multiplication (Austin and Austin, 2012; Amaro *et al*., 2015). *V. vulnificu*s infects fish through water or by contact. It is attracted by gill and/or intestinal mucus, colonizes the epithelium and causes a local inflammation that allows it to invade the bloodstream and produce the septicemia (Amaro *et al.*, 1995; Marco-Noales *et al.*, 2001; Callol *et al.*, 2015a). The zoonotic serotype uses the gills as the main portal of entry into the bloodstream and therefore, the earliest immune response against *V. vulnificus* infection in eels is triggered in gills and later in blood. Callol *et al.*, (2015a,b) performed a transcriptomic and phenotypic study on the eel immune response against the pathogen at the gills. They associated the toxin $RtxA1_3$ with endothelial cells destruction, dendritic cells migration and local inflammation at the gills, a complex process that could be involved in the early steps of the eel vibriosis. Later, Murciano *et al.*, (2017) analyzed the immune response in the blood of mice and related $RtxA1_3$ with an early cytokine storm and death by sepsis. Therefore, we hypothesized that $RtxA1_3$ could also be involved in death by sepsis in fish. This hypothesis is also based on previous: eels infected with a mutant strain deficient in $RtxA1_3$ (Δ*rtxA1*$_3$) are colonized externally and internally by the pathogen but do not die (Lee *et al.*, 2013). In the previous chapter, we performed an *ex vivo* approximation to relate $RtxA1_3$ with an abnormal immune response by RBC and/or WBC. Our main results evidenced an active role of RBC in eel immunity against *V. vulnificus* in terms of pathogen recognition and antigen processing as well as production of some immune effectors, while WBC activated an atypical immune response in which many retrotransposons were involved. Nevertheless, we did not find evidence of any $RtxA1_3$-related cytokine storm. Our main conclusion was that $RtxA1_3$ would be involved in a retrotransposon storm at cell level, which could be related with a new and non-described mechanism of toxin-related sepsis.

The aim of this chapter was to confirm the results obtained *ex vivo* by performing an *in vivo* analysis of the eel immune response in blood against *V. vulnificus.* To this end, we infected eels by immersion with either the wild-type strain (R99) or Δ*rtxA1*$_3$ and analyzed the eel transcriptome in blood (B [whole blood], RBC and WBC) at short and medium term (3 and 12 h post-infection) by using the same eel-specific microarray platform enriched in immune genes used by Callol *et al.*, (2015b).

2. Materials and methods

Bacterial strains and growth conditions

The R99 strain and its derivative mutant Δ*rtxA1*$_3$ (defective in both plasmidic and chromosomic copies of *rtxA1*$_3$ gene (Lee *et al.*, 2013)) were used in this study. Both strains were routinely grown in TSA-1 and LB-1 with gentle agitation (100 rpm) at 28ºC for 24 h to reach a concentration of 10^9 CFU/ml for bath infection. Bacterial concentration was checked before and after bath infection by the drop plate method. Strains were stored in LB-1 plus 20% glycerol at -80ºC.

Animal maintenance, *in vivo* bacterial challenge and sample collection

Eels from a local farm of around 150 g of body weight were maintained and handled in the facilities of the SCSIE of the University of Valencia. Eels were distributed into 2 groups of 24 animals plus a control group of 12 animals and infected as previously described by Callol *et al.*, (2015b). Briefly, eels were infected by bath immersion with R99 or Δ*rtxA1*$_3$ strains at the R99 LD_{50} dose for eels ($1x10^7$ CFU/ml). After 1 h of immersion, eels were transferred into new tanks, containing clean water (1% NaCl, at 28°C) and kept under constant conditions until sampling. Eels were randomly sampled at 0, 3 and 12 h post-infection in 3 groups of 4 individuals each for the collection of B, RBC and WBC. The control group consisted of eels that had been treated as challenged with PBS.

2 ml of blood (1 ml for B samples and 1 ml for RBC and WBC samples) were obtained and separated into blood cells fractions according to Lee *et al.*, (2013) and Callol *et al.*, (2013), as specified in the previous chapter (p. 173). The collected blood and cells were treated with 1 ml of NucleoZOL (Macherey-Nagel) to preserve RNA and stored at -80ºC until use.

Microarray analysis

The experimental design for analysis with eel-microarray platform (Callol *et al.*, 2015b) and the performed comparisons are shown in **FIGURE 1**. *Sample preparation*. Total RNA from B, RBC and WBC obtained at 0, 3 and 12 h post-infection was extracted, labelled and hybridized on microarray as detailed in p. 65. *Data analysis*. The data were analyzed using the GeneSpring 14.5 GX software as described in p. 65 and the comparisons performed to describe transcriptomic profile differences along the infection for each strain and cell type, and also between strains and cell type, are summarized in **FIGURE 1**.

Microarray validation by RT-qPCR

The same RNA samples used for the microarray analysis were analyzed by RT-qPCR as specified in chapter 1 (p. 74) (primers listed in **TABLE 1**). The *act* gene was used as standard and the fold induction ($2^{-\Delta\Delta Ct}$) for each gene was calculated according to Livak and Schmittgen, (2001).

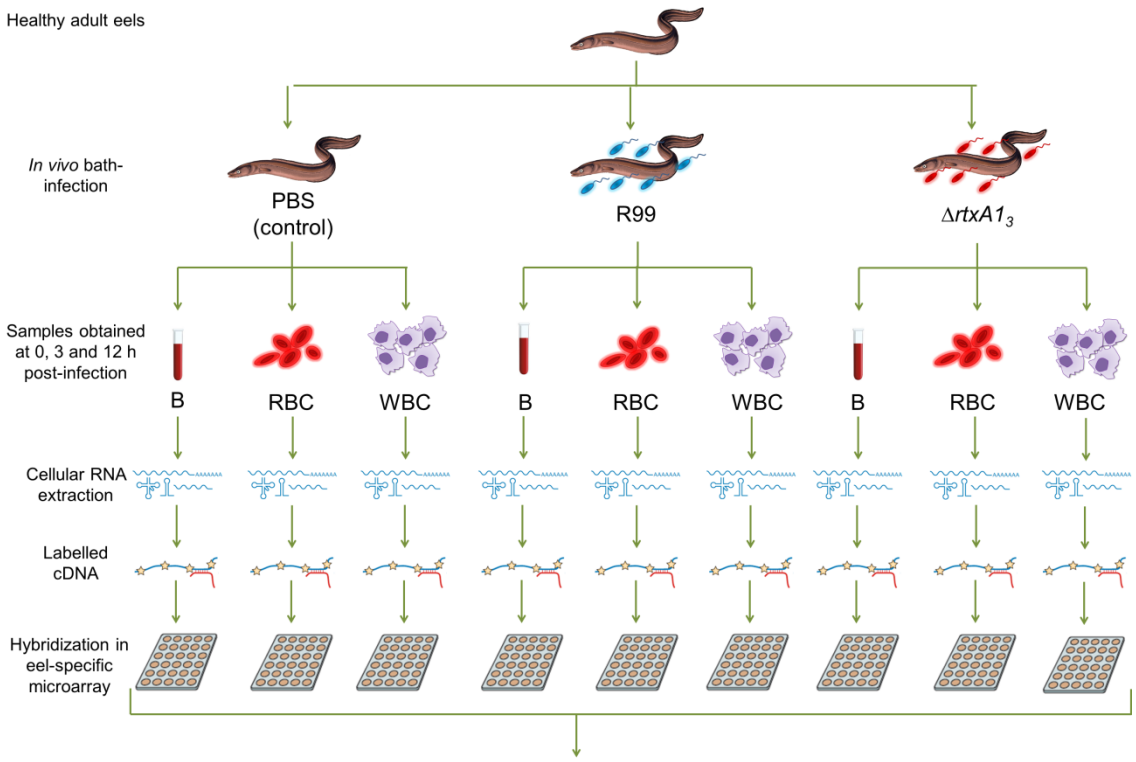

Comparisons and data analysis	B	RBC	WBC
	R99 3 h vs 0 h	R99 3 h vs 0 h	R99 3 h vs 0 h
	R99 12 h vs 0 h	R99 12 h vs 0 h	R99 12 h vs 0 h
	Δ*rtxA1*$_3$ 3 h vs 0 h	Δ*rtxA1*$_3$ 3 h vs 0 h	Δ*rtxA1*$_3$ 3 h vs 0 h
	Δ*rtxA1*$_3$ 12 h vs 0 h	Δ*rtxA1*$_3$ 12 h vs 0 h	Δ*rtxA1*$_3$ 12 h vs 0 h

FIGURE 1 | Experimental design.

TABLE 1 | Primers used in the study and microarray validation. Comparison of fold change values obtained by array and RT-qPCR. In case of RT-qPCR, results were obtained using *act* as the reference gene and the fold induction ($2^{-\Delta\Delta Ct}$) for each gene was calculated.

Gene	Primer sequence	Sample	FC[1]	
			Array	RT-qPCR
Microarray validation by RT-qPCR				
bcl2	Fw: CGCGAGATGACGTCCCAGGT Rv: GGCTTGGAAGGGCTGTGTGC	B R99 3 h vs 0 h	1.52 (=)	1.87 (=)
Il1β	Fw: CGTGCCACGTGCTCTCACAA Rv: CAGCACCACCTAGTGGCTGAACC	B R99 12 h vs 0 h	17.16 (++)	23.44 (++)
Il10	Fw: GAGCACCTACGGCTGTCACG Rv: TCCAGCTCTCTCTAGGCTTTG	B Δ*rtxA1*$_3$ 3 h vs 0 h	-1.79 (=)	-1.61 (=)
Il1β	See above	B Δ*rtxA1*$_3$ 12 h vs 0 h	3.47 (+)	2.28 (+)
Il10	See above	RBC R99 3 h vs 0 h	4.94 (+)	5.24 (+)
bcl2	See above	RBC R99 12 h vs 0 h	-1.9 (=)	-1.03 (=)
Il10	See above	RBC Δ*rtxA1*$_3$ 12 h vs 0 h	-1.81 (=)	-1.01 (=)
p53	Fw: GGAAGGCTGCACGGATCTC Rv: TCTGCGAACCAGCGATTAAA	WBC R99 3 h vs 0 h	9.91 (+)	7.77 (+)
casp3	Fw: CCCAGCCCCTTGAATGTTT Rv: CGCGATGGCACAGACGTA	WBC R99 12 h vs 0 h	1.65 (=)	4.87 (+)
Il18	Fw: CCAGCCACAATGCCGTGTTC Rv: CCCAGCCTCTCTCAGCACCA	WBC Δ*rtxA1*$_3$ 3 h vs 0 h	3.2 (+)	2.49 (+)
Il10	See above	WBC Δ*rtxA1*$_3$ 12 h vs 0 h	-1.81 (=)	-1.21 (=)
Reference gene				
act	Fw: GACATGGAGAAGATCTGGCA Rv: GTCAGGATCTTCATGAGGTAGTC			

[1]FC: fold change values qualitative classification: =, -2<X<2; +, 2≤X<10; ++, 10≤X<25.

3. Results

Transcriptomic response in eel blood during the early vibriosis

To simulate the natural vibriosis and analyze the host reaction against *V. vulnificus* during the early stages of disease, we infected eels by the natural infection route with the wild-type strain and analyzed their transcriptome in the blood by using an eel-specific microarray that is enriched in immune genes (Callol *et al.*, 2015b). To find out the role of each one of the two main cell types in the blood, RBC and WBC, both kinds of cells were separated and their transcriptomes were analyzed independently. Finally, we also included a sample of whole blood (without separating by cell type [B]) to get an overview of the general immune response

in the eel blood. The transcriptomic response was also analyzed in time. Thus, we selected as sampling points, 0h, 3h post-infection (the time at which the toxin is expressed *in vivo* (Lee *et al.*, 2013) and the cytokine storm is activated in mice (Murciano *et al.*, 2017), and 12 h post-infection (the average time at which eels start to die (Amaro *et al.*, 2015)). **FIGURE 1** summarizes all the comparisons performed and **TABLE 1** provides a comparison between fold change values obtained by hybridization with the eel-specific microarray and by RT-qPCR.

The global PCA analysis explained around 70% of the total variance and highlighted a differential response in the eels infected with the wild-type strain and the eels infected with the mutant strain, with the exception of the RBC samples from eels infected with R99 strain at 0 h post-infection, which grouped with those from eels infected with Δ*rtxA1*$_3$, and WBC samples from eels infected with R99 at 3 h post-infection that grouped with those from eels infected with Δ*rtxA1*$_3$ (**FIGURE 2**).

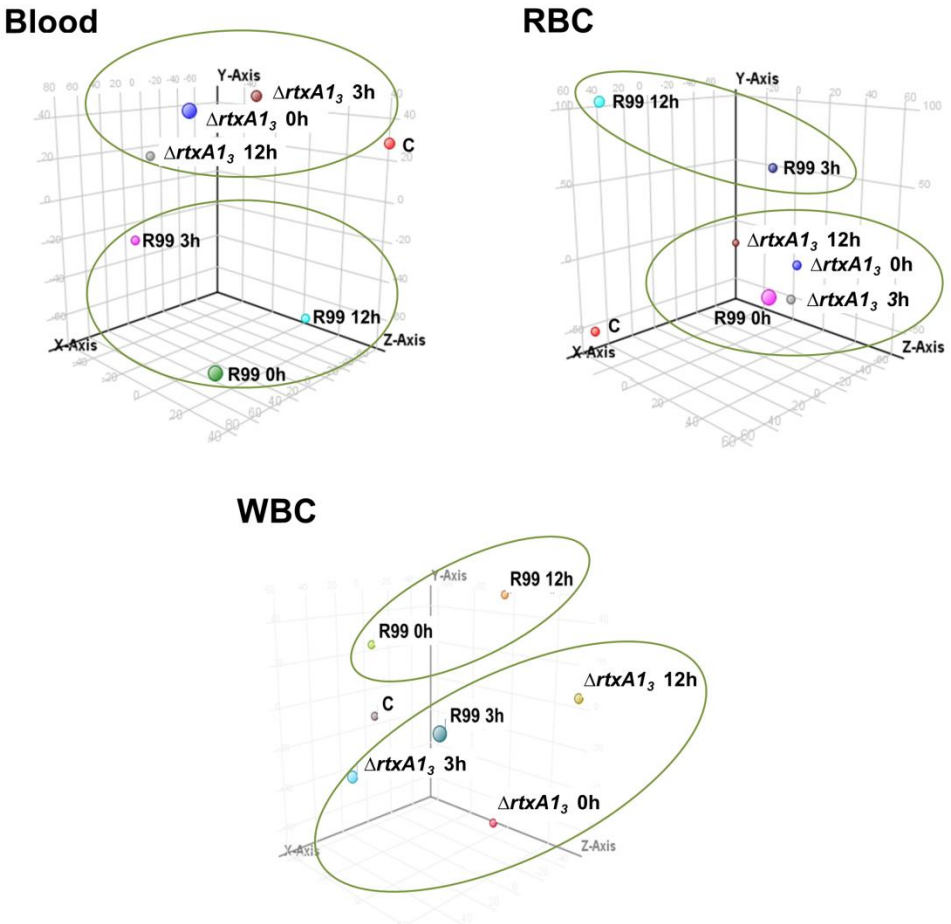

FIGURE 2 | PCA 3-D plot of the eel samples. *Blood samples grouped by challenge.* Three principal components are represented, PC1 on X-axis (40.97%), PC2 on Y-axis (20.99%) and PC3 on Z-axis (13.61%). *RBC samples grouped by challenge.* Three principal components are represented, PC1 on X-axis (36.67%), PC2 on Y-axis (29.14%) and PC3 on Z-axis (10.92%). *WBC samples grouped by challenge.* Three principal components are represented, PC1 on X-axis (45.11%), PC2 on Y-axis (21.69%) and PC3 on Z-axis (12.37%).

The number of DEGs in response to the infection with the wild-type strain was significantly higher than that obtained in response to the mutant Δ*rtxA1*$_3$, independently of the sampling time and type of sample analyzed (**FIGURE 3**). Similarly to the results we obtained *ex vivo* at 3 h post-infection (chapter 4), the highest number of DEGS corresponded to the WBC samples from eels infected with the wild-type strain. However, this strong immune response exhibited by WBC was followed by a dramatic decrease in the number of DEGs at 12 h post-infection (**FIGURE 3**). By contrast, RBC cells showed a response against the wild-type strain that resulted sustained among the analyzed times of vibriosis, while they practically did not react against the mutant strain defective in RtxA1$_3$. Both results suggest that i) RBC are the main cell target for the pathogen *in vivo* and ii) WBC either are mostly destroyed at short term or react against the pathogen at short term and later come back to a silent state. This last hypothesis seems to be the most plausible since WBC also produced a strong immune response at 12 h vs 3 h post-infection, mainly dominated by the downregulation of many of the genes that were upregulated at 3 h vs 0 h post-infection (data not shown). Curiously, the number of DEGs detected in the B samples was much lower than that found in RBC and WBC samples (**FIGURE 3**), and at short term was higher in the eels infected with the mutant strain than in the eels infected with the wild-type strain. This apparent anomaly is probably due to the cell heterogeneity in the blood, which could negatively affect data normalization and be the cause of a high removal of outliers.

TABLE 2 shows a selection of detected DEGs in the B, RBC, and WBC samples. First, we highlight the high number of DEGs that could be related to the toxin, most of which were also found in the experiments performed *ex vivo* (chapter 4): i.e., DEGs related to attack to cytoskeletal, probably linked to the action of the ACD domain; and genes related to apoptosis activation, probably linked to the MCF domain (Satchell, 2011, 2015; Murciano *et al.*, 2017). Second, we also found evidence suggesting that eels responded to the pathogen by activating mechanisms for its removal, such as phagocytosis and autophagy. Phagocytosis could be probably activated through the upregulation of complement-related genes and mannose receptors (lectins) by RBC and WBC, while autophagy could be probably induced by the upregulation of *nod1* (both by RBC and WBC) and some *atg* genes (*atg9* and *atg2* by WBC) (Travassos *et al.*, 2010) (**TABLE 2**). Consequently, a strong activation of WBC death mechanisms was produced, either through apoptosis or autophagy pathways, a response that was exclusively produced by WBC but not by RBC. Third, RBC and WBC also upregulated several genes for PRRs as well as *mhc* I and II, curiously WBC only upregulating *mhcI* (**TABLE 2**). This result supports those obtained in chapter 4 and suggests that RBC act as professional antigen

presenting cells. Among the genes for PRRs, we found upregulated those for TLRs and NLRs (Nod-like receptors) (both of them families of key molecules for PAMPs recognition and mediation in the activation of the immune responses) as early as 3 h post-infection (**TABLE 2**). In case of TLRs, genes for extra- and intra-cellular TLRs were among the DEGs in all the analyzed samples (B, RBC and WBC), although the WBC response was higher in terms of both number of DEGs and fold change values. This result suggests that WBC are more important as antigen presenting cells than RBC. In particular, for extracellular TLRs we detected as DEGs *tlr20a* and *tlr21* that were commonly upregulated by RBC and WBC, while *tlr6* and *tlr5s* (encoding the soluble form of Tlr5) were only overexpressed by WBC. Similarly, encoding intracellular TLRs we detected *tlr3* commonly overexpressed by both blood cell types, while *tlr7* was only upregulated by WBC (as it was previously determined *ex vivo* [chapter 4]) and *tlr9b* was only upregulated by RBC. As we had observed in chapter 4, an intracellular response for *V. vulnificus* recognition was evidenced by the upregulation of PRRs and MHC (*mhcI*) related to intracellular pathogen recognition and processing.

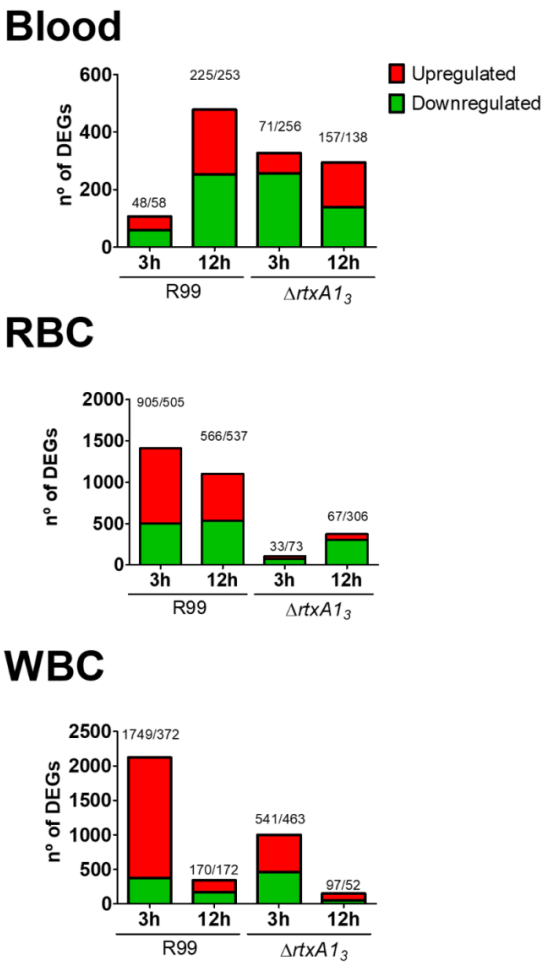

FIGURE 3 | Magnitude of the eel immune response against *V. vulnificus* represented as the number of DEGs in blood, RBC and WBC samples. Bars represent total DEGs (sum of upregulated [red] and downregulated [green] DEGs) at each sampling point against 0 h group of each condition.

Interestingly, cathepsins B, L and S are probably produced by blood cells during the infection as the genes encoding for those cathepsins were detected among the upregulated DEGs when blood samples (B, RBC or WBC) were analyzed (**TABLE 2**). Cathepsins are a group of lysosomal proteases that have a key role in cellular protein turnover, including antigen processing, and they are associated with TLR signaling pathways in blood cells to the point that their inhibition blocks Tlr3, Tlr7 and Tlr9-mediated responses (Matsumoto *et al.*, 2008).

We also found evidence for an early upregulation of different pathways that activate a pro-inflammatory response. Thus, *nod1* and *nod3*, which are involved in the NLR signaling pathway, were upregulated both by RBC and WBC. Nod1 and Nod3 activate Nf-Kβ and Mapks signaling pathways (both also upregulated at 3 h post-infection [**TABLE 2**]), which in turn, enhance transcription of pro-inflammatory cytokines (Kim *et al.*, 2016). We also observed a differential expression of some elements of the Jak/Stat signaling pathway, which are also involved in the activation of the immune response (Rawlings *et al.*, 2004). Specifically, we found *socs3* in B samples (upregulated), *c-myc* and *jak1* in RBC (downregulated) and *stat3* in WBC (upregulated). An important negative regulator of all these activations was found overexpressed by WBC, *nlrc3* (Schneider *et al.*, 2013) (upregulated at 3 h post-infection, both here and in the previous *ex vivo* experiment [chapter 4]), which is suggestive of an attempt to counteract the inflammatory response. In any case, one of the most upregulated genes in B samples was *il1β*, the main marker of inflammation.

In parallel, we found DEGs for the activation of an antibacterial response in all the analyzed samples: i.e., multiple genes encoding complement proteins, factor B, transferrin, hepcidin (the hormone that controls iron sequestering), BPI (an antibacterial protein that is mostly produced by neutrophils), NO, etc. Some of these proteins could be responsible not only for attacking the pathogen but also for endothelial damage. In fact some genes for endothelial regeneration (angiogenesis) were also overexpressed (**TABLE 2**).

Taken into account all the results explained above, we conclude that both RBC and WBC could act together in response to *V. vulnificus* in order to rapidly recognize the pathogen and mediate the innate immune response against the bacterium leading to Nf-Kβ activation, cytokine secretion and inflammatory response through different signaling pathways (Rebl *et al.*, 2010; Kim *et al.*, 2016). Accordingly, a high upregulation of signal transduction-related genes was found, which in turn led to the production of pro-inflammatory cytokines and chemokines (**TABLE 2**). Remarkably, and contrary to our previous *ex vivo* obtained results (chapter 4), we found evidence for cytokine and chemokine production not only by WBC but

also by RBC, and as a result, also in B samples. Therefore, genes encoding for Il1β and its receptors as well as for Il8 precursor were found highly upregulated in the blood at 12 h post-infection, while those encoding for Il6 receptor together with those for Il17, Il12β and Il20 were upregulated by RBC and WBC at 3 h post-infection (**TABLE 2**). All these results are compatible with an early cytokine storm. In addition, genes encoding for progranulin and granulin were upregulated in B samples of eels infected with *V. vulnificus* (**TABLE 2**). Granulins are multifunctional proteins produced as a result of proteolytic processing of progranulin (Bateman *et al.*, 1990) which enhance pro-inflammatory cytokines (such as Tnf and Il8) (Park *et al.*, 2011). Our results are in accordance with previous studies which proved that *V. vulnificus* induces progranulin and granulin production in tilapia which in turn results in the upregulation of C3, Tnf, Il21 and Il8 (Wu *et al.*, 2019). In parallel, a few genes encoding for anti-inflammatory cytokine receptors (i.e., *il10*) were also found early upregulated by RBC and WBC in response to *V. vulnificus* infection (**TABLE 2**). This last observation could be interpreted as an attempt of the organism to control the cytokine storm and reestablish the homeostasis.

As a consequence of the high inflammatory response caused by the bacterium, multiple septicemic markers were upregulated by the cells present in B samples. For instance, genes markers for disseminated intravascular coagulation such as those encoding the coagulation factor VIII, and genes encoding leukotrienes, prostaglandins, and cyclooxygenase considered as markers of the acute phase of disease (Peters-Golden *et al.*, 2005; Gómez-Abellán and Sepulcre, 2016; Wang *et al.*, 2016) were upregulated in B samples at 12 h post-infection. Leukotrienes enhance leukocyte accumulation, phagocyte capacity for microbial ingestion and killing, and generation of other pro-inflammatory mediators (Peters-Golden *et al.*, 2005), while cyclooxygenases potentiate prostaglandin production (Smith *et al.*, 2000) which in turn leads to immune response induction (Gómez-Abellán and Sepulcre, 2016). Moreover, genes for metalloproteinases such as *mmp9*, encoding metalloproteinase 9, involved in endothelial damage (Pedersen *et al.*, 2015), were among the most upregulated genes in B samples in response to vibriosis at 12 h post-infection (**TABLE 2**). Gene duplications are a significant contribution to fish genomes diversity and therefore duplicated or multi-copy genes are commonly found in fish genomes (Palti, 2011). In this sense, more than one copy of *mmp9* was upregulated in eel B samples during vibriosis, highlighting its importance in sepsis.

In addition, several histone-related genes (acetylases, deacetylases, and methyltransferases among others) were found as DEGs (both up and downregulated) mainly by RBC (**TABLE 2**). This, could be associated to an epigenetic response probably related to modulation of the immune response by silencing of genes through methylation (Medzhitov

and Horng, 2009; Shakespear *et al.*, 2011). This observation supports our previous results (chapter 4) and therefore deserves further investigation in future studies.

It is remarkable that here, in a similar way as in the previous *ex vivo* study, we found evidence of a link between systemic and mucosal immunity since *muc2A*, encoding a mucolipin, was upregulated at 3 h post-infection by both RBC and WBC (**TABLE 2**).

The most remarkable result was that we found a gene for a systemic RNAi strongly upregulated in B samples at 12 h post-infection, together with a gene for an anti-silencing protein also strongly upregulated by RBC and WBC at 3 h post-infection (**TABLE 2**). Both of them could be involved in the generation of an unbalanced and atypical immune response related to the retrotransposon storm we observed in response to vibriosis in our previous *ex vivo* study (chapter 4).

TABLE 2 | Effect of *V. vulnificus* infection on eel B, RBC and WBC transcriptome. List of selected transcripts differentially expressed during *V. vulnificus* R99 infection. *: relevant mRNAs with FC<2, however with statistically significant difference (*P<0.05*).

Gene[1]	FC[2]					
	B		RBC		WBC	
	3 h	12 h	3 h	12 h	3 h	12 h
Cytoskeleton rearrangements						
Tubulin-related genes	--	27.2	--	--	2	--
Myosin-related genes	--	5.9	7.6-2.6	6-1.6	8.2-2.2	--
itpr1*, *itpr3	--	--	4.9-2.7	--	--	--
Actin-related genes	--	3.1	3.4	7-1.5(*)	4.7-2	1.8(*)
Coronin-1a	--	--	2.9	--	--	--
Stress-related						
Hypoxia-inducible factor 1 alpha	--	3.5	--	--	--	--
Glutathione peroxidase	--	-2.1	-1.5(*)	-1.7(*)	-2	--
***hsp90* (cochaperone activator of TLR9)**	--	--	3.6	5-1.8(*)	36.9-8.2	--
Inositol hexakisphosphate (*insP6*)	--	--	2	2.9	--	--
hsp70	--	--	--	31.7-2.2	25.2	9.1
Osmotic stress gene	--	--	--	6.7	--	--
Angiogenesis and hematopoiesis						
angpt2	--	5.9	--	--	-3.7	--
angpt1	--	--	5.6	--	7.4	--
cldn19	--	--	3.2	--	11.6	--
cldn1	--	--	3.2	--	7.2	--
cldn18	--	--	--	--	15.4	--

TABLE 2 | Continued.

Gene[1]	FC[2]					
	B		RBC		WBC	
	3 h	12 h	3 h	12 h	3 h	12 h
cldn4	--	--	--	--	4.1	--
cldn29a	--	--	--	--	3	--
Cell death						
p53	--	--	6.8	--	9.9	--
Calpain	--	--	--	-3.9	-4.7	--
p53 apoptosis effector related to PMP-22	--	--	--	--	33.5	--
tnfrsf12a	--	--	--	--	15.9	--
Cell death activator CIDE-3	--	--	--	--	11.3	1.9(*)
Apoptosis-inducing factor 3	--	--	--	--	6.8	--
TNF receptor member 27	--	--	--	--	6	--
atg9	--	--	--	--	3.3	--
atg2a	--	--	--	--	3.3	--
casp8	--	--	--	--	3	--
cell death activator CIDE-A	--	--	--	--	2.4	--
Granzyme	--	--	--	--	--	-6
Chemokines and receptors						
CC CK3	--	3.6	--	--	--	--
C-C receptor type 4	--	--	6.2	--	--	--
CK 21 precursor	--	--	4.1	--	--	--
CCL4	--	--	--	--	8.6	13.4
CK 4 precursor	--	--	--	--	8.2	--
CK 19 precursor	--	--	--	--	5.2	--
CK 10 precursor	--	--	--	--	2.2	--
Complement system						
C5a receptor	--	14.1	--	--	--	--
Complement factor Bf-2	--	6.5-5.3	--	--	--	--
Complement factor B/C2	--	5.9	--	--	2.4	--
Complement factor B	--	4.6	--	--	--	--
C3a receptor 1	--	--	6.5	--	7.5	--
C3c	--	--	4.2	--	4.2	--
C7-1	--	--	4.1	--	3.3	--
C4BPB	--	--	4.1	3	7.7	--
C3	--	--	3.9	--	7.4	--
C3-H2	--	--	3.6	--	4.2	--
C3-H1	--	--	3.5	--	2.9	--
C3-S	--	--	3.1	1.9(*)	5.6-2.6	1.9
factor D precursor	--	--	2.8	--	--	--
C4-2	--	--	2.2	--	2.1	2.7
C5	--	--	--	--	12.8	--

TABLE 2 | Continued.

Gene[1]	FC[2]					
	B		RBC		WBC	
	3 h	12 h	3 h	12 h	3 h	12 h
C5-2	--	--	--	--	6.1	--
C4	--	--	--	--	4.1	--
C4b	--	--	--	--	4	--
C3-3	--	--	--	--	3.6	--
C1R/C1S subunit of Ca^{2+}-dependent	--	--	--	--	3.4-2.9	--
C7	--	--	--	--	3	--
Complement factor I	--	--	--	--	2.3	--
C3 precursor	--	--	--	--	2.2	--
C1q, B chain	--	--	--	--	--	7.7
Migration						
Cd97 precursor	--	--	--	--	2.9	--
Inflammatory cytokines and related proteins						
il1β	--	17.2	--	--	--	--
Granulin	--	9.3	--	--	--	--
IL-8 precursor	--	7.5	--	--	--	--
IL-1β receptor type 1 soluble	--	5.5	--	--	-4.2	--
Progranulin type 1	--	5.5	--	--	--	--
IL-1 receptor type 1	--	4.4	--	--	-6.2	--
il12β	--	--	8.5	--	14.8	--
IL-10 receptor β	--	--	4.9	--	22.2	--
il17a/f1	--	--	4.4	--	--	--
il20	--	--	2.7	--	6	--
nuclear factor interleukin-3-regulated protein	--	--	--	10.1	3.5	--
IL-6 receptor subunit β precursor	--	--	--	6.8	4.3	2.4
irf1	--	--	--	--	3.3-2.8	--
IL-1 receptor-like	--	--	--	--	3.1	--
ifnc1	--	--	--	--	2.6	--
Allograft inflammatory factor-1	--	--	--	--	2.6	--
ifna2	--	--	--	--	2.1	--
IL-17 receptor	--	--	--	--	--	2.2
PRRs						
tlr13	--	4.3	--	--	--	--
tlr9a	--	-2.6	--	--	--	--
tlr20a	--	--	4.2	--	9.6	--
tlr3	--	--	3.4	--	3.7	--
tlr21	--	--	3.1	--	4.9	--
tlr9b	--	--	2.2	1.8(*)	--	--
tlr7	--	--	--	--	4.1	--
tlr6	--	--	--	--	3	--
tlrs5	--	--	--	--	2.2	--
tlr20f	--	--	--	--	-5.5	--

TABLE 2 | Continued.

Gene[1]	FC[2]					
	B		RBC		WBC	
	3 h	12 h	3 h	12 h	3 h	12 h
Antigen presentation						
mhcII	--	2.7	3-1.7(*)	1.5(*)	--	--
mhcI	--	--	4.8-2	84.4	5.3-3.2	30.6
AP-1 complex subunit sigma 3	--	--	--	-2	3.8	--
AP-1 complex subunit gamma 1	--	--	--	--	2.1	--
Signal transducers and transcriptional factors						
klf6	2.2	8.5-5.2	--	--	--	--
src-family tyrosine kinase SCK	--	17.2	--	--	--	--
traf3	--	5.4	--	--	--	--
socs3	--	5.1	--	--	--	--
c-fos	--	3.7	--	16.9	--	--
jun-b	--	3.5	--	11.1	--	--
map2k6	--	--	8.6	--	25.3	--
nod1	--	--	4.9	--	4.3	--
p38	--	--	4.5	4.2	4	--
map3k2	--	--	4.5	--	4.2	--
pak1	--	--	3.3	--	6.9	--
map3k5	--	--	3.1	--	6.9	--
irf3	--	--	2.4	--	--	--
mapk7	--	--	-2	-2	--	--
irak4	--	--	-2.4	--	--	--
jak1	--	--	-2.4	--	--	--
erk1	--	--	-1.9(*)	-2	--	--
NF-Kβ inhibitor alpha	--	--	--	3.3	-4.8	--
nod3	--	--	--	2.8	3.6	--
irf2A	--	--	--	2.7	--	--
irf2B	--	--	--	2.2	--	--
IRF2, promoter region	--	--	--	2.2	--	--
Klf13	--	--	--	2.2	--	--
map3k4	--	--	--	-2.3	--	--
c-myc binding protein	--	--	--	-5.5	--	--
mapk6	--	--	--	--	24.3	--
NF-Kβ p105 subunit	--	--	--	--	4.8	--
Kdel receptor 3	--	--	--	--	4.3	--
mapk14	--	--	--	--	4	--
stat3	--	--	--	--	3.5	3.1
***nlrc3* receptor**	--	--	--	--	2.6	--
cop9	--	--	--	--	2.1	--
Effectors						
Antibacterial response						
LPB/BPI	4.5-3.3	41.7-25	--	--	--	--
Nitric oxide synthase	--	--	--	--	3.4	--

TABLE 2 | Continued.

Gene[1]	FC[2]					
	B		RBC		WBC	
	3 h	12 h	3 h	12 h	3 h	12 h
Cathepsins						
Cathepsin L	--	3.6	--	--	5.6	--
Cathepsin S precursor	--	2.9	1.8(*)	--	--	--
Cathepsin B	--	--	2.5	5.3	--	--
Coagulation						
Platelet receptor Gi24	--	2	--	--	--	--
Antithrombin protein	--	--	3.8	--	4.1	--
Thrombin protein	--	--	3.4	--	--	--
Thrombospondin	--	--	--	--	7.1-3	--
Fibrinogen	--	--	--	--	4	--
Angiotensinogen	--	--	--	--	3.3	--
Plasminogen	--	--	--	--	2	1.9(*)
Iron-related						
Transferrin	--	2.7	2.5-2.1	1.8(*)	--	--
Transferrin receptor (*tfr1*)	--	2.4	--	--	--	--
Aminolevulinic acid	--	2	--	--	--	2.1
Hemoglobin subunit	--	--	--	3.7	--	--
Ferritin	--	--	--	2.8-2.1	--	--
Hepcidin	--	--	--	--	10.2	--
Lectins						
Mannose-6-phosphate receptor-binding protein 1	--	14	--	--	--	--
C-type lectin receptor	--	--	3.8	--	11.5-(-6)	--
Galectin 3	--	--	3.2	--	4.3	1.7(*)
Galectin 4	--	--	2.9	1.7(*)	16.1	--
Intelectin	--	--	2.5	--	12.6	--
Mannose binding lectin 2	--	--	--	3	3.1-2.1	--
Fucolectin 2	--	--	--	--	2.7	--
Fucolectin 4	--	--	--	--	2.1	1.9(*)
Septicemia markers						
Cyclooxygenase 2	5.5	32.1	--	--	--	--
Hyaluronidase-2	2.5	26.6	--	--	--	--
Metalloprotinase 9	--	61.5-40	--	--	--	--
Coagulation factor VIII	--	22.4-9.1	--	--	--	--
Leukotriene	--	5.2	--	--	--	--
Prostaglandin	--	11	--	--	--	--
Coagulation factor V	--	--	--	--	4.6	--
Multiple coagulation factor	--	--	--	--	--	3.1

TABLE 2 | Continued.

Gene[1]	FC[2]					
	B		RBC		WBC	
	3 h	12 h	3 h	12 h	3 h	12 h
Histone modification (epigenetics)						
Histone H2B	--	-2.3	--	--	--	--
Histone H2AFX	--	--	3.2	2.2	--	--
Histone acetyltransferase type B catalytic subunit	--	--	2.2	--	2.6	--
Histone deacetylase 3	--	--	2.2	--	--	--
Histone gene cluster XlH3-A (*h1a*, *h2b*, *h3*, *h4*)	--	--	-1.4(*)	--	--	--
Histone acetyltransferase MYST2	--	--	-1.4(*)	--	--	--
Histone H1x	--	--	-3.5	--	--	--
Histone H3.3	--	--	--	1.3(*)	--	--
euchromatic histone-lysine N-methyltransferase 1b (*ehmt1b*)	--	--	--	-1.7(*)	--	--
Histone acetyltransferase MYST4	--	--	--	-2.7	--	--
Histone deacetylase 1	--	--	--	-2.7	--	--
Histone H2A.Z	--	--	--	-4	--	--
Histone deacetylase 2	--	--	--	-4.3	--	--
Histone H1	--	--	--	--	7.4-5.9	--
Histone H2AV	--	--	--	--	-1.8(*)	-1.6(*)
Special interest						
Systemic RNAi	--	10.5	--	--	--	--
muc2A	--	--	2.5	--	4.4	--
Anti-silencing protein	--	--	2.3	--	3.1	--

[1]Identified DEGs are indicated.
[2]FC: fold change value for each individual gene.
--: not detected as differentially expressed.

Transcriptomic response in the eel blood against a mutant defective in RtxA1$_3$: role of the toxin in vibriosis

To test the hypothesis on the role of RtxA1$_3$ in the animal death, we analyzed the blood transcriptome of eels infected with a double mutant defective in RtxA1$_3$ (Δ*rtxA1$_3$*) and compared it with that of the eels infected with the wild-type strain. **TABLE 3** shows a list of the selected genes that were differentially expressed by blood cells in B, RBC and WBC samples from eels infected with the mutant strain. As expected, the response related to cytoskeletal rearrangements was mostly found in the cells from eels infected with the wild-type strain (**TABLES 2** and **3**), confirming that this response is a consequence of the *in vivo* action of RtxA1$_3$. A minor cytoskeletal-related response was also detected in these cells upon Δ*rtxA1$_3$* infection (**TABLE 3**), but this was probably related to cell motility and activity (i.e., phagocytosis, diapedesis, etc.).

We highlight that the immune response of RBC against the mutant was much lower than that against the wild-type strain, with most of the DEGs involved in signal transduction of immune-related pathways downregulated (i.e., *irf2* and *klf13*) (**FIGURE 3** and **TABLE 3**). Therefore, immune response activation in RBC seems to be strongly dependent on RtxA1$_3$ expression. Similarly, blood cells (B samples) and WBC differentially expressed significantly less genes against the mutant than against the wild-type strain. However, given that eels infected with the mutant strain are able to eliminate the pathogen from its internal organs (Lee *et al.*, 2013) these DEGS should be seen as those essential to activate a protective immune response. This protective immune response consisted on:

i) *A significantly lower activation of TLRs in terms of number of DEGs and fold change value*. Thus, the only *tlrs* that were upregulated were *tlr20a*, a membrane receptor involved in inflammatory response in fish, and *tlr3,* an endosomal receptor for RNA (Rebl *et al.*, 2010), both of them upregulated only by WBC (**TABLE 3**). The upregulation of *tlr3* was unexpected since it is considered an intracellular receptor in humans and mice (Blasius and Beutler, 2010). The most plausible explanation for the upregulation of this intracellular TLR in response to the mutant strain is that either WBC had probably phagocyted bacteria and part of their antigens had been endosomally processed or Tlr3 have other functions in fish. Further studies are needed to prove this hypothesis.

ii) *A significanlt lower activation of inflammation*. Hence, a significant lower fold change values were detected for those genes encoding pro-inflammatory cytokines or genes involved in its production (i.e., *il1β*, *il8*, *irf* genes, progranulin and granulin), together with a

downregulation of genes for anti-inflammatory cytokines (i.e., *il10*) and no differential expression of genes for inhibitors of the innate immune response (i.e., *nlrc3*) (**TABLE 3**).

iii) *A significantly lower activation of septicemia markers related to tissue damage and acute phase of infection*. Thus, *mmp9*, *cox2*, and genes encoding leukotrienes were upregulated against the mutant strain but its upregulation was significantly lower than that showed in response to wild-type strain infection with fold change values up to six times higher in blood of animals infected with the wild-type strain (**TABLES 2** and **3**). This observation is in accordance with the fact that eels infected with the mutant suffer from septicemia but do not die, precisely because the tissue damage is not enough for killing (Lee *et al.*, 2013). In this sense, genes for prostaglandins were not found as DEGs in response to the infection with the mutant strain (**TABLE 3**).

iv) *A lack of response against RNA*. Interestingly, in response to Δ*rtxA1*$_3$ infection, and contrary to what we found in response to wild-type infection, systemic RNAi was downregulated in WBC at 3 h post-infection (**TABLE 3**). By contrast, the microRNA-142a (miR-142a) was upregulated by the same cell type and at the same sampling time (**TABLE 3**). miRNAs (microRNAs) regulate target gene expression either by translational repression or degradation of target mRNAs (Shukla *et al.*, 2011). They are involved in the regulation of various immune-related pathways of both the innate and adaptive immune systems (Baltimore *et al.*, 2008). Concretely, miR-142 has been found to regulate hematopoiesis, inflammation and T cell differentiation in humans and mice (Chen *et al.*, 2004; Talebi *et al.*, 2017). Moreover, miR-142 isoforms could target transcripts which are involved in cytokine signaling, such as *socs1* (Talebi *et al.*, 2017), which was upregulated by RBC in response to the infection with the mutant (**TABLE 3**). Socs1 acts as a negative regulator of cytokine signaling (i.e., inhibition of *stat* and *inf*) (Alexander *et al.*, 1999; Bhattacharyya *et al.*, 2011). Similar results have been reported in grass carp upon *Aeromonas hydrophila* infection in a study where the authors also suggest that miR-142a could be involved in avoidance of bacterial injury in fish (Xu *et al.*, 2016). Therefore, here we propose a similar role for miR-142a in eels with the novelty that miR-142a would be involved in a balanced response against bacterial infections. Further research is needed to prove this hypothesis.

TABLE 3 | Effect of RtxA1$_3$ deletion on eel B, RBC and WBC transcriptome. List of selected transcripts differentially expressed during *V. vulnificus* Δ*rtxA1$_3$* strain infection. *: relevant mRNAs with FC<2, however with statistically significant difference (*P<0.05*).

Gene[1]	FC[2]					
	BLOOD		RBC		WBC	
	3 h	12 h	3 h	12 h	3 h	12 h
Cytoskeleton rearrangements						
Myosin-related genes	2	3.6-2	--	1.4(*)	3.5	--
Tubulin-related genes	1.3(*)	9.7-1.3(*)	--	-2.1	-(2-8.3)	--
Actin-related genes	--	2	--	-2.1	2.7-(-4)	--
Stress-related						
hsp90	--	-(-2.4-3)	--	--	-2.8	--
Angiogenesis and hematopoiesis						
cldn18	--	--	--	--	5	--
cldn1	--	--	--	--	4.2	--
angpt1	--	--	--	--	4	--
Cell death						
TNF receptor 14	--	--	--	--	7.8	--
p53	--	--	--	--	4.9	--
p53 apoptosis effector related to PMP-22	--	--	--	--	3.1	--
traf7	--	--	--	--	-2.3	--
Chemokines and receptors						
CC CK3	-2.3	--	--	--	--	--
CK 13	--	--	--	--	4.2	--
CK 19 precursor	--	--	--	--	3	--
C-X-C motif receptor 3	--	--	--	--	-2.5	--
Complement system						
B/C2	--	10.6	--	--	--	--
Bf-2	--	10.5-7.6	--	--	--	--
C5a receptor	--	6.8	--	--	--	--
C4BPB	--	--	-2.2	--	--	--
C5-2	--	--	--	3.3	--	--
C1q, A subunit	--	--	--	--	4.6	--
C3-H2	--	--	--	--	3.9	--
C7-1	--	--	--	--	3.4	--
C1q, B chain	--	--	--	--	3.1	--
Inflammatory cytokines and related proteins						
il10	-1.8(*)	--	--	-1.8(*)	--	--
IL-1β receptor type 1 soluble	--	6.5	--	--	--	--
Granulin	--	6.2	--	--	--	--
Allograft inflammatory factor-1	--	4.4	--	--	--	--
IL-8 precursor	--	3.8	--	--	--	--
IL-1 receptor type 1	--	3.6	--	--	-2.7	--
il1β	--	3.5	--	--	--	--
Progranulin type I	--	3.3	--	--	--	--

TABLE 3 | Continued.

Gene[1]	FC[2]					
	BLOOD		RBC		WBC	
	3 h	12 h	3 h	12 h	3 h	12 h
irf3	--	2.3	--	--	7.3	--
irf2A	--	--	-1.9(*)	-2.2	--	--
irf2B	--	--	--	-2.3	--	--
irf7	--	--	--	--	7.5	--
il18A	--	--	--	--	3.2	--
il12ß	--	--	--	--	2.6	--
infa	--	--	--	--	2.4	--
il16	--	--	--	--	-2.2	--
PRRs						
tlr20a	--	--	--	--	4.7	--
tlr3	--	--	--	--	4.2	--
tlr13	--	--	--	--	-4.1	--
Antigen presentation						
bl3-7 **(Mhcl)**	55.6	--	--	--	--	--
mhcl	--	--	--	--	2.5	--
AP-1 complex	--	--	--		2.1-(-2)	--
Signal transducers and transcriptional factors						
src-family tyrosine kinase SCK	--	10.6	--	--	--	--
traf3	--	3.2	--	--	--	--
map3k4	--	-1.5(*)	--	--	--	--
c-jun	--	-2.9	--	-3.2	--	--
socs1	--	--	2.5	1.5(*)	--	--
klf13	--	--	--	-3.4	--	--
map2k6	--	--	--	--	6.7	--
c-fos	--	--	--	--	6.1-3.5	--
p38	--	--	--	--	4.4	--
Kdel receptor 3	--	--	--	--	3.8	--
mapk7	--	--	--	--	-2	-1.9(*)
NF-Kβ inhibitor alpha	--	--	--	--	-(3-3.2)	--
mapk2	--	--	--	--	--	2.8
erk1	--	--	--	--	--	-2.4
Effectors						
Antibacterial response						
LBP/BPI	3.6	27-10.8	--	--	-(7-8.4)	--
Nitric oxide synthase	-2.5	--	--	--	--	--
nos1ap **(nitric oxide)**	--	--	--	--	5.5	--
Cathepsins						
Cathepsin S precursor	--	3.5	2.5	1.8(*)	--	--
Cathepsin F precursor	--	--	--	--	2.4	--
Coagulation						
Angiotensinogen	-2.2	--	--	--	--	--
Antithrombin protein	-2.1	--	--	--	2.6	--
Plasminogen	--	--	--	--	-2.3	--

TABLE 3 | Continued.

Gene[1]	FC[2]					
	BLOOD		RBC		WBC	
	3 h	12 h	3 h	12 h	3 h	12 h
Iron-related						
Ferritin M subunit	--	-1.4(*)	--	--	--	--
Hemoglobin subunit	--	--	--	--	11.7-2.1	--
Transferrin receptor (*tfr1*)	--	--	--	--	6.4	--
Lectins						
C-type lectin receptor	-2.2	-3	--	--	3.7	--
Galectin 1	--	--	--	--	14	--
Galectin 2	--	--	--	--	8.1	--
Galectin 4	--	--	--	--	2.9	--
Septicemia markers						
Cyclooxygenase 2 (*cox2*)	--	14.2	--	--	--	--
mmp9	--	8.7-7.4	--	--	--	--
Coagulation factor VIII precursor	--	5.6	--	--	-7.3	--
Leukotriene	--	3.8	--	--	-3	--
Coagulation factor VIII	--	--	--	--	-9.6	--
Histone modification (epigenetics)						
Histone H2A.V	7.6	6.2	--	--	--	--
Histone acetyltransferase MYST2	--	-1.6(*)	--	--	--	--
Histone H1x	--	-1.9(*)	--	--	--	--
Histone H1	--	--	--	--	6.2	--
Histone H2A.Z	--	--	--	--	3.2-2.6	--
Histone H3.3	--	--	--	--	-1.3(*)	-1.8(*)
Special interest						
muc2A	--	--	--	--	3.4	--
***miR-142a* (microRNA)**	--	--	--	--	2	--
systemic RNAi	--	--	--	--	-4.6	--

[1]Identified DEGs are indicated.
[2]FC: fold change value for each individual gene.
--: non detected as differentially expressed.

4. Discussion

The diseased caused by *V. vulnificus* in eels can be divided in three sequential steps; colonization of the gills, invasion of the bloodstream and death by septic shock (Amaro *et al.*, 2015). During the colonization of the gills the major toxin of the species, $RtxA1_3$, plays a key role in the destruction of immune and endothelial cells activating a local inflammation (Callol *et al.*, 2015a). Transcriptomic studies of the gills in response to the infection with *V. vulnificus* revealed that the gills are able to respond very quickly to the infection by upregulating genes for PRRs and signal transductors with a maximum response detected 1 h post-infection. More importantly, part of this response is $RtxA1_3$-dependent (Callol *et al.*, 2015b). In the present chapter, we aimed to describe the eel vibriosis in terms of host immune response in the eel blood as well as to unravel if the toxin acts as a factor that triggers an unbalanced immune response that leads to the eel death by sepsis. **FIGURE 4** summarizes the most important immune-related pathways differentially expressed in eel blood during *V. vulnificus* infection.

Previous studies had already shown that teleost fish RBC are involved in antiviral immune response, mainly through PAMPs recognition and inflammatory cytokine signaling pathway (Workenhe *et al.*, 2008; Dahle *et al.*, 2015; Nombela *et al.*, 2017; Nombela and Ortega-villaizan, 2018). In the previous chapter, we performed an *ex vivo* study that allow us to determine an active and essential role of fish RBC upon bacterial infections for the first time. Here, using an *in vivo* approach, we have confirmed our previous results, and demonstrated that RBC are highly responsive cells during eel immune response against septicemic pathogens, such as *V. vulnificus*, but for that, a cross talk between RBC and WBC (or even platelets) would be necessary, which could be the reason why we did not observe such a relevant RBC response in the previous *ex vivo* experiment where blood cells were infected separately (chapter 4). Nevertheless, in this study we have found strong evidence suggesting that RBC produce an atypical immune response against *V. vulnificus* (in part due to the activation of an antiviral response), which could be the ultimate cause of animal death. Importantly, RBC response is mostly abolished in absence of $RtxA1_3$ (infection with Δ*rtxA1*$_3$ strain), and in absence of the toxin, eels do not die although they suffer from septicemia (Lee *et al.*, 2013). This result suggests that the over-response generated by RBC in response to $RtxA1_3$ could significantly contribute to generate the atypical and detrimental immune response in eels against *V. vulnificus*. Our transcriptomic results evidence that mechanisms for $RtxA1_3$ activation are early enhanced. Therefore, *insP6* is upregulated by RBC upon infection with *V. vulnificus* wild-type strain, and this upregulation is sustained in time (3 and 12 h post-infection) (**TABLE 2**). This allows the resultant InsP6 to bind $RtxA1_3$ CPD domain which in turn results in the release of the

rest of RtxA1$_3$ effector domains, including ACD (Satchell, 2011, 2015). Moreover, we found coronin-1a, together with some genes belonging to its upstream signaling pathway (i.e., *itpr1* and *itpr3*), early upregulated by RBC (3 h post-infection) (**TABLE 2**). Coronin-1a binds to actin which leads to cytoskeleton rearrangements and at the same time induces calcium mobilization (Mueller *et al.*, 2008; Combaluzier *et al.*, 2009; Tokarz-Deptuła *et al.*, 2016). Calcium mobilization in turn potentiates RtxA1$_3$ activity, since it has been described that presence of calcium in the media is required for secretion of the toxin by the bacterium (Kim *et al.*, 2013; Kim, 2018).

Host PRRs, such as TLRs and NLRs are key molecules for PAMPs recognition and mediate in the activation of the immune responses. Our results show an early upregulation (3 h post-infection) of genes encoding TLRs, NLRs and also lectins in eels infected with wild-type *V. vulnificus* in comparison with those infected with Δ*rtxA1$_3$* strain (**TABLES 2** and **3**). Interestingly, the upregulation of genes encoding TLRs in response to the mutant strain is restricted to WBC, stressing the importance of RtxA1$_3$ in the activation of RBC response. As described in previous research, TLRs can be either beneficial or detrimental to the host, depending on the bacterial dose and route of infection (Kawai and Akira, 2011). Similarly, TLRs-encoding gene duplication has been related to systemic autoimmunity in mice (Deane *et al.*, 2007; Krieg, 2007). Here we observed an exacerbated upregulation of multiple TLRs upon wild-type *V. vulnificus* infection (**TABLE 2**). Although this response could be part of a strategy developed to efficiently recognize pathogens, we propose a role of RtxA1$_3$ in provoking an over-dosage of TLRs and its downstream signaling pathways, which in turn would cause an over-magnified immune response that would be detrimental to the host. In fact, our results evidence an early cytokine storm in response to RtxA1$_3$ (a process that we did not observe *ex vivo*), activated at 3 h post-infection by both WBC and RBC that upregulate genes encoding pro-inflammatory cytokines (i.e., *il12β*, *il17*, *il20*) as well as for Tnf, Inf, and Nf-Kβ (this two only upregulated by WBC) (**TABLE 2**). Moreover, the cytokine storm seems to be sustained in the eel blood along the infection, since we detected upregulated *il1β* and its receptor, *il8* precursor and genes encoding for progranulin and granulin. This result is in accordance with the RtxA1$_3$-dependent cytokine storm that has already been described in mice (Murciano *et al.*, 2017). On the contrary, upon RtxA1$_3$ deficient *V. vulnificus* infection a more accurate and beneficial immune response is induced through the activation of only the necessary TLRs and related signaling pathways. As a result, we did not observe evidence of a strong cytokine storm in response to the mutant strain. Interestingly, in RBC the expression of genes encoding pro-inflammatory

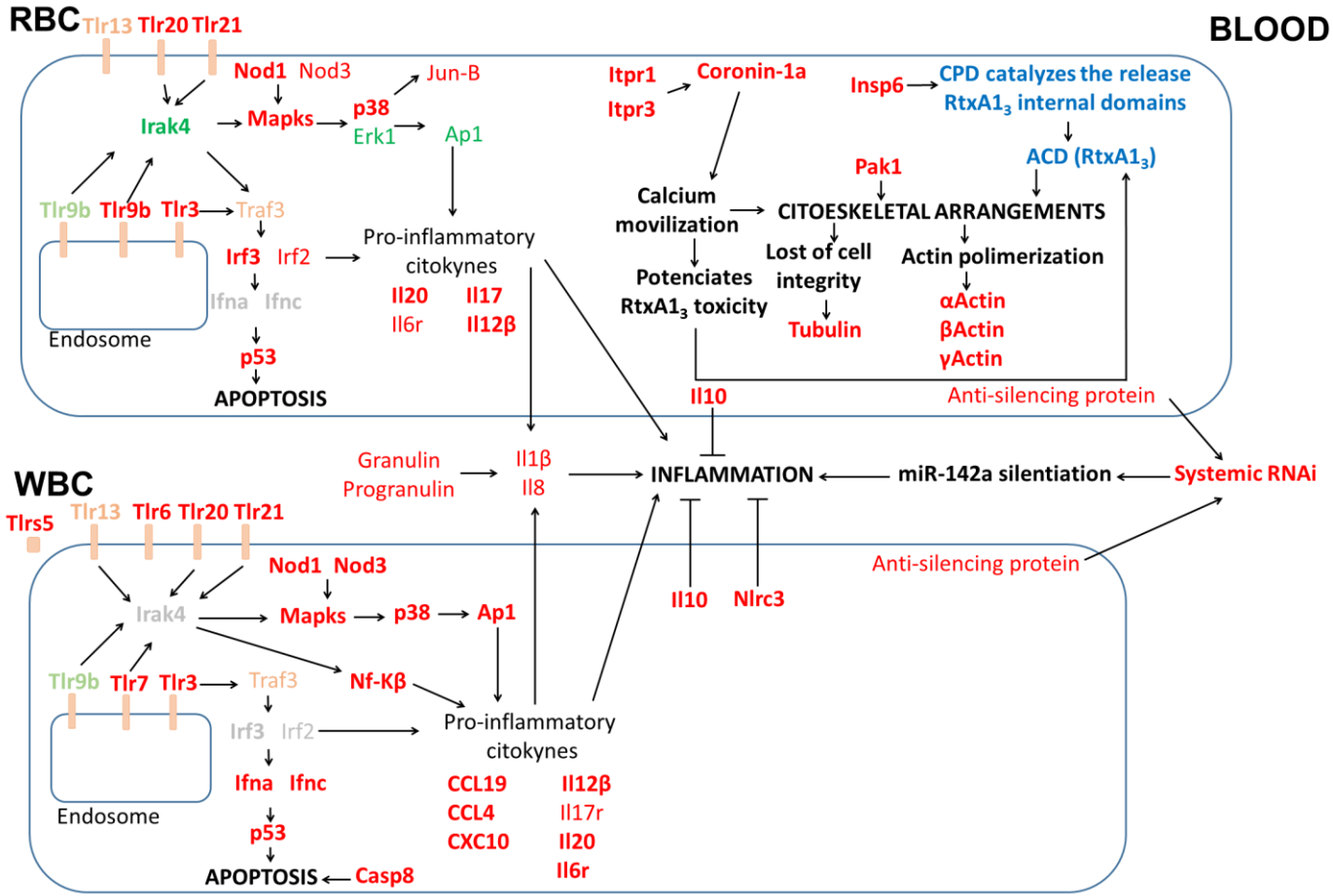

FIGURE 4 | Main immune related pathways differentially expressed in eel blood upon *V. vulnificus* infection. The model show the resultant proteins produced by the main transcripts differentially expressed by eels during *V. vulnificus* R99 strain infection. The putative translated proteins are represented in a code color depending if it is encoded by a gene upregulated (red), downregulated (green), detected differentially expressed in a different cell-type (grey) or if it correspond to $RtxA1_3$ changes in response to eel cells cytoskeleton and calcium mobilization (blue). Those proteins encoded by genes found differentially expressed in blood but not in cells (RBC/WBC) are showed in smooth color (Tlr13, Tlr9b, Traf). The time of production is shown in bold proteins (early codified [3 h]) or not bold (lately codified [12 h]).

cytokines is completely abolished in eels infected with Δ*rtxA1*$_3$ strain, thus confirming that this response is toxin dependent. In WBC *il12β* and *il18* were early upregulated (3 h post-infection) while in B samples genes encoding granulin and progranulin together with *il8* and *il1β* were upregulated at 12 h post-infection. This response can be considered typical against pathogens and would result in an effective and protective immune response.

In addition, TLRs distinguish among classes of pathogens and therefore are essential in inducing the appropriate immune effector molecules (Takeda *et al.*, 2003). Our results not only suggest an over-dosage of TLRs in response to *V. vulnificus* wild-type strain but also the upregulation of inappropriate TLRs for extracellular bacterial recognition. Therefore, we found a high upregulation of genes encoding for Tlr9 and Tlr3, both described as involved in viral detection (Blasius and Beutler, 2010), favoring an atypical immune response which would result ineffective against *V. vulnificus*. Curiously, an upregulation of *tlr9* and *tlr3* in fish upon infection with bacterial pathogens belonging to *Edwarsiella* genus has been reported (*tlr9* in Japanese flounder after *E. tarda* infection (Takano *et al.*, 2007) and *tlr3* in channel catfish and zebrafish in response to *E. ictaluri* (Bilodeau and Waldbieser, 2005; Bilodeau-Bourgeois *et al.*, 2008)). As *Edwarsiella* species are intracellular pathogens, our results support the hypothesis that RtxA1$_3$ provokes the detection of *V. vulnificus* as an intracellular pathogen (an event also observed in mice response to R99 infection (Murciano *et al.*, 2017)). As a result, an unappropriated immune response is activated. To our knowledge, neither the bacterial ligand nor a plausible explanation for those TLRs involved in bacterial recognition has been reported.

Finally, one of the most striking findings in our study was the toxin-dependent differential expression of RNA-related transcriptional modulators such as RNAi, anti-silencing protein and miR-142a. The involvement of miR-142a in regulation of grass carp immune response against the gramnegative bacterial pathogen *A. hydrophila* has been determined by Xu *et al.*, (2016). As miRNA-mediated gene silencing acts faster than most transcriptional regulation responses (Pothof *et al.*, 2009; Yan *et al.*, 2013; O'Brien *et al.*, 2018), Xu *et al.,* proposed a model for the avoidance of bacterial injury in fish in which the rapid upregulation of miR-142a (acting earlier than other innate immune genes) once a fish is exposed to bacterial infection would inhibit inflammation reaction (through the inhibition of *tlr5* and its downstream pathway, including *il1β*, *il8* and *tnfα*) (Xu *et al.*, 2016). Similarly, we found an early upregulation of miR-142a, together with the downregulation of an anti-silencing protein (which would enhance the miRNA-mediated gene silencing) and a decrease in *il1β* expression (which overproduction is associated with non-regulated inflammatory diseases (Chen *et al.*, 2018)) (**TABLES 2** and **3**), in eels after *V. vulnificus* infection, but only when the RtxA1$_3$ was not expressed (Δ*rtxA1*$_3$ strain).

On the contrary, in response to wild-type infection we found an upregulation of a systemic RNAi and an anti-silencing protein, which would prevent miRNA-mediated gene silencing, thus leading to an atypical immune response, somehow mediated by RtxA1$_3$, that eventually causes eel's death. However, more research should be performed in future studies to confirm RNAi and miRNA-mediated modulation of eel immune response upon *V. vulnificus* infection.

In summary, our work provides valuable data about the eel immunotranscriptomic response upon *V. vulnificus* infection, and together with our previous results obtained from *ex vivo* experiments (chapter 4), sets up new objectives for future investigation. Therefore, we have validated most of the results previously obtained *ex vivo* proving that this is a good approximation for studying the host-pathogen interaction. At the same time using an *in vivo* approach we have found new interesting results that we could not bring to light in previous studies. In this sense, we have performed a time-dependent expression analysis of eel blood cells during the infection and determined that the maximum number of DEGs is reached at 3 h post-infection, highlighting the fast immune response induced by *V. vulnificus*. Interestingly, the processes upregulated by eels at 3 h from the beginning of the infection are involved in pathogen recognition and processing and production of inflammatory response; while at 12 h post-infection the most upregulated genes are related to endothelial damage and acute phase of infection. Comparing the immune response triggered by different bacterial strains we have stablished that R99 strain, but not Δ*rtxA1$_3$*, induces an early and deregulated inflammatory response, that could be compatible with a cytokine storm triggered by RtxA1$_3$, similar to that described in mice by Murciano *et al.*, (2017). Interestingly, our results stress the importance of RBC in this atypical and fatal response since their highly response that over-magnified the early cytokine storm is RtxA1$_3$-dependent. Finally, the role of RNAi in silencing miR-142a and triggering a retrotransposon storm (evidenced *ex vivo*) that induce an atypical and non-accurate immune response (R99 infection), together with the probable role of miR-142a for a proper modulation of immunity and host survival (Δ*rtxA1$_3$* infection) deserves further research. Specifically miR-142a stands out as a useful manner to develop new therapeutic tools, based on the utilization of silencing/anti-silencing RNAs in order to prevent vibriosis outbreaks in fish farms.

5. References

Alexander, W.S., Starr, R., Fenner, J.E., Scott, C.L., Handman, E., Sprigg, N.S., et al. (1999) SOCS1 is a critical inhibitor of interferon γ signaling and prevents the potentially fatal neonatal actions of this cytokine. *Cell* **98**: 597–608.

Amaro, C., Biosca, E.G., Fouz, B., Alcaide, E., and Esteve, C. (1995) Evidence that water transmits *Vibrio vulnificus* Biotype 2 infections to eels. *Appl Environ Microbiol* **61**: 1133–1137.

Amaro, C., Sanjuán, E., Fouz, B., Pajuelo, D., Lee, C.T., Hor, L.I, et al. (2015) The fish pathogen *Vibrio vulnificus* Biotype 2: epidemiology, phylogeny and virulence factors involved in warm-water vibriosis. *Microbiol Spectr* **3**: 0005–2014.

Austin, B., and Austin, D.A. (2012) Bacterial fish pathogens: disease of the farmed and wild fish, 5th edn. Dordrecht, the Netherlands: Springer.

Baltimore, D., Boldin, M.P., O'Connell, R.M., Rao, D.S., and Taganov, K.D. (2008) MicroRNAs: New regulators of immune cell development and function. *Nat Immunol* **9**: 839–845.

Bateman, A., Belcourt, D., Bennett, H., Lazure, C., and Solomon, S. (1990) Granulins, a novel class of peptide from leukocytes. *Biochem Biophys Res Commun* **173**: 1161–1168.

Bhattacharyya, S., Zhao, Y., Kay, T.W.H., and Muglia, L.J. (2011) Glucocorticoids target suppressor of cytokine signaling 1 (SOCS1) and type 1 interferons to regulate Toll-like receptor-induced STAT1 activation. *Proc Natl Acad Sci USA* **108**: 9554–9559.

Bilodeau-Bourgeois, L., Bosworth, B.G., and Peterson, B.C. (2008) Differences in mortality, growth, lysozyme, and Toll-like receptor gene expression among genetic groups of catfish exposed to virulent *Edwardsiella ictaluri*. *Fish Shellfish Immunol* **24**: 82–89.

Bilodeau, A.L. and Waldbieser, G.C. (2005) Activation of TLR3 and TLR5 in channel catfish exposed to virulent *Edwardsiella ictaluri*. *Dev Comp Immunol* **29**: 713–721.

Biosca, E.G., Amaro, C., Esteve, C., Alcaide, E., and Garay, E. (1991) First record of *Vibrio vulnificus* biotype 2 from diseased European eel, *Anguilla anguilla*. *J Fish Dis* **14**: 103–109.

Blasius, A.L. and Beutler, B. (2010) Intracellular Toll-like Receptors. *Immunity* **26**: 305–315.

Callol, A., Pajuelo, D., Ebbesson, L., Teles, M., MacKenzie, S., and Amaro, C. (2015a) Early steps in the European eel (*Anguilla anguilla*)-*Vibrio vulnificus* interaction in the gills: role of the

RtxA1$_3$ toxin. *Fish Shellfish Immunol* **43**: 502–509.

Callol, A., Reyes-Lopez, F.E., Roig, F.J., Goetz, G., Goetz, F.W., Amaro, C., et al. (2015b) An Enriched European Eel Transcriptome Sheds Light upon Host-Pathogen Interactions with *Vibrio vulnificus*. *PLoS One* **10**: e0133328.

Callol, A., Roher, N., Amaro, C., and MacKenzie, S. (2013) Characterization of PAMP/PRR interactions in European eel (*Anguilla anguilla*) macrophage-like primary cell cultures. *Fish Shellfish Immunol* **35**: 1216–1223.

Chen, C., Li, L., Lodish, H.F., and Bartel, D.P. (2004) MicroRNAs modulate hematopoietic lineage differentiation. *Science* **303**: 83–6.

Chen, L., Deng, H., Cui, H., Fang, J., Zuo, Z., Deng, J., et al. (2018) Inflammatory responses and inflammation-associated diseases in organs. *Oncotarget* **9**: 7204–7218.

Combaluzier, B., Mueller, P., Massner, J., Finke, D., and Pieters, J. (2009) Coronin 1 is essential for IgM-mediated Ca^{2+} mobilization in B cells but dispensable for the generation of immune responses *in vivo*. *J Immunol* **182**: 1954–1961.

Dahle, M.K., Wessel, Ø., Timmerhaus, G., Nyman, I.B., Jørgensen, S.M., Rimstad, E., et al. (2015) Transcriptome analyses of Atlantic salmon (*Salmo salar* L.) erythrocytes infected with piscine orthoreovirus (PRV). *Fish Shellfish Immunol* **45**: 780–790.

Deane, J.A., Pisitkun, P., Barrett, R.S., Feigenbaum, L., Town, T., Ward, J.M., et al. (2007) Control of TLR7 expression is essential to restrict autoimmunity and dendritic cell expansion. *Immunity* **27**: 801–810.

Gómez-Abellán, V. and Sepulcre, M.P. (2016) The role of prostaglandins in the regulation of fish immunity. *Mol Immunol* **69**: 139–145.

Kawai, T. and Akira, S. (2011) Toll-like receptors and their crosstalk with other innate receptors in infection and immunity. *Immunity* **34**: 637–650.

Kim, B.S. (2018) The modes of action of MARTX toxin effector domains. *Toxins* **10**.

Kim, Y.K., Shin, J.S., and Nahm, M.H. (2016) NOD-like receptors in infection, immunity, and diseases. *Yonsei Med J* **57**: 5–14.

Kim, Y.R., Lee, S.E., Kang, I.C., Nam, K. Il, Choy, H.E., and Rhee, J.H. (2013) A bacterial RTX toxin causes programmed necrotic cell death through calcium-mediated mitochondrial

dysfunction. *J Infect Dis* **207**: 1406–1415.

Krieg, A.M. (2007) The Toll of Too Much TLR7. *Immunity* **27**: 695–697.

Lee, C.T., Pajuelo, D., Llorens, A., Chen, Y.H., Leiro, J.M., Padrós, F., et al. (2013) MARTX of *Vibrio vulnificus* biotype 2 is a virulence and survival factor. *Environ Microbiol* **15**: 419–432.

Livak, K.J. and Schmittgen, T.D. (2001) Analysis of relative gene expression data using real-time quantitative PCR and the $2^{-\Delta\Delta CT}$ method. *Methods* **25**: 402–408.

Marco-Noales, E., Milán, M., Fouz, B., Sanjuán, E., and Amaro, C. (2001) Transmission to eels, portals of entry, and putative reservoirs of *Vibrio vulnificus* Serovar E (Bioype 2). *Appl Environ Microbiol* **67**: 4717–4725.

Matsumoto, F., Saitoh, S.I., Fukui, R., Kobayashi, T., Tanimura, N., Konno, K., et al. (2008) Cathepsins are required for Toll-like receptor 9 responses. *Biochem Biophys Res Commun* **367**: 693–699.

Medzhitov, R. and Horng, T. (2009) Transcriptional control of the inflammatory response. *Nat Rev Immunol* **9**: 692–703.

Mueller, P., Massner, J., Jayachandran, R., Combaluzier, B., Albrecht, I., Gatfield, J., et al. (2008) Regulation of T cell survival through coronin-1-mediated generation of inositol-1,4,5-trisphosphate and calcium mobilization after T cell receptor triggering. *Nat Immunol* **9**: 424–431.

Murciano, C., Lee, C.T., Fernández-Bravo, A., Hsieh, T.H., Fouz, B., Hor, L.I., et al. (2017) MARTX toxin in the zoonotic serovar of *Vibrio vulnificus* triggers an early cytokine storm in mice. *Front Cell Infect Microbiol* **7**: 1–19.

Nombela, I., Carrion, A., Puente-marin, S., Chico, V., Coll, J., Ortega-Villaizan, M.M., et al. (2017) Infectious pancreatic necrosis virus triggers antiviral immune response in rainbow trout red blood cells , despite not being infective. *F1000Research* **6**: 1968.

Nombela, I. and Ortega-Villaizan, M.M. (2018) Nucleated red blood cells: Immune cell mediators of the antiviral response. *PLoS Pathog* **14**: e1006910.

O'Brien, J., Hayder, H., Zayed, Y., and Peng, C. (2018) Overview of microRNA biogenesis, mechanisms of actions, and circulation. *Front Endocrinol* **9**: 1–12.

Palti, Y. (2011) Toll-like receptors in bony fish: From genomics to function. *Dev Comp Immunol* **35**: 1263–1272.

Park, B., Buti, L., Lee, S., Matsuwaki, T., Spooner, E., Brinkmann, M.M., et al. (2011) Granulin is a soluble cofactor for Toll-like receptor 9 signaling. *Immunity* **34**: 505–513.

Pedersen, M.E., Vuong, T.T., Rønning, S.B., and Kolset, S.O. (2015) Matrix metalloproteinases in fish biology and matrix turnover. *Matrix Biol* **44**: 86–93.

Peters-Golden, M., Canetti, C., Mancuso, P., and Coffey, M.J. (2005) Leukotrienes: Underappreciated mediators of innate immune responses. *J Immunol* **174**: 589–594.

Pothof, J., Verkaik, N.S., Van Ijcken, W., Wiemer, E.A.C., Ta, V.T.B., Van Der Horst, G.T.J., et al. (2009) MicroRNA-mediated gene silencing modulates the UV-induced DNA-damage response. *EMBO J* **28**: 2090–2099.

Rawlings, J.S., Rosler, K.M., and Harrison, D.A. (2004) The JAK/STAT signaling pathway. *J Cell Sci* **117**: 1281–1283.

Rebl, A., Goldammer, T., and Seyfert, H.M. (2010) Toll-like receptor signaling in bony fish. *Vet Immunol Immunopathol* **134**: 139–150.

Satchell, K.J.F. (2015) Multifunctional-autoprocessing repeats-in-toxin (MARTX) toxins of *Vibrios*. *Microbiol Spectr* **6**.

Satchell, K.J.F. (2011) Structure and function of MARTX toxins and other large repetitive RTX proteins. *Annu Rev Microbiol* **65**: 71–90.

Schneider, M., Zimmermann, A.G., Roberts, R.A., Zhang, L., Karen, V., Rahman, A.H., et al. (2013) The innate immune sensor NLRC3 attenuates Toll-like receptor signaling via modification of the signaling adaptor TRAF6 and ttranscription factor NF-κB. *Nat Immunol* **13**: 823–831.

Shakespear, M.R., Halili, M.A., Irvine, K.M., Fairlie, D.P., and Sweet, M.J. (2011) Histone deacetylases as regulators of inflammation and immunity. *Trends Immunol* **32**: 335–343.

Shukla, G.C., Singh, J., and Barik, S. (2011) MicroRNAs: Processing, maturation, target recognition and regulatory functions. *Mol Cell Pharmacol* **3**: 83–92.

Smith, W.L., Dewitt, D.L., and Garavito, R.M. (2000) Cyclooxigenases: structural, cellular, and molecular biology. *Annu Rev Biochem* **69**: 145–182.

Takano, T., Kondo, H., Hirono, I., Endo, M., Saito-Taki, T., and Aoki, T. (2007) Molecular cloning and characterization of Toll-like receptor 9 in Japanese flounder, *Paralichtys olivaceus*. *Mol Immunol* **44**: 1845–1853.

Takeda, K., Kaisho, T., and Akira, S. (2003) Toll -Like Receptors. *Annu Rev Immunol* **21**: 335–376.

Talebi, F., Ghorbani, S., Chan, W.F., Boghozian, R., Masoumi, F., Ghasemi, S., et al. (2017) MicroRNA-142 regulates inflammation and T cell differentiation in an animal model of multiple sclerosis. *J Neuroinflammation* **14**: 55.

Tokarz-Deptuła, B., Malinowska, M., Amiak, M.A., and Deptuła, W. (2016) Coronins and their role in immunological phenomena. *Cent Eur J Immunol* **41**: 435–441.

Travassos, L.H., Carneiro, L.A.M., Ramjeet, M., Hussey, S., Kim, Y.G., Magalhes, J.G., et al. (2010) Nod1 and Nod2 direct autophagy by recruiting ATG16L1 to the plasma membrane at the site of bacterial entry. *Nat Immunol* **11**: 55–62.

Wang, T., Yan, J., Xu, W., Ai, Q., and Mai, K. (2016) Characterization of Cyclooxygenase-2 and its induction pathways in response to high lipid diet-induced inflammation in *Larmichthys crocea*. *Sci Rep* **6**.

Workenhe, S.T., Kibenge, M.J.T., Wright, G.M., Wadowska, D.W., Groman, D.B., and Kibenge, F.S.B. (2008) Infectious salmon anaemia virus replication and induction of alpha interferon in Atlantic salmon erythrocytes. *Virol J* **5**: 36.

Wu, S.H., Chou, H.Y., Liu, P.C., Wu, J.L., and Gong, H.Y. (2019) Granulin peptide GRN-41 of Mozambique tilapia is a novel antimicrobial peptide against *Vibrio* species. *Biochem Biophys Res Commun* **515**: 706–711.

Xu, X.Y., Shen, Y.B., Fu, J.J., Yu, H.Y., Huang, W.J., Lu, L.Q., et al. (2016) MicroRNA-induced negative regulation of TLR-5 in grass carp, *Ctenopharyngodon idella*. *Sci Rep* **6**.

Yan, B., Liu, B., Zhu, C.D., Li, K. Le, Yue, L.J., Zhao, J.L., et al. (2013) microRNA regulation of skin pigmentation in fish. *J Cell Sci* **126**: 3401–3408.

GENERAL DISCUSSION, CONCLUSIONS AND FUTURE DIRECTIONS

GENERAL DISCUSSION AND MAIN CONCLUSIONS

V. vulnificus is an aquatic bacterium that alternates between a metabolically inactive state (VBNC state) induced in adverse circumstances (such as low temperatures or low salinities), and a metabolically active state of free (planktonic cells) or sessile cells on mucous surfaces (especially on fish skin mucosae). This pathogen can also be found in the aquatic environment as a part of the microbiota of filter organisms such as oysters, which are considered one of the main reservoirs of the species. *V. vulnificus* is considered as one of the markers for climate change as its abundance in water directly mirrors water temperature. In fact, this species that is autochthonous from warm ecosystems is spreading to traditionally cold areas as close to the North Pole as Greenland or Norway due to global warming.

V. vulnificus is a highly heterogeneous species that comprises virulent and avirulent isolates from multiple hosts, including humans. Among the different groups described in the species, there is one with the unique ability to infect homoeothermic and poikilothermic hosts. This group is highly homogeneous and constitutes a clonal complex within lineage II (pv. *piscis*). In the present thesis, we have focused our research precisely on this group and have formulated a series of questions that we have tried to answer using a combination of omic and gene-based approaches together with confirmatory phenotypic approaches.

The first question was: **do iron and environmental temperature control *V. vulnificus* survival inside and outside its main hosts?** We found that effectively iron is one of the main signals to what the pathogen responses, mainly through the Fur regulator, triggering an environmental-adapted survival strategy. When iron is scarce in the environment *V. vulnificus* would form biofilms as its main survival strategy, while when iron is abundant, the bacterium would be in the water as a capsulated, motile, and highly infective cell (**FIGURE 8** from chapter 1). In addition, temperature also affects *V. vulnificus* survival in the environment and virulence as the pathogen is not infective below 20ºC while it is highly infective over 25ºC. Some of the reasons that explain this virulence dependence on the environmental temperature could be that most of the bacterial activities that facilitate the hosts (including humans) colonization such as motility, chemotaxis and protease secretion, as well as the production of a protective envelope against fish defenses, increase with the temperature, leading to a higher probability of host infection.

The second question was: **what are the bacterial genes essential for septicemia that are controlled by iron?** To answer this question we have used an *ex vivo* model of human and fish septicemia. We have found that *V. vulnificus* not only responds to exogenous iron levels but

also that it is able to change them in blood (by lysing RBC and liberating heme groups) as a consequence of its growth. In fact, 1 out of 2 genes differentially expressed in serum or artificial blood belongs to iron stimulon and/or Fur regulon. In blood, the pathogen also reacts to signals secreted by the host (i.e., ROS and NO) upregulating genes for the inactivation of those signals and membrane regeneration, together with the upregulation of an anaerobic metabolism based in nitrate/nitrite respiration in eels and in glycogen-related compounds in risk humans. According to our transcriptomic results and previous studies, we proposed that the common signal triggering anaerobic metabolism in both hosts is PspABC (enhanced by envelope stress), while in humans, catecholamines levels detected through QseBC are also involved in this process. Moreover, Fur plays a central role determining the nutrient source preferred by *V. vulnificus*, either as apo-Fur (in eels) through Lrp or as holo-Fur (in risk humans) through unknown signaling pathways (**FIGURE 8** from chapter 2). Once in the blood of its main hosts, *V. vulnificus* would express a toxic and host-adapted phenotype mainly based on the production of VvhA and $RtxA1_3$ toxins together with a protective envelope that would allow it to resist host complement and effectively multiply to cause septicemia (**FIGURE 9** from chapter 2). Our transcriptomic results suggest that iron and Fur, through other transcriptional regulators (SmcR and HlyU), trigger the activation of $RtxA1_3$ and VvhA leading to a high toxic phenotype, which explains why this pathogen is so virulent for fish and susceptible humans. We also found that the production of a protective envelope against innate immunity is temperature dependent in case of fish but not in case of humans. Therefore, the production of the capsule, the protective envelope against human innate immunity, is controlled by iron independently of the environmental temperature while that of the O-antigen, the protective envelope against fish innate immunity, is controlled by both iron and temperature being optimal at low levels of iron and 28ºC (water temperature during high mortality outbreaks in fish farms). Furthermore, we have described a new system of survival in fish blood that we have called “survival in fish blood kit”. The kit is formed by two IROMPs that have been horizontally transmitted between different lineages and species, contributing to the emergence of new pathogenic groups in the fish farming environment.

Finally, we wondered **which host genes are involved in response against the pathogen?** *Ex vivo* experiments in artificial eel blood, together with *in vivo* infections have allowed us to shed light to the eel transcriptomic changes during host-pathogen interaction. Hence, we have evidenced the immune-related mechanisms expressed by the eels during *V. vulnificus* infection and revealed that both RBC and WBC take part into the immune response against a bacterial pathogen such as *V. vulnificus*. Based on *ex vivo* results, RBC, the most abundant cells in eel

blood, are mainly involved in antigen recognizing/processing/presentation and TNFa production, although our results point out that they can also act as effectors cells (upregulating genes encoding lectins, prostaglandins, transferrin recycling and coagulation). WBC, on their part, upregulate genes involved in antibacterial compounds secretion (including ROS), professional antigen presentation, signaling transducers, several retrotransposons, and more importantly Il17c and Il6. These two interleukins would act together to coordinate the production of secreted mucins (Muc5B, whose gene is also upregulated in WBC) by mucosal and epithelial cells, thus suggesting a link between systemic and mucosal immunity (**FIGURE 7** from chapter 4). The results obtained *in vivo* are even more interesting and, besides confirming part of the results obtained *ex vivo*, suggest a very fast and strong pro-inflammatory response upon infection, mainly carried out by RBC, together with an atypical response which include the upregulation of a systemic RNAi (**FIGURE 4** from chapter 5).

Finally, we have determined that RtxA1$_3$ is involved in causing eels death by toxic shock after comparing the transcriptomic response in blood of wild-type strain infected eels with those infected with a mutant strain in the toxin. The overall results obtained *ex vivo* and *in vivo* point to a RxA1$_3$-dependent induction of a RBC-mediated and deregulated cytokine storm, probably due to the silencing of miRNA-142a, together with a putative retrotransposon storm (only observed *ex vivo*), whose relevance in the toxin action deserves future research.

From the results of the whole thesis we have extracted and summed up the following main **CONCLUSIONS**:

- **Iron**, not always through Fur, **is one of the main signals impacting the entire life cycle of *V. vulnificus***, from its survival in the marine environment, including biofilm production, motility and chemotaxis, to its survival in the blood of their hosts.

- In blood, **iron concentration is the key external signal triggering a host-adapted virulent phenotype in the zoonotic pathogen *V. vulnificus***. Bacterial transcriptomic analysis of this septicemic bacterium in serum of its main hosts, humans and eels, show the **association between high iron content in blood and septicemia in humans (risk patients), but not in eels**.

- *V. vulnificus* **iron-dependent and host-adapted virulent phenotype** mainly consists of a **generalist but host-dependent protective envelope** plus the **common overexpression of RtxA1$_3$ and VvhA**. In the case of **humans**, the **envelope** is **enriched in the capsule**, while in

eels it contains two plasmid-encoded OMPs, **Fpcrp and Ftbp**, that together conform a **"survival in fish blood kit"** which confer specific ability to resist fish innate immunity.

- **Temperature**, in water and host-infected body in the moment of infection, **contributes to pathogen pre-adaptation for the subsequent invasion and survival in host blood**. Therefore, under infective temperatures, bacterial fitness is enhanced by an increase in metabolic abilities, motility, chemotaxis and protease production. Nevertheless, temperature is not enough to trigger a host-adapted virulent phenotype, for what host and iron markers are essential.

- For the first time, we have established for the first time that **nucleated RBC**, as those of teleost fish, are transcriptionally active cells that **act as immune cells in fish,** not only against viral infections as it has already been described but also **against septicemic bacterial pathogens** such as *V. vulnificus*. Eel RBC take part in the eel immune response against *V. vulnificus* acting as antigen presenting cells and effector cells that respond to cytokines and activate pro-inflammatory cytokine production or even regulate innate immunity response. Moreover, we have proved that **a cross talk between eel RBC and WBC is essential to trigger RBC immune response**, as we have observed by comparing our *ex vivo* and *in vivo* eel transcriptome results.

- Eel **WBC** could **constitute a link between systemic and mucosal immunity** since they are able to activate the production of secreted mucins in response to *V. vulnificus* infection. WBC could be able to migrate towards mucosal tissues and directly secrete mucins against the pathogen, therefore contributing to protection for future infections.

- ***V. vulnificus* is detected as an intracellular pathogen**, through Tlr3, Tlr7 and Tlr9 by eel blood cells probably because of **RtxA1$_3$ intracellular activity**. As a result, **a fatal atypical immune response** against this pathogen is produced, which eventually causes eel death. In fact, in absence of RtxA1$_3$ (infections with a strain defective in RtxA1$_3$ effector domains release) eels are able to generate an effective and protective response in which the animals suffer from septicemia but do not die.

- The atypical immune response generated upon the detection of RtxA1$_3$ seems to be based on a **rapid cytokine/retrotransposon storm, probably mediated by systemic RNAi and anti-silencing protein,** which by unknown mechanisms would lead to **interference with miRNA-142a** activity. As a result, an exacerbated immune would be activated by RBC and cause eel death. On the contrary, in response to atoxic *V. vulnificus*, **miRNA-142a** is

produced very fast in eel blood probably regulating the generation of an accurate and protective inflammatory response that **prevent eels from death by vibriosis**.

- **miR-142a** stands out as a useful manner to **develop new therapeutic tools**, based on the utilization of silencing/anti-silencing RNAs in order to prevent vibriosis outbreaks and *V. vulnificus* spreading in fish farms, the main threat not only for aquaculture economy but also as a public health burden.

FUTURE DIRECTIONS

This thesis provides extensive transcriptomic data about host-pathogen interaction in *V. vulnificus* and its main host, the eel, which opens the door to new hypothesis and could be used to design new experiments. Here, we propose some ideas for **FUTURE STUDIES**:

- **Fpcrp ligand identification**. We have proved that the OMP Fpcrp confers resistance to phagocytosis by eel cells and to eel complement activated by the alternative pathway. We hypothesized that this protein would bind an unknown fish complement inhibitor, preventing bacterial killing and efficient opsonization and phagocytosis. We propose to carry out interatomic studies of *V. vulnificus* and eel serum in order to identify the Fpcrp ligand.

- **Bacterial mutant construction and phenotypic characterization**. Through the bacterial transcriptomic studies performed in this thesis we provide several bacterial mechanisms for host-adaptation and virulence such as maltose or nitrate metabolism for human or eel virulence, respectively. We propose to obtain bacterial mutant strains in those processes and perform specific phenotypic experiments in order to confirm our transcriptomics results.

- **Study the role of $VgrG_1$ and T6SS in *V. vulnificus* defensive response against eel RBC and phagocytosis more in detail.** Our results suggest that $VgrG_1$ is involved both in resistance to *V. vulnificus* natural predators in the aquatic ecosystem and bacterial cytotoxicity towards eel RBC. Nevertheless, more studies are needed to characterize the molecular action of this toxin and its relevance in vibriosis.

- **Establish the link between eel mucosal and systemic immunity.** Our transcriptomic results suggest that pathogen stimulated WBC would be able to migrate to mucosal tissues

and directly secrete mucins against the pathogen, since *muc5B* was upregulated by WBC upon *V. vulnificus* infection in a $RtxA1_3$-induced way. Therefore, *ex vivo* and *in vivo* experiments could be performed to test Muc5B secretion in response to *V. vulnificus* wild-type and defective in $RtxA1_3$ strains infection as well as the putative protection against infection conferred as a consequence of its activation.

- ***In vivo* study of retrotransposon storm.** We have found evidences in an *ex vivo* experiment of a retrotransposon storm produced by eel blood cells upon *V. vulnificus* infection which could be the cause, together with the cytokine storm observed *in vivo*, of the atypical (exacerbated) immune response that ends in animal death. *In vivo* studies should be performed to confirm this hypothesis and in case of confirmation, further research will be necessary to elucidate the molecular mechanisms that produce this massive retrotransposon induction.

- **Investigate miR-142a role in the modulation of a protective immune response in eels and how $RtxA1_3$ can interfere in that response.** We have found transcriptomic evidence that an early upregulation of miR-142a during eel infection with a *V. vulnificus* strain deficient in $RtxA1_3$ activity enhances the inflammatory-related genes silencing, thus leading to an accurate and protective immune response that does not occur in the presence of $RtxA1_3$. We propose to focus further into the study of the undergoing molecular mechanisms of this miRNA-regulated immune response and based on the results obtained, design new therapeutic tools to prevent *V. vulnificus* outbreaks in fish farms.

ANEX

TABLES INDEX

Chapter 4. Cross-talk between *Vibrio vulnificus* and eel blood cells

Chapter 5. Transcriptomic study performed in vivo: eel vibriosis and the role of RtxA1$_3$ of *Vibrio vulnificus* in eel virulence

FIGURES INDEX

Introduction

Hypothesis and objectives

General methodology

Chapter 1. Role of iron and Fur in the life cycle of *Vibrio vulnificus*

Chapter 2. Host-adaptation strategies in *Vibrio vulnificus*

Chapter 3. The effect of environmental temperature on the host-adaptation in *Vibrio vulnificus*

Chapter 4. Cross-talk between *Vibrio vulnificus* and eel blood cells

Chapter 5. Transcriptomic study performed in vivo: eel vibriosis and the role of RtxA1$_3$ of *Vibrio vulnificus* in eel virulence